



National Library
of Canada

Acquisitions and
Bibliographic Services Branch

395 Wellington Street
Ottawa, Ontario
K1A 0N4

Bibliothèque nationale
du Canada

Direction des acquisitions et
des services bibliographiques

395, rue Wellington
Ottawa (Ontario)
K1A 0N4

Your file - Votre référence

Our file - Notre référence

NOTICE

The quality of this microform is heavily dependent upon the quality of the original thesis submitted for microfilming. Every effort has been made to ensure the highest quality of reproduction possible.

If pages are missing, contact the university which granted the degree.

Some pages may have indistinct print especially if the original pages were typed with a poor typewriter ribbon or if the university sent us an inferior photocopy.

Reproduction in full or in part of this microform is governed by the Canadian Copyright Act, R.S.C. 1970, c. C-30, and subsequent amendments.

AVIS

La qualité de cette microforme dépend grandement de la qualité de la thèse soumise au microfilmage. Nous avons tout fait pour assurer une qualité supérieure de reproduction.

S'il manque des pages, veuillez communiquer avec l'université qui a conféré le grade.

La qualité d'impression de certaines pages peut laisser à désirer, surtout si les pages originales ont été dactylographiées à l'aide d'un ruban usé ou si l'université nous a fait parvenir une photocopie de qualité inférieure.

La reproduction, même partielle, de cette microforme est soumise à la Loi canadienne sur le droit d'auteur, SRC 1970, c. C-30, et ses amendements subséquents.

Canada

UNIVERSITY OF ALBERTA

SOLVENT EFFECTS ON THE REACTIVITIES OF SOLVATED ELECTRONS WITH
IONIC SOLUTES IN *n*-BUTANOL/WATER, AND *iso*-BUTANOL/WATER MIXED
SOLVENTS, AND A SERIES OF *n*-ALCOHOL SOLVENTS

by

RUZHONG CHEN



A thesis submitted to the Faculty of Graduate Studies and Research in partial fulfillment
of the requirements for the degree of DOCTOR OF PHILOSOPHY

DEPARTMENT OF CHEMISTRY

Edmonton, Alberta

FALL 1994



National Library
of Canada

Acquisitions and
Bibliographic Services Branch

395 Wellington Street
Ottawa, Ontario
K1A 0N4

Bibliothèque nationale
du Canada

Direction des acquisitions et
des services bibliographiques

395, rue Wellington
Ottawa (Ontario)
K1A 0N4

Author - Votre thèse

Author - Votre thèse

The author has granted an irrevocable non-exclusive licence allowing the National Library of Canada to reproduce, loan, distribute or sell copies of his/her thesis by any means and in any form or format, making this thesis available to interested persons.

L'auteur a accordé une licence irrévocable et non exclusive permettant à la Bibliothèque nationale du Canada de reproduire, prêter, distribuer ou vendre des copies de sa thèse de quelque manière et sous quelque forme que ce soit pour mettre des exemplaires de cette thèse à la disposition des personnes intéressées.

The author retains ownership of the copyright in his/her thesis. Neither the thesis nor substantial extracts from it may be printed or otherwise reproduced without his/her permission.

L'auteur conserve la propriété du droit d'auteur qui protège sa thèse. Ni la thèse ni des extraits substantiels de celle-ci ne doivent être imprimés ou autrement reproduits sans son autorisation.

ISBN 0-315-95161-3

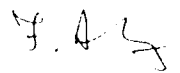
Canada

1000 North Main Street
Boston, Massachusetts 02108
Telephone: (617) 552-1234
Fax: (617) 552-5678
E-mail: info@company.com

Page 1 of 1

1000 North Main Street
Boston, Massachusetts 02108

This document is the property of the company and is to be used only for the purposes stated herein. It is not to be distributed, copied, or otherwise used without the express written consent of the company. If you have received this document in error, please notify the sender immediately. Thank you for your cooperation.



1000 North Main Street
Boston, Massachusetts 02108



*Gordon R. Freeman
Radiation Research Laboratory
Department of Chemistry*

*University of Alberta
Edmonton AB
Canada T6G 2G2*

September 28, 1994

To whom it may concern:

This letter gives permission to Mr. Ruzhong Chen from the co-author, Gordon R. Freeman, for the use of the articles:

1. "Ion Pairing of Ammonium Nitrate in Methanol?" *J Phys. Chem.* **96**, 7107 (1992) by R. Chen and G. R. Freeman.
2. "Solvent Effects on the Reactivity of Solvated Electrons with Ammonium and Nitrate Ions in 1-Butanol/Water Solvents", *Can. J. Chem.* **71**, 1303 (1993) by R. Chen and G. R. Freeman.
3. "Solvent Effects on the Reactivity of Solvated Electrons with Ions in *Iso*-Butanol/Water Mixed Solvents", *Can. J. Chem.* **72**, 1083 (1994) by R. Chen, Y. Avotinsk, and G. R. Freeman.
4. "Solvent Effects on the Reactivity of Solvated Electrons with Nitrate Ion in a series of *n*-Alcohol Solvents", *J. Phys. Chem.* (submitted.) by R. Chen and G. R. Freeman. in the Ph.D. thesis of Mr. Ruzhong Chen.

Yours sincerely,

Gordon R. Freeman

Professor of Chemistry

UNIVERSITY OF ALBERTA

RELEASE FORM

NAME OF AUTHOR: RUZHONG CHEN


TITLE OF THESIS: SOLVENT EFFECTS ON THE REACTIVITIES OF SOLVATED
ELECTRONS WITH IONIC SOLUTES IN *n*-BUTANOL/WATER, AND *iso*-
BUTANOL/WATER MIXED SOLVENTS, AND A SERIES OF *n*-ALCOHOL
SOLVENTS

DEGREE: DOCTOR OF PHILOSOPHY

YEAR THIS DEGREE GRANTED: 1994

Permission is hereby granted to the University of Alberta Library to reproduce single copies of this thesis and to lend or sell such copies for private, scholarly or scientific research purposes only.

The author reserves all other publication and other rights in association with the copyright in the thesis, and except as hereinbefore provided neither the thesis nor any substantial portion thereof may be printed or otherwise reproduced in any material form whatever without the author's prior written permission.



(Signed)

PERMANENT ADDRESS: Apt. 302, 10645-80 Avenue
Edmonton, Alberta
Canada T6E 1V6

Date: Sept 28, 1994

谨以此论文：

献给我的父母亲和大妈，他们的养育之恩永世不忘；


献给我亲爱的妻子，她的爱心是我前进的动力。

*Dedicated to my parents, my aunt in Huainin county, and my
wife, Bo, for their love and care.*

UNIVERSITY OF ALBERTA

FACULTY OF GRADUATE STUDIES AND RESEARCH

The undersigned certify that they have read, and recommend to the Faculty of Graduate Studies and Research for acceptance, a thesis entitled SOLVENT EFFECTS ON THE REACTIVITIES OF SOLVATED ELECTRONS WITH IONIC SOLUTES IN *n*-BUTANOL/WATER, AND *iso*-BUTANOL/WATER MIXED SOLVENTS, AND A SERIES OF *n*-ALCOHOL SOLVENTS submitted by RUZHONG CHEN in partial fulfillment of the requirements for the degree of DOCTOR OF PHILOSOPHY



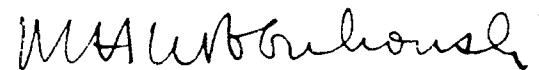
Dr. Gordon R. Freeman, Supervisor



Dr. R. B. Jordan, Chairman



Dr. P. Kebarle



Dr. M. Klobukowski



Dr. J. Tuszynski



Dr. G. V. Buxton, External Examiner

DATE: 28 Sept., 1994

Abstract

We studied solvent effects on e_s^- reactions with solvated ions in 1- and *iso*-butanol/water mixed solvents, and a series of *n*-alcohol solvents.

The value of k_2 for $(e_s^- + NO_{3,s}^-)$ in water is ~ 40 times larger than that in butanols, whereas k_2 for $(e_s^- + NH_{4,s}^+)$ in water is $\sim 10^{-4}$ times smaller than that in butanols. This enormous reversal of solvent effects on e_s^- reaction rates is the first observed for ionic reactants. The e_s^- reactions with H_s^+ , Ag_s^+ , and Cu_s^{2+} are close to the diffusion controlled limit in the butanol/water mixed solvents. The low reactivity of $NH_{4,s}^+$ with e_s^- in water, and the less than diffusion controlled rate of $(e_s^- + OH_{1,s}^+)$, is attributed to the symmetrical hydrogen-bonded solvation structure of NH_4^+ and the partially symmetrical solvation structure of OH_3^+ . The nearly diffusion controlled rates of e_s^- with $NH_{4,s}^+$ and $ROH_{2,s}^+$ in butanols are attributed to the unsymmetrical hydrogen-bonded solvation structures of these ions. The NH_4^+ and H_s^+ ions have no low-lying orbital for an electron to occupy, so either reaction occurs by proton transfer to the electron site, or the neutral species must decompose. We suggest that the proton transfer or decomposition of the neutral species is facilitated by an unsymmetrical solvation structure.

Reaction of e_s^- in $Al(ClO_4)_3$ aqueous solutions is mainly due to H_s^+ from hydrolysis of Al_s^{3+} , and partly to partially hydroxylated aluminum (III) species.

The value of k_2 for e_s^- reaction with nitrate ions in C_1 to C_{10} *n*-alcohols increases with increasing viscosity and dielectric longitudinal relaxation time of the solvent. This relatively slow reaction is assisted by a longer encounter duration, hence a larger η and τ_L . The mean time required for an encounter pair to react, k_r^{-1} , is $\gg \tau_L$ in methanol, whereas $k_r^{-1} < \tau_L$ in 1-octanol and 1-decanol. At the extremes, in methanol and decanol, the activation energy of the overall reaction is similar to that of the fluidity

of the solvent, whereas in intermediate alcohols E_2 is much larger than that of fluidity. The reaction of e_s^- with nitrate is activation *entropy* limited in methanol, mainly activation *energy* limited in C_2 to C_4 *n*-alcohols, and mainly diffusion/dipole rotation limited in 1-decanol.

Acknowledgements

Special thanks are due to Professor Gordon R. Freeman for the direction I received in the course of the thesis work.

I would like to express appreciation to the many persons associated with me during the thesis work including the staff of the Radiation Research Center at the University of Alberta, Mr. L. Coulson and Mr. R. J. Gardner, for aid with electronics and maintenance of the pulse radiolysis equipment. I am very grateful for the help I received from Dr. Norman Gee when I started the graduate study and during the thesis work. It is also a pleasure to express my gratitude to Dr. Y. Avotins, Dr. T. Yoshinari, and Mr. Yixing Zhao for their valuable discussions and cooperation.

Appreciation is extended to the Natural Sciences and Engineering Research Council of Canada for financial assistance to the research project and Department of Chemistry, University of Alberta for teaching and research assistantship.

Table of Contents

Chapter One:	1
Introduction	
I. Solvated Electrons	1
II. Properties of Solvated Electrons.....	3
A. ESR Spectrum and Thermodynamic Properties.....	3
B. Mobility of Solvated Electrons	4
C. Optical Absorption Spectrum.....	4
1. Absorption Band Width	5
2. Transitions	5
3. Optical Absorption Spectrum in Hydroxylic Solvents	6
III. Models of Solvated Electrons.....	7
IV. Structure and Properties of Hydroxylic Solvents	10
A. Structure and Properties of Liquid Water	10
B. Structure and Properties of Alcohols	11
C. Structure and Properties of Water/Alcohol Mixtures	12
1. Static Dielectric Properties	12
2. Thermodynamic Properties.....	13
3. Dynamic Properties	13
V. Reactivity of Solvated Electrons	16
VI. Present Work	19
References	21

Chapter Two:	29
Ion Pairing of Ammonium Nitrate in Methanol?	
I. Introduction	29
II. Experimental Section	30
III. Results and Discussion.....	30
References	39
Chapter Three:	40
Solvent Effects on the Reactivity of Solvated Electrons with Ammonium and Nitrate Ions in 1-Butanol/Water Solvents	
I. Introduction	40
II. Experimental Section	41
A. Materials	41
B. Techniques	41
III. Results and Discussion.....	42
A. Physical Properties	42
B. Rate Constants	42
C. Electrical Conductivities	45
D. Reaction of ($e_s^- + NO_{3,s}^-$).....	46
E. Reaction of ($e_s^- + NH_{4,s}^+$)	47
F. Effective Radii for Mutual Diffusion	49
References	66

Chapter Four:68
**Solvent Effects on the Reactivity of Solvated Electrons with
Ions in *iso*-Butanol/Water Mixed Solvents**

I.	Introduction	68
II.	Experimental Section	70
A.	Materials	70
B.	Techniques.....	71
III.	Results and Discussion.....	72
A.	Physical Properties	72
B.	Rate Constants	73
C.	The Debye Factor f	74
D.	Comparisons of k_2/f in Other Primary Alcohols.....	75
E.	Electrical Conductivities and Effective Reaction Radii (κR_T).....	76
F.	Activation Energies E_2 and E_A	77
G.	Effective Radii R_D for Mutual Diffusion.....	79
H.	Reactions of e_s^- in $Al(ClO_4)_3$ Solutions	81
	References	104

Chapter Five: 107
**Solvent Effects on Reactivity of Solvated Electrons with
Nitrate Ion in C_1 to C_{10} *n*-Alcohols**

I.	Introduction	107
II.	Experimental Section	109
A.	Materials	109
B.	Techniques.....	109
C.	Physical Properties of the Solvents.....	110

III. Results and Discussion.....	110
A. Concentration Dependence of k_{obs}	110
B. Concentration Dependence of Electrical Conductance.....	111
C. Rate Constants k_2	113
D. Dependence of k_2 on Solvent Fluidity and τ_1	113
E. Evaluation of Kk_r for $(e_s^- + NO_{3,s}^-)$ from Equation [5-7].....	115
References	130

Chapter Six 132

General Discussion and Conclusions

I. General Discussion of Molar Conductivities.....	132
II. General Discussion of Solvated Electrons Reactions.....	135
A. Reactions of $(e_s^- + H_s^+)$ and $(e_s^- + NH_{4,s}^+)$	135
B. Reactions of $(e_s^- + Ag_s^+)$, $(e_s^- + Cu_s^{2+})$, and $(e_s^- + NO_{3,s}^-)$	137
III. Conclusions.....	139
References	156

Appendix One..... 158

Experimental Methodology

I. Apparatus for Rate Constant Measurement	158
A. Sample Cells.....	158
B. Removal of Oxygen from Samples	158
C. Irradiation, Optical, and Control Systems	159
1. Van de Graaff Accelerator.....	159
2. Secondary Emission Monitor (SEM)	159
3. Optical System.....	160
4. Temperature Control System.....	161

II.	Apparatus for Electrical Conductivity Measurement.....	162
A.	Impedance Bridge.....	162
B.	Conductance Cells.....	163
C.	Constant Temperature Bath.....	164
III.	Experimental Techniques.....	164
A.	Sample Preparation.....	164
B.	Rate Constant Measurement.....	165
1.	Half-life and k_{obs} Measurement.....	165
2.	k_2 and E_2 Measurement.....	166
3.	Effect of Impurities.....	167
C.	Electrical Conductivity Measurement.....	168
D.	pH Measurement.....	169
	Appendix Two	178
	Experimental Results	
I.	Results of Rate Constant Measurement.....	178
A.	Results of k_{obs} Measurement.....	179
B.	Results of k_2 Measurement.....	201
II.	Results of Molar conductivity Measurement.....	210

List of Tables

Table	Page
2-1. Molar conductivity of ammonium nitrate in methanol.....	34
2-2. Parameter values for curves in Figure 2-1.....	35
3-1. Symbols in Figures 3-1 to 3-3.	50
3-2. The values of pK_a for $NH_4^+ \rightleftharpoons NH_3 + H^+$ in water	50
3-3. Properties of NH_4^+ and H_2O (liquid) compared	51
3-4. Rate parameters for the reaction of solvated electrons with solutes in 1-butanol/water mixed solvents at 298K.....	52
4-1. Symbols in Figures 4-1 to 4-4.....	84
4-2. Rate parameters for reaction of solvated electrons with solvated ions in <i>iso</i> -butanol/water at 298K	85
5-1. Conductivity fitting parameters for ion pairing in lithium nitrate solutions	117
5-2. Rate parameters for the reaction of (e_s^- + nitrate) in C_6 to C_{10} <i>n</i> -alcohols.....	118
5-3. Rate parameters for e_s^- reactions with Ag_s^+ and $NO_{3,s}^-$ in C_1 to C_{10} <i>n</i> -alcohols at 298K	119
5-4. Calculation of k_d for the reaction $e_s^- + Ag_s^+$ in methanol and ethanol at 298K	120
5-5. The values of Kk_f for e_s^- reaction with nitrate in C_1 to C_{10} <i>n</i> -alcohols at 298K	121
6-1. Rate parameters for reaction of solvated electrons with hydrogen ion in 1-butanol/water mixed solvents at 298K	141
A-1. The values of k_{obs} of solvated electrons' reaction with lithium nitrate in 1-butanol/water mixed solvents.....	179

A-2.	The values of k_{obs} of solvated electrons' reaction with ammonium nitrate in 1-butanol/water mixed solvents.....	182
A-3.	The values of k_{obs} of solvated electrons' reaction with ammonium perchlorate in water.....	184
A-4.	The values of k_{obs} of solvated electrons' reaction with ammonium perchlorate in 1-butanol/water mixed solvents.....	186
A-5.	The values of k_{obs} of solvated electrons' reaction with perchloric acid in 1-butanol/water mixed solvents.....	188
A-6.	The values of k_{obs} of solvated electrons' reaction with lithium perchlorate in water, 1-butanol, and <i>iso</i> -butanol.....	191
A-7.	The values of k_{obs} of solvated electrons' reaction with lithium nitrate in <i>iso</i> -butanol solvent.....	192
A-8.	The values of k_{obs} of solvated electrons' reaction with ammonium nitrate in <i>iso</i> -butanol/water mixed solvents.....	192
A-9.	The values of k_{obs} of solvated electrons' reaction with ammonium perchlorate in <i>iso</i> -butanol/water mixed solvents.....	194
A-10.	The values of k_{obs} of solvated electrons' reaction with silver perchlorate in <i>iso</i> -butanol/water mixed solvents.....	196
A-11.	The values of k_{obs} of solvated electrons' reaction with lithium nitrate in 1-hexanol, 1-octanol, and 1-decanol solvents.....	198
A-12.	Temperature and composition dependences of k_2 for the reaction of e_s^- with lithium nitrate in 1-butanol/water mixed solvents.....	201
A-13.	Temperature and composition dependences of k_2 for the reaction of e_s^- with ammonium nitrate in 1-butanol/water mixed solvents.....	202
A-14.	Temperature and composition dependences of k_2 for the reaction of e_s^- with ammonium perchlorate in 1-butanol/water mixed solvents.....	203
A-15.	Temperature and composition dependences of k_2 for the reaction	

	of e_s^- with perchloric acid in 1-butanol/water mixed solvents	204
A-16.	Temperature dependence of k_2 for the reaction of e_s^- with lithium nitrate in <i>iso</i> -butanol solvent	205
A-17.	Temperature and composition dependences of k_2 for the reaction of e_s^- with ammonium nitrate in <i>iso</i> -butanol/water mixed solvents	206
A-18.	Temperature and composition dependences of k_2 for the reaction of e_s^- with ammonium perchlorate in <i>iso</i> -butanol/water mixed solvents.....	207
A-19.	Temperature and composition dependences of k_2 for the reaction of e_s^- with silver perchlorate in <i>iso</i> -butanol/water mixed solvents.....	208
A-20.	Temperature dependence of k_2 for the reaction of e_s^- with lithium nitrate in 1-hexanol, 1-octanol, and 1-decanol solvents.....	209
A-21.	Temperature and composition dependences of molar conductivities of lithium nitrate solutions in 1-butanol/water mixed solvents	211
A-22.	Temperature and composition dependences of molar conductivities of ammonium nitrate solutions in 1-butanol/water mixed solvents	212
A-23.	Temperature and composition dependences of molar conductivities of ammonium perchlorate solutions in 1-butanol/water mixed solvents	213
A-24.	Temperature and composition dependences of molar conductivities of perchloric acid solutions in 1-butanol/water mixed solvents	214
A-25.	Temperature and composition dependences of molar conductivities of lithium nitrate solutions in <i>iso</i> -butanol/water mixed solvents	215
A-26.	Temperature and composition dependences of molar conductivities of ammonium nitrate solutions in <i>iso</i> -butanol/water mixed solvents	216
A-27.	Temperature and composition dependences of molar conductivities of ammonium perchlorate solutions in <i>iso</i> -butanol/water mixed solvents.....	217
A-28.	Temperature and composition dependences of molar conductivities of perchloric acid solutions in <i>iso</i> -butanol/water mixed solvents	218

A-29.	Temperature and composition dependences of molar conductivities of silver perchlorate solutions in <i>iso</i> -butanol/water mixed solvents	219
A-30.	Temperature and composition dependences of molar conductivities of copper (II) perchlorate solutions in <i>iso</i> -butanol/water mixed solvents	220
A-31.	Temperature and composition dependences of the apparent molar conductivities of aluminum (III) perchlorate solutions in <i>iso</i> -butanol/water mixed solvents.....	222
A-32.	Temperature and concentration dependences of the molar conductivities of lithium nitrate solutions in 1-hexanol solvent	223
A-33.	Temperature and concentration dependences of the molar conductivities of lithium nitrate solutions in 1-octanol solvent.....	224
A-34.	Temperature and concentration dependences of the molar conductivities of lithium nitrate solutions in 1-decanol solvent	225

List of Figures

Figure	Page
2-1. Molar conductivity Λ of ammonium nitrate in methanol plotted against (concentration) ^{0.5}	36
2-2. Plot of the Walden product $\Lambda\eta$ against (concentration) ^{0.5}	37
2-3. Comparison of the measured molar conductivities at 298.29K with those that would be expected if $K_2 = 10 \text{ m}^3/\text{mol}$ (dashed line)	38
3-1. Arrhenius plots of k_2 of e_s^- reaction with LiNO_3 in 1-butanol/water mixed solvents	54
3-2. Arrhenius plots of k_2 of e_s^- reaction with NH_4NO_3 in 1-butanol/water mixed solvents	55
3-3. Arrhenius plots of k_2 of e_s^- reaction with NH_4ClO_4 in 1-butanol/water mixed solvents	56
3-4. Solvent composition dependence of k_2 at 298K in 1-butanol/water mixed solvents	57
3-5. Dielectric permittivity dependence of the Debye factor f at 298K.....	58
3-6. Solvent composition dependence of k_2/f at 298K in 1-butanol/water mixed solvents	59
3-7. Solvent composition dependence of the molar conductivities Λ of salts at 298K in 1-butanol/water mixed solvents.....	60
3-8. Solvent composition dependence of κR_f , equation [3-6], at 298K in 1-butanol/water mixed solvents.....	61
3-9. Solvent composition dependence of the activation energies E_2 near 298K in 1-butanol/water mixed solvents	62
3-10. Solvent composition dependence of the activation energies E_Λ of	

	conductance near 298 K in 1-butanol/water mixed solvents.....	63
3-11.	The values of $k_2(e_s^- + NO_{3,s}^-)$ in pure C ₁ -C ₄ alcohol solvents at 298 K, as functions of viscosity η and dielectric relaxation time τ_1	64
3-12.	Solvent composition dependence of R_d at 298K in 1-butanol/water mixed solvents	65
4-1.	Arrhenius plots of k_2 of e_s^- reactions with lithium nitrate in <i>iso</i> -butanol/water mixed solvents.....	88
4-2.	Arrhenius plots of k_2 of e_s^- reactions with ammonium nitrate (A) and ammonium perchlorate (B) in <i>iso</i> -butanol/water solvents	89
4-3.	Arrhenius plots of k_2 of e_s^- reactions with silver perchlorate (A) and perchloric acid (B) in <i>iso</i> -butanol/water solvents	90
4-4.	Arrhenius plots of k_2 of e_s^- reactions with copper(II) perchlorate in <i>iso</i> -butanol/water solvents.....	91
4-5.	Solvent composition dependence of k_2 at 298K in <i>iso</i> -butanol/water solvents.....	92
4-6.	Dielectric permittivity dependence of the Debye factor f at 298K.....	93
4-7.	Solvent composition dependence of k_2/f at 298K in <i>iso</i> -butanol/water solvents.....	94
4- 8.	The values of k_2/f in pure primary C ₁ -C ₄ alcohol solvents at 298K, as functions of viscosity η and dielectric relaxation time τ_1	95
4- 9.	Dielectric relaxation time τ_1 of primary C ₁ -C ₄ alcohols at 298K, as a function of viscosity η	96
4-10.	Solvent composition dependence of the molar conductivities Λ of dilute electrolyte solutions at 298K in <i>iso</i> -butanol/water solvents	97
4-11.	Solvent composition dependence of κR_r , equation [4-10], at 298K in <i>iso</i> -butanol/water solvents.....	98
4-12.	Solvent composition dependence of the activation energies E_2	

of e_s^- reactions, and E_Λ of conductance, near 298K in <i>iso</i> -butanol/water solvents.....	99
4-13. Solvent composition dependence of R_{ij} , equation [4-12], at 298K in <i>iso</i> -butanol/water mixed solvents.....	100
4-14. pH of $Al(ClO_4)_3$ aqueous solutions at 298K as a function of concentration of aluminum (III) added.....	101
4-15. The values of k_{obs} of e_s^- reactions in $Al(ClO_4)_3$ aqueous solutions as a function of concentration of aluminum(III) added.....	102
4-16. Solvent composition dependences of rate constants k'_2 and Arrhenius temperature coefficients E'_2 for reaction of e_s^- in aluminum perchlorate solutions at 298K.....	103
5-1. Concentration and temperature dependences of k_{obs} of e_s^- reaction with lithium nitrate in 1-hexanol.....	122
5-2. Concentration and temperature dependences of k_{obs} of e_s^- reaction with lithium nitrate in 1-octanol.....	123
5-3. Concentration and temperature dependences of k_{obs} of e_s^- reaction with lithium nitrate in 1-decanol.....	124
5-4. Molar conductivities of lithium nitrate solutions at 298K in 1-hexanol, 1-octanol, and 1-decanol.....	125
5-5. Various functions of Λ_0 for lithium nitrate in C_N <i>n</i> -alcohol at 298K.....	126
5-6. Arrhenius plots of measured k_2 for (e_s^- + nitrate) reaction in 1-hexanol, 1-octanol, and 1-decanol.....	127
5-7. Dependences of rate constants on viscosity and dielectric longitudinal relaxation time.....	128
5-8. Activation energy E_2 for (e_s^- + nitrate) reaction in C_1 to C_{10} <i>n</i> -alcohols at 298K, expressed as excess over that of solvent viscosity E_η or that of electrolyte mobility E_Λ	129

6-1.	Arrhenius plots of Λ of LiNO_3 electrolyte solutions in 1-butanol/water mixed solvents.....	142
6-2.	Arrhenius plots of Λ of NH_4NO_3 electrolyte solutions in 1-butanol/water mixed solvents.....	143
6-3.	Arrhenius plots of Λ of NH_4ClO_4 electrolyte solutions in 1-butanol/water mixed solvents.....	144
6-4.	Arrhenius plots of Λ of HClO_4 electrolyte solutions in 1-butanol/water mixed solvents.....	145
6-5.	Arrhenius plots of Λ of LiNO_3 electrolyte solutions in <i>iso</i> -butanol/water mixed solvents.....	146
6-6.	Arrhenius plots of Λ of NH_4NO_3 electrolyte solutions in <i>iso</i> -butanol/water mixed solvents.....	147
6-7.	Arrhenius plots of Λ of NH_4ClO_4 electrolyte solutions in <i>iso</i> -butanol/water mixed solvents.....	148
6-8.	Arrhenius plots of Λ of HClO_4 electrolyte solutions in <i>iso</i> -butanol/water mixed solvents.....	149
6-9.	Arrhenius plots of Λ of AgClO_4 electrolyte solutions in <i>iso</i> -butanol/water mixed solvents.....	150
6-10.	Arrhenius plots of Λ of $\text{Cu}(\text{ClO}_4)_2$ electrolyte solutions in <i>iso</i> -butanol/water mixed solvents.....	151
6-11.	Arrhenius plots of k_2 of e_s^- reactions with perchloric acid in 1-butanol/water solvents.....	152
6-12.	Solvent composition dependence of k_2 for $(e_s^- + \text{H}_s^+)$ at 298K in 1-butanol/water solvents.....	153
6-13.	Solvent composition dependence of Λ of HClO_4 electrolyte solutions at 298K in 1-butanol/water solvents.....	154
6-14.	Solvent composition dependence of κR_r , equation [6-4], at 298K in	

	1-butanol/water mixed solvents.....	155
A-1.	The bubbling system.....	170
A-2.	The secondary emission monitor.....	171
A-3.	Path of analyzing light.....	172
A-4.	The temperature control of the water bath.....	173
A-5.	The temperature regulation system.....	174
A-6.	The sealing technique.....	175
A-7.	The typical solvated electron optical absorption trace.....	176
A-8.	The specific conductance of pure <i>iso</i> -butanol/water mixed solvents.....	177

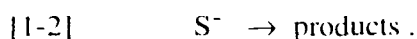
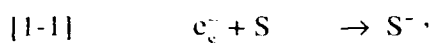
Chapter One

Introduction

I. Solvated Electrons

The discovery of solvated electrons can be traced back to November 1808, when Humphry Davy observed a blue color when he heated potassium metal in dry ammonia gas (1). In 1864, W. Weyl observed a blue color when sodium or potassium was dissolved in liquid ammonia (2). However, it was not until 1922 that C. A. Kraus provided the final proof that the blue color was due to solvated electrons, by comparing transference and conductance properties in solutions of alkali metals dissolved in liquid ammonia (3). Solvated electrons were similarly obtained in other solvents, for example, in amines (4) by dissolving sodium or potassium in them; in water (5); in alcohols (6); in hydrocarbons (7); in ethers (8); etc., by pulse radiolysis.

Solvated electrons have been used to convert a wide range of chemical substances (S) to their reduced form (S^-), which may then undergo further reaction to yield other products.



Pulse radiolysis (9) is one of the most convenient methods to form solvated electrons. It uses pulses of high energy electrons as the source of radiation. When these electrons penetrate the liquid, energy is lost by ionization and excitation of the liquid molecules. Along the path of these high energy electrons local volumes of ionized, excited and

dissociated molecules are formed. These local volumes are called microzones (10). The reactive intermediates in these microzones dissipate in a few nanoseconds by reacting together or diffusing into the bulk of the liquid .

Due to ionization many more electrons are produced along the path of the high energy primary electrons. These lower energy secondary electrons also lose their excess energy by ionization and excitation of the molecules in the liquid medium. The deenergized electrons ultimately enter one of several types of states, depending on the solvent properties:

(i) In an electrophilic solvent, the slowed-down electrons attach to solvent molecules to form negative ions.

(ii) If the electrons are not attached to specific molecules they reach a state of thermal equilibrium with the solvent, resulting in solvated electrons. As discussed in the next section, these solvated electrons can be detected by distinctive properties such as electrical mobility and optical absorption spectrum.

A thermalized electron can be localized in a coulombic (electrostatic) potential well in a solvent whose molecules are polar or anisotropically polarizable: the potential well is created by several suitably oriented solvent molecules (11). On the other hand, if a solvent molecule is isotropically polarizable (with the exception of helium, which has a very small polarizability and repels the electron), the potential well is very shallow and the electron is not then localized to any large extent. Such electrons, which are very mobile, are called "quasifree" electrons (11).

An electron electronically polarizes the medium in about 10^{-15} s. Thus the trapped electron immediately finds itself in an electronically polarized potential well (trap) (12). The electric field of the electron causes the medium molecules to reorient along the axis of a permanent dipole or along that of the maximum polarizability. The trap becomes deeper. The time for this process is related to the dielectric relaxation

time of the medium (13). In water it takes about a picosecond for the trapped electron to relax into the solvated state (11, 12).

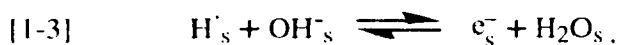
II. Properties of Solvated Electrons

The physical and chemical properties of solvated electrons depend on the nature of the solvent. Geometry and polarity of the solvent molecules affect the electron-solvent interaction, and therefore the energy of solvation.

A. ESR Spectrum and Thermodynamic Properties

An electron is paramagnetic, so electron spin resonance (ESR) studies have shown the nature of the solvated electron states (14). According to an ESR study of solvated electrons in aqueous glasses (15) the electron is solvated at the center of an octahedron made up of six water molecules.

The thermodynamic properties of solvated electrons have also been evaluated, among them are the standard potential (16), and the solvation enthalpy, entropy, and free energy (17-22). All experimental estimations of the thermodynamics of e_s^- have been based on the equilibrium:



and reasonable assumptions for the thermodynamics of H_s^+ (20-23). A recent measurement of the activation energy ($E_a = 39 \pm 2$ kJ/mol and $A = 1.4 \pm 0.4 \times 10^{11}$ m³/mol·s) for reaction [1-3] gave a reassessment of the thermodynamic properties of the solvated electron (20). It showed that the solvated electron thermochemistry is often dominated by the entropy effect rather than the enthalpy effect. The solvated electron has the smallest solvation enthalpy of all aqueous ions ($\Delta H_s^0 = -126 \pm 11$ kJ/mol); and the only positive solvation entropy ($\Delta S_s^0 = 118 \pm 20$ J/mol·K) (20). The

large positive solvation entropy implies a dramatic modification of the water structure in the vicinity of the solvated electron.

B. Mobility of Solvated Electrons

Solvated electrons are different from quasifree electrons. They are much less mobile. The mobility of a delocalized electron could be $\sim 10^{-2} \text{ m}^2/\text{V}\cdot\text{s}$ in comparison to $\sim 10^{-6} \text{ m}^2/\text{V}\cdot\text{s}$ of a localized electron. Conductivity studies provide data on the mobility of solvated electrons. The mobility of the solvated electron is several times higher than that of normal ions. In water, for example, the mobility of the solvated electron is close to that of hydroxide ions and smaller than that of protons (24, 25). In simple alcohols, the mobility of the solvated electrons is also close to that of alkoxy ions (RO^-) (26-28), but why this is so remains a question. In nonpolar liquids, the mobilities depend strongly on the structure of the solvent molecules, and are usually several orders of magnitude greater than those of ordinary ions (29, 30).

C. Optical Absorption Spectrum

Solvated electrons absorb light at wavelengths ranging from ultraviolet to infrared. The absorption band is broad and asymmetric with a long tail extending to higher energies. The energy at the absorption maximum, E_{Amax} , and the width of the band depend on the polarity of the solvent.

In protic solvents such as water, alcohols (31) and ammonia (32a), the energy of maximum absorption E_{Amax} lies in the visible to near-infrared regions, since the interaction of the solvated electrons with these strongly polar molecules is large. In nonpolar aliphatic hydrocarbons, on the other hand, absorption maxima occur further to the infrared where solvation energy arises from interaction with induced dipole moments. Values of E_{Amax} for polar but aprotic solvents such as ethers (8) lie between these extremes.

In general, the values of $E_{\Lambda_{\max}}$ of solvated electrons in organic solvents depend on:

- (i) the types and number of functional groups;
- (ii) the number of alkyl groups attached to the functional group.

Values of $E_{\Lambda_{\max}}$ are temperature and density dependent. Thermal agitation of the solvent molecules and a lower density make the traps shallower. Therefore, values of $E_{\Lambda_{\max}}$ decrease with increasing temperature and decreasing density (31, 33).

1. Absorption Band Width

The solvated electron absorption band has a similar form in a wide range of solvents: it is always broad and asymmetric, skewed to higher energies. This can be interpreted as the result of both homogeneous and heterogeneous broadening effects. Homogeneous broadening assumes that a single species is responsible for the absorption (all traps in the liquid medium are the same), but attributes broadening to the coupling between solvated electron levels in the trap and molecular motions of the surrounding dipolar molecules (34, 35). Heterogeneous broadening, on the other hand, attributes the band width to a wide variation of solvated electron trap depths, each trapped electron state having a different absorption spectrum. Since both factors must play a role, we say that the band is nonhomogeneously broadened.

2. Transitions

The energy absorbed by the ground state solvated electron has been attributed to the following transitions (36-40):

- (i) Bound to bound transition: from the ground state level to an excited state discrete level of the same trap;
- (ii) Bound to continuum transition: from ground state level to continuum levels associated with the liquid as a whole.

The strong skewing of the absorption band toward higher energies has been interpreted as evidence for strong contributions of bound to continuum transitions,

since it is argued that a more symmetric shape would result from bound to bound transitions alone. Evidence for this is given by studies of photo conductivity spectra (41), assuming that higher mobilities generated in photo conductive processes result from excitation of the electron to a continuum level of the liquid. By estimating the threshold or minimum energy E_{th} for photo conductivity and comparing it with the characteristics of the optical absorption spectrum as a whole, an idea of the extent of bound to continuum transitions in the absorption spectrum can be obtained (42-47). The study shows that both bound to bound and bound to continuum transitions contribute to the spectrum; typically E_{th} is less than E_{Amax} (42) and therefore a major portion of the spectrum is due to bound to continuum transitions. In studies of photo conductivity in mixtures of polar/nonpolar solvents (44-47), it has been concluded that bound to bound transitions play an increasing role as the fraction of polar component increases, due to deepening of the traps.

3. *Optical Absorption Spectrum in Hydroxylic Solvents*

The absorption energies of electrons in water, alcohol and their mixtures are greater than those in other polar solvents such as ammonia and amines (48) because of the strong electron interaction with -OH groups.

The values of E_{Amax} of solvated electrons in alcohols are in the order: primary > secondary > tertiary (31, 49). The values of E_{Amax} are almost independent of the chain length for primary alcohol (50), because the alkyl group beyond the α -carbon apparently has little effect on the interaction between the electron and the solvent (48, 50, 51).

A weaker orientational alignment of solvent dipoles around the electron is probably the reason for lower E_{Amax} values in secondary and tertiary alcohols.

The widths of the solvated electron absorption band at half height ($W_{1/2}$) in alcohols are about twice that in water (52). The $W_{1/2}$ values in amines are also about twice that in ammonia (53). In alcohols, the bound to continuum transition mode has

been considered as the major contributor in the absorption spectra of solvated electrons. The extent of bound to bound transition depends on the type of alcohol (43, 52).

III. Models of Solvated Electrons

The progress of theoretical calculations of solvated electrons had been slow due to the statistical aspects of the nonrigid solvated electron structure. Semi-continuum models (54, 55) were not good enough to give a realistic analysis of experimented data. The difficulty was the lack of super computational techniques. In recent years, however, statistical quantum mechanical molecular dynamics simulations have shown promising progress towards the theoretical understanding of solvated electron (56-76). These simulations used a quantum mechanical representation of the electron, but a rather classical representation of the water molecule and a pseudo potential approach for describing the electron-water interaction.

M. J. Klein and his research group mainly concentrated on the simulation of the optical absorption spectrum and diffusion of solvated electrons in ammonia (57, 59-61). Compared to the measured absorption spectrum of e_s^- in ammonia (77), the calculated spectrum was in a higher energy range (60). The calculated diffusion coefficient for e_s^- in ammonia was about 1/3 of the measured one (61). The discrepancy was thought to be due to a nonadiabatic effect in the transport of the electron, and to less realistic features in the models used for both the solvent and the electron-solvent interaction. Also, wave function overlap between e_s^- and an adjacent trap might allow hopping in ammonia, whereas it was ignored in the model calculations. The diffusion coefficient of e_s^- in liquid ammonia is five times that of Cl_s^- (29, 32b).

P. J. Rossky and his research group mainly concentrated on the study of solvated electron dynamics and diffusion in pure water. Early attempts included the

study of electron trapping sites in water, and probing the sites with a test charge to evaluate the capacity of the traps to host an excess electron (63). Recently they did a similar study with a fully quantum mechanical treatment of the excess electronic ground state (64). The results showed that the concentration of effective electron trapping sites is relatively high in the liquid (~ 10 mol/m³). Rossky's group and others also tried to calculate the equilibrium solvated electron absorption spectrum in water, using path-integral Monte Carlo techniques (65, 66), and to simulate electronically adiabatic relaxation of the electronic ground state in a bath of water molecules (67, 68). The simulation results emphasize the role of molecular and structural effects of the solvent.

Studies of solvated electron diffusion in water by statistical quantum molecular dynamics simulation (69, 70) concluded that nonlocal transitions involving adiabatic quantum mechanical wave function overlap and nonadiabatic hopping were absent. The fact that the diffusion rate of e_s^- in water is twice that of Cl_s^- was attributed to the virtually instantaneous, rather than inertial, response of the electron solute to the solvent configuration, resulting in rapid variation of the solvated electron spatial density.

New algorithms for the statistical quantum mechanical molecular dynamics simulation continue to be developed. For example, a mixed classical-quantum system that included nonadiabatic quantum transitions was applied to the problem of solvation dynamics of an initially energetic excess electron in liquid water (71-73). Computed results revealed that there were two possible routes for the solvation of an initially energetic (2eV) quasifree excess electron. One is the case of a rapid localizational cascade through the electronic excited states directly to the electronic ground state; the time to reach the electronic ground state is in the range of 50 to 150 fs and the solvation occurs rapidly once the electron reaches the electronic ground state. The other is the case of the electron going into a localized electronic excited state; the time scale for

appearance of this state is comparable to that in the first case (50-150 fs) and the life time of the electronic excited state is ~ 1 ps. The electron finally would settle into the electronic ground state. This suggested that, if the electron's absorption spectral properties were characterized by an electronic excited state spectrum and a ground state equilibrium spectrum which do not evolve in time, a simple two-state kinetic model could explain the observed spectral dynamics. This is called a two-state model. This is in qualitative agreement with the experimentally measured transient absorption spectra using ultrafast laser spectroscopy (78, 79).

Recently, the influence of solvent intramolecular modes, which are very flexible, on the dynamics of the energetic excess electron solvation in liquid water was studied (74, 75). It was found that the effect of flexibility on relaxation times was substantial, but the effect on the branching ratio for excess electrons passing through alternative intermediate excited states was small. The result also suggested that a two-state model analysis of the dynamics neglected a potentially important role for early time delocalized electrons (74). According to a newly proposed mechanism for the solvation of electrons in pure water, thermalization via spontaneous de-excitations across a manifold of delocalized electronic excited states is followed by a branching between a two-step solvation and a direct trapping path that leads to the electronic ground state of the solvated electron (75).

Recent experimental measurements by ultra fast transient spectroscopy of photo excited solvated electrons in pure water detected complicated spectral transients, indicating a break down of the simple two-state model (80). The molecular dynamics calculation indicated that the observed complexity of the ultrafast spectral dynamics was due to a combination of spectral changes in electronic excited state solvation and electronic ground state bleaching dynamics (76).

IV. Structure and Properties of Hydroxylic Solvents

In the present work, we use 1-butanol/water, *iso*-butanol/water mixtures and a series of normal alcohols as solvents to study the reactivities of solvated electrons with solvated ions in these solvents. The reactivities of solvated electrons depend not only on the nature of the solvated electron itself and the co-reactant but also on the structural features of the solvent and resulting properties such as diffusion coefficients, viscosity, dielectric relaxation times, etc. We here give a brief introduction to these topics.

A. Structure and Properties of Liquid Water

Many X-ray and neutron scattering, and dielectric and ultrasonic measurements have been carried out and modern spectroscopic techniques (IR, Raman, and NMR) utilized to determine the microscopic structure of liquid water (81). Based on experimental results statistical mechanical calculations (82, 83) and computer simulation (84) have been carried out to build models for the structure of liquid water.

Liquid water was considered to have a "broken down" ice structure (85) according to earliest model based on radial distribution functions. In ice, each water molecule is hydrogen bonded tetrahedrally to four other molecules. The distribution functions of water (86, 87) indicate slightly more than four nearest neighbors. At high temperatures it becomes close to five indicating a more random order.

Since this early model, numerous models have been proposed for the structure of water. These models fall into two broad categories:

- (i) uniformist models (88, 89);
- (ii) mixture models (90-93).

According to the uniformist models, water consists of a single type of three-dimensional random hydrogen bond network. There are no significant amounts of

monomer water. There is an equilibrium between free and bonded hydroxyl groups. The structure is regarded as a network of cavities with structural order that is approximately tetrahedral.

According to the mixture models, water consists of a mixture of two or more species. These are water molecules with no hydrogen bonds or with up to four hydrogen bonds. The hydrogen bonded water molecules form an open network full of cavities or clusters of water molecules. These exist in equilibrium with monomer water and clusters, which make the medium denser than ice. Recent efforts have focused on exploring the feasibility of long-lived clusters of water molecules to account for the observed large heat capacity of liquid water, and a simple two-structure model for liquid water has been proposed (94). In this model, the structure of water is considered as primarily a mixture of tetramers and octamers. However, no single model can explain all the properties of water. Experimental results are usually explainable with one or the other of these models

B. Structure and Properties of Alcohols

In contrast to water, the liquid structure of alcohols is simpler than that of water because there is only one hydroxyl group per molecule. The hydroxyl groups in alcohols can hydrogen bond with each other. Alcohols have the ability to form up to three hydrogen bonds per molecule. Water, on the other hand, can form up to four hydrogen bonds. Various spectroscopic studies have shown that monomers, dimers, and polymers all exist (95-97).

There are chain and ring structures where approximately two hydrogen bonds per alcohol molecule are formed. Alcohols with larger alkyl groups tend to exist mainly as monomers and ring-like polymers because of the steric hindrance (98). Lower alcohols can make a third hydrogen bond which leads to a three-dimensional linkage of polymer chains (99, 100).

C. *Structure and Properties of Water/Alcohol Mixtures*

An alcohol contains both a hydrophilic hydroxyl group and a hydrophobic alkyl group. It is this bifunctional nature of the alcohol molecule that gives rise to strong composition-dependent physical properties in alcohol/water mixtures. The amount of hydrogen bonding between the alcohol hydroxyl group and water molecules depends on the sizes of the hydrophobic alkyl groups and the number of hydrophobic hydroxyl groups in the alcohols. For *n*-alkanols with small hydrophobic alkyl groups ($n \leq 3$), they are completely miscible with water at any composition. As the hydrophobic alkyl group becomes larger the solubility decreases. For butanol/water mixtures, except for *t*-butanol, they are only miscible with water within the range of 0 to ~50 mol% water and > 97 mol% water (101); *t*-butanol is completely miscible with water.

1. Static Dielectric Properties

Information about the short range order in a liquid can be obtained from dielectric properties. The Kirkwood structure factor, g_k , which is calculated from the dielectric constant, dipole moment and density, is a measure of the short-range order (102). When the molecular dipoles are oriented in series, which amplify their effects, the value of g_k is greater than one. For head-to-tail interaction between molecular dipoles, which tend to cancel each other's effect, the value of g_k is less than one. Random orientation gives $g_k = 1$.

As a result of the existence of short-range order in water and primary alcohols the g_k values are greater than unity (53, 103). The value of g_k increases with increasing chain length for primary alcohols because the alcohols with longer chains are better aligned. Small alcohols can form a third hydrogen bond cross-linking the polymer chains. This must be the reason for its lower g_k value which arises because of the difficulty of alignment.

The g_k values increase slightly when water is added to methanol or tertiary alcohols (103, 104). Water can make hydrogen bonds with those alcohol molecules resulting in a better linear arrangement of dipoles. Thus water has a structure-building effect in these cases. On the other hand, the g_k values decrease when water is added to other alcohols (103), and water acts as a structure breaker on these alcohols.

2. *Thermodynamic Properties*

The thermodynamic functions of mixing of alcohols and water have been useful in the study of the structure of alcohol/water mixtures (105, 106). The extent of change depends on the alkyl group. Hydrogen bond formation gives rise to a negative enthalpy of mixing and a positive value of enthalpy of mixing implies hydrogen bond rupture.

When a small amount of alcohol is dissolved into water a decrease in enthalpy and entropy results. The interpretation is that:

- (i) the alcohol molecule promotes water-water hydrogen bonding (107, 108);
- or
- (ii) water molecules order around the alcohol molecule and form clathrate-like structures (109).

Therefore, the structure of water is strengthened by adding of small amount of alcohol molecules in this case (108).

When water is added to small alcohols, some of these alcohol molecules make hydrogen bonds with water, the enthalpy of mixing is negative (exothermic) and water acts as a structure maker. The enthalpy of mixing of higher alcohols with water is positive (endothermic), and water acts as a structure breaker (105, 106).

3. *Dynamic Properties*

The dynamic properties are important for the study of kinetics in liquids, because kinetics involves movement of species. Viscosity and dielectric relaxation

time are among the most important dynamic properties for our study of reactivity of solvated electrons with solvated ions in alcohol/water mixed solvents.

(a) Viscosity (η): The viscosity of a liquid is related to the rate of diffusion in a liquid. The viscosity is higher in alcohols with longer or branched alkyl groups. The bulkiness of the alkyl group makes it difficult to flow. Viscosities are strongly composition dependent in mixtures of alcohol and water. The following are the important qualitative features of viscosity of butanol/water mixtures (110, 111):

(i) A maximum in viscosity occurs at a composition near the miscibility edge in alcohol-rich range, except for iso-butanol/water mixtures in which the maximum is in 0 mol% water composition;

(ii) A sharp increase in viscosity occurs when a few mole percent of alcohol is added to water;

(iii) Only small changes in viscosity occur when a few mole percent of water is added to alcohol.

Viscosity is increased when some alcohol is added to water. This is perhaps due to the clathrate-like structure formation (109). In the small alcohols, water acts as a structure maker, indicated by an increase in viscosity. Viscosity decreases when water is added to larger alcohols which can be explained by the formation of water-nucleated alcohol complexes (31, 105); or by the breakdown of alcohol structure by water (112).

(b) Dielectric Relaxation Times (τ): The dielectric relaxation time is related to the reorientation of the molecular dipoles along the applied field in a liquid. The reorientation of solvent dipoles around the charged reactant species is necessary for the solvated electron to react with solvated ions.

Water has a single dielectric relaxation process, with a dielectric relaxation time (τ) equal to 10^{-11} s at normal temperature and pressure. In contrast, several dielectric relaxation processes are observed in alcohols. They are represented by (113):

(i) τ_1 : the time required for the collective breaking of intermolecular hydrogen bonds and reorientation of molecules;

(ii) τ_2 : the reorientation time of a free monomer;

(iii) τ_3 : the reorientation time of free -OH dipoles.

The process that relates to the liquid structure is given by τ_1 . This is called the primary relaxation process. The reorientation of larger alcohol molecules depends on the steric hindrance of the alkyl group and the hydrogen bonds (114). Reorientation of these molecules needs the cooperation of the other molecules. Small alcohol molecules display relatively small steric effects, hence reorientation depends mostly on hydrogen bond breaking; relaxation times in these alcohols are shorter (115).

When a small amount of water is added to an alcohol, the dielectric relaxation time varies as follows (116, 117):

(i) In the smallest alcohol methanol, it is practically constant up to 10 mol% water and then decreases at 303K; at 273K and 248K, it increases at the beginning and a maximum is present; at lower temperature, it increases with increasing mol% water;

(ii) In ethanol and 2-propanol, it decreases monotonously with increasing mol% water.

Water has a structure breaking effect in most alcohols.

Dielectric relaxation time decreases and viscous flow becomes easier when temperature increases. This is because of the increasing thermal agitation of the molecules.

The dielectric relaxation time in the constant charge case is called longitudinal relaxation time τ_L (118): $\tau_L = \tau_1 \epsilon_\infty / \epsilon_s$, where ϵ_∞ and ϵ_s are relative permittivities at infinite and low (static) frequency, respectively. τ_L is related to the dynamic behavior of polar solvents in electron transfer processes (119).

V. Reactivity of Solvated Electrons

Another useful way to gain understanding of the solvated electron is to study their reactivities with different types of solute. An enormous amount of kinetic data has been reported. Rates of the solvated electron reactions have been measured in water (120-123); alcohols (124-131); alcohol mixtures (132); and alcohol/water mixtures (27, 28, 111, 133-146). The present work continues and extends this work to the particular case of ionic solutes.

In models of kinetics of chemical reactions in solution, the solution is generally assumed to be a continuum dielectric with a frequency dependent dielectric constant $\epsilon(\omega)$, and generally two kinds of approaches were used to determine how fast the reaction will be:

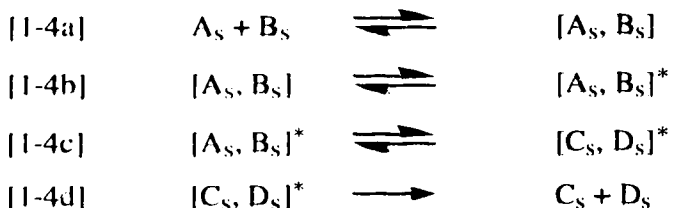
(i) Quantum statistical or semiclassical theories were used to evaluate the intrinsic rate at which the reaction occurs, which is a molecular level quantity (147);

(ii) Statistical theories were used to account for the probability of existence of encounter pair of the two reactant species in solution, the Smoluchowski-Debye-Stokes-Einstein model being such an example (148-151).

The reactions of the solvated electron are usually electron transfer reactions (152). Possible exceptions are $e_{\zeta}^{-} + ROH \rightarrow H + RO_{\zeta}^{-}$ and $e_{\zeta}^{-} + ROH_{2,\zeta}^{+} \rightarrow H + ROH$ in water and alcohols, where a proton from a solvating $-OH$ or $-OH_{2}^{+}$ group might transfer to the site of the electron (153, 154). Proton transfer to the "cavity" of the electron site might avoid the work needed to create a new site for the H atom if the electron were to transfer first, followed by decomposition of the transient ROH^{-} or ROH_2 . The electron and proton are both elementary particles, but the former has a much smaller mass and, other things being equal, would have a larger transfer

probability. Protons have larger mobilities than do electrons in water and alcohols, which means that the transport mechanisms are different.

For electron transfer between two species A and B in liquid media, according to Marcus' model we have the following mechanism (147, 155):



where the subscript s signifies "solvated". The first step represents the random diffusion of two reactants, which by chance encounter each other and thereby form an encounter pair. The second step represents thermal activation of the encounter pair to the transition state, which involves random reorientations of solvent dipoles around the encounter pair in a manner that accidentally facilitates electron transfer from A to B, for example. The third step is the rapid transfer of the electron, restricted by the Franck-Condon principle. The last step represents relaxation of the product state, followed by diffusive separation of the products C and D.

The observed second order reaction rate constant k_2 can be related to the foregoing mechanism through the steady state approximation for the concentrations of the intermediates:

$$[1-5] \quad \frac{1}{k_2} = \frac{1}{k_{4a}} + \frac{(k_{-4b} + k_{4d}) k_{4c} + k_{-4b} k_{4d}}{K_{4a} k_{4b} k_{4c} k_{4d}}$$

where $K_{4a} = k_{4a}/k_{-4a}$ is the equilibrium constant of reaction [1-4a], and reaction [1-4c] is assumed to be thermoneutral, with $k_{4c} = k_{-4c}$. If one further sets $k_{4d} = k_{-4b}$, one obtains:

$$[1-6] \quad \frac{1}{k_2} = \frac{1}{k_{4a}} + \frac{2k_{4c} + k_{-4b}}{K_{4a} k_{4b} k_{4c}}$$

In the limiting case of $k_{4c} \gg k_{-4b}$ one obtains:

$$\begin{aligned}
 [1-7] \quad \frac{1}{k_2} &= \frac{1}{k_{4a}} + \frac{2}{K_{4a}k_{4b}} \\
 &= \frac{1}{k_{4a}} + \frac{1}{K_{4a}k_r}
 \end{aligned}$$

where $k_d = k_{4a}$ = diffusion controlled upper limit of the reaction rate constant, and $k_r = k_{4b}/2$ = rate of formation of products from encounter pairs when half of the initially formed transition states revert back to reactants ($k_{-4c} = k_{4c}$).

In water ($\eta \sim 10^{-3}$ Pa·s, $\tau_L \sim 10^{-12}$ - 10^{-11} s) typical value of the diffusion rate constants is $k_d \approx 10^7$ m³/mol·s, $k_{-d} \approx 10^{12}$ s⁻¹, hence $K_{4a} \approx 10^{-5}$ m³/mol. The value of $k_{4b} \propto \exp(-\Delta G_{4b}/RT)$ is related mainly to the entropy of reorganization of solvent dipoles around the reactant encounter pair to assist, by fluctuations in the polarization potential, electron transfer from A_s to B_s .

We analyze large values of k_2 from the viewpoint of the Smoluchowski-Debye-Stokes-Einstein model (151):

$$[1-8] \quad k_2 \approx k_d = 4 \pi N_A (D_A + D_B) R_f f$$

where N_A = Avogadro's constant, D_A and D_B are diffusion coefficients, R_f is the average center-to-center distance between A and B when electron transfer occurs, and f is a factor that accounts for the effect of the coulombic interaction between the reactants on their probability of diffusing to within a distance R_f of each other.

$$[1-9] \quad f = \frac{U(R_f)}{k_B T} \left| \exp\left(\frac{U(R_f)}{k_B T}\right) - 1 \right|^{-1}$$

where, $U(R_f)$ is the potential energy of interaction between the reactants at distance R_f , k_B is Boltzmann's constant, and T is the absolute temperature.

The potential energy when S is an ion of charge $z\xi$ is given by:

$$[1-10] \quad U(R_f) = - \frac{z\xi^2}{4\pi\epsilon_0\epsilon_r R_f}$$

where $-\xi$ is the charge on the electron, ϵ_0 is the permittivity of vacuum, and ϵ_r is the relative permittivity of the solvent between the electron and the ion.

The relative contributions of k_d and k_r to limiting the observed reaction rate are reflected in the ratio k_2/k_d . If $k_2 \approx k_d$, then $K_{4a}k_r \gg k_d$; if $k_2 = 0.5 k_d$, then $K_{4a}k_r \approx k_d$; if $k_2 \ll k_d$, then $k_2 \approx K_{4a}k_r$.

We have introduced the probability κ that reaction occurs during the lifetime of an encounter pair (151). Then,

$$[1-11] \quad k_2 = \kappa k_d = 4 \pi N_A (D_A + D_B) \kappa R_r f$$

For example, when $\kappa \leq 0.10$, then $K_{4a}k_r \leq k_d/9$. To the extent that this model is satisfactory, we evaluate solvent effects on k_2/f . Although this model ignores the effects that solvent structure (molecular packing and relative orientation) exerts on reactant diffusion rates and reaction probabilities, the equation is useful in evaluating effects of bulk fluid properties such as viscosity and dielectric constant on the rate constants of the solvated electron with solvated ions in solutions.

The effect of temperature on reaction rates also provides valuable information for postulating mechanisms. Changes in rates due to temperature change are generally expressed in terms of the activation energy (E_2) and the frequency factor (A_2) of the Arrhenius equation (156):

$$[1-12] \quad k_2 = A_2 \exp(-E_2/RT)$$

VI. Present Work

The objective of this study is to learn more about the behavior of the solvated electron in 1-butanol/water and *iso*-butanol/water mixed solvents, and in a series of normal alkanol solvents. The effects of the different solvents on the reactions of the solvated electron with solvated ions were measured at different temperatures. Electrical conductivity measurement was made to obtain information about the diffusion coefficients of ions, since the diffusion coefficients of the reacting species are related to their molar conductivities. The activation energies of nearly diffusion

- 20 -

controlled reactions are similar to those of diffusion of the corresponding ions in solution, so the temperature dependence of the molar conductivities was also investigated. pH measurement was made to provide information about ion dissociation equilibria in aluminum(III) perchlorate aqueous solutions.

References:

1. P. P. Edwards. *Adv. Inorg. Chem. Radiachem.* **25**, 135 (1982).
2. W. Weyl. *Ann. Phys.* **121**, 601 (1864), quoted by J. C. Thompson. *in* *Electrons in Liquid Ammonia*. Clarendon Press, Oxford. 1976. p. 2.
3. C. A. Kraus. *The Properties of Electrically Conducting System*. Chemical Catalogue Co., New York. 1922. Section 5 of chapter 14, p. 375.
4. P. Fowles, W. R. McGregor, and M. C. R. Symons. *J. Chem. Soc.* 3329 (1957).
5. E. J. Hart and J. W. Boag. *J. Am. Chem. Soc.* **84**, 4090 (1962).
6. S. Arai and L. M. Dorfman. *J. Chem. Phys.* **41**, 2190 (1964).
7. G. R. Freeman. *In Radiation Research Reviews*. Vol. **1**. Edited by G. O. Phillips and R. B. Cundall. Elsevier, Amsterdam. 1968. p. 1.
8. F. Y. Jou and G. R. Freeman. *Can. J. Chem.* **54**, 3693 (1976).
9. L. M. Dorfman and M. S. Matheson. *In Progress in Reaction Kinetics*. Vol. **3**. Edited by G. Porter. Pergamon Press, London. 1965. Chapter 6, p. 237.
10. G. R. Freeman. *In Kinetics of Nonhomogeneous Processes*. 1 ed. Edited by G. R. Freeman. John Wiley & Sons Inc., New York. 1987. Section 1 of chapter 6, p. 278.
11. J. Jortner and A. Gaathon. *Can. J. Chem.* **55**, 1801 (1977).
12. G. R. Freeman. *In Radiation Research*. Edited by G. Silini. North Holland, Amsterdam. 1967. p. 113.
13. Y. Wang, M. K. Crawford, M. J. McAuliffe, and K. B. Eisenthal. *Chem. Phys. Lett.* **74**, 160 (1980).
14. D. F. Feng and L. Kevan. *Chem. Rev.* **80**, 1 (1980).
15. L. Kevan. *J. Phys. Chem.* **84**, 1232 (1980).

16. U. Schindewolf. *Angew. Chem. Intl. Ed.* **7**, 190 (1968).
17. J. Jortner and R. M. Noyes. *J. Phys. Chem.* **70**, 770 (1966).
18. R. M. Noyes. *In Radiation Chemistry I. Vol. 1. Adv. Chem. Ser. No. 81. Edited by R. F. Gould. American Chemical Society, Washington, DC. 1968. p. 65.*
19. B. Hickel and K. Sehested. *J. Phys. Chem.* **89**, 5271 (1985).
20. P. Han and D. M. Bartels. *J. Phys. Chem.* **94**, 7294 (1990).
21. H. A. Schwarz. *J. Phys. Chem.* **95**, 6697 (1991).
22. H. A. Schwarz. *J. Phys. Chem.* **96**, 8937 (1992).
23. J. H. Baxendale. *Radiat. Res. Suppl.* **4**, 139 (1964).
24. G. C. Barker, P. Fowles, D. C. Sammon, and B. Stringer. *Trans. Faraday Soc.* **66**, 1498 (1970).
25. K. H. Schmidt, P. Han, and D. M. Bartels. *J. Phys. Chem.* **96**, 199 (1992).
26. P. Fowles. *Trans. Faraday Soc.* **67**, 428 (1971).
27. O. I. Micic and B. Cercek. *J. Phys. Chem.* **81**, 833 (1977).
28. Y. Maham and G. R. Freeman. *J. Phys. Chem.* **92**, 1506 (1988).
29. G. R. Freeman. *In Kinetics of Nonhomogeneous Processes. 1 ed. Edited by G. R. Freeman. John Wiley & Sons Inc., New York. 1987. Appendix of chapter 2, p. 66.*
30. P. H. Tewari and G. R. Freeman. *J. Chem. Phys.* **51**, 1276 (1969).
31. A. D. Leu, K. N. Jha, and G. R. Freeman. *Can. J. Chem.* **60**, 2342 (1982).
32. J. C. Thompson. *Electrons in Liquid Ammonia. 1 ed. Clarendon press, Oxford. 1976. (a) p. 279; (b) p. 80.*
33. F. Y. Jou and G. R. Freeman. *J. Phys. Chem.* **81**, 909 (1977).
34. D. Huppert, P. Avouris, and P. M. Rentzepis. *J. Phys. Chem.* **82**, 2282 (1978).
35. T. R. Tuttle Jr., S. Golden, S. Lwenje, and C. M. Stupak. *J. Phys. Chem.* **88**, 3811 (1984).

36. N. R. Kestner and J. Jortner. *J. Phys. Chem.* **77**, 1040 (1973).
37. A. Kajiwara, K. Funabashi, and C. Naleway. *Phys. Rev.* **A6**, 808 (1972).
38. R. Lugo and P. Delahay. *J. Chem. Phys.* **57**, 2122 (1972).
39. G. L. Hug and I. Carmichael. *J. Phys. Chem.* **86**, 3410 (1982).
40. K. Funabashi, I. Carmichael, and W. H. Hamill. *J. Chem. Phys.* **69**, 2652 (1978).
41. T. Ichikawa and H. Yoshida. *J. Chem. Phys.* **73**, 1540 (1980).
42. J. K. Baird, L. K. Lee, and E. J. Meehan, Jr. *J. Chem. Phys.* **83**, 3710 (1985).
43. T. Kimura, K. Hirao, N. Okabe, and K. Fueki. *Can. J. Chem.* **62**, 64 (1984).
44. J. K. Baird and C. H. Morales. *J. Phys. Chem.* **89**, 774 (1985).
45. K. F. Baverstock and P. J. Dyne. *Can. J. Chem.* **48**, 2182 (1970).
46. T. Shida, S. Iwata, and T. Watanabe. *J. Phys. Chem.* **76**, 3683 (1972).
47. N. Kato, S. Takagi, and K. Fueki. *J. Phys. Chem.* **85**, 2684 (1981).
48. G. R. Freeman. *J. Phys. Chem.* **77**, 7 (1973).
49. A. D. Leu, K. N. Jha, and G. R. Freeman. *Can. J. Chem.* **61**, 1115 (1983).
50. R. R. Hentz and G. A. Kenney-Wallace. *J. Phys. Chem.* **78**, 514 (1974).
51. G. E. Hall and G. A. Kenney. *Chem. Phys.* **32**, 313 (1978).
52. F. Y. Jou and G. R. Freeman. *Can. J. Chem.* **57**, 591 (1979).
53. F. Y. Jou and G. R. Freeman. *Can. J. Chem.* **60**, 1809 (1982).
54. D. A. Copeland, N. R. Kestner, and J. Jortner. *J. Chem. Phys.* **53**, 1189 (1970).
55. D. F. Feng, K. Fueki, and L. Kevan. *J. Chem. Phys.* **58**, 3281 (1973).
56. D. Chandler, Y. Singh, and D. M. Richardson. *J. Chem. Phys.* **81**, 1975 (1984).
57. M. Sprik, R. W. Impey, and M. L. Klein. *J. Chem. Phys.* **83**, 5802 (1985).
58. M. Sprik, R. W. Impey, and M. L. Klein. *Phys. Rev. Lett.* **56**, 2326 (1986).
59. M. Sprik and M. L. Klein. *J. Chem. Phys.* **87**, 5987 (1987).
60. M. Sprik and M. L. Klein. *J. Chem. Phys.* **89**, 1592 (1988).
61. M. Sprik and M. L. Klein. *J. Chem. Phys.* **91**, 5665 (1989).

62. Z. Deng, G. J. Martyna, and M. L. Klein. *J. Chem. Phys.* **100**, 7590 (1994).
63. J. Schnitker, P. J. Rossky, and G. A. Kenney-Wallace. *J. Chem. Phys.* **85**, 2986 (1986).
64. K. Motakabbir, J. Schnitker, and P. J. Rossky. *J. Chem. Phys.* **97**, 2055 (1992).
65. J. Schnitker, K. Motakabbir, P. J. Rossky, and R. Friesner. *Phys. Rev. Lett.* **60**, 456 (1988).
66. A. Wallqvist, G. Martyna, and B. J. Berne. *J. Phys. Chem.* **92**, 1721 (1988).
67. P. J. Rossky and J. Schnitker. *J. Phys. Chem.* **92**, 4277 (1988).
68. R. B. Barnett, U. Landman, and A. Nitzan. *J. Chem. Phys.* **90**, 4413 (1989).
69. J. Schnitker and P. J. Rossky. *J. Phys. Chem.* **93**, 6965 (1989).
70. G. S. Del Buono, P. J. Rossky, and T. H. Murphrey. *J. Phys. Chem.* **96**, 7761 (1992).
71. J. C. Tully. *J. Chem. Phys.* **93**, 1061 (1990).
72. F. A. Webster, J. Schnitker, M. S. Friedrichs, and others. *Phys. Rev. Lett.* **66**, 3172 (1991).
73. F. A. Webster, P. J. Rossky, and R. A. Friesner. *Comput. Phys. Commun.* **93**, 494 (1991).
74. T. H. Murphrey and P. J. Rossky. *J. Chem. Phys.* **99**, 515 (1993).
75. E. Keszei, S. Nagy, T. H. Murphrey, and P. J. Rossky. *J. Chem. Phys.* **99**, 2004 (1993).
76. B. J. Schwartz and P. J. Rossky. *J. Phys. Chem.* **98**, 4489 (1994).
77. F. Y. Jou and G. R. Freeman. *J. Phys. Chem.* **85**, 629 (1981).
78. F. H. Long, H. Lu, and K. B. Eisenthal. *Phys. Rev. Lett.* **64**, 1469 (1990).
79. H. Lu, F. H. Long, and K. B. Eisenthal. *J. Opt. Soc. Am. B.* **7**, 1511 (1990).
80. J. C. Alfano, P. K. Walhout, Y. Kimura, and P. F. J. Barbara. *J. Chem. Phys.* **98**, 5996 (1993).

81. F. Franks (*Editor*). *Water; A Comprehensive Treatise*. Vol. **1**. Plenum, New York. 1972.
82. P. J. Rossky. *Ann. Rev. Phys. Chem.* **36**, 321 (1985).
83. J. P. Hansen and I. R. McDonald. *Theory of Simple Liquids*. Academic Press, New York. 1976.
84. M. P. Allen and D. J. Tildesley. *Computer Simulation of Liquids*. Clarendon Press, Oxford, UK. 1987.
85. J. D. Bernal and P. H. Fowler. *J. Chem. Phys.* **1**, 515 (1933).
86. A. H. Narten and H. A. Levy. *J. Chem. Phys.* **55**, 2263 (1971).
87. A. H. Narten. *J. Chem. Phys.* **56**, 5681 (1972).
88. J. A. Pople. *Proc. Royal Soc.* **A205**, 163 (1954).
89. S. A. Rice and M. G. Sceats. *In Water: A Comprehensive Treatise*. Vol. **7**. Edited by F. Franks. Plenum, New York. 1982. Chapter 2, p. 83.
90. H. S. Frank and Y. W. Wen. *Discuss Faraday Soc.* **24**, 133 (1957).
91. G. Nemethy and H. A. Scheraga. *J. Chem. Phys.* **36**, 3382 (1962).
92. M. S. Jhon, J. Grosh, T. Ree, and H. Eyring. *J. Chem. Phys.* **44**, 1465 (1966).
93. G. J. Safford, P. S. Leung, A. W. Naumann, and P. C. Schaffer. *J. Chem. Phys.* **50**, 4444 (1969).
94. S. W. Benson and E. D. Siebert. *J. Am. Chem. Soc.* **114**, 4269 (1992).
95. P. Huyskens. *J. Mol. Struct.* **100**, 403 (1983).
96. P. Schuster, G. Zundel, and C. Sandorfy (*Editor*). *The Hydrogen Bond*. Vol. **3**. North Holland Publishing, Amsterdam. 1976. p. 1070.
97. M. C. R. Symons and V. K. Thomas. *J. Chem. Soc. Faraday Trans.* **177**, 1883 (1981).
98. H. H. Eysel and J. E. Bertie. *J. Mol. Struct.* **142**, 227 (1986).
99. B. M. Petit and P. J. Rossky. *J. Chem. Phys.* **78**, 7296 (1983).
100. W. L. Jorgensen. *J. Phys. Chem.* **90**, 1276 (1986).

101. J. M. Sorensen and W. Arlt (*Editor*). Liquid-Liquid Equilibrium Data Collection, DECHEMA Chem. Data Series. Frankfurt. 1979.
102. J. G. J. Kirkwood. *J. Chem. Phys.* **7**, 911 (1939).
103. J. B. Hasted. *In* Aqueous Dielectrics. Chapman and Hall, London. 1973. p. 176.
104. A. D'Aprano and I. D. Donato and G. D'Arrigo, D. Bertolini, M. Cassettari, and G. Salvetti. *Molecular Physics.* **55**, 475 (1985).
105. A. C. Brown and D. J. G. Ives. *J. Chem. Soc. II.* 1608 (1962).
106. B. Marongiu, I. Perino, R. Monaci, V. Solinas and S. Torrazza. *J. Molecular Liq.* **28**, 229 (1984).
107. H. Tanaka, K. Nakanishi, and H. Touhara. *J. Chem. Phys.* **81**, 4065 (1984).
108. T. M. Bender and R. Pecora. *J. Phys. Chem.* **90**, 1700 (1986).
109. W. L. Jorgensen, J. Gao, and C. Ravimohan. *J. Phys. Chem.* **89**, 3470 (1985).
110. P. C. Senanayake, N. Gee, and G. R. Freeman. *Can. J. Chem.* **65**, 2441 (1987).
111. Y. Maham and G. R. Freeman. *J. Phys. Chem.* **91**, 1561 (1987).
112. A. D'Aprano, D. Donato, E. Caponetti, and V. Agrigento. *J. Sol. Chem.* **8**, 793 (1979).
113. S. K. Garg and C. P. Smyth. *J. Phys. Chem.* **69**, 1294 (1965).
114. W. Dannhauser and A. F. Flueckinger. *Phys. Chem. Liq.* **2**, 37 (1970).
115. J. Barthel, K. Bachhuber, R. Buchner, and H. Hetzenauer. *Chem. Phys. Lett.* **165**, 369 (1990).
116. D. Bertolini, M. Cassettari, and G. Salvetti. *J. Chem. Phys.* **76**, 3285 (1982).
117. D. Bertolini, M. Cassettari, and G. Salvetti. *J. Chem. Phys.* **78**, 365 (1983).
118. H. Sumi and R. A. Marcus. *J. Chem. Phys.* **84**, 4272 (1986).
119. M. J. Weaver. *Chem. Rev.* **92**, 463 (1992).
120. G. V. Buxton, C. L. Greenstock, W. P. Helman, and A. B. Ross. *J. Phys. Chem. Ref. Data.* **17**, (1988).

121. A. J. Elliot, D. R. McCracken, G. V. Buxton, and N. D. Wood. *J. Chem. Soc. Faraday Trans.* **86**, 1539 (1990).
122. G. V. Buxton and S. R. Mackenzie. *J. Chem. Soc. Faraday Trans.* **88**, 2833 (1992).
123. M. Anbar, M. Bambenek, and A. B. Ross. Selected Specific Rates of Reactions of Transients from Water in Aqueous Solution. 1. Hydrated Electron. *Nat. Stand. Ref. Data Ser., Nat. Bur. Stand. (U.S.)* **43**, 1973.
124. E. J. Waston and S. Roy. Selected Specific Rates of Reactions of the Solvated Electron in Alcohols. *Nat. Stand. Ref. Data Ser., Nat. Bur. Stand. (U.S.)* **42**, 1972.
125. G. L. Bolton and G. R. Freeman. *J. Am. Chem. Soc.* **98**, 6825 (1976).
126. B. Hickel. *J. Phys. Chem.* **82**, 1005 (1978).
127. K. Okazaki and G. R. Freeman. *Can. J. Chem.* **56**, 2313 (1978).
128. A. M. Afanassiev, K. Okazaki, and G. R. Freeman. *J. Phys. Chem.* **83**, 1244 (1979).
129. A. M. Afanassiev, K. Okazaki, and G. R. Freeman. *Can. J. Chem.* **57**, 839 (1979).
130. Farhataziz, S. Kalachandra, and M. S. Tunuli. *J. Phys. Chem.* **88**, 3837 (1984).
131. M. S. Tunuli and Farhataziz. *J. Phys. Chem.* **90**, 6587 (1986).
132. M. A. Rauf, G. H. Stewart, and Farhataziz. *Radiat. Phys. Chem.* **26**, 433 (1985).
133. F. Barat, L. Gilles, B. Hickel, and L. Lesigne. *J. Phys. Chem.* **77**, 1711 (1973).
134. B. H. Milosavljevic and O. I. Micic. *J. Phys. Chem.* **82**, 1359 (1978).
135. H. A. Schwarz and P. S. Gill. *J. Phys. Chem.* **81**, 22 (1977).
136. Y. Maham and G. R. Freeman. *J. Phys. Chem.* **89**, 4347 (1985).
137. Y. Maham and G. R. Freeman. *Can. J. Chem.* **66**, 1706 (1988).
138. P. C. Senanayake and G. R. Freeman. *J. Phys. Chem.* **91**, 2123 (1987).

139. P. C. Senanayake and G. R. Freeman. *J. Chem. Phys.* **87**, 7007 (1987).
140. P. C. Senanayake and G. R. Freeman. *J. Phys. Chem.* **92**, 5142 (1988).
141. C. C. Lai and G. R. Freeman. *J. Phys. Chem.* **94**, 302 (1990).
142. C. C. Lai and G. R. Freeman. *J. Phys. Chem.* **94**, 4891 (1990).
143. S. A. Peiris and G. R. Freeman. *Can. J. Phys.* **68**, 940 (1990).
144. S. A. Peiris and G. R. Freeman. *Can. J. Chem.* **69**, 157 (1991).
145. S. A. Peiris and G. R. Freeman. *Can. J. Chem.* **69**, 884 (1991).
146. T. B. Kang and G. R. Freeman. *Can. J. Chem.* **71**, 1297 (1993).
147. M. D. Newton and N. Sutin. *Ann. Rev. Phys. Chem.* **35**, 437 (1984).
148. M. V. Smoluchowski. *Z. Phys. Chem.* **92**, 129 (1917).
149. R. Fürth (*Editor*). *A. Einstein's Investigations on the Theory of Brownian Movement*. Dover Publications, New York. 1956. p. 75. *Translation by A. D. Cowper of Z. Elektrochemie* **14**, 235 (1908).
150. P. Debye. *Trans. Electrochem. Soc.* **82**, 265 (1942).
151. R. Chen and G. R. Freeman. *Can. J. Chem.* **71**, 1303 (1993).
152. E. J. Hart and M. Anbar. *The Hydrated Electron*. Wiley-Interscience, New York. 1970.
153. G. L. Bolton, M. G. Robinson, and G. R. Freeman. *Can. J. Chem.* **54**, 1177 (1976).
154. P. Han and D. M. Bartels. *J. Phys. Chem.* **96**, 4899 (1992).
155. R. A. Marcus. *J. Chem. Phys.* **24**, 966 (1956).
156. A. Frost and R. G. Pearson. *Kinetics and Mechanism*. 2nd ed. John Wiley & Sons, New York. 1961.

Chapter Two^a

Ion Pairing of Ammonium Nitrate in Methanol?

I. Introduction

In a recent report (1) of the reactivities of lithium and ammonium nitrates in liquid methanol with solvated electrons, and with electrons prior to solvation, it was suggested that the association constant of ammonium ions with nitrate ions was much greater than that of lithium with nitrate:



with $K_1 \leq 0.0205 \text{ m}^3/\text{mol}$ (20.5M^{-1}) and $K_2 \gg 10 \text{ m}^3/\text{mol}$ (10^4M^{-1}) at room temperature. The salt concentrations used were within the range $100\text{-}1000 \text{ mol}/\text{m}^3$ ($0.1\text{-}1.0 \text{ M}$) in both cases. The enormous value of K_2 compared to K_1 seemed surprising to us, but relatively little is known about the behavior in concentrated solutions of salts in alcohols. An enormous value of K_2 in methanol would have several interesting implications for our embryonic understanding of solvation effects in different solvents, so we checked it by electrical conductance measurements.

^a A version of this chapter has been published. R. Chen and G. R. Freeman. *Journal of Physical Chemistry*. **96**, 7107 (1992).

II. Experimental Section

Methanol (Aldrich, 99.9%, Spectrophotometric grade, freshly opened bottle) and ammonium nitrate (Aldrich, 99.999%, opened bottle kept in a vacuum desiccator containing P₂O₅) were used without further purification. Solutions of 995, 123, and 38.0 mol/m³ were made by weighing nitrate into 100 mL or 25 mL volumetric flasks and adding appropriate amounts of methanol, with intermittent shaking of the flasks. Aliquots ≥ 2.7 mL, measured to ≤ 1%, of these solutions were diluted to obtain solutions ≥ 10.0 mol/m³, and the last was diluted further to obtain 1.08 mol/m³.

The conductance cells were Yellow Springs Instrument Co. model YSI3403, calibrated at 298.15 K using the secondary standard solution YSI3161. Temperature was controlled to ± 0.01 K, and conductances were measured when the specified temperature had been constant for 30 minutes.

The impedance bridge was General Radio Co. model 1608-A. The measurements were made at 1 kHz.

III. Results and Discussion

The conductance data are listed in Table 2-1.

The conductances measured at 283.28 to 328.21 K vary with the square root of the concentration (Figure 2-1) in the manner expected for strong electrolytes. The Debye-Hückel-Onsager equation (2) for the variation of conductivity Λ (S·m²/mol) with concentrations C (mol/m³) below about 100 mol/m³ is:

$$[2-3] \quad \Lambda = \Lambda_0 - (A + B\Lambda_0)C^{1/2} + DC$$

where Λ_0 is the conductivity per mole at infinite dilution, D is an empirical constant, and, for a 1,1-electrolyte,

$$[2-4] \quad A = \frac{\xi F^2}{3\pi\eta} \left(\frac{2}{\epsilon RT} \right)^{1/2}$$

and

$$[2-5] \quad B = \frac{0.586 \xi F^2}{6\pi} \left(\frac{1}{2\epsilon RT} \right)^{3/2}$$

where ξ is the protonic charge, F the Faraday, η the shear viscosity of the solvent, $\epsilon = \epsilon_0 \epsilon_r$ the electric permittivity of the solvent, R the gas constant, and all units are SI.

Preliminary calculations showed that the data up to 100 mol/m³ in Figure 2-1 fit equations [2-3] to [2-5] within a few percent. The empirical best-fit values of Λ_0 , (A + B Λ_0) and D are listed in Table 2-2. Values of (A + B Λ_0) calculated using equations [2-4] and [2-5] are listed for comparison; the average difference between the calculated and empirical values is $\pm 6\%$.

The Arrhenius temperature coefficient of Λ_0 is 8.5 kJ/mol, which is about RT (2.5 kJ/mol) lower than the Arrhenius temperature coefficient for shear viscosity (10.7 kJ/mol) (3) in this temperature range. The behavior is thus normal.

The value of Λ_0 at 298 K is within the experimental uncertainty of that (11.8 $\times 10^{-3}$) derived from data in Tables IV, 15 and IV, 22 of ref. 4.

At concentrations between 100 and 1000 mol/m³ the solution viscosity η increases appreciably, reaching about 1.5 η_0 at the highest concentration. While the viscosities of NH₄NO₃ solutions in methanol have not been reported, those of NH₄Cl up to 351 mol/m³ and of KI up to 603 mol/m³ at 298K have been (5). The viscosities of solutions of these two salts are virtually the same in the overlapping concentration range, so we assumed that the viscosities of NH₄NO₃ solutions would be similar. Extrapolation of the viscosities of the KI solutions to 1000 mol/m³, using the Jones and

Dole type plot (Figure 1 of ref. 5), gave $\eta/\eta_0 = 1.49$. The data are only available for 298K. We applied Walden's rule and multiplied each value of Λ at 298.29 K by the value of η at the same concentration, and examined the concentration dependence of $\Lambda\eta$ (Figure 2-2). The full curve in Figure 2-2 represents the equation of Onsager and Fuoss (6), normalized for the changing viscosity:

$$[2-6] \quad \Lambda\eta = \Lambda_0\eta - aC^{1/2} + bC - cC\log C$$

where the values of a , b , and c were adjusted to obtain the best over-all fit to the experimental data. The curve in Figure 2-2 corresponds to $\Lambda_0\eta = 6.34 \times 10^{-6} \text{ S}\cdot\text{m}^2\text{mol}^{-1}\text{Pa}\cdot\text{s}$, $a = 4.7 \times 10^{-7} \text{ S}\cdot\text{m}^{3.5}\text{mol}^{-1.5}\text{Pa}\cdot\text{s}$, $b = 3.9 \times 10^{-8} \text{ S}\cdot\text{m}^5\text{mol}^{-2}\text{Pa}\cdot\text{s}$, and $c = 9.2 \times 10^{-9} \text{ S}\cdot\text{m}^5\text{mol}^{-2} \text{ Pa}\cdot\text{s}$.

The first two terms on the right-hand side of equation [2-6] are equal to the Λ_0 and $(A + B\Lambda_0)C^{1/2}$ terms of equation [2-3] multiplied by η_0 . The value of D in equation [2-3] is greatly modified to the $(b - c \log C)$ in equation [2-6].

The suggestion (1) that $K_2 \gg 10 \text{ m}^3/\text{mol}$ is not correct. Even if the ion association constant were only $K_2 = 10 \text{ m}^3/\text{mol}$ the conductance would have followed the dashed curve in Figure 2-3. The conductance at $123 \text{ mol}/\text{m}^3$ would have been only 6% of the observed value.

The decrease of conductance with increasing concentration is adequately explained by the ion-atmosphere model of Milner (7), which was simplified eleven years later when Debye and Hückel introduced further approximations and greatly reduced the range of concentrations to which it applied (8). The conductance equation of Onsager and Fuoss (6) is an extension of the Milner-Debye-Hückel-Onsager equation [2-3]. The actual equation of Onsager and Fuoss was not normalized for viscosity, and one might argue that the changing viscosity can be accommodated in the adjustable parameters b and c of the un-normalized form of equation [2-6]. However, the equation is very crude; a more exact one would require a much greater understanding of the behavior of the liquid

state than presently exists. Even at the present level of approximation, the value of a in equation [2-6] should vary with concentration because the values of A and B in equations [2-4] and [2-5] depend on the values of η and ϵ , both of which change appreciably at high salt concentrations; at 1000 mol/m^3 $\eta \approx 1.5 \eta_0$ (5), and $\epsilon \approx 0.4 \epsilon^0$ (9), where η_0 and ϵ^0 refer to pure methanol. Equation [2-6] should be replaced by a functional.

High concentrations of ions in water and alcohols have larger effects on bulk properties than existing models accommodate (6, 9, 10). A new attack on the theory should be made by computer simulation.

The rate constant data of Duplâtre and Jonah has been re-interpreted elsewhere (11).

Table 2-1. Molar conductivity of ammonium nitrate in methanol

C (mol/m ³)	Λ (10 ⁻³ S·m ² /mol) ^a			
1.08	8.71	10.8	12.4	14.4
10.0	7.57	9.10	10.7	12.3
38.0	6.39	7.59	8.94	10.2
61.5	5.63	6.68	7.84	8.93
123.	4.90	5.83	6.84	7.76
199.	4.52	5.47	6.29	7.22
398.	3.71	4.51	5.22	6.00
597.	3.23	3.95	4.59	5.29
796.	2.89	3.54	4.12	4.75
995.	2.59	3.16	3.71	4.29

a. T(K) for columns 2 to 5 were, respectively, 283.28, 298.29, 313.53, and 328.21.

Table 2-2. Parameter values for curves in Figure 2-1.

T (K)	283.28	298.29	313.53	328.21
η (10^{-4} Pa·s) ^a	7.0	5.45	4.54	3.75
ϵ_r ^b	35.6	32.5	29.6	27.2
Λ_0 (extrap) (10^{-3} S·m ² /mol) ^c	9.3	11.6	13.3	15.5
A (10^{-4} S·m ^{3.5} mol ^{-1.5})	3.71	4.86	5.96	7.37
B (10^{-2} m ^{1.5} mol ^{-0.5})	2.57	2.72	2.90	3.08
10^4 (A + B Λ_0) _{calc}	6.1	8.0	9.8	12.1
10^4 (A + B Λ_0) _{emp} ^d	6.0	8.7	9.1	11.2
D _{emp} (10^{-5} S·m ⁵ /mol ²) ^d	1.8	3.1	3.0	3.8

a. Ref. 3.

b. Interpolated from a combined plot of data from (i) F. Buckley and A. A. Maryott. Tables of Dielectric Dispersion Data for Pure Liquids and Dilute Solutions. NBS Circular 589. Washington, D.C. 1958. p. 7; (ii) Y. Y. Akhadov. Dielectric Properties of Binary Solutions. Pergamon, Oxford. 1980. p. 273.

c. Extrapolated with the empirically best-fit equation.

d. Empirical best-fit values for equation [2-3].

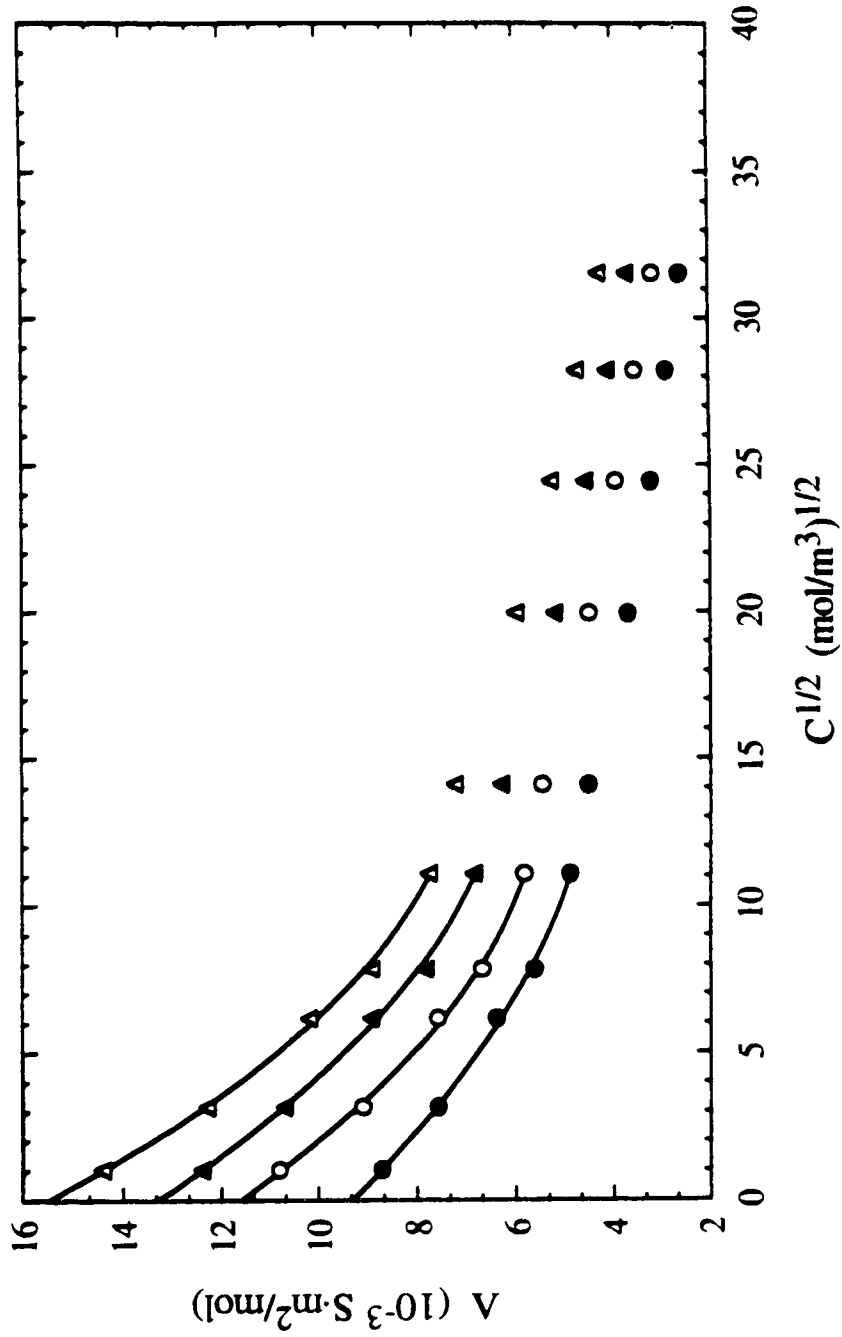


Figure 2-1. Molar conductivity Λ of ammonium nitrate in methanol plotted against $(\text{concentration})^{0.5}$.
T(K): ●, 283.28; ○, 298.29; ▲, 313.53 K; △, 328.21. The full curves were calculated from equation [2-3] and the empirical constants in Table 2-2.

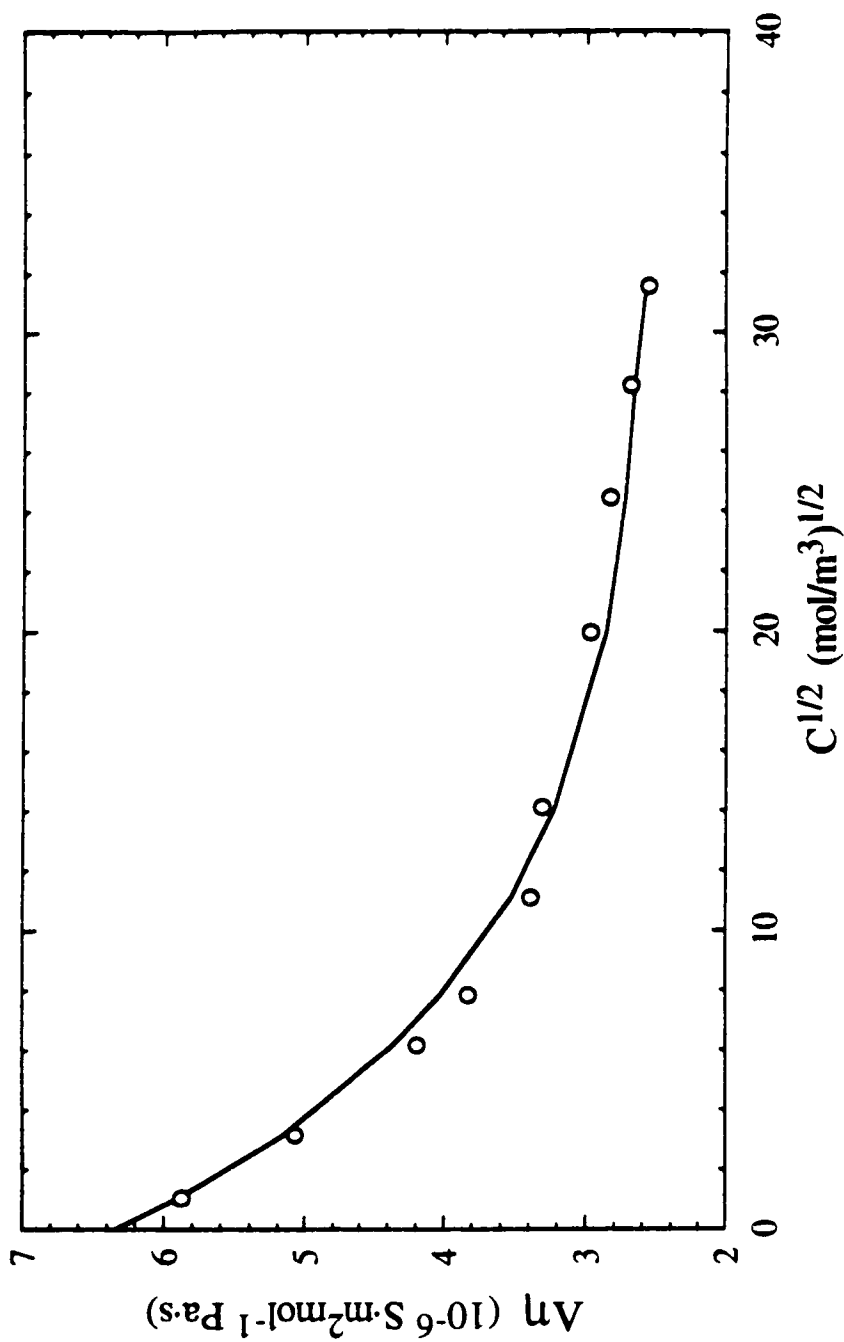


Figure 2-2. Plot of the Walden product $A\eta$ against (concentration)^{0.5}. $T = 298.29\text{K}$. The curve represents equation [2-6].

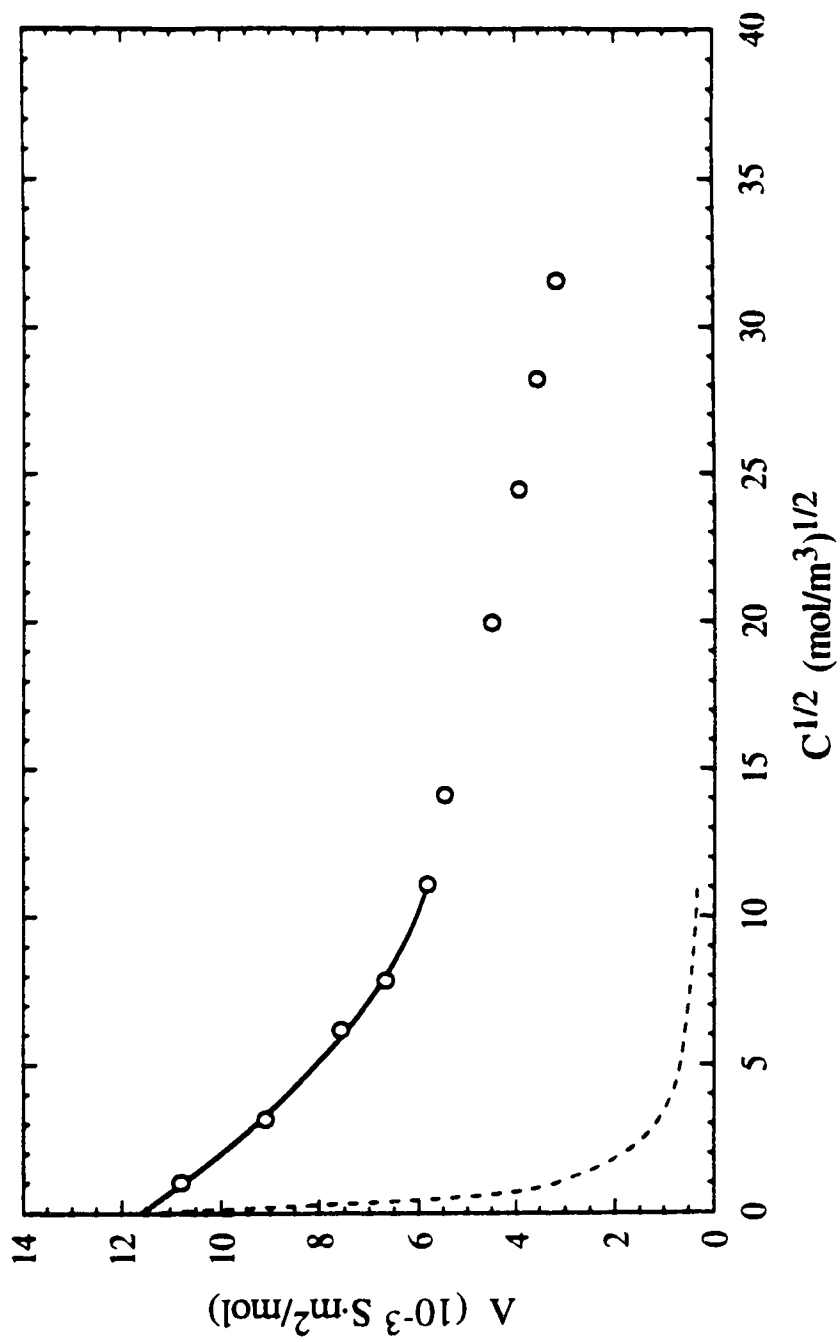


Figure 2-3. Comparison of the measured molar conductivities at 298.29 K with those that would be expected if $K_2 = 10 \text{ m}^3/\text{mol}$ (dashed line).

References:

1. G. Duplâtre and C.D. Jonah. *J. Phys. Chem.* **95**, 897 (1991).
2. P. W. Atkins. *Physical Chemistry*. 4th ed. Freeman, New York. 1990. pp. 760-1, note that B requires F^2 .
3. R. C. Weast (*Editor*). *Handbook of Chemistry and Physics*. 70th ed. CRC Press, Boca Raton, FL. 1989. p. F-43.
4. B. E. Conway. *Electrochemical Data*. Elsevier, Amsterdam. 1952. pp. 155 and 162.
5. G. Jones and H. J. Fornwalt. *J. Am. Chem. Soc.* **57**, 2041 (1935).
6. A. L. Horvath (*Editor*). *Handbook of Aqueous Electrolyte Solutions*. Wiley, New York. 1985. p. 252.
7. S. R. Milner. *Philos. Mag.* (a) **23**, 551 (1912); (b) **25**, 742 (1913).
8. P. Debye and E. Hückel. *Phys. Z.* **24**, 185, 305, 335 (1923).
9. J. B. Hasted and G. W. Roderick. *J. Chem. Phys.* **29**, 17 (1958).
10. N. E. Hill, W. E. Vaughan, A. H. Price, and M. Davies. *Dielectric Properties and Molecular Behavior*. van Nostrand, New York. 1969. pp. 348-354.
11. T. B. Kang and G. R. Freeman. *Can. J. Chem.* **71**, 1297 (1993).

Chapter Three^a

Solvent Effects on the Reactivity of Solvated Electrons with Ammonium and Nitrate Ions in 1-Butanol/Water Solvents

I. Introduction

In the present work we report solvent effects on the rate of reaction of solvated electrons with solvated ions, and on the transport (conductance) of ions in solution. Rates of reaction between two species depend on the coming together (transport) of the species, and on the probability that they react when they encounter each other. Division of the reaction rate constant by the ionic conductance in the same solvent partially separates the solvent effect on transport from that on the probability of reaction of the encounter pair. We used 1-butanol/water binary solvents over the entire range of miscibility (1), and the newly discovered "switchover" reactant, ammonium nitrate (2).

Alcohols (3) and alcohol binary solvents (4, 5) have a wide range of physical and solvation properties (6, 7), so they are excellent media in which to study solvent effects on reaction kinetics.

^a A version of this chapter has been published. R. Chen and G. R. Freeman. *Canadian Journal of Chemistry*. **71**, 1303 (1993).

II. Experimental Section

A. *Materials*

All chemicals and 1-butanol were from Aldrich Chemical Co. Lithium nitrate (99.999%), ammonium nitrate (99.999%), lithium perchlorate (reagent grade), and ammonium perchlorate (99.8%) were used as received; after opening a fresh bottle, it was stored in a vacuum desiccator that contained P₂O₅ powder. 1-Butanol (spectrometric grade, 99.5%, gold label) was dried for 1 week on Davison Molecular Sieves (3Å), then treated for one day under ultra high pure argon (99.999%, Liquid Carbonic Canada Ltd.) with sodium borohydride (2 g/L) at 330 K. The alcohol was then fractionally distilled under argon, through an 80 x 2.3 cm column packed with glass helices, discarding the first 20% and last 40%. The middle 40% portion was collected and stored in a flask under argon. The water content, measured by Karl-Fisher titration, was 0.05 mol%. The solvated electron half-life after a 100 ns pulse of 340 fJ electrons (4 J/kg) at 298 K was about 10 μs.

Water was purified in a Barnstead Nanopure II ion exchange system. The solvated electron half-life after a 100 ns pulse of 2.1 MeV electrons was about 12 μs.

B. *Techniques*

The methods of sample preparation and kinetic optical absorption spectroscopy were the same as those in the preceding work (2).

Electrical conductivity measurements were done with an impedance bridge (model 1608-A, General Radio Co.) at 1 kHz. Most of the time the conductance mode (G_p) was used. For conductances < 0.6 μS, the bridge was set to one of the capacitance modes (C_p) and the conductance was calculated from the capacitance data. The conductance cells were obtained from Yellow Springs Instruments (Model YSI3403),

and calibrated at 298.15 K using the secondary standard solution YSI1361. Temperature was controlled to within ± 0.01 K at 273 K, and ± 0.02 K at 344 K. Conductances were measured when the specified temperature had been constant for 30 minutes. The molar conductance (Λ) was obtained from the plot of specific conductance against solute concentration.

III. Results and Discussion

A. Physical Properties

1-Butanol is not completely miscible with water (8). The rate constants were measured over the miscible range. The following mol% water were used: 0, 10.0, 20.0, 35.0, 45.0, 99.0, and 100.0. The values of viscosities for the mixed solvents were obtained from ref. 1. The values of relative permittivities for the mixed solvents were obtained from ref. 9. However, only data in the range of 0-23 mol% water were available, so we use those for iso-butanol/water mixed solvents (10) as an approximation for other compositions.

B. Rate Constants

Arrhenius plots of k_2 for LiNO_3 , NH_4NO_3 , and NH_4ClO_4 in mixed solvents are given in Figures 3-1 to 3-3. The mol% of water represented by the symbols in these Figures are shown in Table 3-1. Due to the low solubility of NH_4ClO_4 in solvents of 0 and 10 mol% water, its k_2 was not measured at these compositions.

For the reaction of e_s^- with $\text{NH}_{4,s}^+$ in NH_4ClO_4 solutions at 100 and 99 mol% water, the equilibrium $\text{NH}_{4,s}^+ \rightleftharpoons \text{NH}_3 + \text{H}_s^+$ affects the measured rate constants. The value of k_2 for $\text{NH}_{4,s}^+$ in water is $\sim 10^{-4}$ times smaller than that for H_s^+ , so a small amount of dissociation of NH_4^+ causes a significant increase in the observed rate of

reaction of e_s^- . The concentration of H_s^+ when $[NH_{4,s}^+] = 10\text{-}100 \text{ mol/m}^3$ is $[H_s^+] \approx \sqrt{K_a [NH_{4,s}^+]}$, where K_a is the dissociation constant. Values of K_a in water at different temperatures (11) are listed in Table 3-2. Values of K_a in the 99 mol% H_2O mixed solvent are not available, so we used those for water as an approximation. The values of $k_2(e_s^- + NH_{4,s}^+)$ were calculated from the slopes of plots of $(k_{obs} - k_2' [H_s^+])$ against $[NH_{4,s}^+]$, where k_2' is the rate constant for the reaction of e_s^- with H_s^+ in water (5).

In alcohol solvent we have the following equilibrium: $NH_{4,s}^+ + BuOH \rightleftharpoons NH_3 + BuOH_{2,s}^+$. Values of K_a for 1-BuOH/ H_2O are not available, but those for methanol/water and ethanol/water have been reported (12a); K_a in pure ethanol is about 6 times larger than that in pure water (12b). In the alcohol-rich region k_{obs} is $> 1 \times 10^5/s$ at 298 K for the concentration range of $[NH_{4,s}^+] = (0.02\text{-}0.2) \text{ mol/m}^3$. Based on K_a in ethanol, the estimated $k_2'[H_s^+]$ is $< 10^4/s$ for the range of $[NH_{4,s}^+]$ we used. Therefore, the influence of $[H_s^+]$ on k_{obs} is negligible and the values of $k_2(e_s^- + NH_{4,s}^+)$ were directly calculated from the slopes of plots of k_{obs} against $[NH_{4,s}^+]$.

The solvent composition dependences of k_2 at 298 K are shown in Figure 3-4. In the water-rich region the reaction of e_s^- with $NH_{4,s}^+$ is very slow ($k_2 = 1.5 \times 10^3 \text{ m}^3/\text{mol}\cdot\text{s}$ in water, which agrees with a recently reported value (13)). However, in the alcohol-rich region, the reaction is fast ($k_2 \approx 10^7 \text{ m}^3/\text{mol}\cdot\text{s}$). Therefore, the observed rate constants with NH_4NO_3 are mainly due to $NO_{3,s}^-$ in the water-rich region and mainly due to $NH_{4,s}^+$ in the alcohol-rich region.

The rate constants at 297 K for the reaction of e_s^- with $LiCO_4$ are $1.0 \times 10^2 \text{ m}^3/\text{mol}\cdot\text{s}$ in water, and $< 1.0 \times 10^2 \text{ m}^3/\text{mol}\cdot\text{s}$ in 1-butanol, so these ions did not contribute appreciably to the measured e_s^- reaction rates in the other solutions.

In models of the kinetics of chemical reactions in solution, the solvent is generally assumed to be a uniform continuum, and two effects determine how fast the

reaction will be (14). Foremost is the intrinsic rate at which the reaction occurs, which is a molecular-level quantity that requires a quantum or semiclassical theory for its evaluation. The other effect for bimolecular reaction rates is statistical and accounts for the probability of existence of adjacent reactive entities in solution. The Smoluchowski-Debye-Stokes-Einstein model is such an example (15-18). We here use it to examine the reactions of solvated electrons with ionic solutes. Once the effects of the bulk fluid are accounted for, the unexplained features are attributed to effects of the nonhomogeneous structure of the solvent.

For a diffusion-controlled reaction between species i and j (18):

$$[3-1] \quad k_2 = 4\pi N_A (D_i + D_j) \kappa R_r f$$

where 4π steradians indicates that all directions of approach of i and j lead to reaction, N_A is Avogadro's constant, D_i , and D_j (m^2/s) are the diffusion coefficients of i and j, R_r is the reaction radius of the reacting pair, and κ is the probability of reaction during one encounter. The factor f reflects the effect of coulombic interaction between the reactants on their probability of obtaining the closeness of approach at which reaction occurs (17),

$$[3-2] \quad f = \frac{U(R_r)}{k_B T} \left[\exp\left(\frac{U(R_r)}{k_B T}\right) - 1 \right]^{-1}$$

where, $U(R_r)$ is the potential energy of interaction between the reactants at distance R_r , k_B is Boltzmann's constant, and T is the absolute temperature.

The potential energy when S is an ion of charge $z\xi$ is given by:

$$[3-3] \quad U(R_r) = - \frac{z\xi^2}{4\pi\epsilon_0\epsilon_r R_r}$$

where $-\xi$ is the charge on the electron, ϵ_0 is the permittivity of vacuum, and ϵ_r is the relative permittivity of the solvent between the electron and the ion.

Values of f were calculated for a range of ϵ_r , using a value of R_r appropriate to each solute. The results for 298 K are shown in Figure 3-5. When the reactants attract

each other ($z = +1$) the value of f is >1 ; for repulsion ($z = -1$) f is <1 . The solvent composition dependences of k_2/f at 298 K are shown in Figure 3-6. For the reaction of ($e_s^- + NO_{3,s}^-$) the observed values of k_2 decrease monotonically with increasing alcohol content of the solvent (Figure 3-4). Removal of the coulombic interaction (k_2/f) reduces the apparent difference between the water-rich and alcohol-rich regions. Values of f at other temperatures were not calculated, because values of ϵ_r are not available.

The coulombic interaction does not explain the shape of the curve of $k_2(e_s^- + NH_{4,s}^+)$ against solvent composition (Figure 3-6). The diffusion coefficients and effective reaction radii (κR_r) also influence the reaction rates.

C. Electrical Conductivities

The diffusion coefficients in equation [3-1] are related to the molar electrical conductivities λ (S·m²/mol) of the respective ions (19):

$$[3-4] \quad D = \lambda k_B T / z_i^2 \xi^2 N_A \quad .$$

Combining equation [3-1] with [3-4] we get:

$$[3-5] \quad \kappa R_r = \frac{\xi^2}{4\pi k_B} \times \frac{k_2}{f T \left[\frac{\lambda_i}{z_i^2} + \lambda_e \right]}$$

$$= 1.48 \times 10^{-16} k_2 / f T \left[\left(\lambda_i / z_i^2 \right) + \lambda_e \right]$$

where λ_i and λ_e are the molar conductivities of the reactant ion and e_s^- , respectively.

The values of the individual ionic conductivities in the mixed solvents are not known, so we have used approximations based on measured salt conductances. In pure water at 298 K the ratios of the λ 's of e_s^- (20): $NH_{4,s}^+$ (21): $NO_{3,s}^-$ (21) are 2.59: 1.04: 1.00. The diffusion coefficients ($\propto \lambda_i / z_i^2$) are in the same ratios. Thus, diffusion of e_s^- dominates the relative motion of each reactant pair.

In water we have the following ratios: $[\lambda(e_s^-) + \lambda(NO_{3,s}^-)] / \Lambda_0(Li_s^+ + NO_{3,s}^-)$

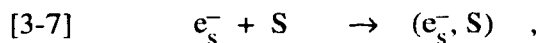
$$= 2.3 ; [\lambda(e_s^-) + \lambda(\text{NH}_{4,s}^+)] / \Lambda_0 (\text{NH}_{4,s}^+ + \text{ClO}_{4,s}^-) = 1.6 ; [\lambda(e_s^-) + \lambda(\text{NH}_{4,s}^+)] / \Lambda_0 (\text{NH}_{4,s}^+ + \text{NO}_{3,s}^-) = 1.7 ; \text{ and } [\lambda(e_s^-) + \lambda(\text{NO}_{3,s}^-)] / \Lambda_0 (\text{NH}_{4,s}^+ + \text{NO}_{3,s}^-) = 1.7.$$

Thus, equation [3-5] can be approximated as

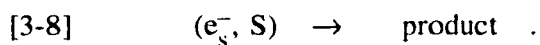
$$[3-6] \quad \kappa R_r \approx 1 \times 10^{-16} k_2 / fT \Lambda$$

where Λ is the molar conductivity in the diluted solutions.

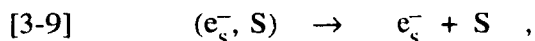
The solvent composition dependence of the molar conductivities Λ of the salts at 298 K, and the approximate values of κR_r at 298 K, are shown in Figures 3-7 and 3-8, respectively. The most interesting observation is that κR_r for the reaction $(e_s^- + \text{NH}_{4,s}^+)$ increases by a factor of more than 10^3 when the mixed solvent changes from the water-rich region to the alcohol-rich region. The activation energy of the reactions, E_2 , and the activation energy of the conductance, E_Λ , of the salts are plotted against solvent composition in Figures 3-9, and 3-10, respectively. For a diffusion controlled reaction, E_2 is essentially that for the mutual diffusion of e_s^- and S, which encounter each other at random,



and react,



In slow reactions most encounter pairs diffuse apart again,



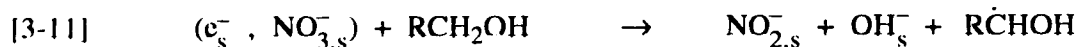
in which case the measured E_2 is mainly due to the activation energy of reaction [3-8].

D. *Reaction of $(e_s^- + \text{NO}_{3,s}^-)$*

E_Λ of the reactant salts is similar to the E_2 that might be expected for a diffusion controlled reaction. The values of E_2 for the reaction $(e_s^- + \text{NO}_{3,s}^-)$ increase with

increasing alcohol content, reaching a maximum in pure 1-butanol which is about three times larger than that in pure water (Figure 3-9). The values of E_A decrease with increasing alcohol content in the alcohol-rich region, and the magnitude of change is much smaller than that of E_2 . This agrees with the observation that the reaction ($e_s^- + NO_{3,s}^-$) is a nearly diffusion controlled reaction in water and gradually deviates away from it as the alcohol content is increased.

The reaction ($e_s^- + NO_{3,s}^-$) in alcohol solvents is complex. The proposed reaction sequence is (2, 5, 18, 22):



Alcohol molecules apparently participate chemically in the reaction. The change of k_2 for the reaction ($e_s^- + NO_{3,s}^-$) in different pure alcohol solvents is shown in Figure 3-11 as functions of solvent viscosity (23) and dielectric relaxation time (24, 25). As the length of the alkyl group in the primary alcohols is increased, the solvent fluidity *decreases* and k_2 *increases*. This inverse relationship between k_2 and solvent fluidity is attributed to the increasing duration of reactant encounter pairs as solvent fluidity decreases, and a greatly enhanced probability of reaction [3-11] with increasing encounter duration.

For secondary alcohol solvents, k_2 is 4-7 times larger than in their primary alcohol counterparts. This is attributed to the relatively reactive α -C-H group on the secondary alcohol.

E. Reaction of ($e_s^- + NH_{4,s}^+$)

The reaction ($e_s^- + NH_{4,s}^+$) is nearly diffusion controlled in the alcohol-rich region and much slower in the water-rich region. The value of kR_f in pure 1-butanol is

10^3 times larger than that in pure water at 298 K (Figure 3-8). In ammonium nitrate solution, E_2 represents the reaction ($e_s^- + NH_{4,s}^+$) in the alcohol-rich region and ($e_s^- + NO_{3,s}^-$) in the water-rich region. The value of E_2 for the reaction ($e_s^- + NH_{4,s}^+$) is larger in pure 1-butanol than in pure water (Figure 3-9).

The rate constants in water for several other cations, Ag_s^+ (4c), H_s^+ , Tl_s^+ , and Cu_s^{2+} (5), are all $(2.5-4.2) \times 10^7$ m³/mol·s, so the respective values of κR_r are much larger than that for $NH_{4,s}^+$ in water.

The solvation of ammonium ions in aqueous solution has been extensively studied by the method of apparent volume of individual ions (26); of entropies of dilution (27); of viscosities (28); of water activity (29); of NMR (30); and of IR and Raman spectra (31, 32). All these studies show that the ammonium ion in aqueous solution has properties similar in many respects to those of a water molecule (structure, volume, molecular weight, charge distribution; see Table 3-3). Its influence on water properties is usually negligible compared with the change caused by the other cations.

In a study of entropies of solution, Frank and Robinson stated that (27) "... the difference [between NaCl and NH_4Cl] is in the direction to be expected if the NH_4^+ exerts an additional stabilizing influence on the water structure by virtue of its tetrahedral shape and its ability to form hydrogen bonds". In a study of Raman spectra of aqueous electrolyte solution, Vollmar wrote (32) "... the electrostatic forces exerted on their nearest neighbors by H_2O and by NH_4^+ are probably very similar. In particular both H_2O and NH_4^+ form hydrogen bonds of about the same strength". As this unique property of solvated ammonium ions in water is responsible for many thermodynamic and spectroscopic properties of the aqueous solutions of ammonium salts, we believe that it is also responsible for the kinetic behavior of the solvated ammonium ion in water: Since $NH_{4,s}^+$ is symmetrically solvated in water, it has little tendency to accept an electron.

Relatively little is known about the behavior of electrolyte solutions in alcohols. Each alcohol molecule contains one -OH group which can bond with others to form a

chain or ring structure in the liquid, but not a three-dimensional structure like that of water. This would greatly influence the solvation structure of an ammonium ion in it. It is, therefore, reasonable to suggest that NH_4^+ is unsymmetrically solvated in an alcohol, and that this greatly facilitates electron attachment and subsequent decomposition, $\text{NH}_4 \rightarrow \text{H} + \text{NH}_3$. More thermodynamic and spectroscopic studies of electrolyte solutions in alcohols would be of great help for our embryonic understanding of solvation effects in different solvents. The rate parameters for the reactions in 1-butanol/water mixed solvents are summarized in Table 3-4.

F. Effective Radii for Mutual Diffusion

The Stokes radius, R_d , for mutual diffusion of ions in an electrolyte solution is given by (19):

$$\begin{aligned}
 [3-12] \quad R_d &= \left(\frac{1}{R_{d_i}} + \frac{1}{R_{d_j}} \right)^{-1} \\
 &= 8.2 \times 10^{-16} / \eta \left(\frac{\lambda_i}{z_i^2} + \frac{\lambda_j}{z_j^2} \right) .
 \end{aligned}$$

In our case, $i = e_s^-$, $j = \text{NH}_4^+$ or NO_3^- , so $|z_i| = |z_j| = 1$. As discussed before for κR_r , we use the approximation $(\lambda_{e_s^-} + \lambda_j) \approx 1.8 \Lambda$, so

$$[3-13] \quad R_d \approx 5 \times 10^{-16} / \eta \Lambda .$$

The solvent composition dependences of R_d are shown in Figure 3-12. Equation [3-12] shows that R_d emphasizes the more mobile ion. In the alcohol-rich region, R_d increases as the alcohol content increases. This is attributed to the larger size of the molecules that solvate the ions. The decrease of R_d as a small amount of alcohol is added to water indicates that the microscopic viscosity of the liquid in the vicinity of the ions is lower than the shear viscosity of the bulk liquid; the ions remain in the disordered water.

Table 3-1. Symbols in Figures 3-1 to 3-3.

Symbol	mol % H ₂ O	Symbol	mol % H ₂ O
+	0	■	45
Δ	10	○	99
▲	20	●	100
□	35		

Table 3-2. The values of pK_a for NH_{4,s}⁺ ⇌ NH₃ + H_s⁺ in water.^a

T(K)	pK _w	pK _b	pK _a
277.0	14.78	4.84	9.94
298.0	14.00	4.75	9.25
313.5	13.54	4.73	8.81
328.5	13.13		8.41
343.2			8.08

a. Values of pK_w and pK_b from ref. 11. pK_a = pK_w - pK_b. Values of pK_a at 328.5 and 343.2 K are extrapolated from a plot of pK_a against T.

Table 3-3. Properties^a of NH_4^+ and H_2O (liquid) compared

Molecule	Mass (g/mol)	Partial molar volume (ml/mol)	H-X-H angle (degree)	X-H distance (nm)
NH_4^+	18.05	18.0	109.5	0.103
H_2O	18.02	18.0	104.5	0.101

a. from ref. 32, p. 2241.

Table 3-4. Rate parameters for reactions of solvated electrons with solvated ions in 1-butanol/water mixed solvents at 298 K.

ϵ_r^a	η^b (10^{-3} Pa·s)	mol % H ₂ O	f^c	k_2 (10^6 m ³ /mol·s)	k_2/f (10^6 m ³ /mol·s)	E_2^d (kJ/mol)	Λ^e (10^{-3} S·m ² /mol)	E_A^f (kJ/mol)
$NO_{3,s}^-^g$								
78.5	0.89	100	0.78	9.2	12.	16.	10.8	15
75.8	1.09	99	0.77	7.7	10.	15.	10.4	17
19.8	2.92	45	0.34	1.2	3.5	21.	2.05	21
18.4	2.81	35	0.31	1.1	3.5	22.	1.92	20
17.8	2.70	20	0.29	0.72	2.5	30.	1.74	20
17.5	2.66	10	0.29	0.53	1.8	32.	1.52	19
17.4	2.60	0	0.28	0.19	0.68	43.	1.28	18
$NH_{4,s}^+, NO_{3,s}^-^h$								
		100	0.78	10.	13.	16.	14.8	18.
		99	0.77	8.0	10.	17.	13.4	18.
		45	i	5.2	4.6	32.	2.35	19.
		35		11.	6.9	30.	2.14	18.
		20		13.	6.2	27.	1.89	18.
		10		11.	4.8	26.	1.60	18.
		0		8.3	3.1	25.	1.37	20.
$NH_{4,s}^+^i$								
		100	1.40	1.5×10^{-3}	1.1×10^{-3}	20.	14.0	16.
		99	1.42	1.5×10^{-3}	1.1×10^{-3}	20.	12.6	16.
		45	3.01	4.6	1.5	33.	2.50	20.
		35	3.20	9.2	2.9	29.	2.47	20.
		20	3.29	12.	3.6	26.	2.30	20.

Table 3-4. continued

ϵ_r^a	η^b (10^{-3} Pa·s)	mol% H ₂ O	f^c	k_2 (10^6 m ³ /mol·s)	k_2/f (10^6 m ³ /mol·s)	E_2^d (kJ/mol)	Λ^e (10^{-3} S·m ² /mol)	E_Λ^f (kJ/mol)
<i>Li_s⁺, ClO_{4,s}⁻ ^j</i>								
		100		1.0×10^{-4}		20.		
		0		$<1. \times 10^{-4}$		—		

- a. Relative dielectric permittivity. Those for 99, 45, and 35 mol% are for iso-butanol/water mixtures. Data from refs. 9, 10.
- b. Viscosity. Data from ref. 1.
- c. Debye factor.
- d. Temperature coefficient at 298 K from Arrhenius plots of k_2 .
- e. Molar conductivity of the dilute solutions.
- f. Temperature coefficient at 298 K from Arrhenius plots of Λ .
- g. $\text{NO}_{3,s}^-$ in LiNO_3 solutions, concentrations 0.02-1.8 mol/m³.
- h. $\text{NH}_{4,s}^+$ and $\text{NO}_{3,s}^-$ in NH_4NO_3 solutions, concentrations 0.02-0.2 mol/m³. The value of f was calculated according to $z = -1(\text{NO}_{3,s}^-)$ in 100 and 99 mol % H₂O; in the other compositions, k_2/f was calculated from the proportionate contributions of each ion and the appropriate f .
- i. $\text{NH}_{4,s}^+$ in NH_4ClO_4 solutions, concentrations 1-140 mol/m³ for mol% H₂O of 100, 99; 0.02-0.2 for mol% H₂O of 45, 35, and 20.
- j. LiClO_4 concentrations 60-600 mol/m³ in water, and 90-440 mol/m³ in 1-butanol.

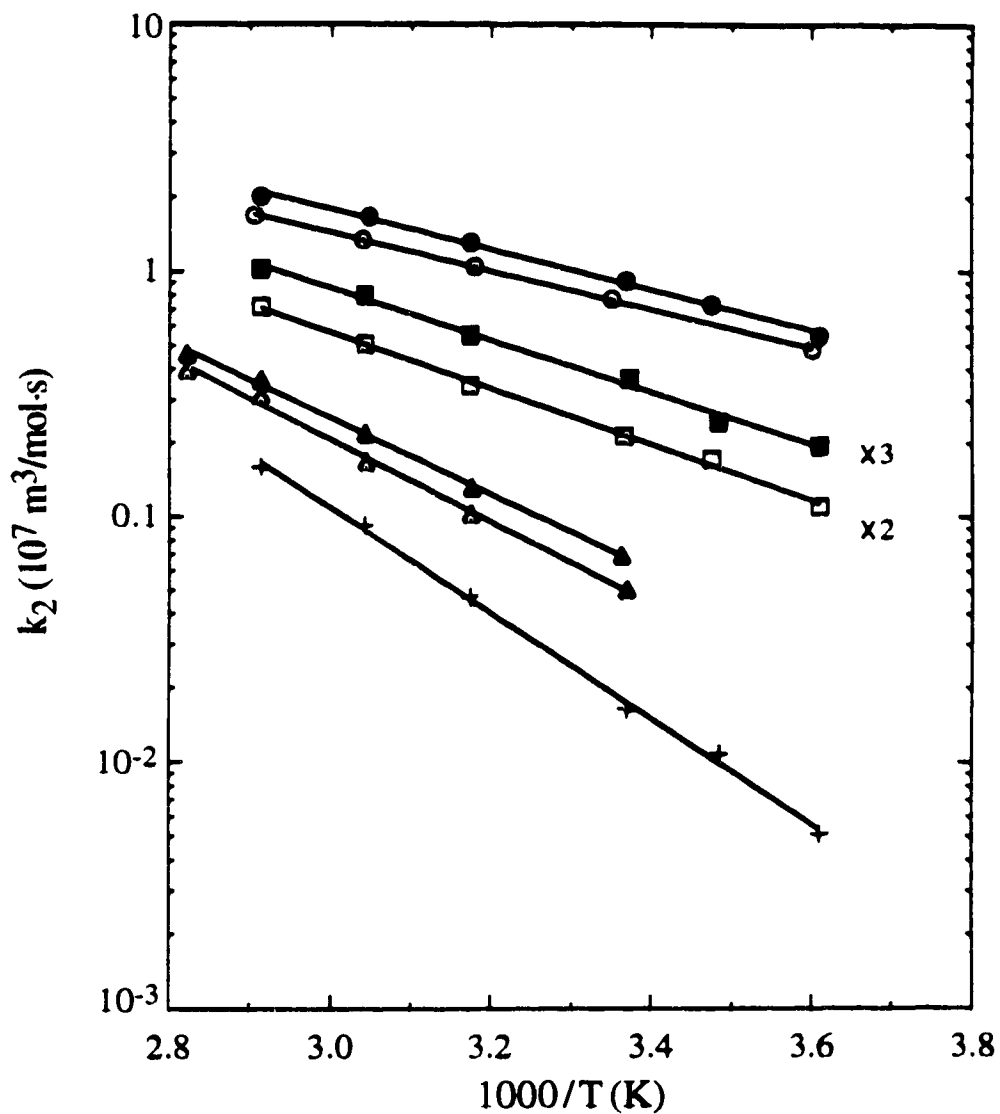


Figure 3-1. Arrhenius plots of k_2 of e^-_s reaction with LiNO_3 in 1-butanol/water mixed solvents. Symbols representing mol% water are given in Table 3-1. To separate the lines, some values of k_2 have been multiplied by the factors indicated.

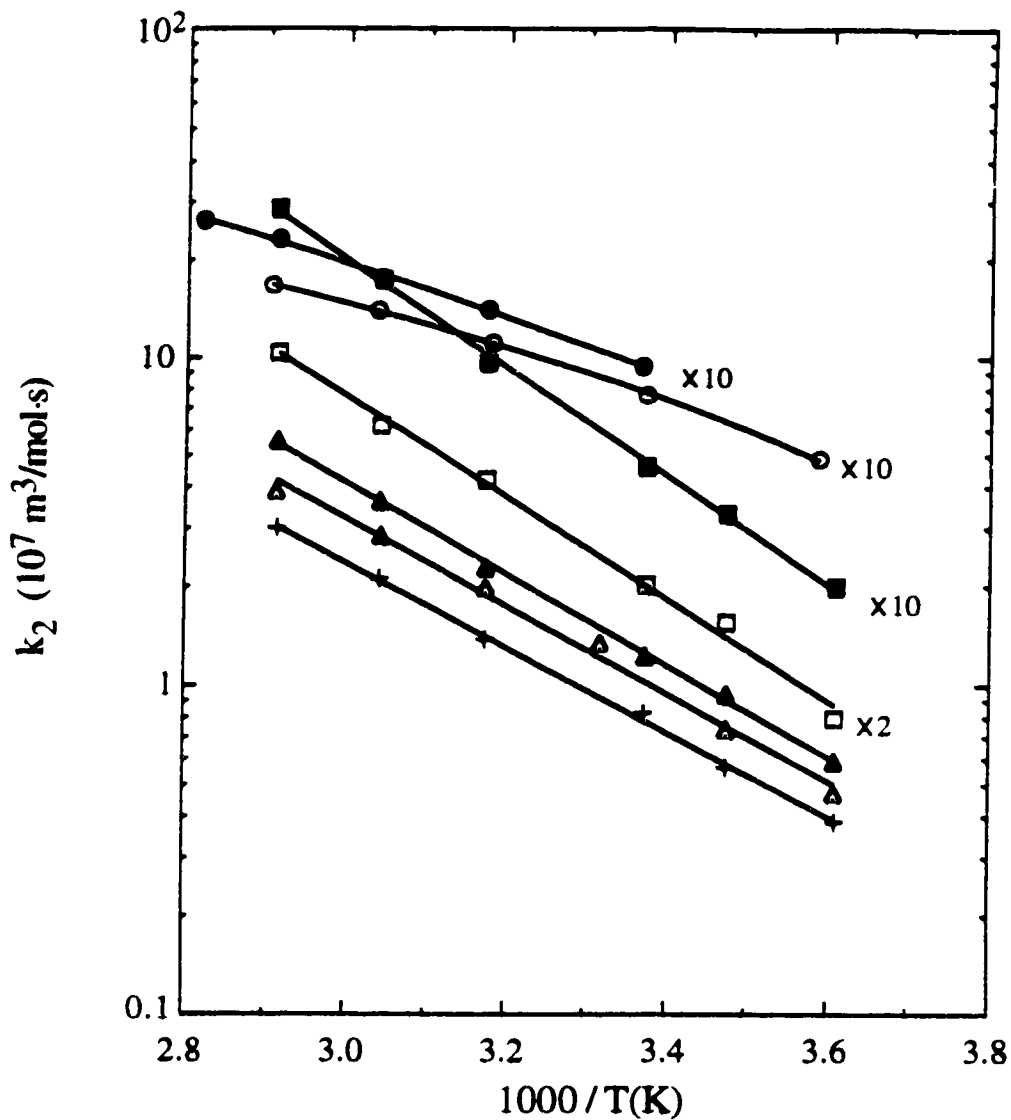


Figure 3-2. Arrhenius plots of k_2 of e_s^- reaction with NH_4NO_3 in 1-butanol/water mixed solvents. Symbols representing mol% water are given in Table 3-1. To separate the lines, some values of k_2 have been multiplied by the factors indicated.

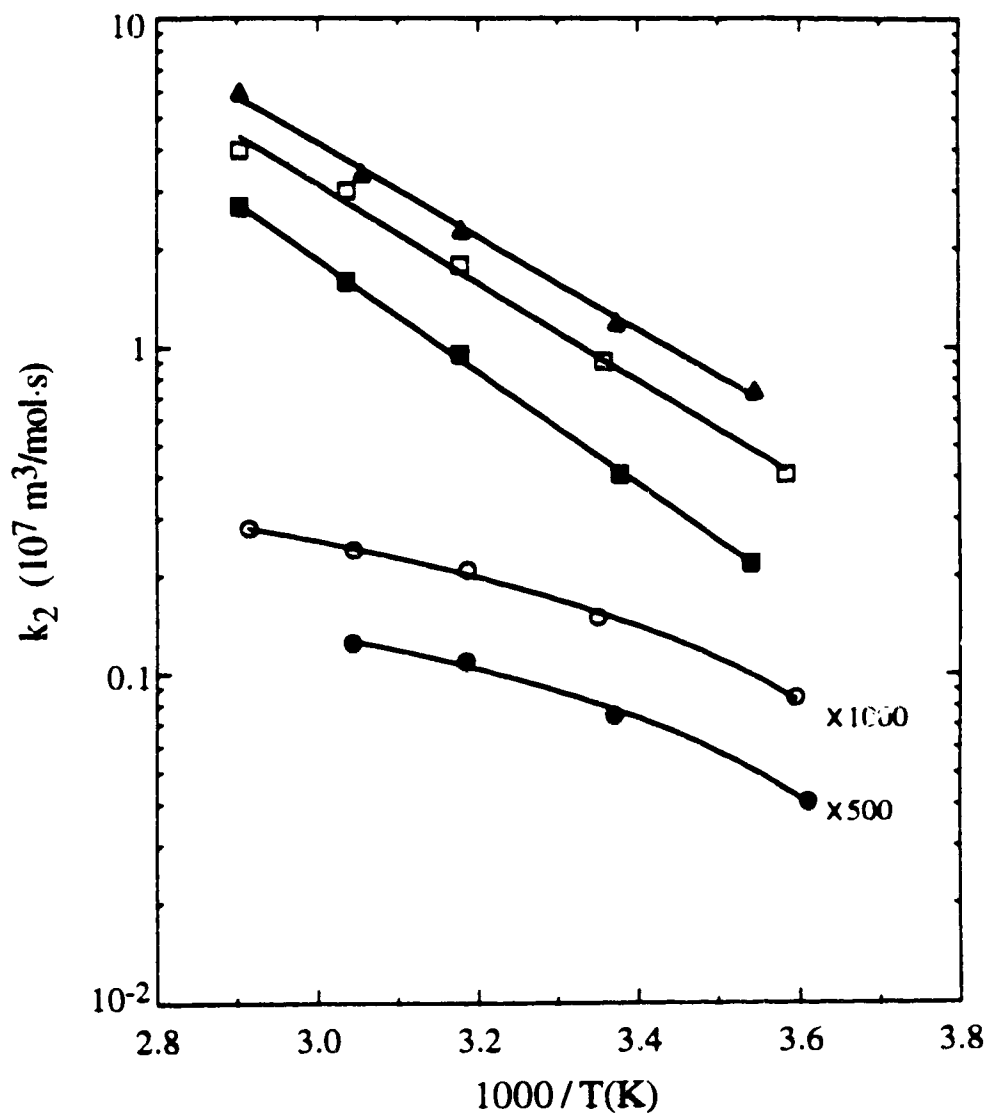


Figure 3-3. Arrhenius plots of k_2 of e_s^- reaction with NH_4ClO_4 in 1-butanol/water mixed solvents. Symbols representing mol% water are given in Table 3-1. To separate the lines, some values of k_2 have been multiplied by the factors indicated.

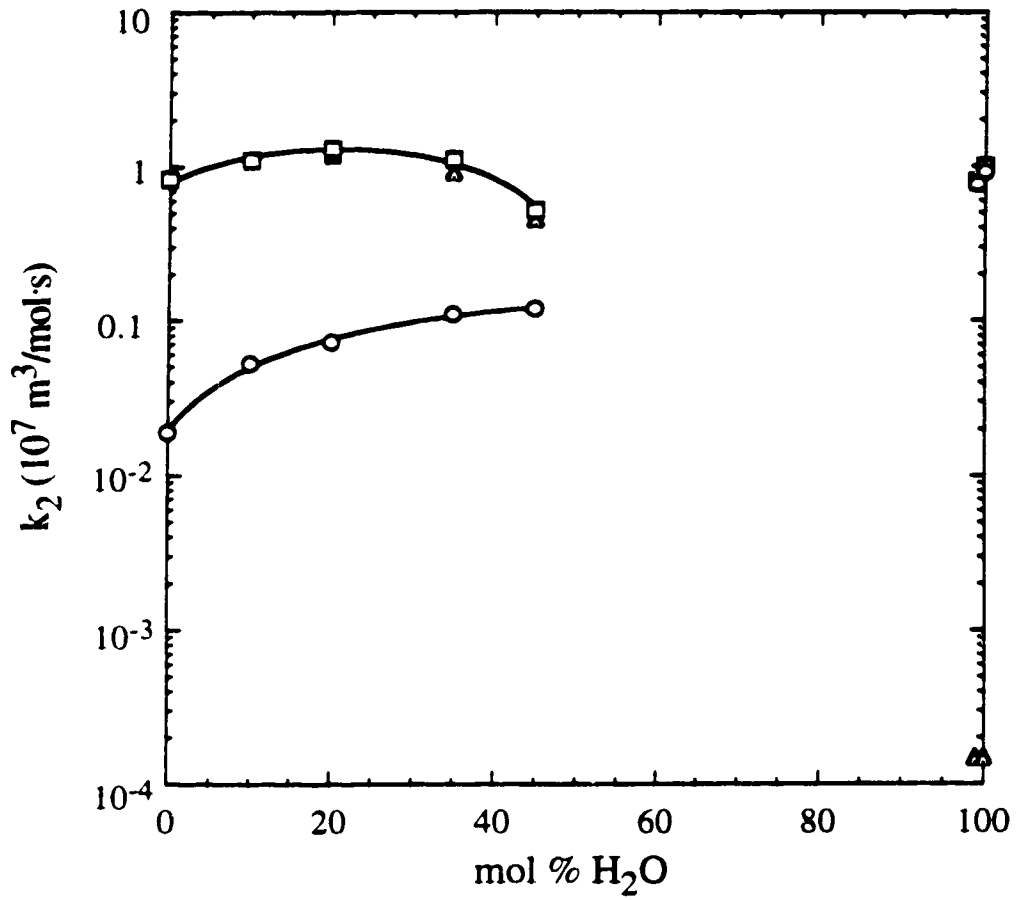


Figure 3-4. Solvent composition dependence of k_2 at 298 K in 1-butanol/water solvents. \circ LiNO_3 , \square NH_4NO_3 , \triangle NH_4ClO_4 .

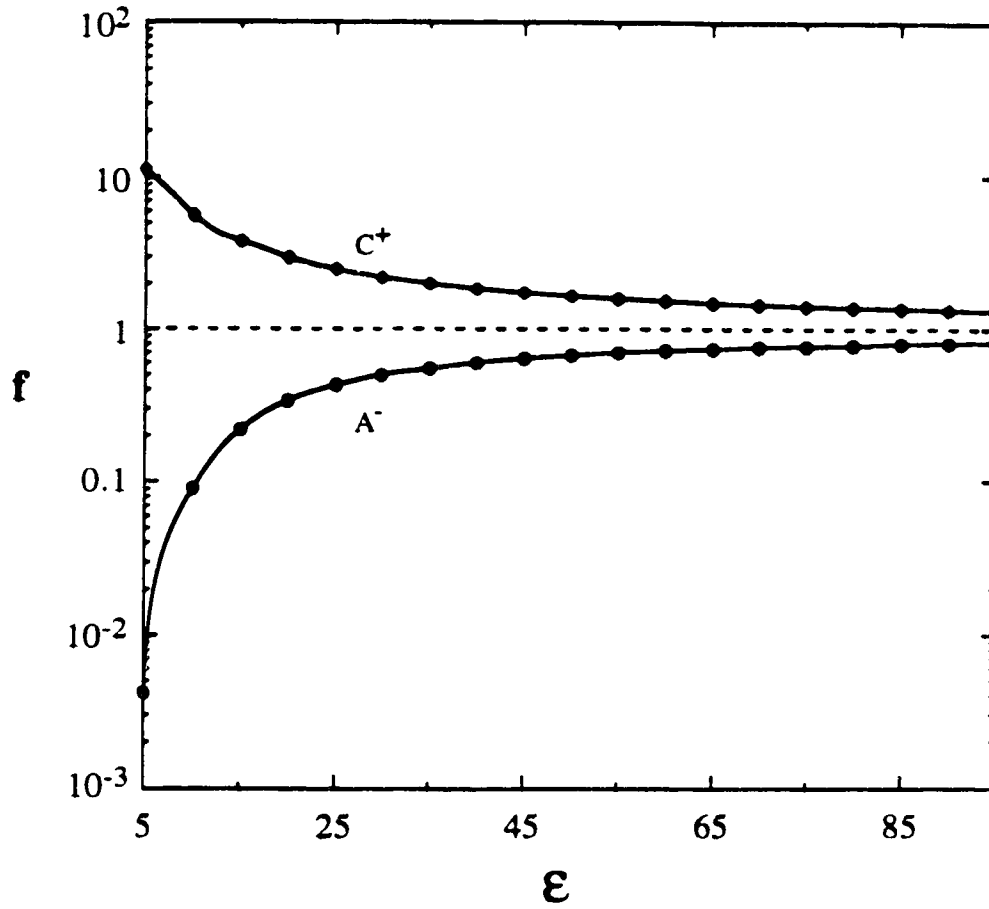


Figure 3-5. Dielectric permittivity dependence of the Debye factor f at 298 K. C^+ , ammonium ion, using $R_r = 1.0$ nm; A^- , nitrate ion, using $R_r = 1.5$ nm.

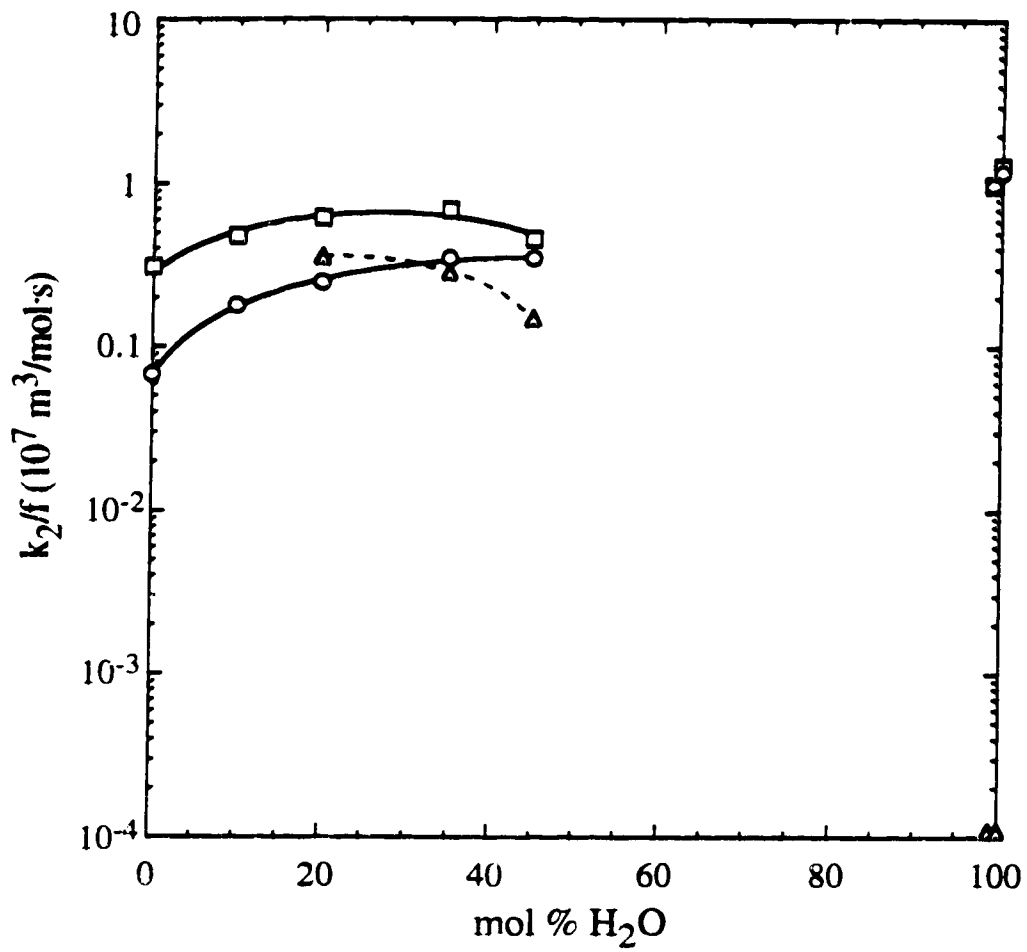


Figure 3-6. Solvent composition dependence of k_2/f at 298 K in 1-butanol/water mixed solvents. Symbols as in Figure 3-4.

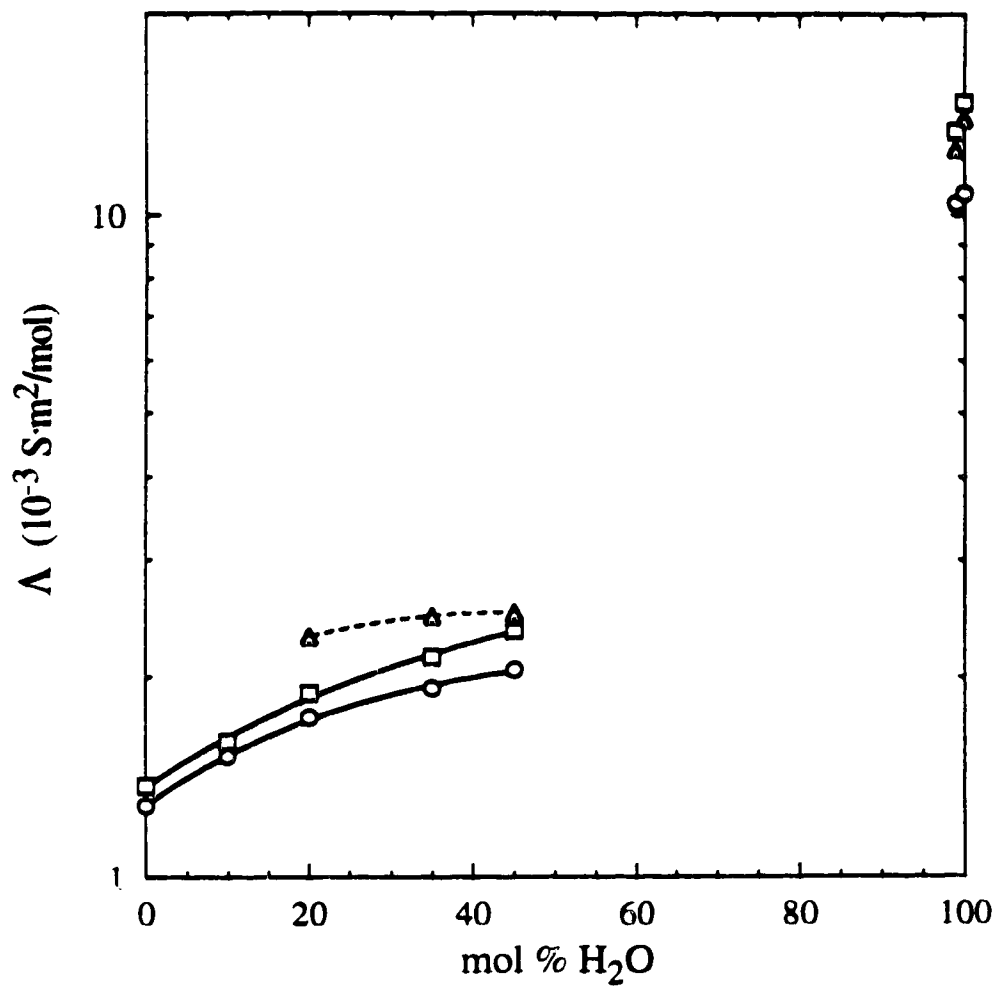


Figure 3-7. Solvent composition dependence of the molar conductivities Λ of salts at 298 K in 1-butanol/water mixed solvents. Symbols as in Figure 3-4.

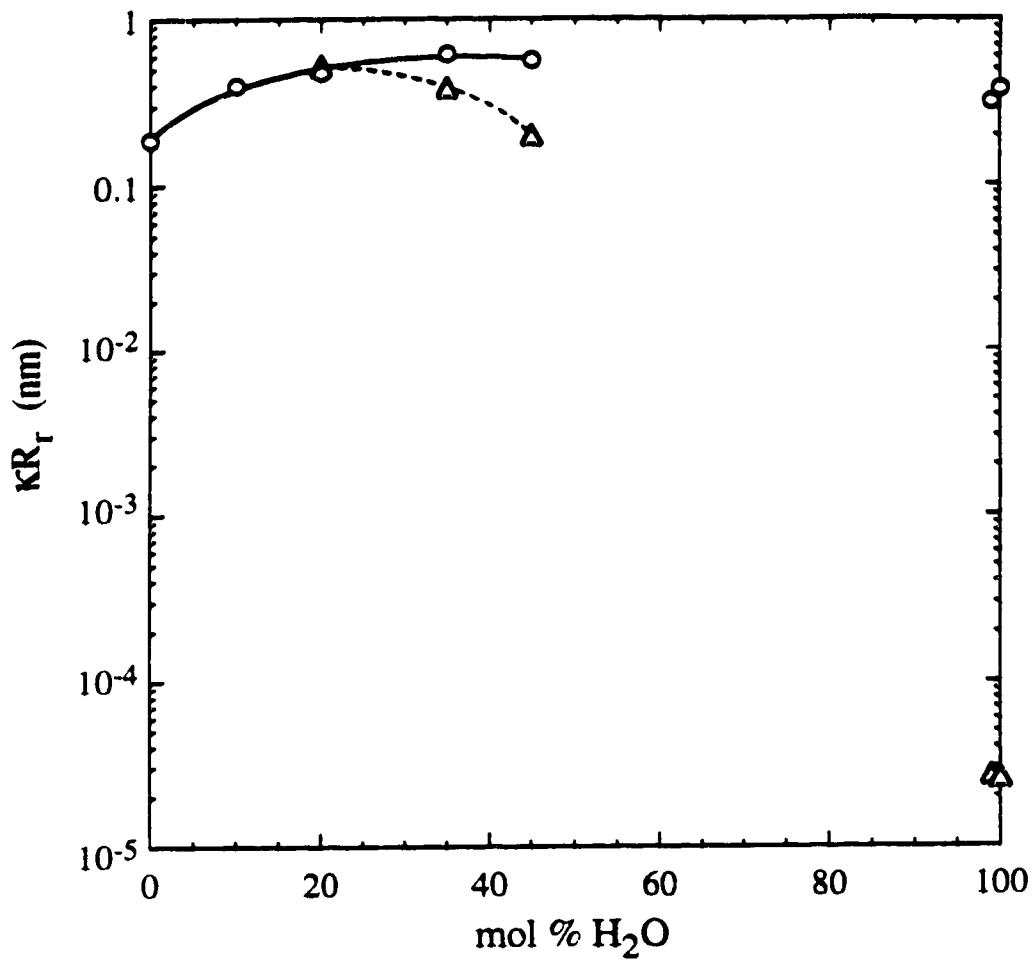


Figure 3-8. Solvent composition dependence of κR_r , equation [3-6], at 298 K in 1-butanol/water mixed solvents. Symbols as in Figure 3-4.

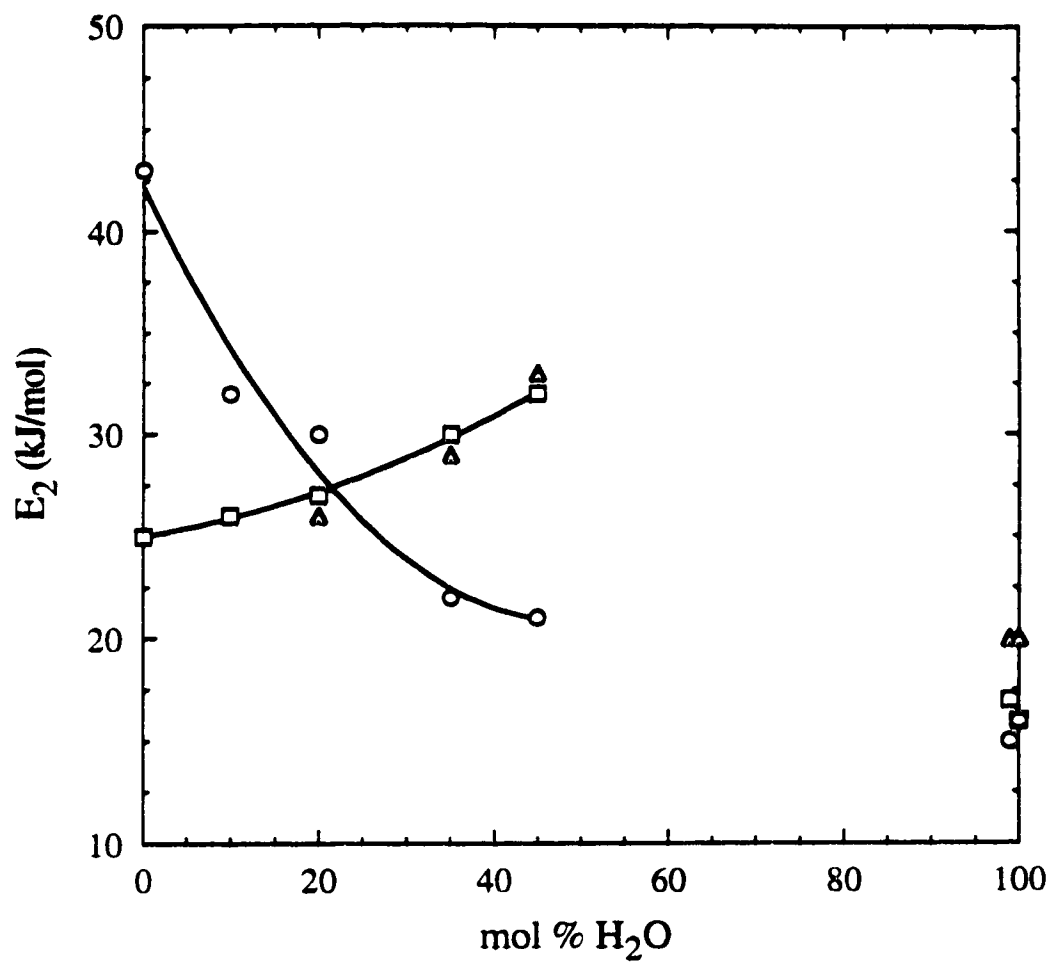


Figure 3-9. Solvent composition dependence of the activation energies E_2 near 298 K in 1-butanol/water mixed solvents. Symbols as in Figure 3-4.

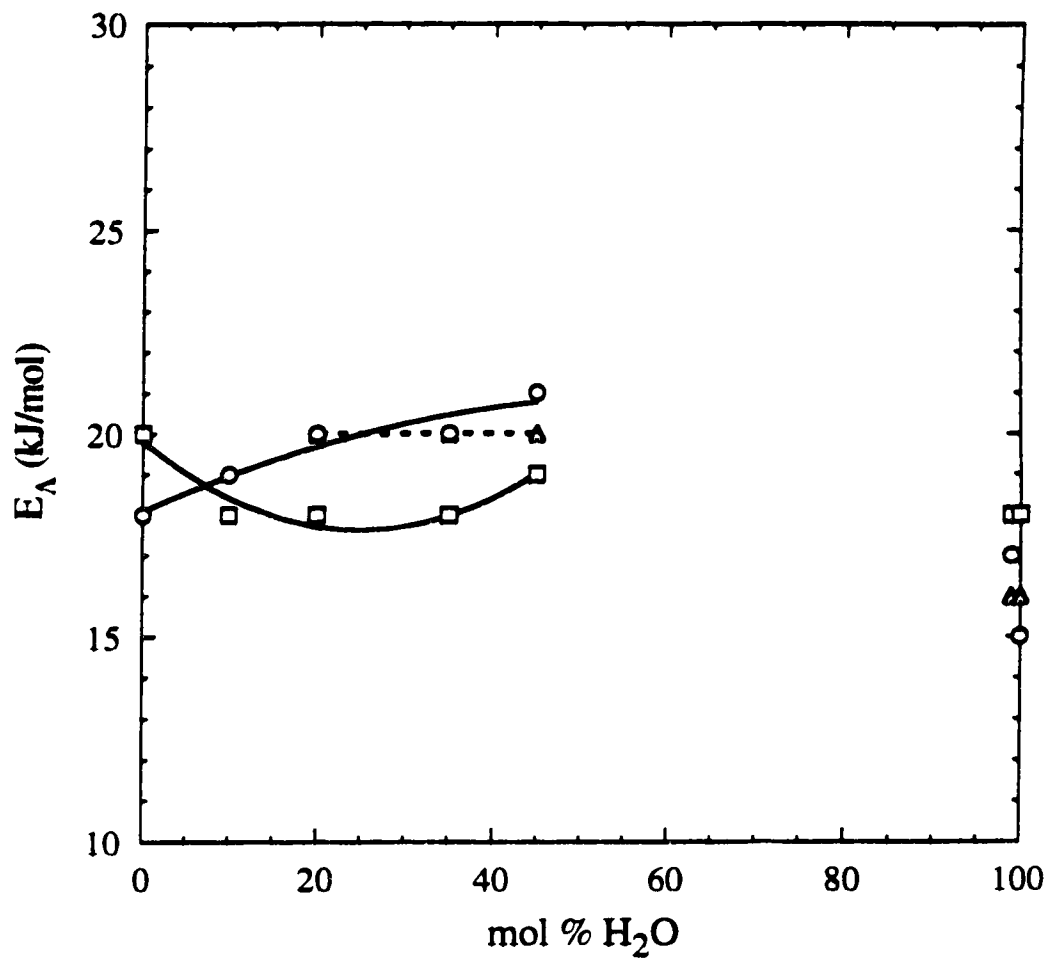


Figure 3-10. Solvent composition dependence of the activation energies E_A of conductance near 298 K in 1-butanol/water mixed solvents. Symbols as in Figure 3-4.

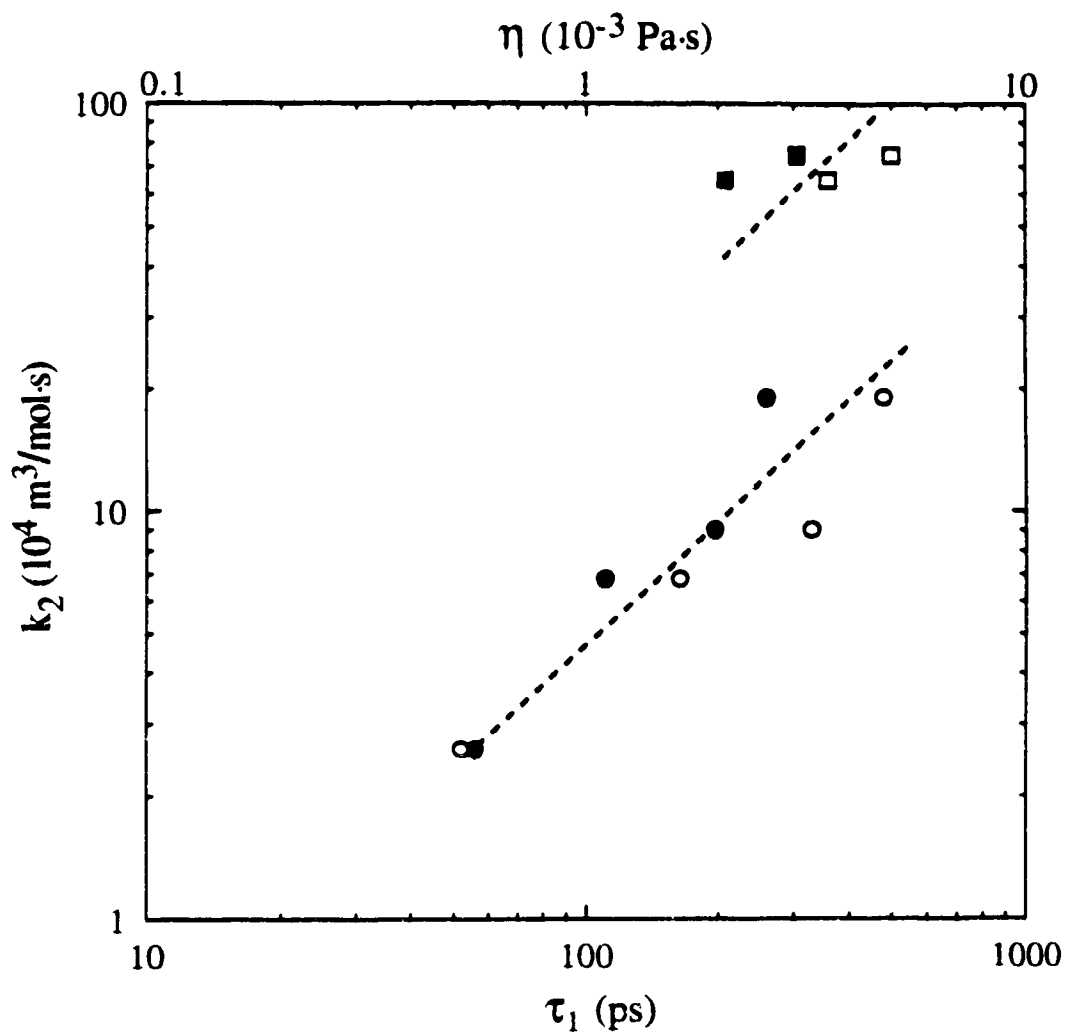


Figure 3-11. The values of k_2 for e_s^- reaction with nitrate ion in pure C_1 - C_4 alcohol solvents at 298 K, as functions of viscosity η (●, ■) and dielectric relaxation time τ_1 (○, □). ●, ○ primary alcohols; ■, □ secondary alcohols. Refs. for k_2 : C_1 and C_2 (22); C_3 (18); 1- C_4 (present work); 2- C_4 (5). Solvent properties: η (23); τ_1 (24, 25). The dashed lines have slopes = 1.0.

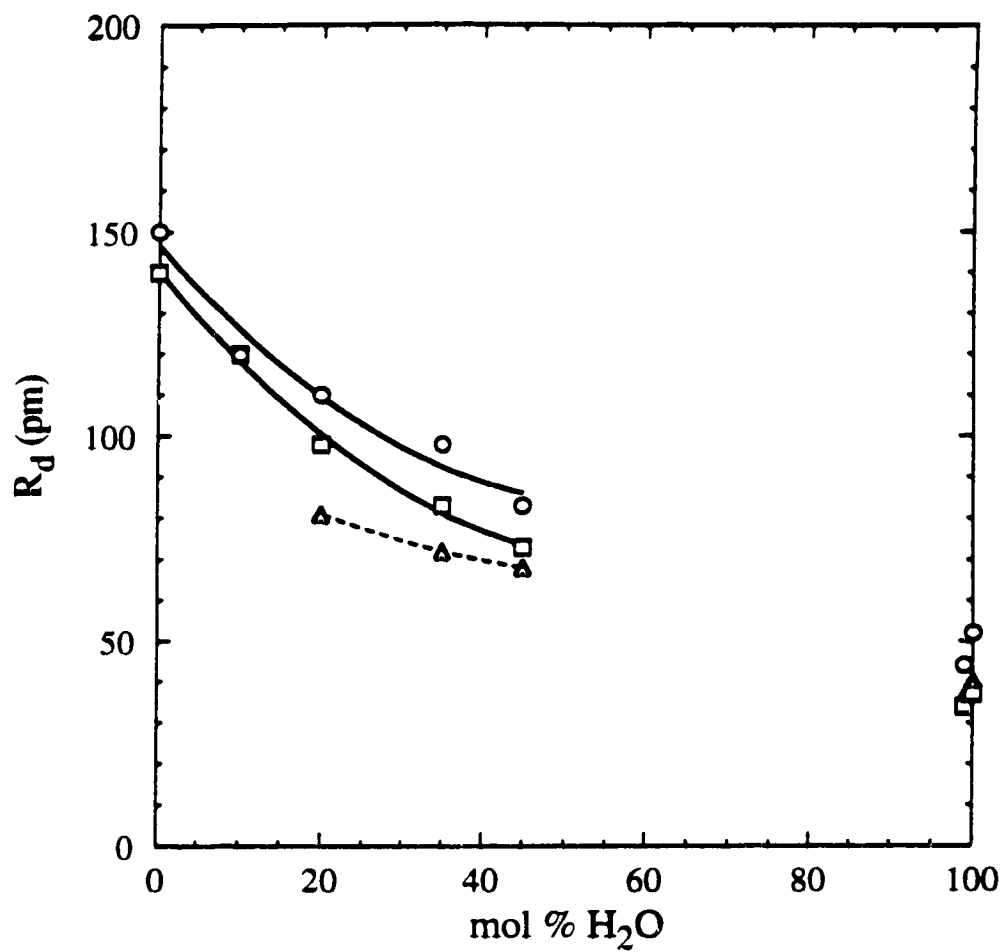


Figure 3-12. Solvent composition dependence of R_d at 298 K in 1-butanol/water mixed solvents. Symbols as in Figure 3-4.

References:

1. Y. Maham and G. R. Freeman. *J. Phys. Chem.* **91**, 1561 (1987).
2. T. B. Kang and G. R. Freeman. *Can. J. Chem.* **71**, 1297 (1993).
3. A. M. Afanassiev, K. Okazaki and G. R. Freeman. (a) *J. Phys. Chem.* **83**, 1244 (1979); (b) *Can. J. Chem.* **57**, 839 (1979).
4. P. C. Senanayake and G. R. Freeman. (a) *J. Chem. Phys.* **87**, 7007 (1987); (b) *J. Phys. Chem.* **91**, 2123 (1987); (c) *J. Phys. Chem.* **92**, 5142 (1988).
5. S. A. Peiris and G. R. Freeman. *Can. J. Chem.* **69**, 884 (1991).
6. A.-D. Leu, K. N. Jha and G. R. Freeman. *Can. J. Chem.* (a) **60**, 2342 (1982); (b) **61**, 1115 (1983).
7. K. M. Idriss-ali and G. R. Freeman. *Can. J. Chem.* **62**, 2217 (1984).
8. J. M. Sorensen and W. Arlt (*Editor*). *Liquid-Liquid Equilibrium Data Collection, DECHEMA Chem. Data Series*. Frankfurt. 1979. p. 237.
9. A. D'Aprano, D. Donato and E. Caponetti. *J. Solution Chem.* **8**, 135 (1979).
10. A. C. Brown and D. G. Ives. *J. Chem. Soc. II*, 1608 (1962);
11. R. C. Weast (*Editor*). *Handbook of Chemistry and Physics*. 70th ed. CRC Press, Boca Raton, FL. 1989. pp. D165-166.
12. (a) O. Popovych. *Anal. Chem.* **46**, 2009 (1974); (b) R. P. Bell. *Acids and Bases, Their Quantitative Behavior*. 2nd ed. Methuen, London. 1969. p. 27.
13. H. A. Schwarz. *J. Phys. Chem.* **95**, 6697 (1991).
14. J. Keizer. *J. Phys. Chem.* **86**, 5053 (1982).
15. M. V. Smoluchowski. *Z. Phys. Chem.* **92**, 129 (1917).
16. R. Fürth (*Editor*). *A. Einstein's Investigations on the Theory of Brownian Movement*. Dover Publications, New York. 1956. p. 75. *Translation by A. D. Cowper of Z. Elektrochemie* **14**, 235 (1908).

17. P. Debye. *Trans. Electrochem. Soc.* **82**, 265 (1942).
18. A. Peiris Sedigallage and G. R. Freeman. *Can. J. Phys.* **68**, 940 (1990).
19. P. W. Atkins. *Physical Chemistry*. 2nd ed. Freeman, New York. 1982. pp. 904-905.
20. K. H. Schmidt, P. Han and D. M. Bartels. *J. Phys. Chem.* **96**, 199 (1992).
21. A. L. Horvath (*Editor*). *Handbook of Aqueous Electrolyte Solutions*. Wiley, New York. 1985. pp. 262-263.
22. C. C. Lai and G. R. Freeman. *J. Phys. Chem.* **94**, 302 (1990).
23. R. W. Gallant. *Physical Properties of Hydrocarbons*. vol. 1. Gulf Publishing, Houston, TX. 1968.
24. J. Barthel, K. Bachhuber, R. Buchner and H. Hetzenauer. *Chem. Phys. Lett.* **165**, 369 (1990).
25. F. Buckley and A. A. Maryott. *Tables of Dielectric Dispersion Data for Pure Liquids and Dilute Solutions*. NBS Circular 589, Washington, D.C. 1958.
26. K. Fajans and O. Johnson. *J. Am. Chem. Soc.* **64**, 668 (1942).
27. H. S. Frank and A. L. Robinson. *J. Chem. Phys.* **8**, 933 (1940).
28. M. Kaminsky. *Discussions Faraday Soc.* **24**, 171 (1957).
29. Z. Libus and K. Chachulska. *J. Molecular Liquids* **46**, 53 (1990).
30. J. C. Hindman. *J. Chem. Phys.* **36**, 1000 (1962).
31. E. Ganz. *Z. Physik Chem.* **B35**, 1 (1937).
32. P. M. Vollmar. *J. Chem. Phys.* **39**, 2236 (1963).

Chapter Four^a

Solvent Effects on the Reactivity of Solvated Electrons with Ions in *Iso*-Butanol/Water Mixed Solvents

I. Introduction

The present article continues the studies of solvated electron reactions with ions in mixed solvents (1), in this case *iso*-butanol/water.

The reactions of solvated electrons (e_s^-) are usually electron transfer reactions (2). Possible exceptions are $e_s^- + ROH \rightarrow H + RO_s^-$ and $e_s^- + ROH_{2,s}^+ \rightarrow H + ROH$ in water and alcohols, where a proton from a solvating $-OH$ or $-OH_2^+$ group might transfer to the site of the electron (3). Proton transfer to the "cavity" of the electron site might avoid the work needed to create a new site for the H atom if the electron were to transfer first, followed by decomposition of the transient ROH^- or ROH_2 . The electron and proton are both elementary particles, but the former has a much smaller mass and, other things being equal, would have a larger transfer probability. Protons have larger mobilities than do electrons in water and alcohols, which means that the transport mechanisms are different.

For electron transfer between two species A and B in liquid media one may write:



^a A version of this chapter has been published. R. Chen, Y. Avotinsk, and G. R. Freeman. *Canadian Journal of Chemistry*. **72**, 1083 (1994).



where the subscript s signifies "solvated". The first step represents the random diffusion of two reactants, which by chance encounter each other and thereby form an [encounter pair], and which might diffuse apart again. The second step represents electron transfer within the encounter pair, which might involve thermal activation of the solvated species A_s and B_s in concert (4, 5).

The overall second order reaction rate constant k_2 may be represented by

$$[4-2] \quad \frac{1}{k_2} = \frac{1}{k_{1a}} + \frac{1}{K_{1a}k_{1b}}$$

$$= \frac{1}{k_d} + \frac{1}{K_{1a}k_r}$$

where $k_d = k_{1a}$ = diffusion controlled upper limit of the reaction rate constant, $K_{1a} = k_{1a}/k_{-1a}$, and $k_r = k_{1b}$ = rate of formation of products from encounter pairs. The value of K_{1a} is typically $10^{-5} \text{ m}^3/\text{mol}$.

We analyze large values of k_2 from the viewpoint of the Smoluchowski-Debye model (1, 6):

$$[4-3] \quad k_2 \approx k_d = 4 \pi N_A (D_A + D_B) R_f f$$

where N_A = Avogadro's constant, D_A and D_B are diffusion coefficients, R_f is the average center-to-center distance between A and B when electron transfer occurs, and f is a factor that accounts for the effect of the coulombic interaction between the reactants on their probability of diffusing to within a distance R_f of each other.

The relative contributions of k_d and k_r to limiting the observed reaction rate are reflected in the ratio k_2/k_d . If $k_2 \approx k_d$, then $K_{1a}k_r \gg k_d$; if $k_2 = 0.5 k_d$, then $K_{1a}k_r \approx k_d$; if $k_2 \ll k_d$, then $k_2 \approx K_{1a}k_r$. We have introduced the probability κ that reaction occurs during the lifetime of an encounter pair (1). Then,

$$[4-4] \quad k_2 = \kappa k_d = 4 \pi N_A (D_A + D_B) \kappa R_f f$$

For example, when $\kappa \leq 0.10$, then $K_{1a}k_r \leq k_d/9$. we evaluate solvent effects on k_2/f . Partial information is obtained about the diffusion coefficients of ionic reactants by measuring molar conductances of the reactant electrolyte solutions.

II. Experimental Section

A. Materials

Is-butanol (Aldrich, 99+%, Spectrophotometric Grade, Gold Label) was dried for one week on Davison Molecular Sieves (3Å), then treated for one day under ultra-pure argon (99.999%, Liquid Carbonic Canada Ltd.) with sodium borohydride (2 g/L) at 330 K. The alcohol was then fractionally distilled under argon, through an 80 × 2.3 cm column packed with glass helices, discarding the first 20% and last 40%. The middle 40% portion was collected and stored in a flask under argon. The water content, measured by Karl-Fisher titration, was 0.05 mol %. The solvated electron half-life after a 100 ns pulse of 340 fJ (2.1 MeV) electrons (4 J/kg) at 298 K was about 10 μs.

Singly distilled water was further purified in a Barnstead Nanopure II ion exchange system. The half-life of solvated electrons after a 100 ns pulse of 340 fJ electrons (4J/kg) was about 12 μs.

The following chemicals were obtained from Aldrich: lithium nitrate (99.999%, gold label), ammonium nitrate (99.999%), ammonium perchlorate (99.8%), lithium perchlorate (reagent grade), copper(II) perchlorate (98%, reagent grade), and aluminum (III) perchlorate (98%, reagent grade). Silver perchlorate (reagent grade) was from Strem. After opening a fresh bottle, it was stored in a vacuum desiccator that contained P₂O₅ powder.

Perchloric acid (70 wt %, in water) was obtained from Fisher Scientific.

The salts and acid were used as received.

B. Techniques

Butanol/water mixed solvents were prepared in a one L volumetric flask, by volume measurements at 298 K.

Solid solutes were weighed into 25 mL volumetric flasks and dissolved in the mixed solvent to get the stock solution. Sample solutions were made by diluting aliquots of stock solution, using syringes or volumetric pipettes. Perchloric acid samples were prepared through several steps of dilution from the 70 wt % aqueous solution, and the concentrations of the stock solution were checked with the calibrated pH meter.

Four to six sample solutions with different concentrations were prepared for each solute. The solutions were poured into 10 mm Spectrosil optical cells, deaerated by bubbling with UHP argon, and sealed. All components of the solution were of low volatility, so their concentration changed negligibly during bubbling.

Electrons were produced by pulse radiolysis. The radiation was a 100 ns pulse of 340 fJ (2.1 MeV) electrons, delivering a dose of ~ 4 Gy(J/kg). The number of pulses per sample was 2 or 3 at each temperature, and the number of temperatures per sample was 4 or 5. A pure solvent sample was part of each series, so the effect of the $\sim 3 \times 10^{-3}$ mol/m³ of aldehyde produced during three pulses would not affect the value of k_2 obtained from the slope of the plot of k_{obs} against added solute concentration.

The light source was a 1000 W Xe arc lamp (Optical Radiation Co., model XLN) contained in a lamp housing (Photochemical Research Assoc., model PRA ALH220). A Bausch and Lomb monochromator housing, type 33-86-25, was used with the grating type 33-86-03 (700–1000 nm), and a Corning filter type CS-2-64 (700–1000 nm). The light intensity reaching the detector was controlled by adjusting the slits on the monochromator. The wavelength of the analyzing light was 850 nm with bandwidth 9 nm, to obtain an optimal absorption signal.

The silicon detector (pin photodiode SGD 040) was sensitive over the wavelength range 400–1100 nm. The 3 to 97% response time of the detector, amplifier

and transient digitizer (Tektronix R7912) was 6 ns. The signal to noise ratio of the differential amplifier (Tektronix 7A13) was increased by using the 5 MHz filter, which gave a system response time of 96 ns.

The cell holder in the thermostated box was repeatedly rotated full cycles clockwise and counterclockwise between pulse measurements, to obtain a temperature uniformity of ± 0.1 K within the box.

The decay half-life of the solvated electron absorption was computed as a function of time after each pulse, and recorded on the absorption trace (1b). The first-order decay constants were plotted against solute concentration, and second order rate constants obtained from the slope of the line. At high concentrations in butanol the plots were curved due to ionic strength effects, in which case initial slopes were used.

Electrical conductivity measurements were made as described earlier (1a).

pH measurements were made with a Fisher Accumet digital pH/ion meter (model 520) with a glass indicating electrode (Fisher No. 13-639-3) and a reference electrode (Fisher No. 13-639-52). The meter was calibrated with two standard buffer solutions at 298 K, SO-B-108 (pH = 7.00 ± 0.01) and SO-B-98B (pH = 4.00 ± 0.01).

III. Results and Discussion

A. Physical Properties

Iso-butanol is not miscible with water in the composition range 45.4–97.8 mol % water at 298 K (7). Reaction rate constants were measured in solvents containing the following mol % water: 0.0, 10.0, 20.0, 35.0, 45.0, 98.0, 100.0. Values of the viscosities of the mixed solvents were obtained from ref. 8, and of the relative permittivities at 298 K from ref. 9.

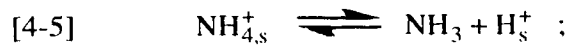
B. Rate Constants

Arrhenius plots of k_2 for LiNO_3 , NH_4NO_3 , NH_4ClO_4 , AgClO_4 , HClO_4 and $\text{Cu}(\text{ClO}_4)_2$ in the mixed solvents are given in Figures 4-1 to 4-4. The symbols that represent the different solvent compositions are listed in Table 4-1.

The precision of k_2 values is 5-10% in pure water solvent and 10-15% in mixed and pure alcohol solvents.

Due to the low solubilities of NH_4ClO_4 and NH_4NO_3 in pure *iso*-butanol, and of NH_4ClO_4 in the 10 mol % water mixture, these values of k_2 could not be measured.

The observed rate of electron reaction in NH_4ClO_4 solutions in 100 and 98 mol % water was affected by reaction of e_s^- with H_s^+ obtained from the dissociation (1a)



$$[4-6] \quad [\text{H}^+] = (K_a[\text{NH}_{4,s}^+])^{0.5} .$$

Values of the dissociation constant K_a of $\text{NH}_{4,s}^+$ are only known for pure water solvent (1a), but they are a reasonable approximation for the 98 mol % water solvent as well. The values of $k_2(e_s^- + \text{NH}_{4,s}^+)$ were calculated from the slopes of plots of $(k_{\text{obs}} - k_2[\text{H}_s^+])$ against the concentration of undissociated $\text{NH}_{4,s}^+$, where k_2 is the rate constant for $(e_s^- + \text{H}_s^+)$ in the appropriate solvent. The corrections are ~50% at 277K and ~80% at 328K; the values of $k_2(e_s^- + \text{NH}_{4,s}^+)$ are very low in these solvents.

In the alcohol-rich solvents the values of $k_2(e_s^- + \text{NH}_{4,s}^+)$ are so high that, unless K_a is >10x the value in pure water solvent, the corrections for $k_2[\text{H}_s^+]$ are negligible. The values of k_2 in alcohol-rich solvents were taken directly from the slopes of plots of k_{obs} against added $[\text{NH}_{4,s}^+]$.

The overall rate constants at 297 K for reaction of e_s^- with $\text{Li}_s^+ + \text{ClO}_{4,s}^-$ are $100 \pm 20 \text{ m}^3/\text{mol}\cdot\text{s}$ in water and $<40 \text{ m}^3/\text{mol}\cdot\text{s}$ in *iso*-butanol. Thus the rate constants of e_s^- with the ions Li_s^+ and $\text{ClO}_{4,s}^-$ are negligible by comparison with those with $\text{NO}_{3,s}$, $\text{NH}_{4,s}^+$, H_s^+ , Ag_s^+ , and Cu_s^{2+} .

Figure 4-5 displays the solvent composition dependence of k_2 at 298 K for NO_3^- , NH_4^+ , H_3^+ , Ag_s^+ , and Cu_s^{2+} , and for NH_4^+ and NO_3^- in combination. As found in other mixed solvents (1a), the reaction of e_s^- with NH_4^+ is 4 orders of magnitude faster in the alcohol-rich solvent than in pure water solvent. The low reactivity in water is attributed (1b) to a symmetric structure of NH_4^+ hydrogen bonded into the structure of water, which would tend to spread out the positive charge and reduce the electron affinity of the ion. The reaction might actually happen by proton transfer to the electron site (3). In alcohol, NH_4^+ is unsymmetrically solvated, which evidently facilitates electron attachment and the subsequent decomposition of $\text{NH}_4 \rightarrow \text{H} + \text{NH}_3$ (1b), or approach of the electron site and proton transfer to it.

The observed rate constants for NH_4NO_3 solutions are mainly due to NO_3^- in the water-rich region and to NH_4^+ in the alcohol-rich region.

C. The Debye Factor f

The coulombic interaction between e_s^- and a reactant of charge $z\xi$ increases their probability of approach to within the distance R_r if z is positive, and decreases it if z is negative (6; Figure 6):

$$[4-7] \quad f = \frac{U(R_r)}{k_B T} \left[\exp\left(\frac{U(R_r)}{k_B T}\right) - 1 \right]^{-1} ,$$

where $U(R_r)$ is the potential energy of interaction between the reactants at center-to-center distance R_r , and k_B is Boltzmann's constant. For the electron and ion,

$$[4-8] \quad U(R_r) = - \frac{z\xi^2}{4\pi\epsilon_0\epsilon_r R_r} ,$$

where ϵ_0 is the permittivity of vacuum, and ϵ_r is the relative permittivity of the medium between the electron and ion.

The estimated value of f depends on the choice of values of ϵ_r and R_r . Some authors used the hydrated ion radius for R_r (10), which seems too small for solvated electron reaction with a solvated ion (4). The van der Waals diameter of a water

molecule is 0.29 nm^b (11). To use the bulk value of ϵ_r for water one would need at least three water molecules between the reactants (one polarized by each reactant, and one relatively free), so $\epsilon_r = 78$ would require $R_r \geq 0.9 \text{ nm}$. We took $R_r = 1.0 \text{ nm}$ for reaction of e_s^- with positive ions. The repulsion between a negative ion and an electron makes it somewhat more difficult for them to approach each other closely, so we took $R_r = 1.5 \text{ nm}$ for reaction of e_s^- with anions and used the bulk value of the static dielectric constant of the solvent. Values of f at 298 K are shown as functions of ϵ_r and z in Figure 4-6. Values of f at other temperatures were not calculated because the variation of ϵ_r with temperature is not known for the mixed solvents.

The solvent composition dependences of k_2/f at 298 K are shown in Figure 4-7. When adjusted for the coulombic interactions in this way, the rate constants k_2/f are all similar and increase with increasing water content. Exceptions are the low values for $e_s^- + \text{NO}_{3,s}^-$ in pure alcohol solvent and $e_s^- + \text{NH}_{4,s}^+$ in water, which are inefficient reactions (1). The points for ammonium nitrate are higher than the rest because both ions are reactants; the overall k_2 was partitioned between $\text{NH}_{4,s}^+$ and $\text{NO}_{3,s}^-$ using the ratio of ammonium perchlorate and lithium nitrate rate constants, then each part was divided by the appropriate f , and the results added to obtain an overall k_2/f .

D. Comparisons of k_2/f in Other Primary Alcohols

Alcohols that have longer alkyl groups have lower molecular diffusion rates, indicated by the higher shear viscosities η (12), and lower molecular rotation rates, indicated by the longer dielectric relaxation times τ_1 (13). The changes of k_2/f with η and τ_1 for reactions of e_s^- with a number of cations and anions in a series of primary alcohol solvents (1,14,15) are shown in Figure 4-8.

^b $r_{\text{vdW}} = \left(\frac{3}{4\pi N_A} \cdot \frac{b}{4} \right)^{1/3} = 4.63 \times 10^{-9} b^{1/3}$.

Reactions of e_s^- with the positive ions (H_s^+ , $NH_{4,s}^+$, Ag_s^+ , Cu_s^{2+}) display values of k_2/f that vary approximately as η^{-1} and τ_1^{-1} (Figure 4-8). The correlation with η^{-1} and the near equality of the values for the different ions indicates that the reactions in alcohol solvents are essentially diffusion-controlled (16a). The somewhat larger rate constants for H_s^+ are due to the proton-hopping mechanism of diffusion (16b).

For the e_s^- reaction with $NO_{3,s}^-$ the value of k_2/f increases as η^{+1} (Figure 4-8) so the diffusion process [4-1a] is not rate limiting. The duration of an encounter between a pair of reactants increases with increasing η ; the multistep reaction that results in the permanent capture of e_s^- by $NO_{3,s}^-$ (1) evidently becomes more probable as the encounter duration increases, in spite of the fact that the rate of new encounters decreases. This indicates that the probability of reaction per encounter increases approximately as the square of the encounter duration.

There is a correlation between the viscosity and the longest dielectric relaxation time τ_1 in alcohols (Figure 4-9). The correlation of k_2/f for ($e_s^- + NO_{3,s}^-$) with τ_1^{+1} is better than that with η^{+1} (Figure 4-8), which we do not yet understand. The line through the points in Figure 4-9 intersects the η axis, which indicates that the rounder shaped alcohol molecules (methanol) can rotate more freely (small τ_1) than they can bump past each other (η). This might mean that the duration of an e_s^- encounter with a $NO_{3,s}^-$ is determined by the molecular dipole rotation time. Dipole reorientation must accompany charge migration in polar solvents, because of the large polarization energy of the solvent molecules around the ion or electron.

E. Electrical Conductivities and Effective Reaction Radii (κR_T)

The diffusion coefficients in equation [4-4] are related to the molar electrical conductivities λ ($S \cdot m^2/mol$) of the respective ions (16b). However, the conductivities of solvated electrons in the mixed solvents are not known, so the ionic conductivities Λ of the dilute reactant electrolyte solutions are used as an approximation. The ratios of the

conductance of e_s^- (17) to that of the various reactant ions (18) in water are known and are roughly assumed to have similar values in the mixed solvents (15):

$$[4-9] \quad \lambda(e_s^-) + \lambda(B^z)/z^2 \approx 1.8\Lambda/z .$$

where z is the number of charges on the reactant in B^z , Λ is the molar conductivity of its electrolyte solutions at low concentration, and the factor 1.8 has an average deviance of ± 0.2 for the present solutes in water. By rearranging equation [4-4] and making appropriate use of equation [4-9] one can obtain (15b):

$$[4-10] \quad \kappa R_T \approx 1 \times 10^{-16} z k_2 / f T \Lambda .$$

The solvent composition dependences of Λ of the reactant electrolytes at 298 K, and of the approximate values of κR_T at 298 K, are shown in Figures 4-10 and 4-11, respectively. The rate parameters are listed in Table 4-2. In most cases the concentrations of salts are $\leq 0.2 \text{ mol/m}^3$ for k_2 and Λ measurements, so ion pairing is negligible. The low reactivity of NH_4ClO_4 in water required concentrations up to 100 mol/m^3 for measurement of k_2 , and the same concentration range was used for Λ measurement; the Debye-Hückel-Onsager equation (16c) describes the Λ data, so ion pairing is negligible.

Most of these values of κR_T are relatively insensitive to solvent composition. The greatest exception is for NH_4^+ , which is only 10^{-4} times as reactive in water as in *iso*-butanol. The next largest exception is for H_s^+ , which is only 0.2 times as reactive in pure water solvent as in the alcohol-rich solvents; this supports the previous conclusion that reaction of e_s^- with H_s^+ in water is 0.2 times slower than diffusion controlled (19, 20), and that the reaction is diffusion controlled in alcohol.

F. Activation Energies E_2 and E_Λ

The Arrhenius temperature coefficients E_2 and E_Λ of reaction and conductance near 298 K are plotted against solvent composition in Figure 4-12. The most remarkable feature is the large increase of E_Λ upon addition of 2 mol % of *iso*-butanol to the aqueous

solutions of AgClO_4 and $\text{Cu}(\text{ClO}_4)_2$, as seen on the right-hand side of Figure 4-12D. This effect is reproducible and corresponds to an increase in conductivity at 298 K (Figure 4-10), which contrasts with the decrease of conductivity of the other aqueous solutions when 2 mol % of *iso*-butanol was added (Figure 4-10). The decrease of Λ and relatively small increase of E_Λ of the other solutions is due to the increased η upon addition of 2 mol % of alcohol to water (Table 4-2). The *increase* of Λ and large increase of E_Λ of the AgClO_4 and $\text{Cu}(\text{ClO}_4)_2$ solutions is worth a separate study. The increase of Λ with T is reproducible with different heating times. It is not due to oxidation of the alcohol by ClO_4^- . The pH measurement in these solutions would be useful to the understanding of the mechanism and a pH meter would have to be calibrated for each solvent and temperature.

The Arrhenius temperature coefficients of the e_s^- reactions in pure water solvent are 2 ± 2 kJ/mol greater than those of conductance of the electrolyte solutions; this difference is essentially the mean thermal agitation energy $RT = 2.5$ kJ/mol, since conductance is driven by the electric field rather than by thermal energy. The values of E_2 in pure water solvent are 3 ± 1 kJ/mol lower than the temperature coefficient of solvated electron diffusion, 20 kJ/mol (17). The exception is $(e_s^- + \text{H}_s^+)$, where $E_2 = 12$ kJ/mol equals the temperature coefficient of proton diffusion in water near 298 K (17; Table 4-2, $E_\Lambda(\text{H}_s^+ + \text{ClO}_{4,s}^-) + 2.5$ kJ/mol).

In the alcohol-rich mixed solvents E_2 is ~ 6 kJ/mol greater than E_Λ for the transition metal ions Ag^+ and Cu^{2+} and the acidic ions H_s^+ and $\text{NH}_{4,s}^+$, indicating a need for a slightly greater agitation energy to react. At the miscibility edge of 45 mol % water, $(E_2 - E_\Lambda)$ for the acidic ions increases to ~ 12 kJ/mol, possibly indicating that e_s^- and the acidic ions are selectively solvated by different components of the solvent, or that they are selectively solvated in the same component but separated by a microstructure of the other component.

The effect of greatest magnitude is the opposite changes of E_2 and E_A for the LiNO_3 solutions on going from pure *iso*-butanol to the water solubility edge at 45 mol % water (Figures 4-12 A and C): E_2 decreases from 41 to 25 kJ/mol while E_A increases from 19 to 25 kJ/mol. Thus, $E_2 - E_A = 22$ kJ/mol in pure *iso*-butanol solvent, but it decreases upon addition of water, reaching zero at the water solubility limit of 45 mol %, and remains at essentially zero in pure water solvent. Electron capture by NO_3^- is clinched by subsequent reaction of the initial NO_3^{2-} ; the reaction is evidently a relatively easy protonation by water in pure water solvent, but involves a more difficult reaction of the alcohol in alcohol solvent (1).

A plot of $(E_2 - E_A)$ against E_A for the various solvent compositions breaks the data into alcohol-rich and water-rich regions, which have been demonstrated in greater detail for other alcohols by plots of k_2 against η at 298 K (21, 22). The $(E_2 - E_A)$ plot is therefore not shown.

Alcohol/water mixed solvents form composite structures, as indicated by their thermodynamic properties (23). Dilute solutions of electrolytes in mixtures near the critical 2-phase composition might have properties characteristic of nanoemulsions. The study of liquids and of liquid solutions for their own sake has reached the beginning of a new cycle of great interest and value to general science.

G. Effective Radii R_d for Mutual Diffusion

We obtain further insight into equations [4-4] and [4-10] by considering R_d . The Stokes radius R_d for mutual diffusion of ions i and j in an electrolyte solution is

(16a):

$$\begin{aligned}
 [4-11] \quad R_d &= \left(\frac{1}{R_{di}} + \frac{1}{R_{dj}} \right)^{-1} \\
 &= 8.62 \times 10^{-16} / \eta \left(\frac{\lambda_i}{z_i^2} + \frac{\lambda_j}{z_j^2} \right)
 \end{aligned}$$

In our case, $i = e_s^-$ and $j = \text{reactant ion}$. As discussed earlier, values of $\lambda_{e_s^-}$ are not available for the mixed solvents, so we use the approximation $[\lambda_{e_s^-} + (\lambda_j/z_j^2)] \approx 1.8\Lambda/z_j$, hence

$$[4-12] \quad R_d \approx 5 \times 10^{-16} z_j / \eta \Lambda \quad ,$$

where Λ is the molar conductance of dilute solutions of the electrolyte that contains reactant ion j .

The solvent composition dependences of R_d are shown in Figure 4-13. Equation [4-12] emphasizes the more mobile ion. In water the mobility of e_s^- (17, 24) is greater than that of all the ions we studied except H_s^+ ; the last has a high mobility due to a solvent-structure-dependent proton hopping mechanism (16b). This is why R_d for $HClO_4$ is only 14 pm, while the rest are in the vicinity of 45 pm in pure water solvent.

The values of R_d for $AgClO_4$ and $Cu(ClO_4)_2$ in pure water reduce to half upon addition of 2 mol% of *iso*-butanol (Figure 4-13): the values of Λ , η , and E_Λ all increase by factors of 1.4 to 1.5 upon addition of 2 mol % of *iso*-butanol to water. A possible reason for the increases in Λ and E_Λ is a reaction that produces H_s^+ , for example,



This uncertainty is why the dashed lines do not acknowledge the apparent decrease of R_d in Figure 4-13 or of κR_T in Figure 4-11 for Ag^+ or Cu^{2+} on going from 100 to 98 mol % water. The copper(II) ion hydrolyzes to a small extent even in pure water solvent (Table 4-1, p. 50 of ref. 25a; Table 12-2, p. 274 of ref. 25b), which was detectable with the pH meter. However, addition of 2 mol % (10 vol. %) of *iso*-butanol to the water or to the dilute salt solutions did not change their indicated pH's appreciably (± 0.03 units), possibly due to an effect of the alcohol on the electrode.

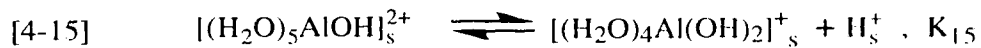
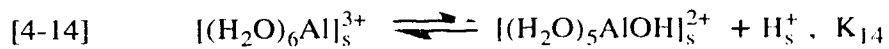
The fact that R_d for $H^+ClO_4^-$ is also smaller in pure alcohol and the mixed solvents, than R_d for the other electrolytes (Figure 4-13), indicates that proton hopping also occurs in those solvents. The ratio $R_d(H^+ClO_4^-)/R_d(\text{other salts}) \approx 0.3$ in water and is usually ~ 0.6 in *iso*-butanol, so proton hopping is less efficient in alcohol than in

water. However, $\text{Ag}^+\text{ClO}_4^-$ has an exceptionally high conductance in alcohol solvents (Figure 4-13 and ref. 15b), which again suggests that reaction [4-13] occurs.

The larger values of R_{i1} for electrolytes in alcohol than in water are attributed to the larger size of the solvating molecules that attach to the ions.

H. Reactions of e_s^- in $\text{Al}(\text{ClO}_4)_3$ Solutions

The reaction rate of e_s^- with Al_s^{3+} cannot be measured directly, because Al_s^{3+} hydrolyses extensively (25). The identities of the species present in aluminum salt solutions at different pH's are not well known, because the hydrolyzed ions can form charged clusters and polymers (25–28). For example, Rubin and coworkers studied the influence of pH on clustering and coagulation in Al(III) solutions, and concluded that in acidic aqueous solutions the main species in equilibrium are Al_s^{3+} , AlOH_s^{2+} , and a polymer $[\text{Al}_8(\text{OH})_{20}]_s^{4+}$. However, for the very dilute, natural pH solutions of $\text{Al}(\text{ClO}_4)_3$ used in our work, only the first two steps of the equilibria are important (25, 28):



where K_{14} and K_{15} are the equilibrium constants.

Measured values of pH of aqueous $\text{Al}(\text{ClO}_4)_3$ solutions at 298 K are plotted against added Al(III) concentration in Figure 4-14, along with data from ref. 28. The e_s^- reaction rate constant data were obtained at $\text{Al}(\text{ClO}_4)_3$ concentrations $< 0.10 \text{ mol/m}^3$, but pH was also measured at higher concentrations to sort out the hydrolysis equilibria. We attempted to fit the data in Figure 4-14 by selecting a value of K_{15}/K_{14} and adjusting the value of K_{14} to give calculated pH values as near as possible to the experimental values. Curves for $K_{15}/K_{14} = 0, 1, 2,$ and 4 are shown in Figure 4-14, and the corresponding values of K_{14} are given in the legend. The best fit was obtained with $K_{15}/K_{14} = 2$ and $K_{14} = 4.7 \times 10^{-3} \text{ mol/m}^3$, which corresponds to $\text{p}K_{14} = 5.33$ and $\text{p}K_{15} = 5.03$. The

value of $pK_{14}+pK_{15}$ is in good agreement with that (10.5) estimated based on the assumption that the logarithms of the stepwise constants decrease linearly with the step of hydrolysis (p. 115 of ref. 25b). The dashed line for $K_{15}/K_{14} = 0$ corresponds to the single stage hydrolysis with $pK = 5.02$ reported earlier (28). Figure 4-14 confirms that multistep hydrolysis (25–28) is significant even at these low concentrations.

Measured half-lives of e_s^- in these solutions gave the first-order k_{obs} values displayed in Figure 4-15. These values were corrected for reaction of e_s^- with H_s^+ , using the measured pH values and $k_2(e_s^- + H_s^+) = 2.4 \times 10^7 \text{ m}^3/\text{mol}\cdot\text{s}$. The net reaction rate with aluminum species is represented by $(k_{obs} - 2.4 \times 10^7 [H_s^+])$; the curve is sublinear (Figure 4-15). The net reaction rate also gives sublinear curves when plotted against the equilibrium values of $[Al_s^{3+}]$ or $[HOAl_s^{2+}]$; it gives a superlinear curve when plotted against $[(HO)_2Al_s^+]$. It appears that e_s^- does not react appreciably with Al_s^{3+} , but that it reacts with a partially hydroxylated species with a rate constant $k_2 > 3 \times 10^6 \text{ m}^3/\text{mol}\cdot\text{s}$.

An early report of $k_2(e_s^- + Al_s^{3+}) = 2 \times 10^6 \text{ m}^3/\text{mol}\cdot\text{s}$ in water at room temperature, at pH = 6.8 (29a), is unclear, because at pH = 6.8 hydrated alumina precipitates. We observed the e_s^- reaction rate in the aluminum perchlorate "solutions" at pH = 6.4 to be the same as that in aqueous $H_2PO_4^-/HPO_4^{2-}$ buffer at that pH. Anbar and Hart might have obtained pH = 6.8 with $H_2PO_4^-/HPO_4^{2-}$ buffer (29b) in which case the observed reaction rate could have been due to the $H_2PO_4^-$. We obtained $k_2(e_s^- + H_2PO_4^-) = 1.2 \times 10^4 \text{ m}^3/\text{mol}\cdot\text{s}$ at $[H_2PO_4^-] = 72 \text{ mol}/\text{m}^3$ and pH = 6.42 at 298 K, whereas Anbar (29c) reported $0.8 \times 10^4 \text{ m}^3/\text{mol}\cdot\text{s}$ at $[H_2PO_4^-] = 100 \text{ mol}/\text{m}^3$ and pH = 7.1 at room temperature.

We could not measure $[H_s^+]$ in the alcoholic solvents. Uncorrected values of k'_2 obtained from plots of k_{obs} against added $[Al(ClO_4)_3]$, and the corresponding Arrhenius temperature coefficients E'_2 , are displayed against solvent composition in Figure 4-16. The relatively low values of k'_2 and high values of E'_2 in pure water and

98 mol % water solvents indicate that the hydrolysis reactions, possibly [4-14] and [4-15], have activation energies of about 20 kJ/mol. The higher values of k'_2 and lower E'_2 in the *iso*-butanol-rich solvents indicate that either the acid dissociation constants of the solvated Al_s^{3+} are higher in these solvents, or that the solvated ions themselves are more reactive with e_s^- .

Table 4-1. Symbols in Figures 4-1 to 4-4

Symbol	mol % H ₂ O	Symbol	mol % H ₂ O
+	0	■	45
Δ	10	○	98
▲	20	●	100
□	35		

Table 4-2. Rate parameters for reactions of solvated electrons with solvated ions in *iso*-butanol/water mixed solvents at 298 K.

ϵ_r^a	η^b (10^{-3} Pa·s)	mol % H ₂ O	f^c	k_2 (10^6 m ³ /mol·s)	k_2/f (10^6 m ³ /mol·s)	E_2^d (kJ/mol)	Λ^e (10^{-3} S·m ² /mol)	E_A^f (kJ/mol)
<i>NO</i> _{3,s} ⁻ ^g								
78.5	0.89	100	0.78	9.2	12.	16.	10.8	15
73.0	1.30	98	0.77	9.6	12.	17.	8.7	20.
19.8	3.25	45	0.34	1.4	4.1	24.	1.35	25.
18.4	3.15	35	0.31	1.1	3.5	28.	1.63	23.
17.6	3.13	20	0.29	0.70	2.4	32.	1.40	23.
17.5	3.20	10	0.29	0.69	2.4	35.	1.25	21.
17.6	3.40	0	0.29	0.29	0.86	41.	0.86	19.
<i>NH</i> _{4,s} ⁺ , <i>NO</i> _{3,s} ⁻ ^h								
		100	0.78	10.	13.	16.	14.8	18.
		98	0.77	7.4	9.6	17.	12.3	19.
		45	h	4.5	4.6	35.	1.64	22.
		35		11.	7.0	32.	1.88	22.
		20		11.	5.4	29.	1.58	22.
		10		9.3	5.0	28.	1.26	23.
		0						
<i>NH</i> _{4,s} ⁺ ⁱ								
		100	1.40	1.5×10^{-3}	1.1×10^{-3}	20.	14.0	16.
		98	1.43	2.6×10^{-3}	1.8×10^{-3}	21.	12.5	20.
		45	3.01	3.9	1.3	36.	2.05	25.
		35	3.20	8.6	2.7	32.	1.98	24.
		20	3.32	11.	3.3	29.	1.61	23.

Table 4-2. continued

ϵ_r ^a	η ^b (10^{-3} Pa·s)	mol % H ₂ O	f ^c	k_2 (10^6 m ³ /mol·s)	k_2/f (10^6 m ³ /mol·s)	E_2 ^d (kJ/mol)	Λ ^e (10^{-3} S·m ² /mol)	E_Λ ^f (kJ/mol)
Ag_s^+ ^j								
78.5	0.89	100	1.40	45.	32.	18.	13.4	15.
73.0	1.30	98	1.43	35.	24.	20.	21.0	22.
19.8	3.25	45	3.01	14.	4.7	29.	2.43	24.
18.4	3.15	35	3.20	13.	4.1	28.	2.20	23.
17.6	3.13	20	3.32	12.	3.6	28.	1.62	23.
17.5	3.20	10	3.34	10.	3.0	28.	1.57	23.
17.6	3.40	0	3.32	8.0	2.4	30.	1.22	23.
H_s^+ ^k								
		100	1.40	24.	17.	12.	40.3	10.
		98	1.43	24.	17.	12.	31.5	12.
		45	3.01	16.	5.3	27.	2.95	18.
		35	3.20	16.	5.0	26.	2.58	21.
		20	3.32	15.	4.5	27.	1.91	22.
		10	3.34	12.	3.6	29.	1.56	23.
		0	3.32	9.5	2.9	30.	1.41	24.
Cu_s^{2+} ^l								
		100	1.88	38.	20.	16.	24.3	16.
		98	1.96	29.	15.	17.	34.3	24.
		45	5.68	25.	4.4	31.	3.15	26.
		35	6.11	21.	3.4	27.	3.04	24.
		20	6.38	22.	3.4	26.	2.84	24.
		10	6.42	19.	3.0	27.	2.48	24.
		0	6.38	13.	2.0	36.	1.88	25.

Table 4-2. continued

- a. Relative dielectric permittivity, ref. 9.
- b. Viscosity, ref. 8.
- c. Debye factor.
- d. Arrhenius temperature coefficient of k_2 at 298 K.
- e. Molar conductivity of the salt solutions at concentrations $<0.2 \text{ mol/m}^3$.
- f. Arrhenius temperature coefficient of Λ at 298 K.
- g. NO_3^- in LiNO_3 solutions, concentrations $0.02\text{--}0.4 \text{ mol/m}^3$.
- h. NH_4^+ and NO_3^- in NH_4NO_3 solutions, concentrations $0.02\text{--}0.2 \text{ mol/m}^3$. The value of f was calculated according to $z = -1(\text{NO}_3^-)$ in 100 and 98 mol % H_2O ; in the other compositions, k_2/f was calculated from the proportionate contributions of each ion and the appropriate f and summed.
- i. NH_4^+ in NH_4ClO_4 solutions, concentrations $2\text{--}170 \text{ mol/m}^3$ for mol % H_2O of 100 and 98; $0.02\text{--}0.2 \text{ mol/m}^3$ for mol % H_2O of 45, 35, and 20.
- j. Ag_s^+ in AgClO_4 solutions, concentrations $0.01\text{--}0.08 \text{ mol/m}^3$.
- k. H_s^+ in HClO_4 solutions, concentrations $0.01\text{--}0.07 \text{ mol/m}^3$.
- l. Cu_s^{2+} in $\text{Cu}(\text{ClO}_4)_2$ solutions, concentrations $0.01\text{--}0.1 \text{ mol/m}^3$.

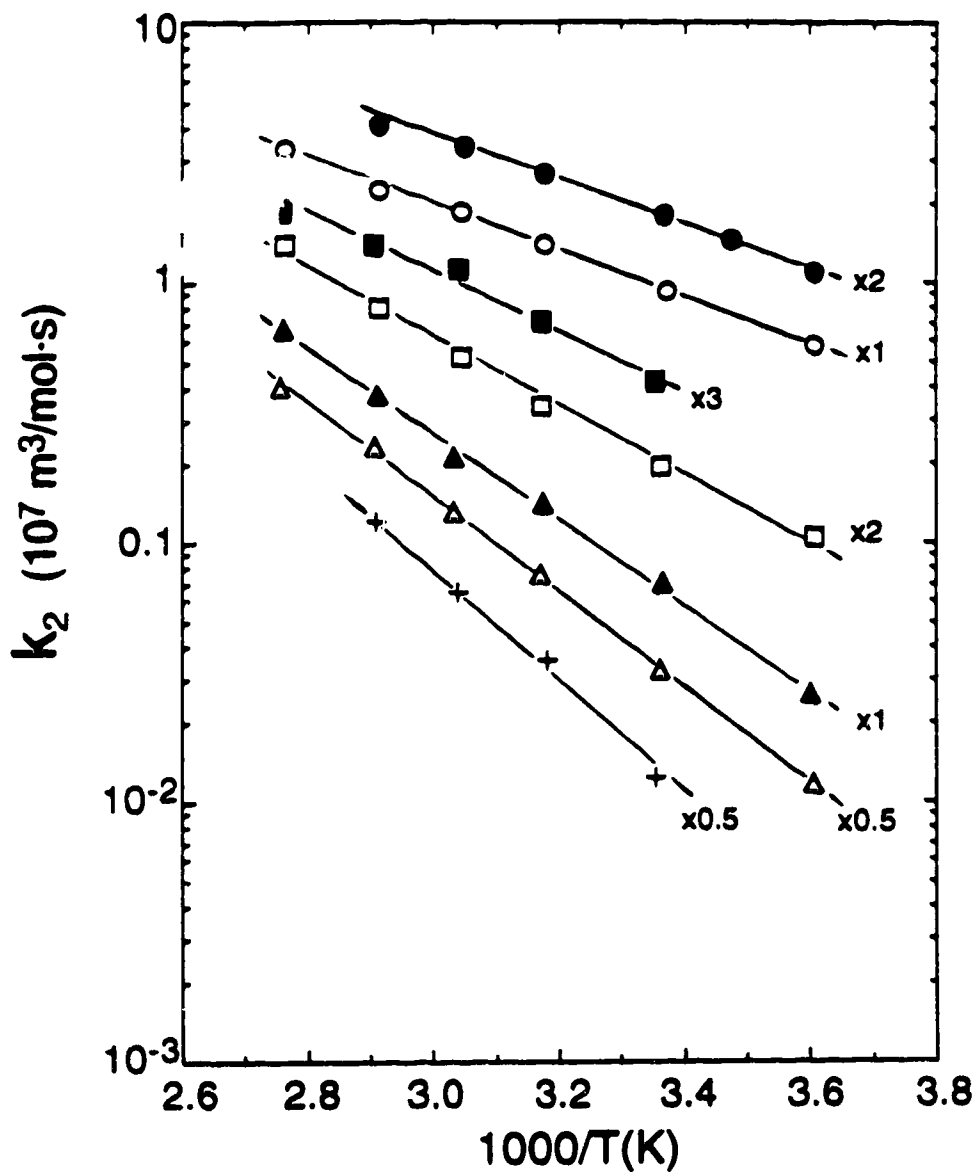


Figure 4-1. Arrhenius plots of k_2 of e_s^- reactions with lithium nitrate in *iso*-butanol/water mixed solvents. Symbols are explained in Table 4-1. To separate the lines, the values of k_2 have been multiplied by the factors indicated.

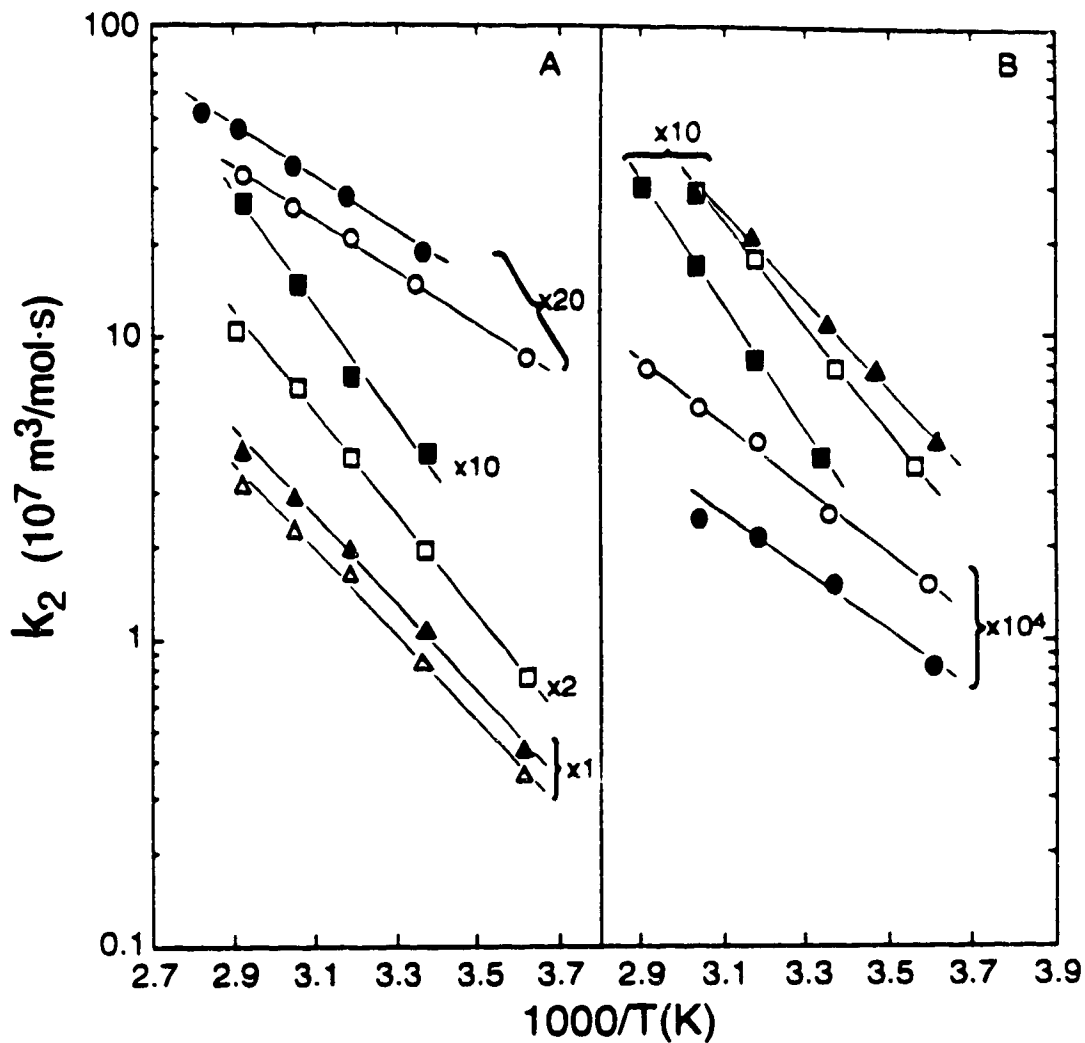


Figure 4-2. Arrhenius plots of k_2 of e_s^- reactions with ammonium nitrate (A) and ammonium perchlorate (B) in *iso*-butanol/water solvents. Symbols are explained in Table 4-1. The values of k_2 have been multiplied by the factors indicated. Data for NH_4^+ in (B) in 100 and 98 mol % of water have been corrected for reaction of H_5^+ from NH_4^+ dissociation (see text).

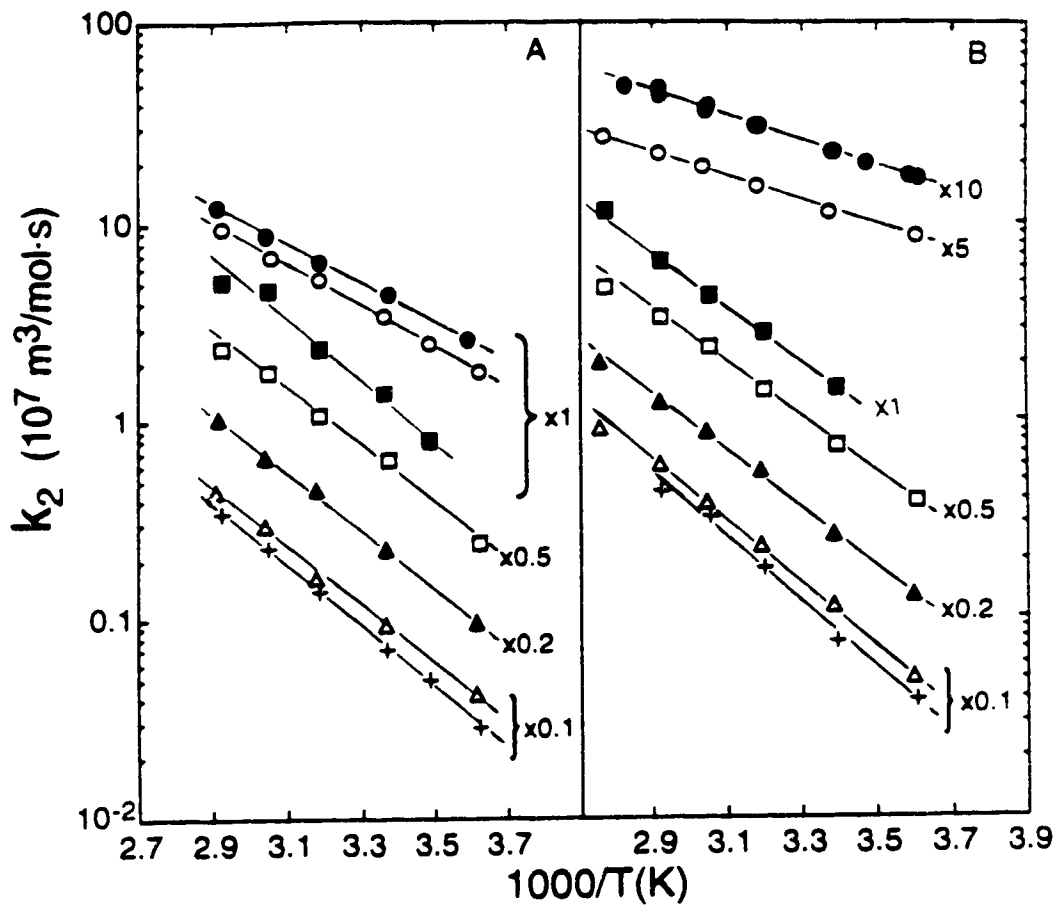


Figure 4-3. Arrhenius plots of k_2 of e_s^- reactions with silver perchlorate (A) and Perchloric acid (B) in *iso*-butanol/water solvents. Symbols are explained in Table 4-1. Values of k_2 have been multiplied by the factors indicated.

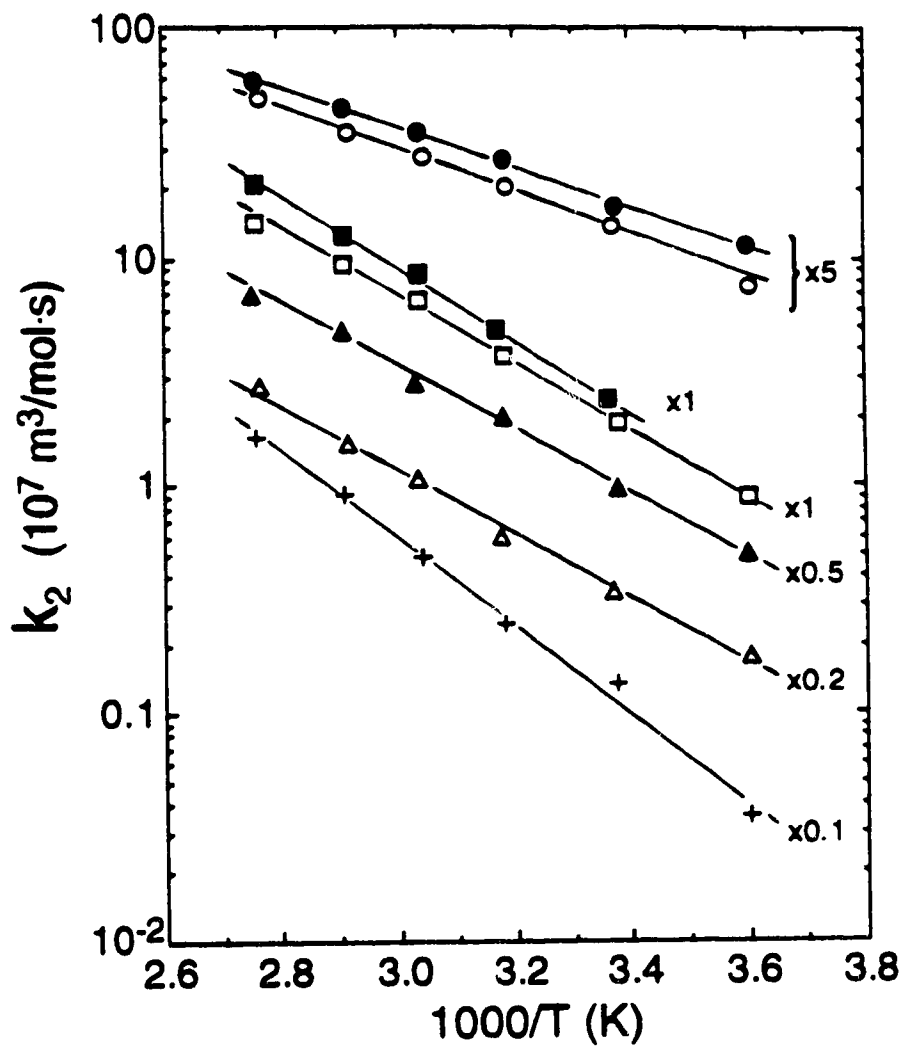


Figure 4-4. Arrhenius plots of k_2 of e_s^- reactions with copper(II) perchlorate in *iso*-butanol/water solvents. Symbols are explained in Table 4-1. Values of k_2 have been multiplied by the factors indicated.

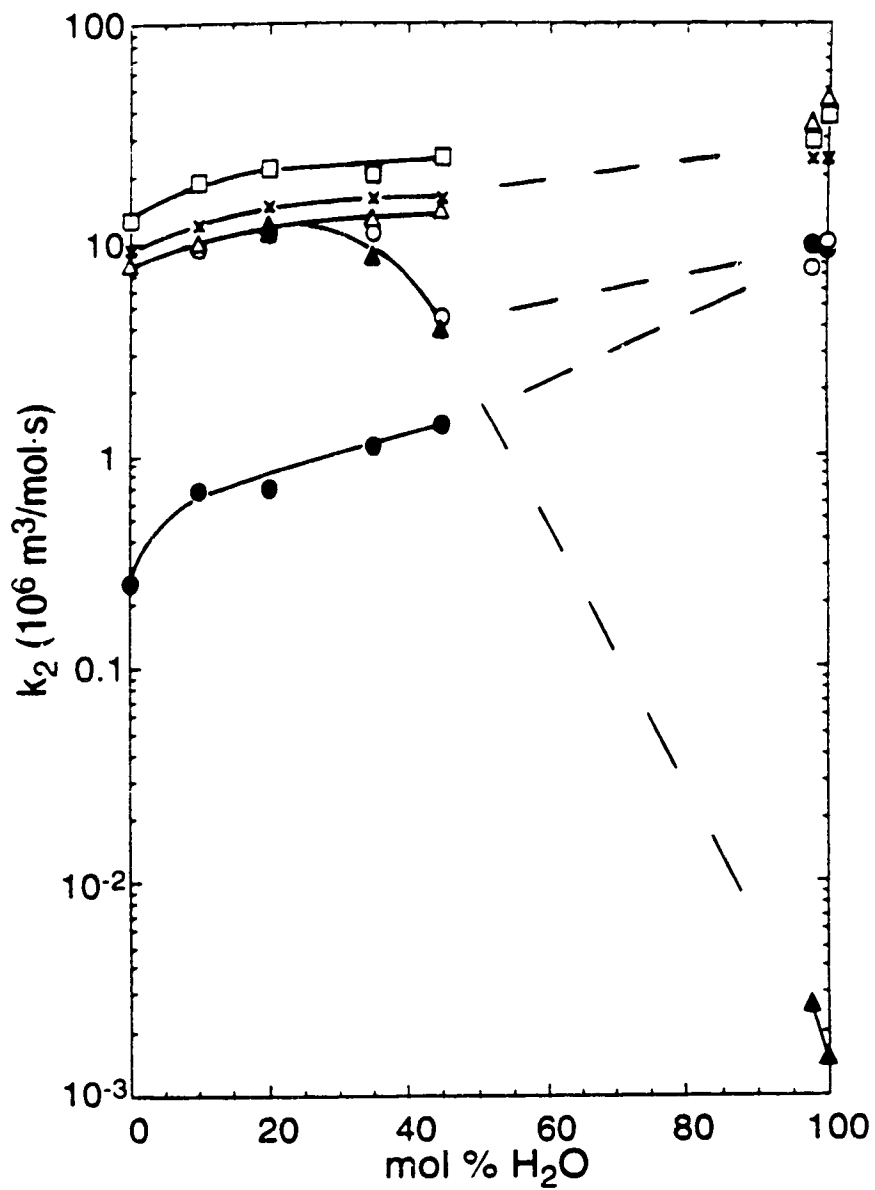


Figure 4-5. Solvent composition dependence of k_2 at 298 K in *iso*-butanol/water solvents. ● LiNO_3 , ○ NH_4NO_3 , ▲ NH_4ClO_4 , △ AgClO_4 , × HClO_4 , □ $\text{Cu}(\text{ClO}_4)_2$.

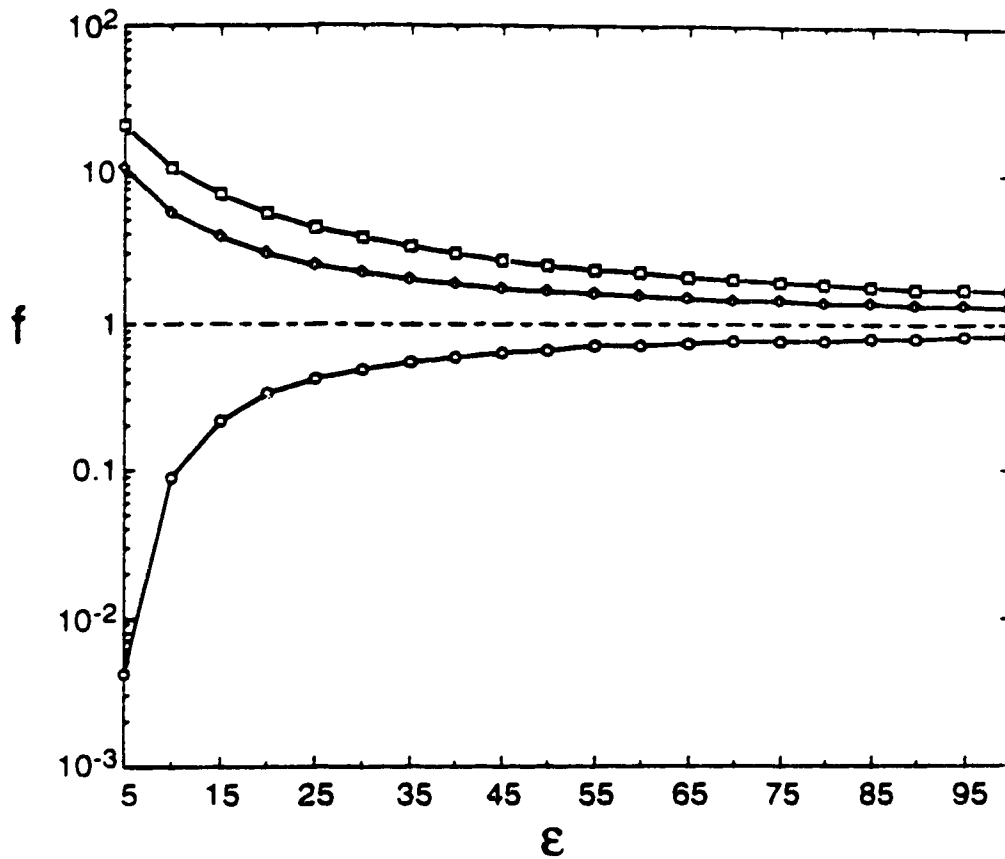


Figure 4-6. Dielectric permittivity dependence of the Debye factor f at 298 K. \square $z = +2$ and \diamond $z = +1$, using $R_T = 1.0$ nm; \circ $z = -1$, using $R_T = 1.5$ nm.

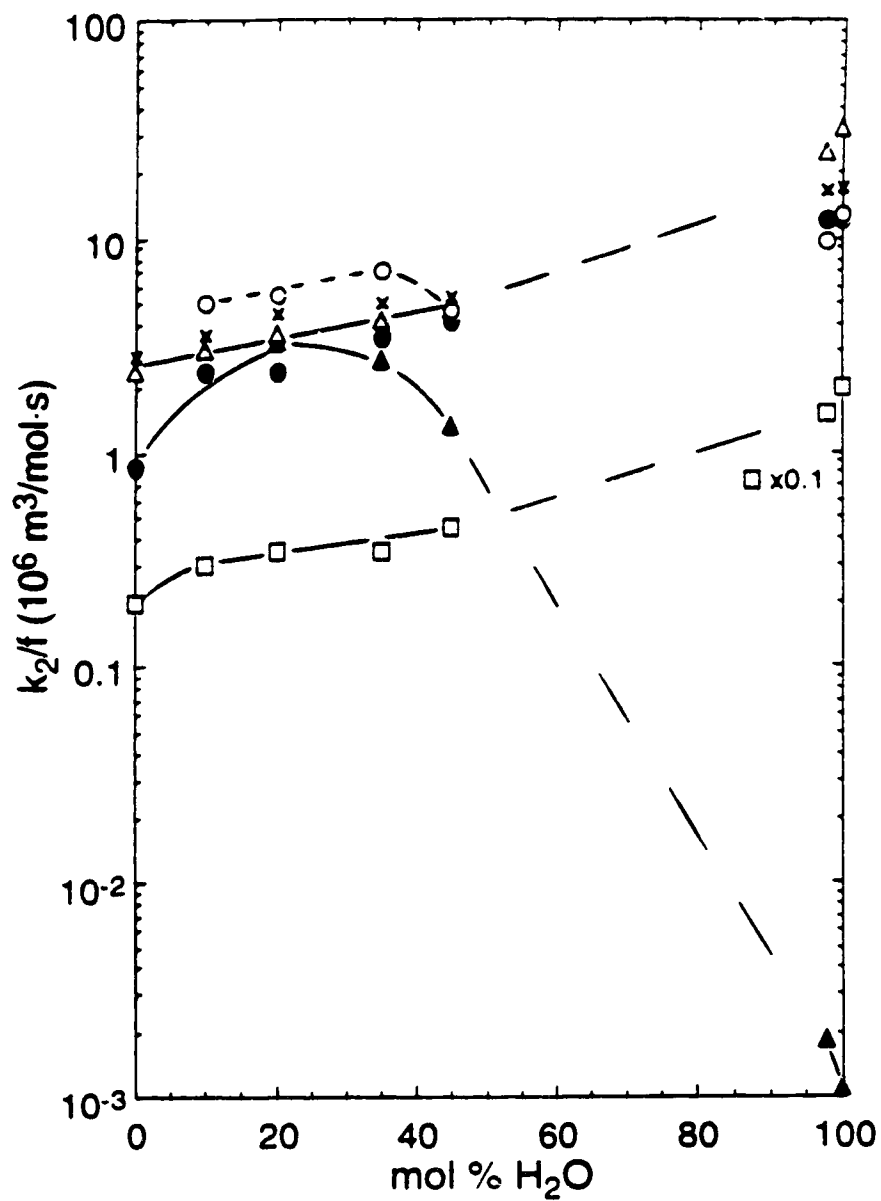


Figure 4-7. Solvent composition dependence of k_2/f at 298 K in *iso*-butanol/water solvents. See Table 4-2 for values of f . Symbols as in Figure 4-5. To separate the lines, some values of k_2/f have been multiplied by the factors indicated.

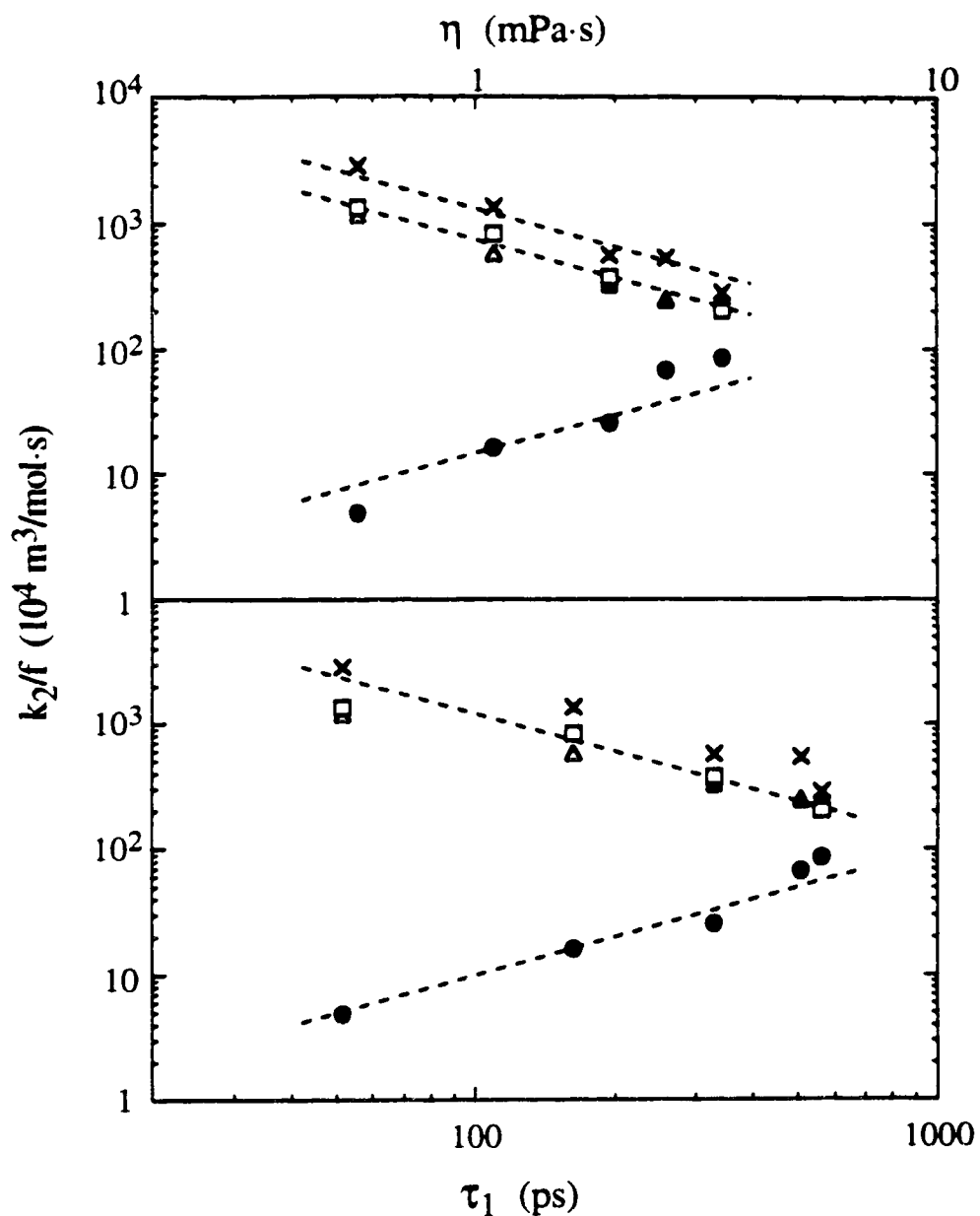


Figure 4-8. The values of k_2/f in pure primary C₁-C₄ alcohol solvents at 298 K, as functions of viscosity η and dielectric relaxation time τ_1 . Symbols as in Figure 4-5. Refs. for k_2 : C₁ and C₂ (14); C₃ (1b, 15); C₄ (1a and present work, data for H⁺ in 1-BuOH, unpublished data measured by the authors). Solvent properties: η (12); τ_1 (13). The dashed lines have slopes of 1.0.

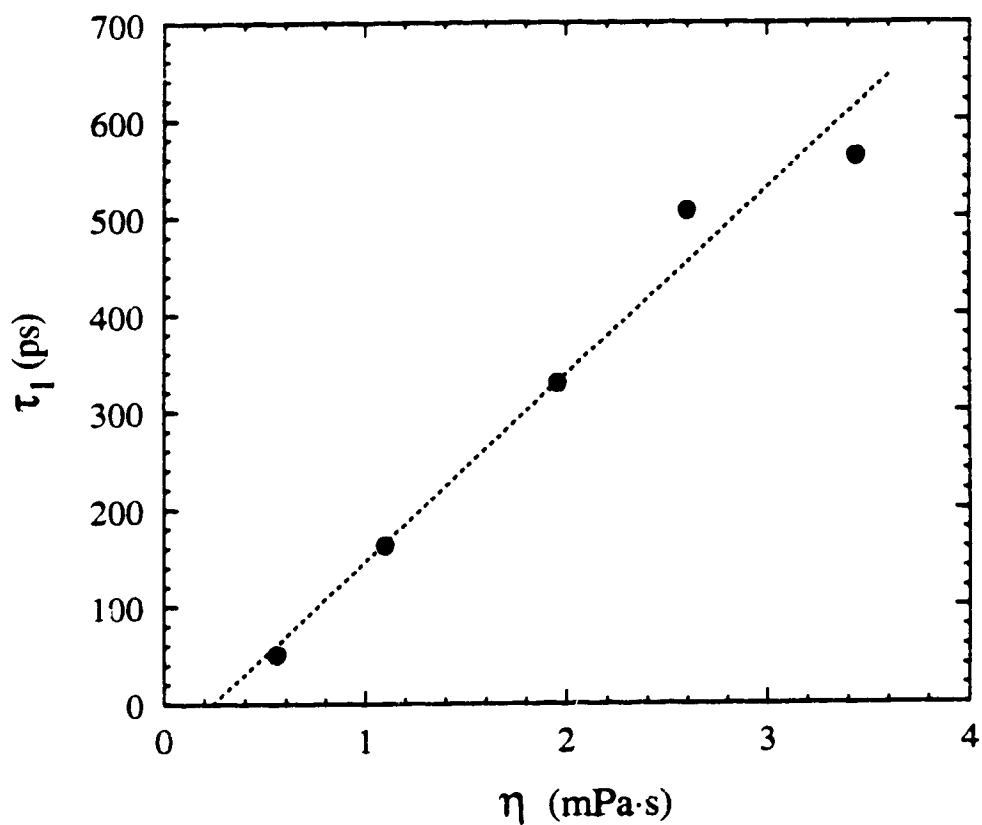


Figure 4-9. Dielectric relaxation time τ_1 (13a, b) of primary C₁–C₄ alcohols at 298 K, as a function of viscosity η (12). The dashed line represents $\tau_1/\text{ps} = 192 (\eta - 0.24)/\text{mPa}\cdot\text{s}$.

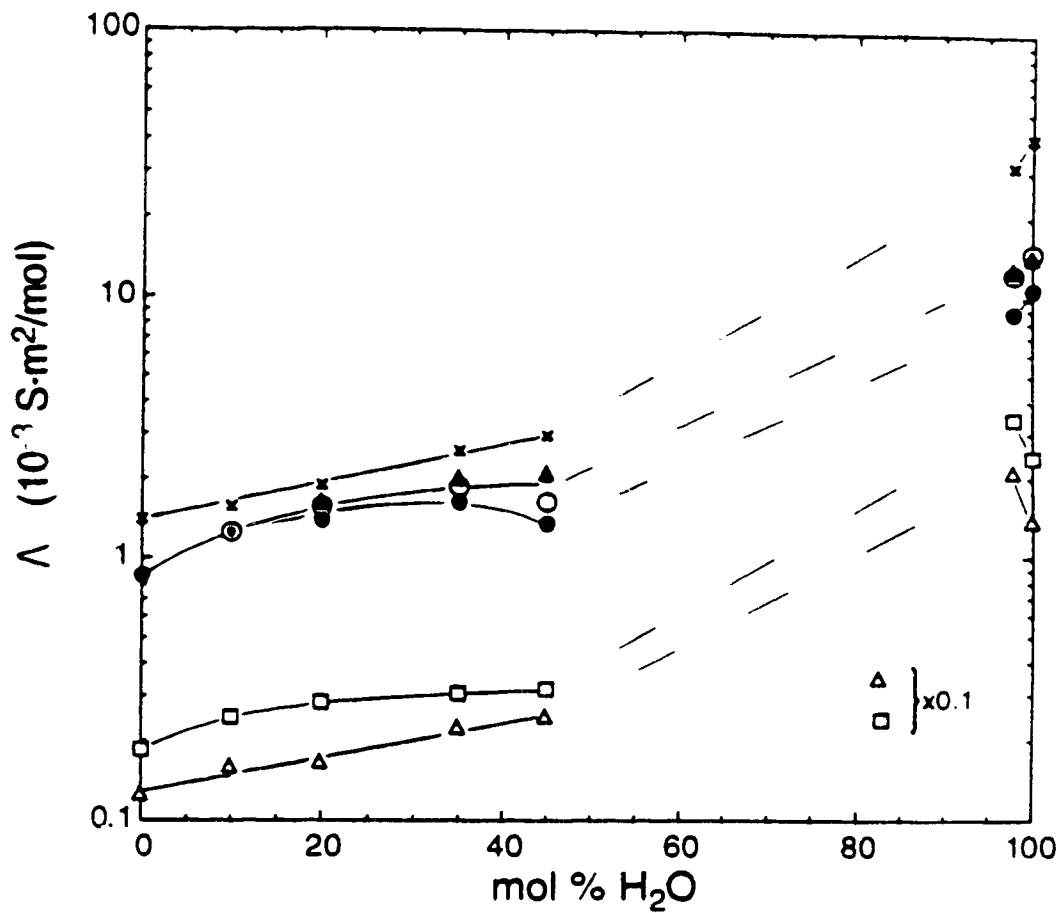


Figure 4-10. Solvent composition dependence of the molar conductivities Λ of dilute electrolyte solutions at 298 K in *iso*-butanol/water solvents. Symbols as in Figure 4-5. Some values of Λ have been multiplied by the factors indicated.

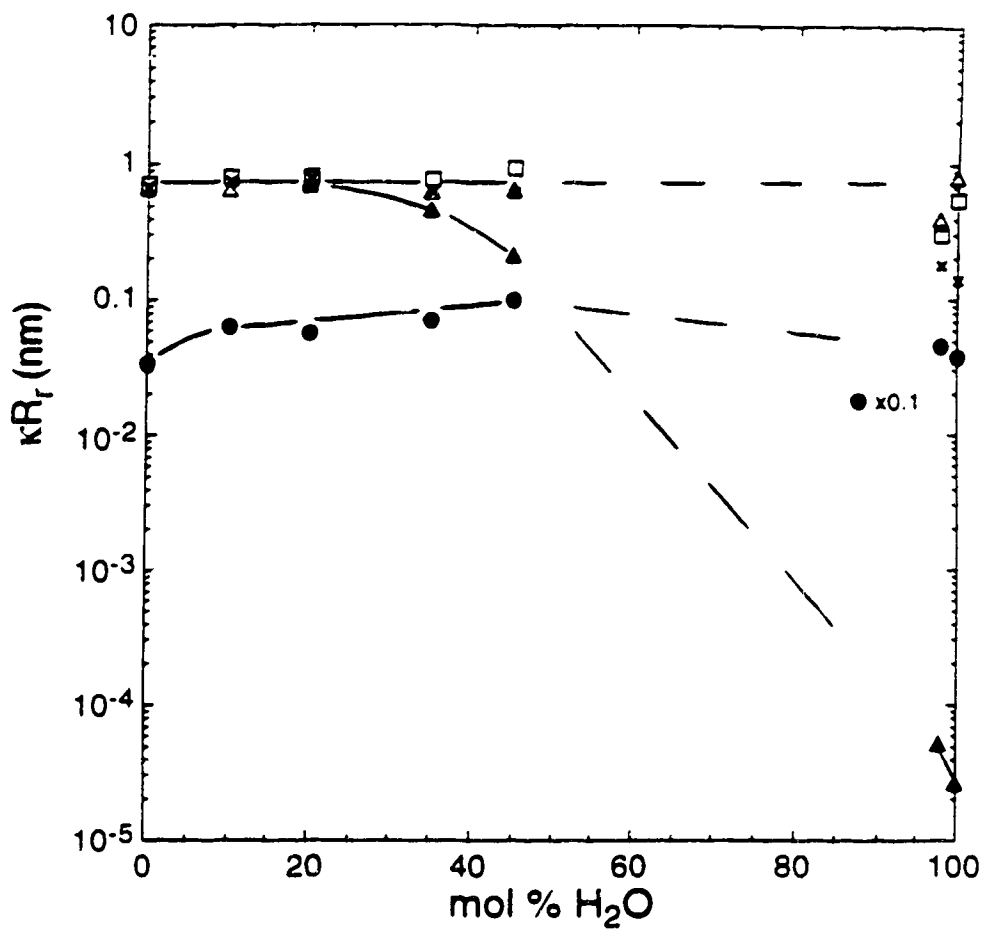


Figure 4-11. Solvent composition dependence of κR_r , equation [4-10], at 298 K in *iso*-butanol/water solvents. Symbols as in Figure 4-5. Some values of κR_r have been multiplied by the factors indicated.

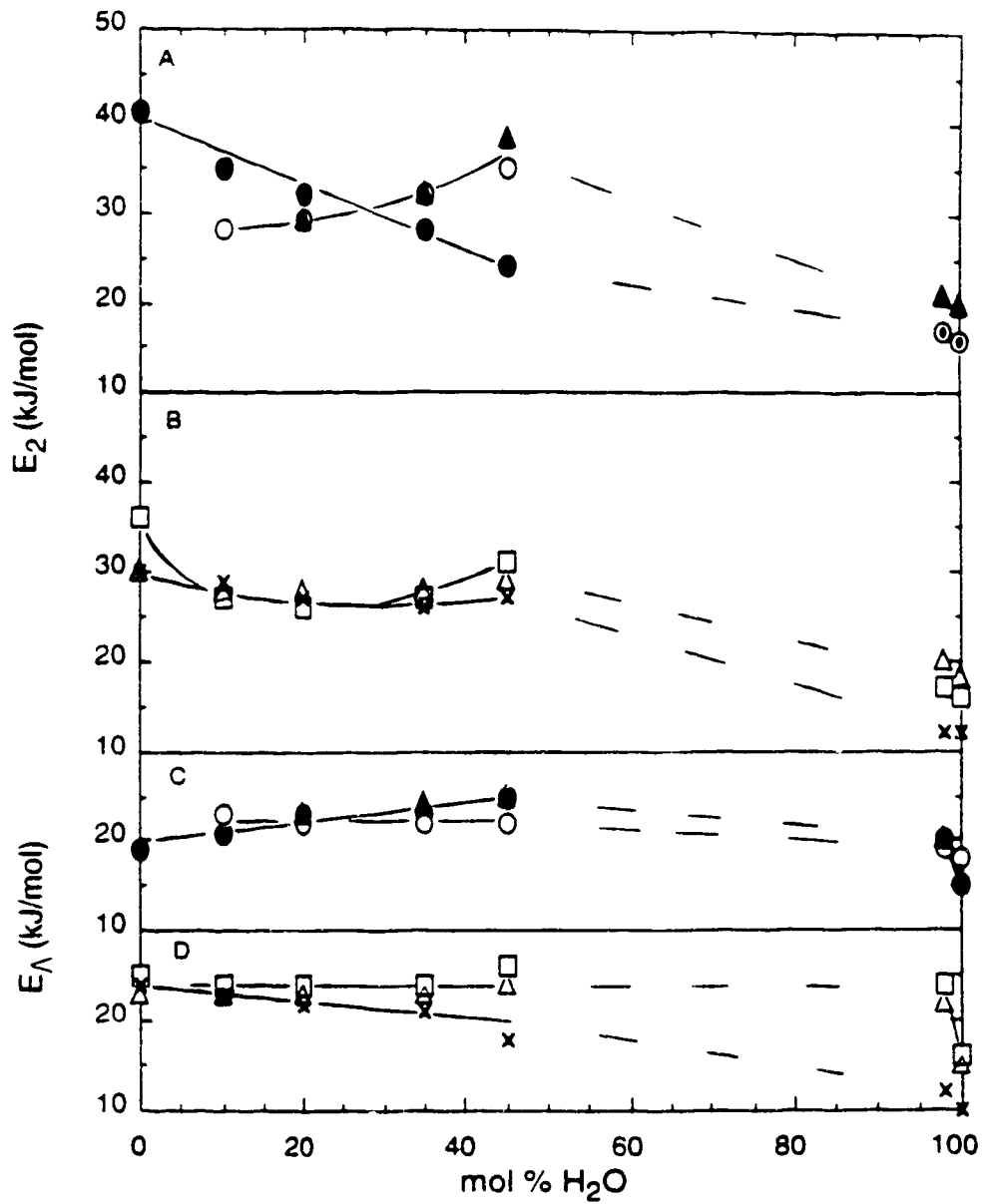


Figure 4-12. Solvent composition dependences of the activation energies E_2 of e_3^- reactions, and E_A of conductance, near 298 K in *iso*-butanol/water solvents. Symbols as in Figure 4-5. A, C: LiNO_3 , NH_4NO_3 , and NH_4ClO_4 . B, D: AgClO_4 , HClO_4 , and $\text{Cu}(\text{ClO}_4)_2$.

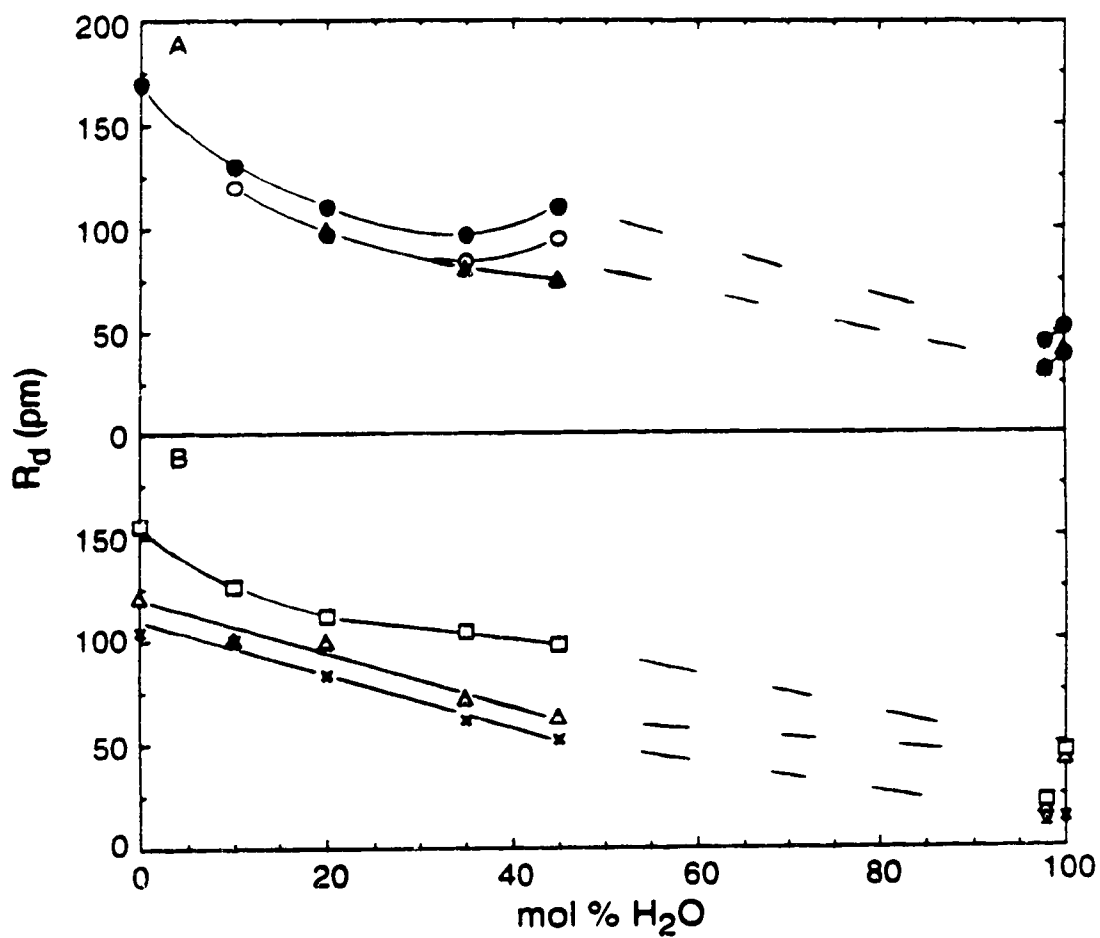


Figure 4-13. Solvent composition dependence of R_d , equation [4-12], at 298 K in *iso*-butanol/water mixed solvents. Symbols as in Figure 4-5. A: LiNO₃, NH₄NO₃, and NH₄ClO₄. B: AgClO₄, HClO₄, and Cu(ClO₄)₂.

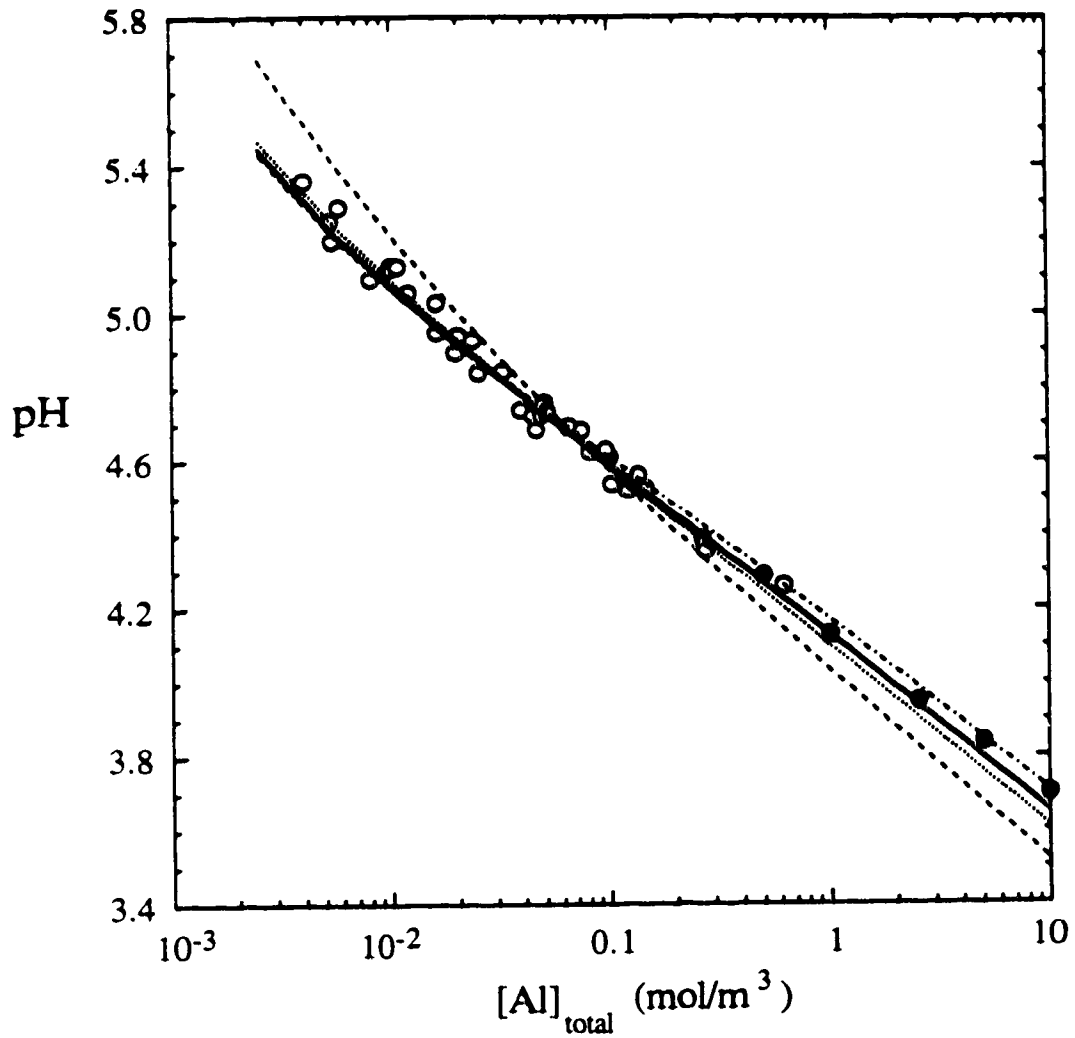


Figure 4-14. pH of $\text{Al}(\text{ClO}_4)_3$ aqueous solutions at 298 K as a function of concentration of aluminum (III) added. O present measurements; ● ref. 28. — calculated for reactions [4-14] and [4-15], with $K_{15}/K_{14} = 2$ and $K_{14} = 4.7 \times 10^{-3} \text{ mol/m}^3$; ---- $K_{15}/K_{14} = 0$ and $K_{14} = 9.6 \times 10^{-3} \text{ mol/m}^3$; ... $K_{15}/K_{14} = 1$ and $K_{14} = 6.0 \times 10^{-3} \text{ mol/m}^3$; -.-.- $K_{15}/K_{14} = 4$ and $K_{14} = 3.5 \times 10^{-3} \text{ mol/m}^3$.

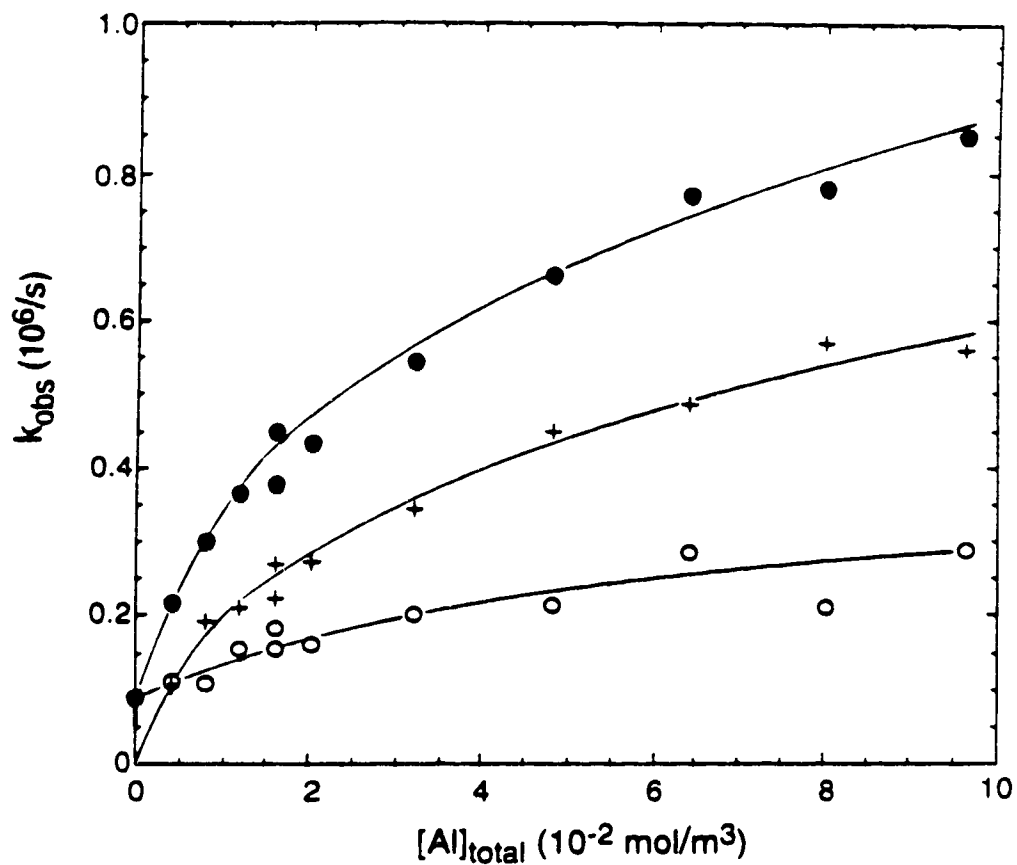


Figure 4-15. The values of k_{obs} of e_s^- reactions in $\text{Al}(\text{ClO}_4)_3$ aqueous solutions as a function of concentration of aluminum(III) added. ●, experimentally measured k_{obs} ; +, $2.4 \times 10^7 [\text{H}_s^+]$, with $[\text{H}_s^+]$ from pH measurement; ○ ($k_{\text{obs}} - 2.4 \times 10^7 [\text{H}_s^+]$).

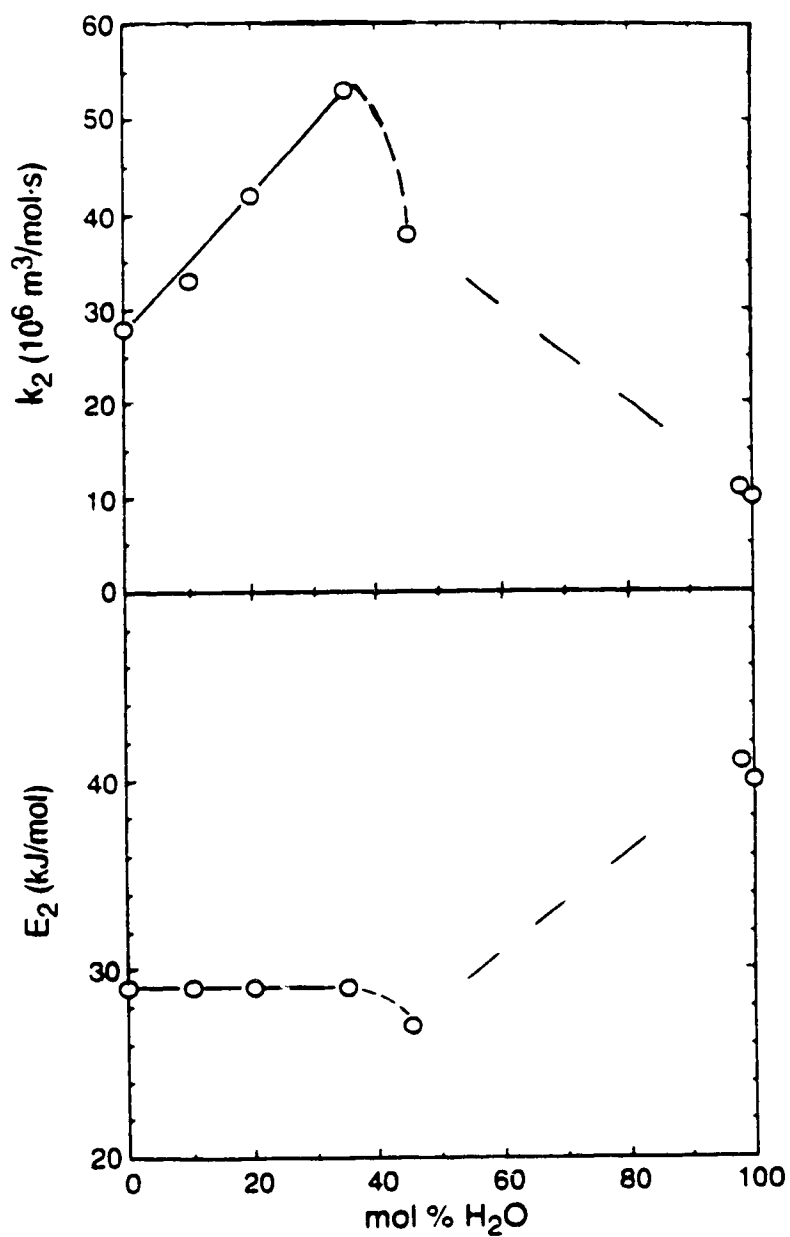


Figure 4-16. Solvent composition dependences of rate constants k_2' and Arrhenius temperature coefficients E_2' for reaction of e_s^- in aluminum perchlorate solutions at 298 K. See text.

References:

1. (a) R. Chen and G. R. Freeman. *Can. J. Chem.* **71**, 1303 (1993); (b) T. B. Kang and G. R. Freeman. *Can. J. Chem.* **71**, 1297 (1993).
2. E. J. Hart and M. Anbar. *The Hydrated Electron*. Wiley-Interscience, New York. 1970.
3. (a) G. L. Bolton, M. G. Robinson, and G. R. Freeman. *Can. J. Chem.* **54**, 1177 (1976); (b) P. Han and D. M. Bartels. *J. Phys. Chem.* **96**, 4899 (1992).
4. R. A. Marcus. *J. Chem. Phys.* **24**, 966 (1956).
5. M. D. Newton and N. Sutin. *Ann. Rev. Phys. Chem.* **35**, 437 (1984).
6. P. Debye. *Trans. Electrochem. Soc.* **82**, 265 (1942).
7. J. M. Sorensen and W. Arlt (*Editor*). *Liquid-Liquid Equilibrium Data Collection, DECHEMA Chem. Data Series*. Frankfurt. 1979. p. 245.
8. P. C. Senanayake and G. R. Freeman. *Can. J. Chem.* **65**, 2441 (1987).
9. A. C. Brown and D. J. G. Ives. *J. Chem. Soc. II*. 1608 (1962).
10. A. J. Elliot, D. R. McCracken, G. V. Buxton, and N. D. Wood. *J. Chem. Soc. Faraday Trans.* **86**, 1539 (1990).
11. R. C. Weast (*Editor*). *Handbook of Chemistry and Physics*. 70th ed. CRC Press, Boca Raton, FL. 1989. p. D-190.
12. R. W. Gallant. *Physical Properties of Hydrocarbons*. Vol. **1**. Gulf Publishing, Houston, TX. 1968.
13. (a) J. Barthel, K. Bachhuber, R. Buchner, and H. Hetzenauer. *Chem. Phys. Lett.* **165**, 369 (1990); (b) H. Sato, H. Nakamura, K. Itoh, and k. Higasi. *Chem. Lett. Chem. Soc. Jpn.* 1167 (1985); (c) F. Buckley and A. A. Maryott.

Tables of Dielectric Dispersion Data for Pure Liquids and Diluted Solutions.
NBS Circular 589. Washington, D.C. 1958.

14. C. C. Lai and G. R. Freeman. *J. Phys. Chem.* **94**, 4891 (1990).
15. S. A. Peiris and G. R. Freeman. (a) *Can. J. Phys.* **68**, 940 (1990); (b) *Can. J. Chem.* **69**, 157 (1991).
16. P. W. Atkins. *Physical Chemistry*. 4th ed. Freeman, New York. 1990. (a) pp. 763-766; (b) pp.754-757; (c) p. 760.
17. K. H. Schmidt, P. Han, and D. M. Bartels. *J. Phys. Chem.* **96**, 199 (1992).
18. A. L. Horvath (*Editor*). *Handbook of Aqueous Electrolyte Solutions*. Wiley, New York. 1985. pp. 262-263.
19. M. Anbar. *Adv. Chem. Ser.* **50**, 55 (1965).
20. K. N. Jha and G. R. Freeman. *J. Chem. Phys.* **48**, 5480 (1968).
21. P.C. Senanayake and G. R. Freeman. *J. Phys. Chem.* **91**, 2123 (1987).
22. Y. Maham and G. R. Freeman. *Can. J. Chem.* **66**, 1706 (1988).
23. B. Marongiu, I. Perino, R. Monaci, V. Solinas, and S. Torrazza. *J. Molecular Liq.* **28**, 229 (1984).
24. G. R. Freeman. *In Kinetics of Nonhomogeneous Processes. Edited by G. R. Freeman*. Wiley-Interscience, New York. 1987. p. 80.
25. (a) J. P. Hunt. *Metal Ions in Aqueous Solution*. Benjamin, New York. 1963. Chap. 4.; (b) C. F. Baes Jr. and R. E. Mesmer. *The Hydrolysis of Cations*. Wiley-Interscience, New York. 1976. Chapters 6 and 12.
26. J. Bjerrum, G. Schwarzenbach, and L. G. Sillen. *Stability Constants of Metal-ion Complexes, with Solubility Products of Inorganic Substances. Part II: Inorganic Ligands*. Chemical Society, London. 1958. pp. 20-21; and the references therein.
27. A. J. Rubin. *Aqueous-Environmental Chemistry of Metals*. Ann Arbor Science Publishers, Ann Arbor, Michigan. 1976. Chap. 9.

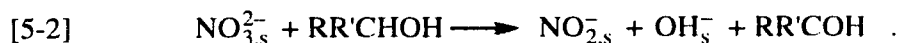
28. C. R. Frink and M. Peech. *Inorganic Chemistry*. **2**, 473 (1963).
29. (a) M. Anbar and E. J. Hart. *J. Phys. Chem.* **69**, 973 (1965); (b) J. K. Thomas, S. Gordon, and E. J. Hart. *J. Phys. Chem.* **68**, 1524 (1964); (c) M. Anbar and E. J. Hart. *Adv. Chem. Ser.* **81**, 79 (1968).

Chapter Five^a

Solvent Effects on Reactivity of Solvated Electrons with Nitrate Ion in C₁ to C₁₀ *n*-Alcohols

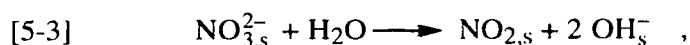
I. Introduction

The reaction of solvated electrons with nitrate ions in alcohol solvents is complex, and in pure alcohol solvents the solvent molecule participates chemically in the overall ($e_s^- + NO_{3,s}^-$) reaction (1-3). The proposed reaction mechanism is:



In reaction [5-2], hydrogen atom transfer occurred, and might involve correlated electron and proton transfers (3).

In aqueous solutions, the suggested reactions were (4):



or

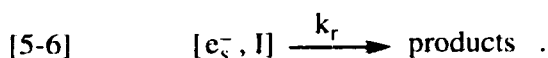
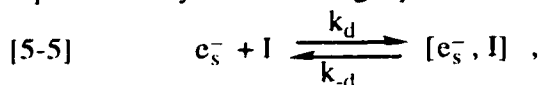


Reaction [5-3] is the protolysis of $NO_{3,s}^{2-}$ by water, followed by reaction [5-4]. The measured rate constant for the reaction ($e_s^- + NO_{3,s}^-$) in water is much larger than those in pure alcohols. This is consistent with the protolysis mechanism in water, since the ionic dissociation of water and hence concentration of H_s^+ in water is greater than

^a A version of this chapter has been submitted for publication to the Journal of Physical Chemistry. R. Chen and G. R. Freeman.

those in alcohols.

The reactions of solvated electrons with solvated ions or molecules, I, can be represented by the following equations (5, 6):



The overall second order reaction rate constant k_2 may be written as (6):

$$[5-7] \quad \frac{1}{k_2} = \frac{1}{k_d} + \frac{1}{Kk_r} \quad ,$$

where, k_d = diffusion controlled upper limit of the rate constant of the forward reaction [5-5], $K = k_d/k_{-d}$, and k_r is the rate of formation of products from encounter pairs.

The relative contributions of k_d and k_r to limiting the observed reaction rate are reflected in the ratio of k_2/k_d (7). If $Kk_r \gg k_d$ then $k_2 \approx k_d$, and the reaction is diffusion-controlled, which could be analyzed according to the Smoluchowski-Debye model (8, 9). If $Kk_r \ll k_d$, then $k_2 \approx Kk_r$ and the reaction is reactivity controlled.

Solvated electron reaction rates with several neutral molecules and with the positive silver ion have been compared in C_1 to C_{10} *n*-alcohols (10, 11). The value of k_2 at 298 K decreases with increasing viscosity η . The slope of a log-log plot of k_2 against η is approximately -1 for Ag_s^+ , pyrene, and 1, 12-benzperylene; and roughly -0.5 for phenanthrene.

However, for reaction of e_s^- with the negative nitrate ion in C_1 to C_4 *n*-alcohols at 298 K, a log-log plot of k_2 against η (or the dielectric relaxation time τ_1) has a slope of about +1 (7, 12). Consistent with refs. 10 and 11, plots of k_2 for several positive ions (Cu_s^{2+} , Ag_s^+ , H_s^+ , $NH_{4,s}^+$) had slopes of about -1 (7). When the values of k_2 were divided by the Debye factor f (2, 9), the extended lines of log-log plots of k_2/f at 298 K against η (or τ_1) from the $NO_{3,s}^-$ and cation data indicated that the two values of k_2/f might be equal in an alcohol that had $\tau_1 \approx 1$ ns or $\eta \approx 7$ mPa·s. The present

work checks this prediction by measuring $k_2(e_s^- + NO_3^-)$ in C_6 , C_8 and C_{10} *n*-alcohols. The nitrate solubility in *n*- $C_{12}H_{25}OH$ was too small to permit measurement.

We estimated values of k_d for each solvent, then obtained information about Kk_r from k_2 and equation [5-7] (13).

Molar conductivities Λ of lithium nitrate solutions were also measured to obtain information about association of the ions in the alcohols.

II. Experimental Section

A. Materials

1-Hexanol (Alfa, 99+%) was refluxed for one day under ultra high pure argon (99.999%, Liquid Carbonic Ltd.) with sodium borohydride (~1 g/l) at 410 K. The alcohol was then fractionally distilled under argon, through an 80 x 2.3 cm column packed with glass helices, discarding the first 20% and last 40%. The middle 40% portion was collected and stored in a flask under argon. The solvated electron half-life after a 100 ns pulse of 340 fJ (2.1 MeV) electrons (~4 J/kg) at 298 K was about 8 μ s.

1-Octanol (Aldrich, 99+%, anhydrous), and 1-decanol (Alfa, 99+%) were used as received. After opening a fresh bottle, the alcohol was transferred to a flask under argon for storage. The solvated electron half-life after a 100 ns pulse of electrons (~4 J/kg) at 298 K was about 3 μ s in both cases.

Lithium nitrate (Aldrich, 99.999%, gold label) was used as received. After opening a fresh bottle, it was stored in a vacuum desiccator that contained P_2O_5 powder.

B. Techniques

The methods of sample preparation and kinetic optical absorption spectroscopy were reported earlier (7).

Electrolyte conductivity measurements were made in an impedance bridge

(model 1608-A, General Radio Co.) at 1 kHz (14). For conductances $<0.1 \mu\text{S}$, the bridge was set to the capacitance mode C_s . For conductances within the range $0.1\text{-}0.6 \mu\text{S}$, the bridge was set to the capacitance mode C_p . In both cases, the conductance was calculated from the capacitance data. For conductances $>0.6 \mu\text{S}$, conductance mode G_p was used.

C. *Physical Properties of the Solvents*

The values of η and their activation energies E_η were obtained from data in ref. 15a for 1-hexanol, refs. 15b and 16 for 1-octanol, and ref. 16 for 1-decanol.

Relative permittivities ϵ_r were obtained from combined plots of data in refs. 17a and 18 for 1-hexanol, refs. 17b and 19a for 1-octanol, and refs. 19b and 20 for 1-decanol.

Values of the longest dielectric relaxation time τ_1 were obtained from ref. 19b. Values of the dielectric longitudinal relaxation time τ_L were calculated from data in refs. 19 and 20.

III. Results and Discussion

A. *Concentration Dependence of k_{obs}*

The measured first order rate constants k_{obs} are plotted as functions of added lithium nitrate concentration in 1-hexanol, 1-octanol, and 1-decanol in Figures 5-1 to 5-3. The points are from two separate runs in most cases. The dependences are linear within the experimental scatter in 1-hexanol and 1-octanol, but the dependence of k_{obs} on added concentration in 1-decanol is perceptibly sublinear at the higher concentrations (Figure 5-3). Before proceeding with an analysis of k_{obs} , we examine ion pairing in these solutions by electrical conductance measurements.

In C_1 to C_4 *n*-alcohols and *iso*-butanol, the electrical conductances of lithium

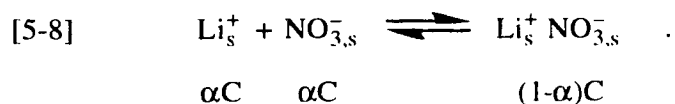
nitrate solutions varied linearly with added concentration of salt in the range used for rate constant measurement (1, 2, 7, 12). This meant that ion pairing was negligible under the conditions used.

The overall rate constant for e_s^- reaction with lithium perchlorate solutions was negligible by comparison with that with lithium nitrate solutions (7). Therefore the measured rate constants in C₁ to C₄ alcohols were due to $e_s^- + NO_{3,s}^-$.

In C₆ to C₁₀ alcohols the coulombic attraction between Li_s^+ and $NO_{3,s}^-$ increases as the permittivity $\epsilon = \epsilon_0\epsilon_r$ becomes smaller; the probability of ion pairing increases with increasing carbon number. This might affect k_{obs} .

B. Concentration Dependence of Electrical Conductance

Let the total concentration of lithium nitrate added be C and the degree of dissociation of ion-pairs be α . Then one may write:



The association constant K_a is:

$$[5-9] \quad K_a = \frac{1-\alpha}{\alpha^2 C}$$

If the Debye-Hückel-Onsager equation for conductivity applies we have (21):

$$[5-10] \quad \Lambda = \alpha[\Lambda_0 - (A + B\Lambda_0)(\alpha C)^{1/2}]$$

where Λ_0 is the molar conductivity at infinite dilution and, for a 1,1-electrolyte (22a),

$$[5-11] \quad A = \frac{\xi F^2}{3\pi\eta} \left(\frac{2}{\epsilon RT} \right)^{1/2}$$

and

$$[5-12] \quad B = \frac{0.586 \xi F^2}{6\pi} \left(\frac{1}{2\epsilon RT} \right)^{3/2}$$

where ξ is the protonic charge, F the Faraday, η the shear viscosity of the solvent, $\epsilon =$

$\epsilon_0\epsilon_r$ the electric permittivity of the solvent, R the gas constant, and all units are SI.

Equations [5-9]-[5-12], with K_a and Λ_0 in each solvent selected to best fit the data, are adequate for 1-hexanol solutions at lithium nitrate concentrations up to ~ 3 mol/m³, and up to ~ 1 mol/m³ in 1-octanol (Figure 5-4). At higher concentrations the calculated conductivities are too low because larger clusters of ions form; while dimers are neutral, trimers are charged and contribute to the conductivity.

Equations [5-9]-[5-12] failed completely for the lithium nitrate solutions in 1-decanol (Figure 5-4). In 1-decanol clusters larger than pairs dominate the conductivity behavior at these concentrations. No adequate model for this behavior exists yet.

The model was adequate for conductivities in 1-hexanol at all temperatures used. The parameter values for Equations [5-9] and [5-12] are listed in Table 5-1. The ion association constant *increases* with increasing temperature because the value of ϵ_r decreases relatively more rapidly than T increases, so the increasing coulombic attraction energy of the ions dominates their increasing thermal agitation energy.

The model was barely adequate for conductivities in 1-octanol at 298 K, but was inadequate at higher temperatures. We include the parameter values at 298 K in Table 5-1 because plots of various functions of Λ_0 of lithium nitrate in methanol to 1-octanol at 298 K show that the octanol value is consistent with the others (Figure 5-5).

The value of Λ_0 decreases with increasing size of the alcohol as expected (Figure 5-5), because the viscosity increases. However, multiplying Λ_0 by η is not enough to normalize the conductances; $\eta\Lambda_0$ is not constant. The solvating molecules are larger when the carbon number N of the alcohol is larger. If the carbons and oxygen are considered as a random chain with $N+1$ links, the radius of the solvated ion increases roughly as $\sqrt{N+1}$. Stokes' equation then suggests that $\eta\sqrt{N+1}\Lambda_0$ might be constant; it nearly is (Figure 5-5). Finally, diffusing charges in a polar solvent carry local polarization with them, even if all the individual solvating molecules do not migrate with the ion. Therefore, an appropriate normalizing factor might be the

longitudinal relaxation time $\tau_L = \tau_1 \epsilon_\infty / \epsilon_s$; values of $\tau_L \Lambda_0$ are constant except for the lower value in methanol (Figure 5-5).

The $\tau_L \Lambda_0$ and $\eta \sqrt{N+1} \Lambda_0$ curves in Figure 5-5 indicate that the Λ_0 value in 1-octanol at 298 K is satisfactory.

C. *Rate Constants k_2*

The conductance data indicate that, at the concentrations of lithium nitrate used to determine k_2 in 1-hexanol, e_s^- was reacting mainly with $\text{NO}_{3,s}^-$ at 274 K and with a mixture of $\text{NO}_{3,s}^-$ and $\text{Li}_s^+ \text{NO}_{3,s}^-$ pairs at higher temperatures. The variations of k_{obs} with added lithium nitrate concentration shown in Figure 5-1 indicate that the values of k_2 for reaction of e_s^- with the free ion is similar to that with the ion pair. The similarity could be due to the approximate cancellation of two effects. In $e_s^- + \text{NO}_{3,s}^-$ coulombic repulsion inhibits the close approach of the two reactants and slows the reaction (Debye factor $f < 1$). The $\text{Li}_s^+ \text{NO}_{3,s}^-$ ion pair would act as a dipole; the e_s^- would tend to be attracted toward the positive end, which would increase the Debye factor to $f > 1$, but then the unreactive Li_s^+ would be a barrier to electron transmission from the e_s^- site to the $\text{NO}_{3,s}^-$. The values of k_2 reported herein are therefore averages over the various species present.

In 1-octanol k_2 corresponds mainly to reaction of e_s^- with pairs, and in 1-decanol with larger clusters of ions. The apparent values of k_2 in 1-decanol are therefore lower than the true values, because the effective concentration of $\text{NO}_{3,s}^-$ in clusters is smaller than the assumed free ion concentration in the plots.

The values of k_2 are listed in Table 5-2 and shown as Arrhenius plots in Figure 5-6. The apparent activation energies E_2 are listed in Table 5-2.

D. *Dependence of k_2 on Solvent Fluidity and τ_L*

The reaction of e_s^- with the fused-ring aromatic hydrocarbon pyrene (Py) is

nearly diffusion controlled (10). The values of $k_2(e_s^- + \text{Py})$ in alcohols at 298 K are nearly the same as those of the normalized rate constant k_2°/f for $e_s^- + \text{Ag}_s^+$, where k_2° is k_2 from refs. 1 and 11 corrected for the ionic strength effect (23), and f is the Debye factor (2) (Figure 5-7). The value of f depends on the value of the reaction radius R_r and of the permittivity of the solvent molecules between the electron and reactant ion at the moment of reaction. By considering the relative orientations of the solvent molecules between e_s^- and a reactant cation or anion, it seems reasonable that there are three intervening molecules when e^- reacts with a cation, and four when e^- reacts with an anion (24). Thus $R_r(\text{nm}) \approx 0.15 + r_{\text{ion}} + nd_s$, where 0.15 nm is taken to represent the approximate expansion of the solvent structure in the vicinity of the electron, $r_{\text{ion}} = 0.13$ nm for Ag^+ and 0.19 nm for NO_3^- (25), $n = 3$ or 4 is the number of intervening solvent molecules of diameter $d_s \approx 2r_{\text{rcp}}$, where $r_{\text{rcp}} = 6.1 \times 10^{-9} V_m^{1/3}$ is the random-close-packed radius of the solvent molecules^b (26), and V_m is the molar volume. Parameter values are gathered in Table 5-3.

Pyrene is neutral, so there is no ionic strength effect and $k_2 = k_2^\circ$, and $f = 1$. Hence for Py and Ag_s^+ in C_1 to C_{10} n -alcohols at 298 K we have (Figure 5-7): $k_2^\circ/f \propto \eta^{-0.83} \propto \tau_L^{-0.54}$.

The values of $k_2(e_s^- + \text{NO}_{3,s}^-)$ in C_1 to C_4 n -alcohols (1, 2, 12) have been corrected for the ionic strength to obtain k_2° , and k_2°/f is plotted in Figure 5-7. For this reaction at 298 K in the C_1 to C_4 n -alcohols: $k_2^\circ/f \propto \eta^{1.2} \propto \tau_L^{0.63}$.

The occurrence of ion pairing and clustering in the lithium nitrate solutions in 1-hexanol, 1-octanol and 1-decanol prevented the estimation of f values and ionic strength. The apparent value of k_2 in 1-decanol, where ion clustering was most extensive, is considered to be lower than it would have been in the absence of clustering. We therefore conclude that the reaction ($e_s^- + \text{NO}_{3,s}^-$) would become essentially diffusion controlled in a larger n -alcohol with $\eta \approx 10$ mPa·s or $\tau_L \approx 1$ ns at

^b Free volume $\approx 43\%$, see reference 26.

298 K.

E. Evaluation of Kk_r for $(e_s^- + NO_{3,s}^-)$ from Equation 5-7

If k_d is known, the value of Kk_r can be estimated from k_2 and equation 5-7. In methanol and ethanol at 298 K the values of the diffusion coefficients D can be calculated from the mobility data for e_s^- (27) and the conductivity data for Ag_s^+ (15c) using the Nernst-Einstein equation (22b), so k_d can be estimated from the Smoluchowski-Debye equation (8, 9):

$$[5-13] \quad k_d = 4\pi N_A (D_{e^-} + D_{Ag^+}) R_r f \quad ,$$

where N_A is Avogadro's constant. The values are listed in Table 5-4.

The estimated values of $k_d(e_s^- + Ag_s^+)$ are about double the k_2° values (Table 5-3). We therefore take $2k_2^\circ(e_s^- + Ag_s^+)$ in each alcohol as a reference.

For $e_s^- + Ag_s^+$ the value of f is >1 , whereas for $e_s^- + NO_{3,s}^-$ f is <1 . We therefore normalize for the different f values by taking $k_d(e_s^- + NO_{3,s}^-) \approx 2k_2^\circ(e_s^- + Ag_s^+) [f_{NO_{3,s}^-} / f_{Ag_s^+}]$.

Values of Kk_r estimated for $e_s^- + NO_{3,s}^-$ in C_1 to C_4 n -alcohols are listed in Table 5-5. The reaction in C_6 to C_{10} alcohols involves ion pairs and clusters, so we put $f = 1$ for lack of better information; the resulting estimates of Kk_r are included in Table 5-5.

When k_2 is sufficiently small the value of Kk_r is not very sensitive to the value of k_d . In the C_1 to C_4 n -alcohols $Kk_r \approx k_2^\circ$ (Table 5-5). Even in C_{10} alcohol, if $k_d \approx 4k_2$ the estimated Kk_r is only ~30% greater than k_2 .

The value of K is the ratio of the rate of the diffusion process k_d to the rate of breaking of an encounter pair k_{-d} . In ethanol the value would be $K \approx 10^7 m^3 mol^{-1} s^{-1} / 10^{11} s^{-1} \approx 10^{-4} m^3/mol$ for the reaction of $(e_s^- + NO_{3,s}^-)$; the value of k_{-d} corresponds to the time required for the e_s^- and the $NO_{3,s}^-$ of an encounter pair to diffuse apart by about 20% of R_r . we take this ratio for other alcohols as well. We thus estimate values

of k_r , and the mean time required for an encounter pair to react, k_r^{-1} (Table 5-5).

The rate is governed by reactions [5-1] and [5-2], which are the formation of the intermediate NO_3^{2-} and subsequent reaction with a solvent molecule. A slow reaction [5-2] is assisted by a longer encounter duration, hence a larger τ_L or η . The smallest value of k_r^{-1} occurs in the alcohol with the largest τ_L and η , and the other way around (Tables 5-3 and 5-5).

When $k_r^{-1} \gg \tau_L$ many encounters are required to complete the reaction. This condition is most extreme in methanol (Tables 5-3 and 5-5), and in this system the observed activation energy E_2 of the overall reaction is similar to those of viscosity and ionic conductance (Figure 5-8). In methanol the encounter duration is so short, compared to the time required for reaction of NO_3^{2-} with a methanol molecule, that reaction depends on the chance that a methanol molecule is oriented favorably for reaction at the time the NO_3^{2-} is formed. The reaction is said to have a large, negative entropy of activation.

In C_2 to C_4 *n*-alcohols E_2 is sufficiently larger than E_η or E_A (Figure 5-8) that the reaction is progressively more enthalpy driven.

In the large alcohols C_8 and C_{10} , where $k_r^{-1} < \tau_L$ (Tables 5-3 and 5-5), E_2 falls toward the energy required for diffusion (fluidity, conductivity) as the reaction approaches diffusion control (Figure 5-8).

Table 5-1. Conductivity fitting parameters for ion pairing in lithium nitrate solutions.

T (K)	ϵ_r^a	η^b (10^{-3} Pa·s)	A ^c (10^{-4} S·m ^{3.5} /mol ^{1.5})	B ^d (m ^{1.5} /mol ^{0.5})	Λ_0 (10^{-4} S·m ² /mol)	K_a (m ³ /mol)
<i>l</i> -hexanol						
298.2	13.3	4.29	0.965	0.104	5.1	0.74
313.2	11.8	2.77	1.55	0.116	7.7	2.4
328.5	10.2	1.84	2.44	0.133	9.5	4.1
343.4	8.71	1.28	3.72	0.159	12.	11.
353.2	7.72	1.03	4.86	0.182	14.	30.
<i>l</i> -octanol						
298.2	10.1	7.37	0.646	0.158	3.	20.

- a. Relative permittivity of solvent; see *Experimental Section* for references.
- b. Viscosity of solvent; see *Experimental Section* for references.
- c. calculated from equation [5-11].
- d. calculated from equation [5-12].

Table 5-2. Rate parameters for the reaction of (e^-_s + nitrate) in C_6 to C_{10} *n*-alcohols.

T (K)	ϵ_r^a	η^b (10^{-3} Pa·s)	α^c	k_2^d (10^6 $m^3/mol\cdot s$)	E_2^e (kJ/mol)
<i>l</i> -hexanol					
273.6	16.0	9.78	0.94	0.10	34
296.9	13.3	4.46	0.73	0.34	
319.0	11.1	2.36	0.45	0.83	
342.2	9.1	1.32	0.25	2.0	
<i>l</i> -octanol					
274.7	12.4	17.8		0.16	30
297.5	10.1	7.54	0.23	0.40	
328.5	7.4	2.83		1.4	
347.9	6.0	1.68		2.4	
<i>l</i> -decanol					
296.3	7.6	11.8		0.53	30
314.1	6.5	6.19		1.0	
328.9	5.8	3.81		1.7	

- a. Relative permittivity of solvent; see *Experimental Section* for references.
- b. Viscosity of solvent; see *Experimental Section* for references.
- c. Degree of dissociation of $LiNO_3$ at the average concentration used to determine k_2 , calculated from equation [5-9] with the value of K_a interpolated or extrapolated in Arrhenius plots of K_a (data in Table 5-1).
- d. Rate constants calculated from slopes of k_{obs} against C plots in Figures 5-1 to 5-3.
- e. Activation energy from Arrhenius plots of k_2 .

Table 5-3. Rate parameters for e_s^- reactions with Ag_s^+ and $NO_{3,s}^-$ in C_1 to C_{10} n -alcohols at 298 K.

C_n^a	ϵ_r	η (10^{-3} Pa·s)	τ_L^b (ps)	r_{rcp}^c (nm)	$(e_s^- + Ag_s^+)$			$(e_s^- + NO_{3,s}^-)$		
					R_r^d (nm)	f^e	k_2^{0f} (10^6 $m^3/mol\cdot s$)	R_r^d (nm)	f^e	k_2^{0f} (10^4 $m^3/mol\cdot s$)
1	32.5	0.56	4.4	0.21	1.5	1.7	28	2.0	0.63	2.1
2	24.3	1.10	18.	0.24	1.7	1.8	16	2.2	0.57	4.3
3	20.1	1.96	41.	0.26	1.8	2.0	12.	2.4	0.53	6.9
4	17.4	2.60	74.	0.28	1.9	2.1	9.1	2.5	0.49	10.
5	13.9	3.35	116.	0.29	2.0	2.3	7.1			
6	13.3	4.29	172.	0.31	2.1	2.4	6.0			
7	11.4	5.68	230.	0.32	2.2	2.6	6.7			
8	10.1	7.37	315.	0.33	2.2	2.7	4.6			
9	9.1	9.10	415.	0.34	2.3	2.9	4.2			
10	7.8	11.0	460.	0.35	2.4	3.2	3.8			

- a. Number of carbons in n -alcohols.
- b. Longitudinal dielectric relaxation time, see *Experimental Section* for refs.
- c. Random-close-packed radius of solvent molecules; see text.
- d. Reaction radius; see text.
- e. Debye factor; equation in ref. 2.
- f. Rate constant corrected for ionic strength effect.

Table 5-4. Calculation of k_d for the reaction $e^-_s + Ag^+_s$ in methanol and ethanol at 298 K.

n-ROH	D_{e^-} ^a	D_{Ag^+} ^b	R_r ^c	f ^d	k_d ^e
	(10^{-9} m ² /s)		(nm)		(10^6 m ³ /mol·s)
methanol	1.5	1.2	1.5	1.7	52.
ethanol	0.77	0.49	1.7	1.8	29.

- a. Diffusion coefficient of the solvated electron calculated from mobility data in ref. 30.
- b. Diffusion coefficient of Ag^+ ion calculated from conductivity data in ref. 15c using Ag^+ ion transport number of 0.36 for $AgClO_4$ in ethanol (p.1013 of ref. 15).
- c. Reaction radius; see text.
- d. Debye factor.
- e. Diffusion controlled reaction limit calculated from equation [5-13].

Table 5-5. The values of Kk_r for e_s^- reaction with nitrate in C_1 to C_{10} n -alcohols at 298 K.

n -ROH	k_2^a (10^4 $m^3/mol\cdot s$)	f^b	Kk_r^c (10^4 $m^3/mol\cdot s$)	$\sim k_r^{-1d}$ (ps)	E_2^e	E_η^f	E_Λ^g	$E_{\tau_l}^h$
					(kJ/mol)			
methanol	2.1	0.63	2.1	4800	9.	11.	9.	15.
ethanol	4.3	0.57	4.3	2300	40.	13.	13.	14.
<i>l</i> -propanol	6.9	0.53	7.0	1400	46.	18.	16.	19.
<i>l</i> -butanol	10.	0.49	10.	1000	43.	19.	18.	22.
<i>l</i> -hexanol	35.	~1	38.	260	34.	23.	16.	26.
<i>l</i> -octanol	43.	~1	49.	200	30.	26.		29.
<i>l</i> -decanol	53.	~1	68.	150	30.	28.		30.

- a. Rate constant; for C_1 - C_4 alcohols, values are k_2^0 . Data from: ref. 1 for C_1 and C_2 ; ref. 2 for C_3 ; ref. 12 for C_4 ; others, present work.
- b. Debye factor.
- c. Calculated from equation [5-7]; see text.
- d. Taking $K=10^{-4} m^3/mol$; mean time for an encounter pair to react.
- e. Activation energy from Arrhenius plot of measured k_2 . Refs as in a.
- f. Activation energy of shear viscosity. Values of η : for C_1 to C_4 from: R. C. Weast (*Editor*). Handbook of Chemistry and Physics. 70th ed. CRC Press, Boca Raton, FL. 1989. pp. F41-44; for C_6 - C_{10} , see **Experimental Section** for references.
- g. Activation energy of molar conductivity; Refs. as in a.
- h. Activation energy of the longitudinal relaxation time; estimated from data in refs. 19b and 20.

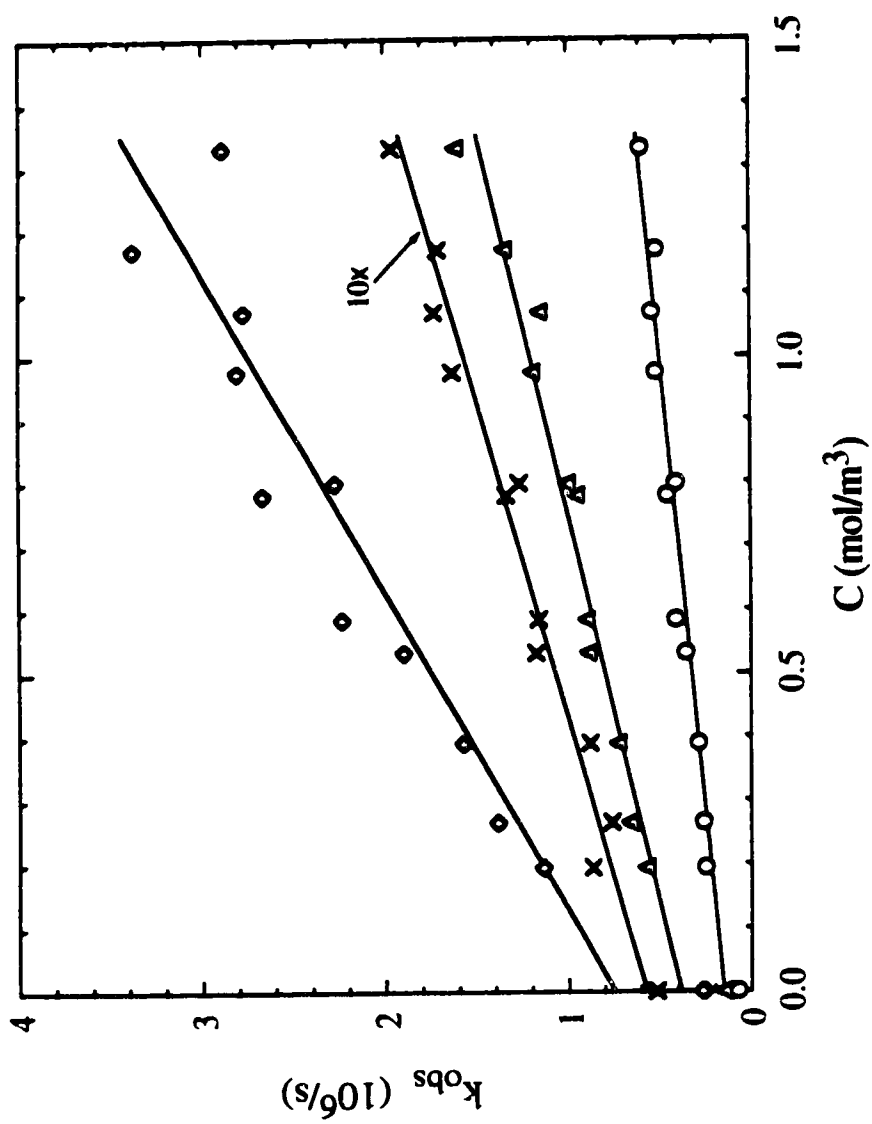


Figure 5-1. Concentration and temperature dependences of k_{obs} for e_s^- reaction with lithium nitrate in 1-hexanol. T(K): x (times 10), 273.6; \circ , 296.9; Δ , 319.0; \diamond , 342.2.

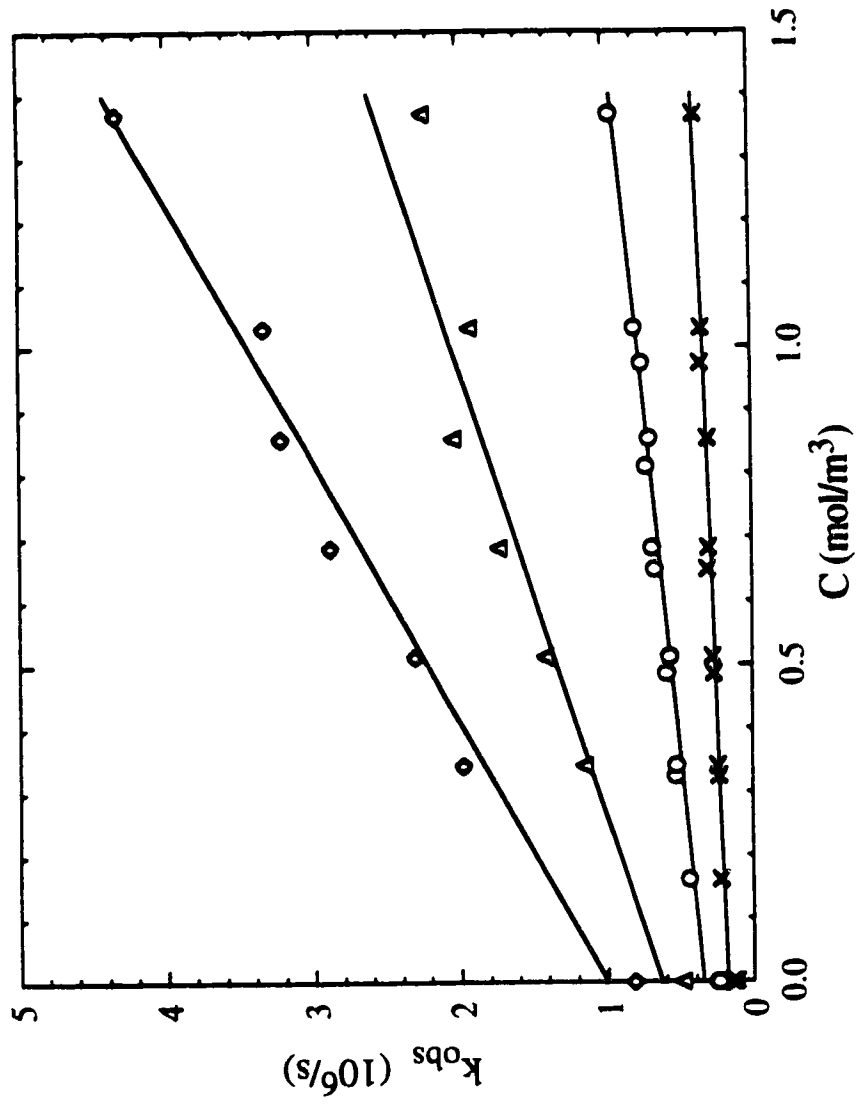


Figure 5-2. Concentration and temperature dependences of k_{obs} for e_s reaction with lithium nitrate in 1-octanol. T(K): x, 274.7; O, 297.5; Δ, 328.5; ◊, 347.9.

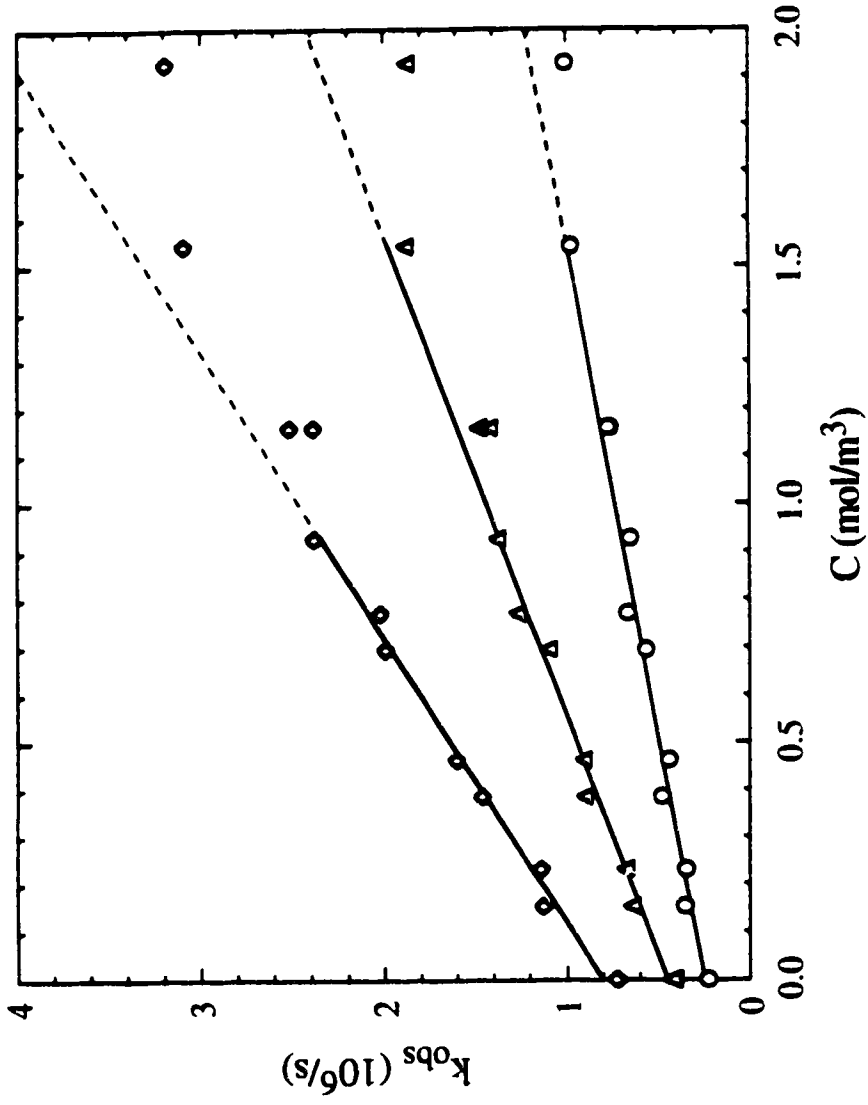


Figure 5-3. Concentration and temperature dependences of k_{obs} for e_s reaction with lithium nitrate in 1-decanol. T(K): O, 296.3; Δ, 314.1; ◇, 328.9.

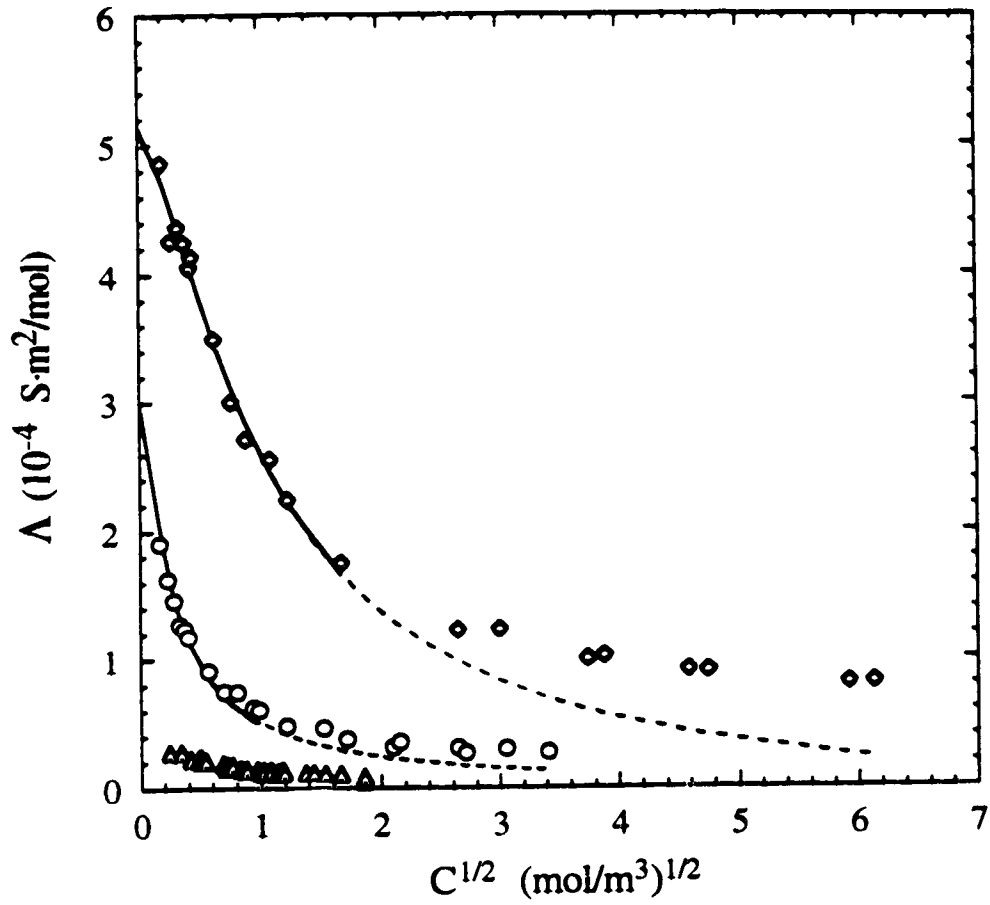


Figure 5-4. Molar conductivities of lithium nitrate solutions at 298K in 1-hexanol (\diamond), 1-octanol (\circ), and 1-decanol (Δ). The full curves were calculated from equations [5-10] - [5-12], with the empirical parameters in Table 5-1.

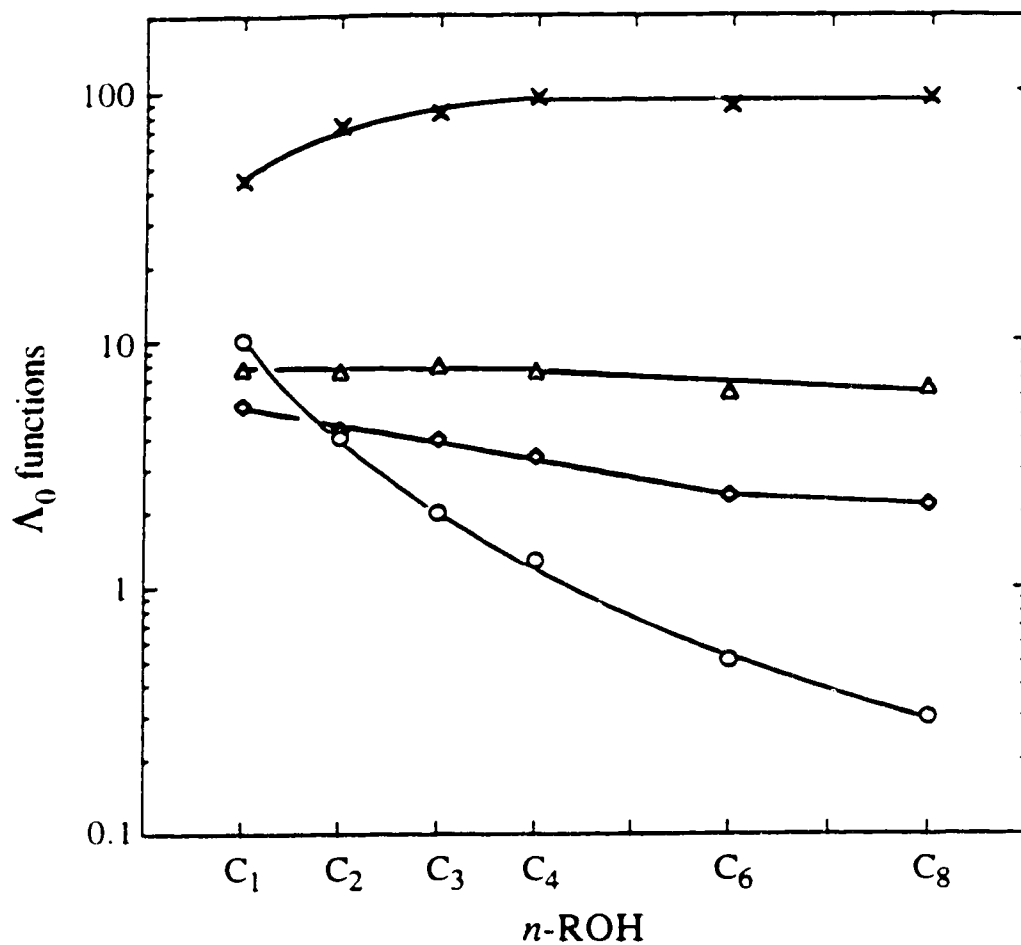


Figure 5-5. Various functions of Λ_0 for lithium nitrate in C_N n -alcohol at 298K; $N=1$ to 8. \circ , Λ_0 ($10^{-3} \text{ S}\cdot\text{m}^2/\text{mol}$); \diamond , $\eta \Lambda_0$ ($10^{-6} \text{ Pa}\cdot\text{s}\cdot\text{S}\cdot\text{m}^2/\text{mol}$); Δ , $\eta (N+1)^{1/2} \Lambda_0$ ($10^{-6} \text{ Pa}\cdot\text{s}\cdot\text{S}\cdot\text{m}^2/\text{mol}$); \times , $\tau_L \Lambda_0$ ($10^{-15} \text{ s}\cdot\text{S}\cdot\text{m}^2/\text{mol}$).

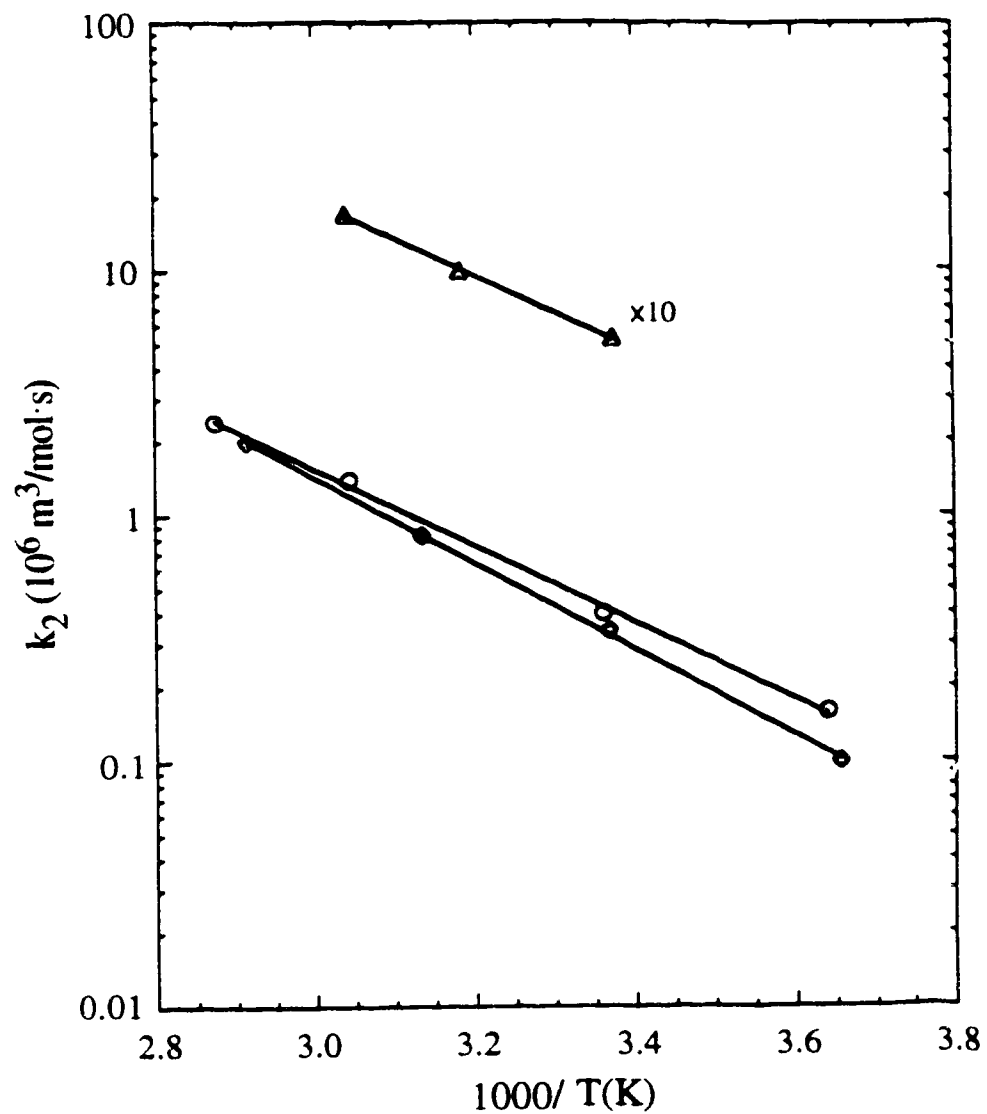


Figure 5-6. Arrhenius plots of measured k_2 for ($e_s^- + \text{nitrate}$) reaction in 1-hexanol (\diamond), 1-octanol (\circ), and 1-decanol (Δ). To separate the lines, k_2 in 1-decanol has been multiplied by 10.

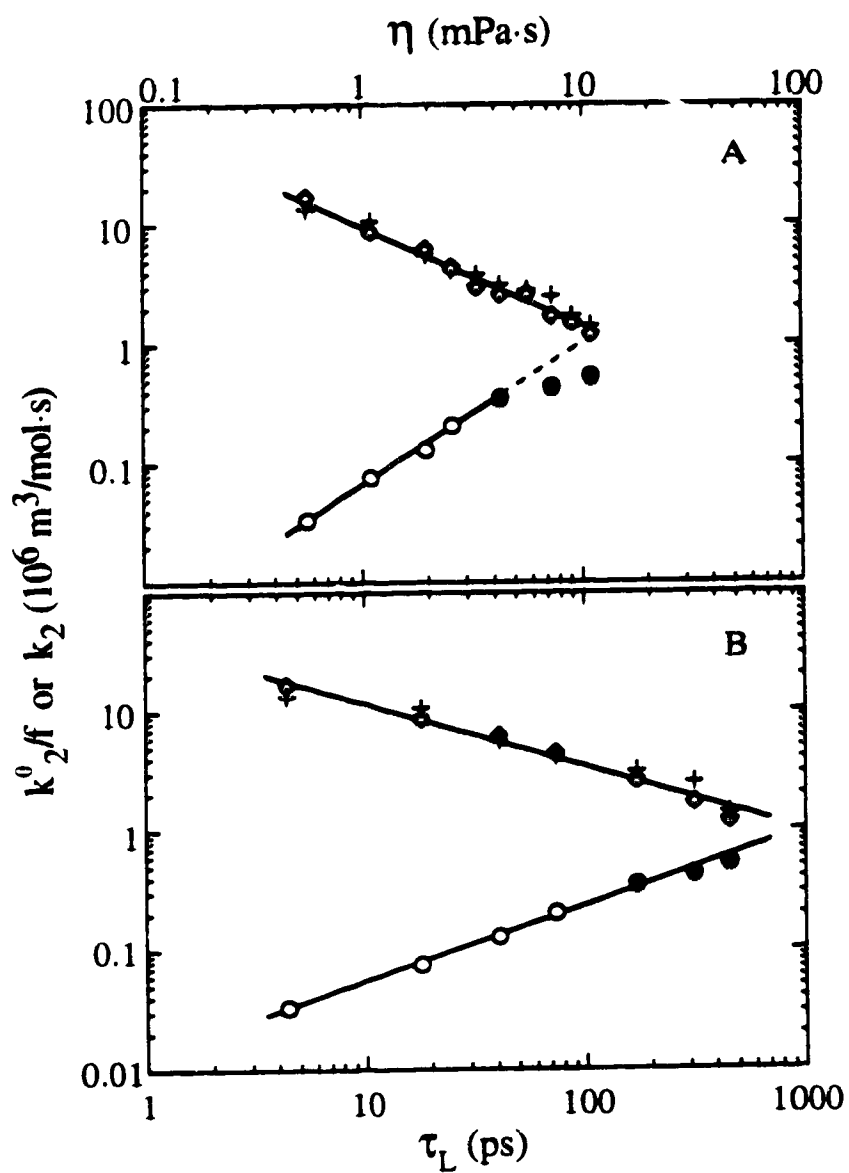


Figure 5-7. Dependences of rate constants on viscosity η (A) and dielectric longitudinal relaxation time τ_L (B) at 298K. k_2^0/f : +, (e_s^- + Pyrene), data from ref. 10; \diamond , (e_s^- + Ag_s^+), data from refs. 1, 11; \circ , (e_s^- + $NO_3_s^-$). \bullet , apparent k_2 for (e_s^- + lithium nitrate), see text.

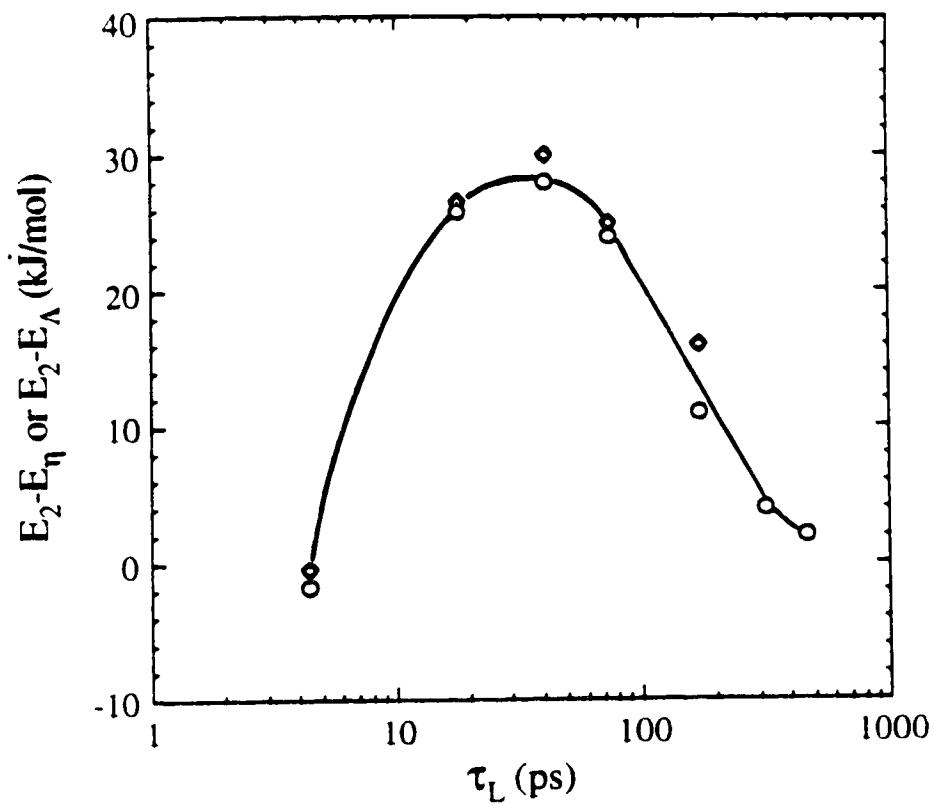


Figure 5-8. Activation energy E_2 of ($e^-_s + \text{nitrate}$) reaction in C_1 to C_{10} n -alcohols, expressed as excess over that of solvent viscosity E_η (O) or that of electrolyte mobility E_Λ (◊), plotted against τ_L at 298K.

References:

1. C. C. Lai. and G. R. Freeman. *J. Phys. Chem.* **94**, 4891(1990).
2. S. A. Peiris. and G. R. Freeman. *Can. J. Phys.* **68**, 940 (1990).
3. T. B. Kang and G. R. Freeman. *Can. J. Chem.* **71**, 1297 (1993).
4. M. Grätzel, A. Henglein, and S. Taniguchi. *Ber. Bunsen-Ges. Phys. Chem.* **74**, 292 (1970).
5. R. A. Marcus. *J. Chem. Phys.* **24**, 966 (1956).
6. M. D. Newton and N. Sutin. *Ann. Rev. Phys. Chem.* **35**, 437 (1984).
7. R. Chen, Y. Avotins, and G. R. Freeman. *Can. J. Chem.* **72**, 1083 (1994).
8. M. V. Smoluchowski. *Z. Phys. Chem.* **92**, 129 (1917).
9. P. Debye. *Trans. Electrochem. Soc.* **82**, 265 (1942).
10. Farhataziz, S. Kalachandra, and M. S. Tunuli. *J. Phys. Chem.* **88**, 3837 (1984).
11. M. S. Tunuli and Farhataziz. *J. Phys. Chem.* **90**, 6587 (1986).
12. R. Chen and G. R. Freeman. *Can. J. Chem.* **71**, 1303 (1993).
13. A. J. Elliot, D. R. McCracken, G. V. Buxton, and N. D. Wood. *J. Chem. Soc. Faraday Trans.* **86**, 1539 (1990).
14. R. Chen and G. R. Freeman. *J. Phys. Chem.* **96**, 7107 (1992).
15. G. J. Janz and R. P. T. Tomkins (*Editor*). *Nonaqueous Electrolytes Handbook*. Vol. 1. Academic Press, New York. 1972; (a) pp. 48 and 976; (b) p. 57; (c) p. 405.
16. M. A. Rauf, G. H. Stewart, and Farhataziz. *J. Chem. Eng. Data*, **28**, 324 (1983).
17. Y. Y. Akhadov (*Editor*). *Dielectric Properties of Binary Solutions*. Pergamon, Oxford. 1980; (a) pp. 427 and 450; (b) pp. 428 and 451.
18. A. D'Aprano, D. Donato, and E. Caponetti. *J. Solution Chem.* **8**, 135 (1979).

19. (a) A. A. Maryott and E. R. Smith. Tables of Dielectric Constants of Pure Liquids. NBS Circular 514. Washington, D.C. 1951; p. 29. (b) F. Buckley and A. A. Maryott. Tables of Dielectric Dispersion Data for Pure Liquids and Diluted Solutions. NBS Circular 589. Washington, D.C. 1958; pp. 12-15, 47. (c) G. Åkerlöf. J. Am. Chem. Soc. **54**, 4125 (1932).
20. S. K. Garg and C. P. Smyth. J. Phys. Chem. **69**, 1294 (1965).
21. C. W. Davies. Ion Association. Butterworths, London. 1962. p. 12.
22. P. W. Atkins. Physical Chemistry. 4th ed. Freeman, New York. 1990. (a) pp. 760, note that B requires F^2 ; (b) p. 764.
23. A. L. Horvath (*Editor*). Handbook of Aqueous Electrolyte Solutions. Wiley, New York. 1985. pp. 210.
24. Y. Zhao and G. R. Freeman. Can. J. Chem. (*submitted*). "Solvent Effects on Reactivity of Solvated Electrons with Ions in t-Butanol/Water Mixtures."
25. Y. Marcus. Ion Solvation. Wiley, New York. 1985. pp. 46-47.
26. G. R. Freeman. Radiation Chemistry; lecture notes. 1993. p. 243.
27. G. R. Freeman. In Kinetics of Nonhomogeneous Processes. Edited by G. R. Freeman. Wiley-Interscience, New York. 1987. p. 80.

Chapter Six

General Discussion and Conclusions

In this chapter, we first present the experimental results not included in the previous four chapters. We then give general discussion of all experimental results and correlate them with each other. Finally, We summarize the conclusions reached from the studies.

I. General Discussion of Molar Conductivities

Molar conductivities of the dilute reactant electrolyte solutions in both 1-butanol/water and *iso*-butanol/water mixed solvents have been measured. Arrhenius plots of LiNO_3 , NH_4NO_3 , NH_4ClO_4 , and HClO_4 , in 1-butanol/water mixed solvents; and for LiNO_3 , NH_4NO_3 , NH_4ClO_4 , HClO_4 , AgClO_4 , and $\text{Cu}(\text{ClO}_4)_2$ in *iso*-butanol/water mixed solvents are shown in Figures 6-1 to 6-10.

Molar conductivity measurement provides information about the diffusion coefficient of the reactant ion in the solutions; the diffusion coefficient is related to the conductivity by the Nernst-Einstein relation (1a). Diffusion coefficients of the solvated electrons in the mixed solvents are not known, so we used molar conductivity Λ of the reactant electrolyte and the known diffusion coefficient of the solvated electrons in water (2) to estimate the diffusion coefficients of the reactant ion and the solvated electrons in the mixed solvents (3,4).

Molar conductivity measurement also provides information about the ion pairing

of the reactant ion in the solutions. We used Λ to evaluate the extent of ion pairing of LiNO_3 in C_6 to C_{10} *n*-alcohols (5). In 1-butanol/water and *iso*-butanol/water mixed solvents, the specific electrical conductances of the dilute reactant electrolyte solutions varied linearly with added concentration of salt in the range used for rate constant measurement in most case. This meant that ion pairing was negligible under the conditions used. Exceptions are LiNO_3 and NH_4NO_3 at ≤ 10 mol% water mixed solvents at high temperature ($>328\text{K}$). Arrhenius plots of Λ in these cases are bent downwards at high temperatures (Figures 6-1, 6-2, 6-5, and 6-6). The activation energies in these cases were calculated from the slopes near 298K. The bending is due to the decreasing of the value of $\epsilon_r T$ as T increases; ϵ_r decreases relatively faster than T increases. This has two effects.

First, according to Debye-Hückel-Onsager equation (1b):

$$[6-1] \quad \Lambda = \Lambda_0 - (A + B\Lambda_0)C^{1/2}$$

where, Λ_0 is the molar conductivity at infinite dilution, C the concentration of the salt, and A , B are functions of $\epsilon_r T$ (1b).

$$[6-2] \quad A = \frac{\xi F^2}{3\pi\eta} \left(\frac{2}{\epsilon_r T} \right)^{1/2}$$

and

$$[6-3] \quad B = \frac{0.586\xi F^2}{6\pi} \left(\frac{1}{2\epsilon_r T} \right)^{3/2}$$

where ξ is the protonic charge, F the Faraday, η the shear viscosity of the solvent, $\epsilon = \epsilon_0\epsilon_r$ the permittivity of the solvent, R the gas constant, and all units are SI.

The decrease of $\epsilon_r T$ makes A and B increase. This would give Λ a more negative dependence on C . At lower temperatures, Λ is a good approximation of Λ_0 , whereas at high temperatures, Λ may be noticeably smaller than Λ_0 even in the dilute solutions.

Secondly, decreasing $\epsilon_r T$ increases the probability of ion pairing, so there may be a small extent of ion pairing in these solutions at high temperatures. Arrhenius plots of rate constants for the reactions of ($e_s^- + NO_{3,s}^-$) and ($e_s^- +$ ammonium nitrate) are linear in the whole temperature range in ≤ 10 mol% water mixed solvents. This indicates that the first effect may be the main reason for the bending of Λ against $1/T$ plots.

Another remarkable feature is the higher values of Λ for $AgClO_4$ in 98 mol% water and for $Cu(ClO_4)_2$ in 99.5, 99, and 98 mol% water *iso*-butanol/water mixed solvents, which are even larger than those in pure water, and the strong bending of Arrhenius plots (Figures 6-9 and 6-10). Arrhenius plots of Λ for NH_4NO_3 , NH_4ClO_4 , and $HClO_4$ are also bent in 98 mol% water *iso*-butanol/water mixed solvents, but the values of Λ are lower than those in pure water (Figures 6-6 to 6-8). We need more study to understand the increase of Λ for $AgClO_4$ and $Cu(ClO_4)_2$ solutions. The decrease of Λ for the other solutions is due to an increase of solvent viscosity upon addition of 2 mol% alcohol to water.

We do not understand the curvatures of the Arrhenius plots of Λ in <100 but ≥ 98 mol% water mixed solvents. They are not due to the decrease of $\epsilon_r T$ and also ion pairing is negligible, since ϵ_r is larger than those in alcohol-rich region and the specific electrical conductances of the dilute reactant electrolyte solutions varied linearly with added concentration of salt. It might be related to the complicated liquid structure change in this narrow range near the critical two phase composition. Recent experimental investigations from small-angle X-ray scattering (6, 7), neutron scattering (8, 9), and fluorescence probing and ultrasonic absorption (10, 11) suggest that short-chain alcohols form micelle-like aggregates in aqueous solutions at above a certain concentration range. Fluorescence probing (11) conclude that C_2 to C_4 monoalcohols self-associate in water to form aggregates which share many properties with micelles of conventional surfactants. The critical aggregation mole percent is 2.5 mol% alcohol for 1-butanol and 6.7 mol% alcohol for *iso*-butanol at 298K. These investigations and others (12) showed

that alcohol/water mixtures form composite structures. We suggest that dilute solutions of electrolytes in alcohol/water mixtures near the critical 2 phase composition might have properties characteristic of nanoemulsions. This is worth a future separate study.

II. General Discussion of Solvated Electrons Reactions

A. Reactions of $(e_s^- + H_s^+)$ and $(e_s^- + NH_{4,s}^+)$

The experimental results of k_2 for $(e_s^- + NH_{4,s}^+)$ reaction in 1-butanol/water mixed solvents are in chapter three (3); those of $(e_s^- + NH_{4,s}^+)$ and $(e_s^- + H_s^+)$ reactions in *iso*-butanol/water mixed solvents are in chapter four (4). We here first present the experimental results of k_2 for $(e_s^- + H_s^+)$ reaction in 1-butanol/water mixed solvents and then give a general discussion on these reactions.

Arrhenius plots of k_2 for $HClO_4$ solutions in 1-butanol/water mixed solvents are given in Figure 6-11. The mol% water represented by the symbols in the figure are as in Table 3-1, p. 50. The reaction in $HClO_4$ solution is due to $(e_s^- + H_s^+)$, since the rate constant for $(e_s^- + ClO_{4,s}^-)$ reaction is very low (3). Figure 6-12 displays the solvent composition dependence of k_2 at 298K for this reaction in 1-butanol/water mixed solvent, along with those of $(e_s^- + NO_{3,s}^-)$, $(e_s^- + NH_{4,s}^+)$, and e_s^- reaction with $NH_{4,s}^+$ and $NO_{3,s}^-$ in combination. The coulombic interaction of e_s^- with different kinds of ions is accounted for by the Debye factor f (13). Dividing of k_2 by f reduces the apparent difference between $(e_s^- + H_s^+)$ and $(e_s^- + NO_{3,s}^-)$ reactions. We obtain information about solvent effects on e_s^- reactivity with ions by estimating the effective reaction radius, κR_r (4):

$$[6-4] \quad \kappa R_r \approx 1 \times 10^{-16} z k_2 / f T \Lambda .$$

where κ is the probability that reaction occurs during the lifetime of an encounter pair, z the number of charges on the reactant ion, T the absolute temperature, and Λ the molar conductivity in the dilute solutions.

Molar conductivities of HClO_4 solutions in 1-butanol/water mixed solvents at 298K are shown in Figure 6-13. Rate parameters for $(e_s^- + H_s^+)$ reaction in 1-butanol/water mixed solvents are listed in Table 6-1. Solvent composition dependence of κR_f for e_s^- reactions with H_s^+ , along with those with $\text{NO}_{3,s}^-$ and $\text{NH}_{4,s}^+$ in 1-butanol/water mixed solvents, are shown in Figure 6-14. The change of κR_f with solvent composition for $(e_s^- + H_s^+)$ reaction is similar to that in *iso*-butanol/water mixed solvents (4). The value of κR_f for $(e_s^- + H_s^+)$ reaction in water is lower than that for $(e_s^- + \text{NO}_{3,s}^-)$, whereas the reverse is true in both 1-butanol and *iso*-butanol. The H_s^+ is only ~ 0.2 times as reactive in pure water as in the alcohol-rich solvents. The reaction $(e_s^- + H_s^+)$ in water is ~ 0.2 times slower than diffusion controlled (14, 15) and the reaction is diffusion controlled in alcohol. The change in rate is somewhat similar to that of reaction $(e_s^- + \text{NH}_{4,s}^+)$, although the magnitude of change is much smaller.

Both $\text{NH}_{4,s}^+$ and H_s^+ have no low-lying orbital for an electron to occupy, so their reactions with the solvated electrons occur either by proton transfer to the electron site or the electron transfer, followed by the decomposition of the neutral species. Although the opinion of electron transfer mechanism dominated in the 1960s (14, 16), J. Jortner and coworkers found that a number of moderately slow e_s^- reactions with Brønsted acids in water giving H atoms as product could be correlated with a logarithmic plot of reaction rate constant against pK_a for the Brønsted acid (17, 18). A recent study of $\text{H}_{\text{aq.}} \rightleftharpoons e_{\text{aq.}}^-$ inter conversion also favored proton transfer mechanism for the explanation of $e_{\text{aq.}}^-$ reactions (19). Both $\text{NH}_{4,s}^+$ and H_s^+ are Brønsted acids. Their rates of reaction with the solvated electrons are related to their acidity in the solutions. The H_s^+ ion is a stronger Brønsted acid than $\text{NH}_{4,s}^+$ and the rate for $(e_s^- + H_s^+)$ reaction in water is much faster than that for $(e_s^- + \text{NH}_{4,s}^+)$ reaction, but still ~ 0.2 times slower than diffusion controlled. The H_s^+ ion in water is an exceptionally poor scavenger of the presolvated electrons (20, 21).

A lot of experimental results support the conclusion that ammonium ion is

stabilized by hydrogen bonding of its hydrogen atoms with water molecules to fit into the water hydrogen bonding network, and that its acidity is decreased from what it would be in the absence of such stabilization (22-24). We suggest that the tetrahedral, symmetrical hydrogen bonded solvation structure of ammonium ion in water reduces the probability of proton transfer from it to the electron site, or of the electron attachment to it. The hydronium ion ($\text{OH}_{3,s}^+$) has a partially symmetrical, tetrahedral hydrogen bonded solvation structure in water that reduces to a less extent the probability of proton transfer from it to the electron site, or of the electron attachment to it. In monoalcohols, each alcohol molecule contains one -OH group that can bond with others to form a chain or ring structure in the liquid, but not a three-dimensional structure like that of water. This would greatly influence the solvation structure of ammonium ion and hydrogen ion in them. It is, therefore, reasonable to suggest that both $\text{NH}_{4,s}^+$ and $\text{ROH}_{2,s}^+$ are unsymmetrically solvated in monoalcohols and this would greatly facilitate the proton transfer from $\text{NH}_{4,s}^+$ and $\text{ROH}_{2,s}^+$ to the electron site, or electron attachment to them and subsequent decomposition of the neutral species.

B. Reactions of ($e_s^- + \text{Ag}_s^+$), ($e_s^- + \text{Cu}_s^{2+}$), and ($e_s^- + \text{NO}_{3,s}^-$)

Reactions of ($e_s^- + \text{Ag}_s^+$) and ($e_s^- + \text{Cu}_s^{2+}$) are close to diffusion controlled reaction limit in *iso*-butanol/water mixed solvents. The normalized rate constants, k_2/f , are essentially the same for both ($e_s^- + \text{Ag}_s^+$) and ($e_s^- + \text{Cu}_s^{2+}$) reactions in alcohol-rich region; that for ($e_s^- + \text{Ag}_s^+$) is larger than that for ($e_s^- + \text{Cu}_s^{2+}$) in water-rich region. (Figure 4-7, p. 94). The modified Smoluchowski-Debye model considers the effects of solvent transport properties and coulombic interactions between ions on the reaction rates and can be applied to these nearly diffusion controlled reactions (4). The change in solvent transport properties and coulombic interactions between ions can be normalized for different reactions by considering the effective reaction radius κR_f (see equation [6-4]). The values of κR_f are relatively insensitive to the change of solvent composition for

both ($e_s^- + Ag_s^+$) and ($e_s^- + Cu_s^{2+}$) reactions in *iso*-butanol/water mixed solvents (see Figure 4-11, p. 98). The average value of κR_T is 0.7 nm. For these nearly diffusion controlled reactions, the normalized rates of reactions, k_2/f , are more influenced by changes in solvent transport properties than changes in solvation structures, in contrast of the cases of ($e_s^- + H_s^+$) and ($e_s^- + NH_{4,s}^+$) reactions.

Reaction of ($e_s^- + NO_{3,s}^-$) in water is close to the diffusion controlled reaction limit, and gradually deviates from it as the alcohol content increases in both 1-butanol/water and *iso*-butanol/water mixed solvents (Figure 3-6, p. 59 and Figure 4-7, p. 94). The normalized rate constant, k_2/f , decreases faster when the water content is ≤ 10 mol%. In these solvents the ($e_s^- + NO_{3,s}^-$) reaction is mainly reactivity controlled. This relatively slow reaction *increases* with *increasing* viscosity η and dielectric longitudinal relaxation time τ_L , which means it is assisted by a longer encounter duration (4, 5). Due to lack of τ_L data in the mixed solvents, only the data in pure alcohol solvents have been analyzed (4, 5). The main conclusions we reached there (5), however, would also apply to ≤ 10 mol% water 1-butanol/water and *iso*-butanol/water mixed solvents.

III. Conclusions

The main conclusions reached in these experimental studies are:

1. The value of k_2 for $(e_s^- + NO_{3,s}^-)$ reaction in water solvent is ~ 40 times larger than that in 1-butanol or *iso*-butanol solvent, whereas the values of k_2 for $(e_s^- + NH_{4,s}^+)$ reaction in water is $\sim 10^{-4}$ times smaller than the value in 1- or *iso*-butanol-rich solvents. This enormous reversal of solvent effects on e_s^- reaction rates is the first observed for ionic reactants. A similar change like that of $(e_s^- + NH_{4,s}^+)$, but with a less extent, also happens in $(e_s^- + H_s^+)$ reaction. The low reactivity of $NH_{4,s}^+$ with e_s^- in water, and the less than diffusion controlled rate of $(e_s^- + OH_{3,s}^+)$, is attributed to the symmetrical hydrogen-bonded solvation structure of NH_4^+ and the partially symmetrical solvation structure of OH_3^+ . We suggest that the proton transfer or decomposition of the neutral species of these reactions in alcohols is facilitated by an unsymmetrical solvation structure.
2. The reaction rate constants k_2 for solvated electron reaction with nitrate ions in C_1 to C_{10} *n*-alcohols increase with *increasing* viscosity η and longitudinal relaxation time τ_L of the solvent. This relatively slow reaction is assisted by a longer encounter duration. The mean time required for an encounter pair to react, k_r^{-1} , is $\gg \tau_L$ in methanol, whereas $k_r^{-1} < \tau_L$ in 1-octanol and 1-decanol. The reaction of e_s^- with nitrate is activation *entropy* limited in methanol, mainly activation *energy* limited in C_2 to C_4 *n*-alcohols, and mainly diffusion/dipole rotation limited in 1-decanol.
3. Reactions of $(e_s^- + Ag_s^+)$ and $(e_s^- + Cu_s^{2+})$ are close to the diffusion controlled reaction limit in the whole range of *iso*-butanol/water mixed solvents. For these nearly diffusion controlled reactions, the normalized rates of reactions, k_2/f , are mainly influenced by changes in solvent transport properties. The larger values of k_2/f for $(e_s^- + H_s^+)$ reaction in both 1- or *iso*-butanol-rich solvents are due to the larger

diffusion coefficient of H_s^+ by proton hopping than those of other ions in these solvents.

4. Reaction of e_s^- in $Al(ClO_4)_3$ solutions in water is due mainly to H_s^+ from hydrolysis of Al_s^{3+} , and partly to partially hydroxylated aluminum (III) species. Reaction of e_s^- with Al_s^{3+} itself appears to be negligible in water. The reactivity of the solutions of $Al(ClO_4)_3$ in *iso*-butanol-rich solvents is 3–5 times greater than that in water. This may be due to the higher concentration of H_s^+ from the larger extent of hydrolysis of Al_s^{3+} in these solutions.

5. The values of Λ for $AgClO_4$ in 98 mol% water and for $Cu(ClO_4)_2$ in 99.5, 99, and 98 mol% water *iso*-butanol/water mixed solvents are higher than those in pure water. This is attributed to an increase of hydrolysis of metal ions to form H_s^+ . The curvatures of the Arrhenius plots of Λ in these mixed solvents are not due to the decrease of $\epsilon_r T$ and ion pairing. They might relate to the complicated liquid structure change in this narrow range near the critical two phase composition.

6. Electrical conductivity measurement demonstrates that ammonium nitrate behaves as a normal, strong electrolyte in methanol. The molar conductivities are fitted by the Onsager-Fuoss equation, the second term of which contributes the greatest reduction in conductivity and corresponds to the ion-atmosphere (long range coulombic interactions) model of Milner, Debye and Hückel.

Table 6-1. Rate parameters for reaction of solvated electrons with hydrogen ion in 1-butanol/water mixed solvents at 298 K.

ϵ_r^a	η^b (10^{-3} Pa·s)	mol % H ₂ O	f^c	k_2 (10^6 m ³ /mol·s)	k_2/f (10^6 m ³ /mol·s)	E_2^d (kJ/mol)	Λ^e (10^{-3} S·m ² /mol)	E_A^f (kJ/mol)
H_s^+ ^g								
78.5	0.89	100	1.40	24.	17.	12.	40.3	10.
19.8	2.92	45	3.01	20.	6.6	28.	3.08	21.
18.4	2.81	35	3.20	21.	6.6	27.	2.58	21.
17.8	2.70	20	3.29	18.	5.5	25.	1.83	21.
17.5	2.66	10	3.34	14.	4.2	26.	1.66	21.
17.4	2.60	0	3.35	18.	5.4	27.	1.46	21.

- a. Relative dielectric permittivity. Those for 45 and 35 mol % are for *iso*-butanol/water mixtures. Data from refs. 9, 10 of chapter three.
- b. Viscosity. Data from ref. 1 of chapter three.
- c. Debye factor.
- d. Temperature coefficient at 298 K from Arrhenius plots of k_2 .
- e. Molar conductivity of the dilute solutions.
- f. Temperature coefficient at 298 K from Arrhenius plots of Λ .
- g. H_s^+ in HClO₄ solutions, concentrations 0.007-0.18 mol/m³.

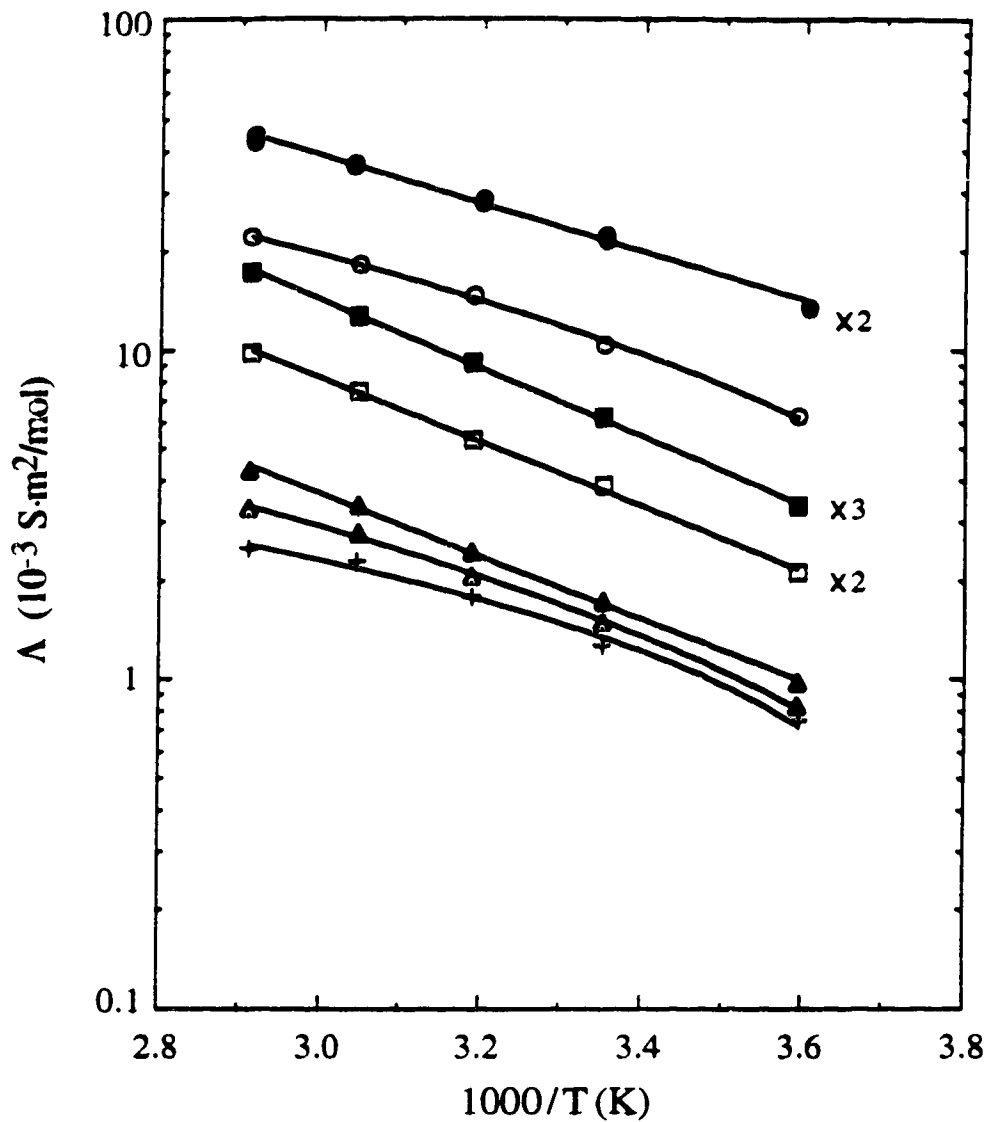


Figure 6-1. Arrhenius plots of Λ of LiNO_3 solutions in 1-butanol/water mixed solvents. Symbols representing mol% water are given in Table 3-1. To separate the lines, some values of Λ have been multiplied by the factors indicated.

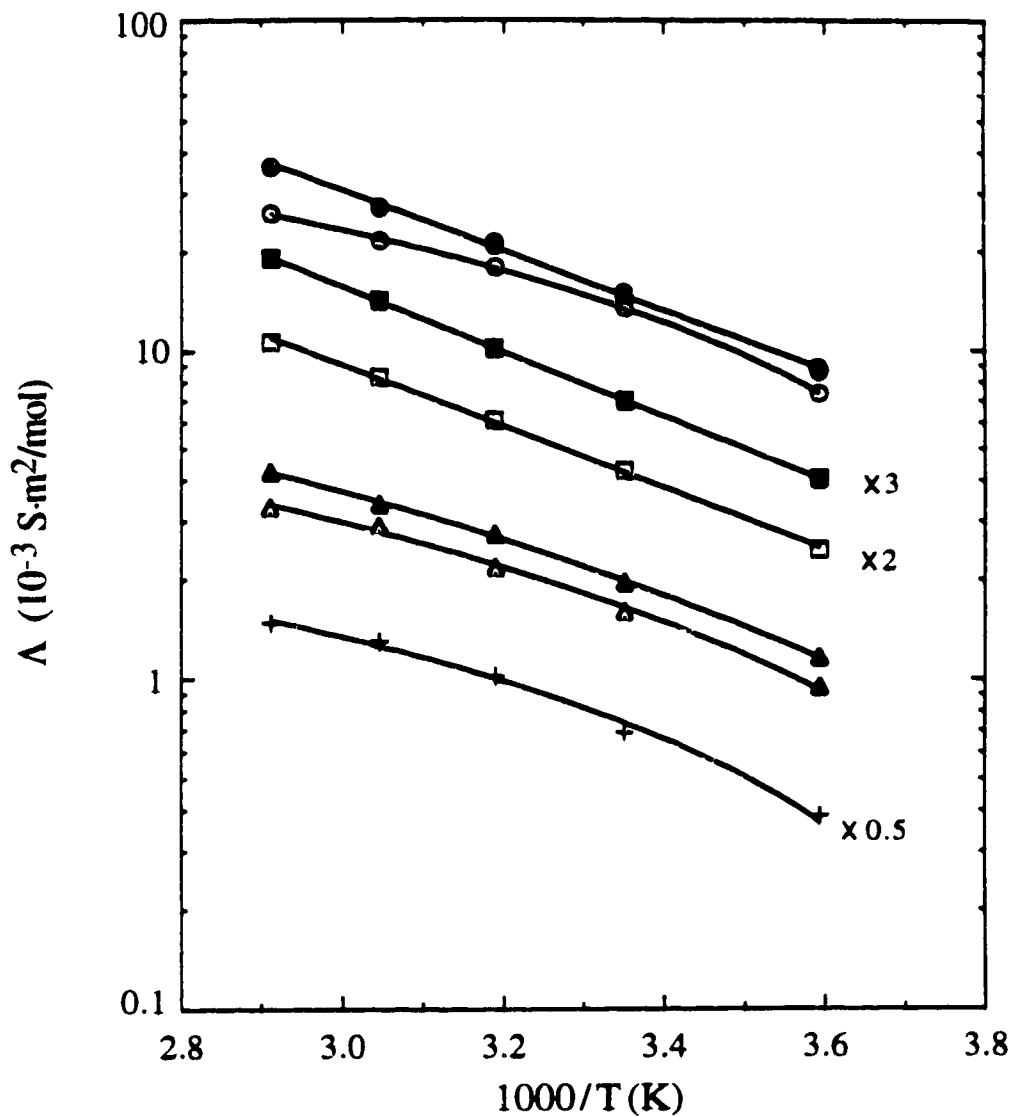


Figure 6-2. Arrhenius plots of Λ of NH_4NO_3 solutions in 1-butanol/water mixed solvents. Symbols representing mol% water are given in Table 3-1. To separate the lines, some values of Λ have been multiplied by the factors indicated.

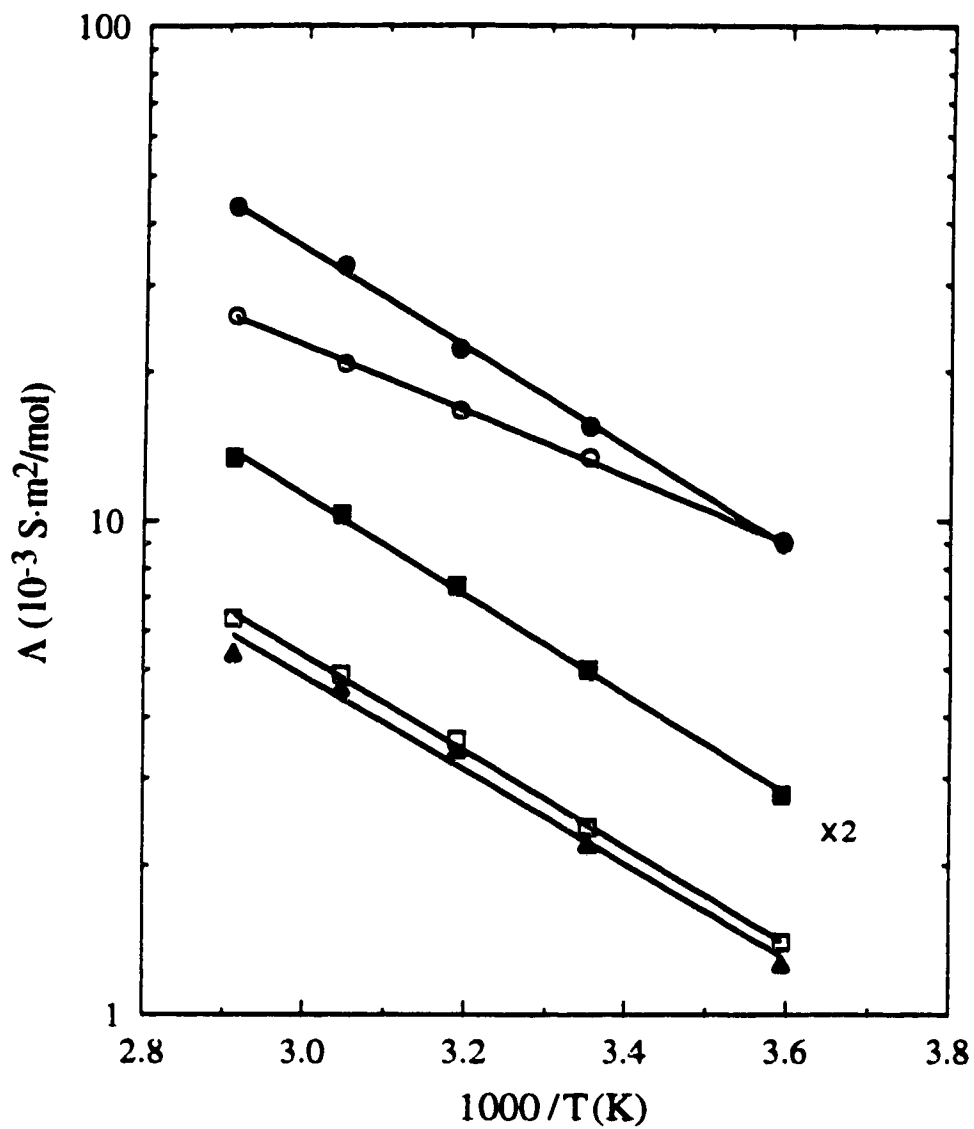


Figure 6-3. Arrhenius plots of Λ of NH_4ClO_4 solutions in 1-butanol/water mixed solvents. Symbols representing mol% water are given in Table 3-1. To separate the lines, some values of Λ have been multiplied by the factors indicated.

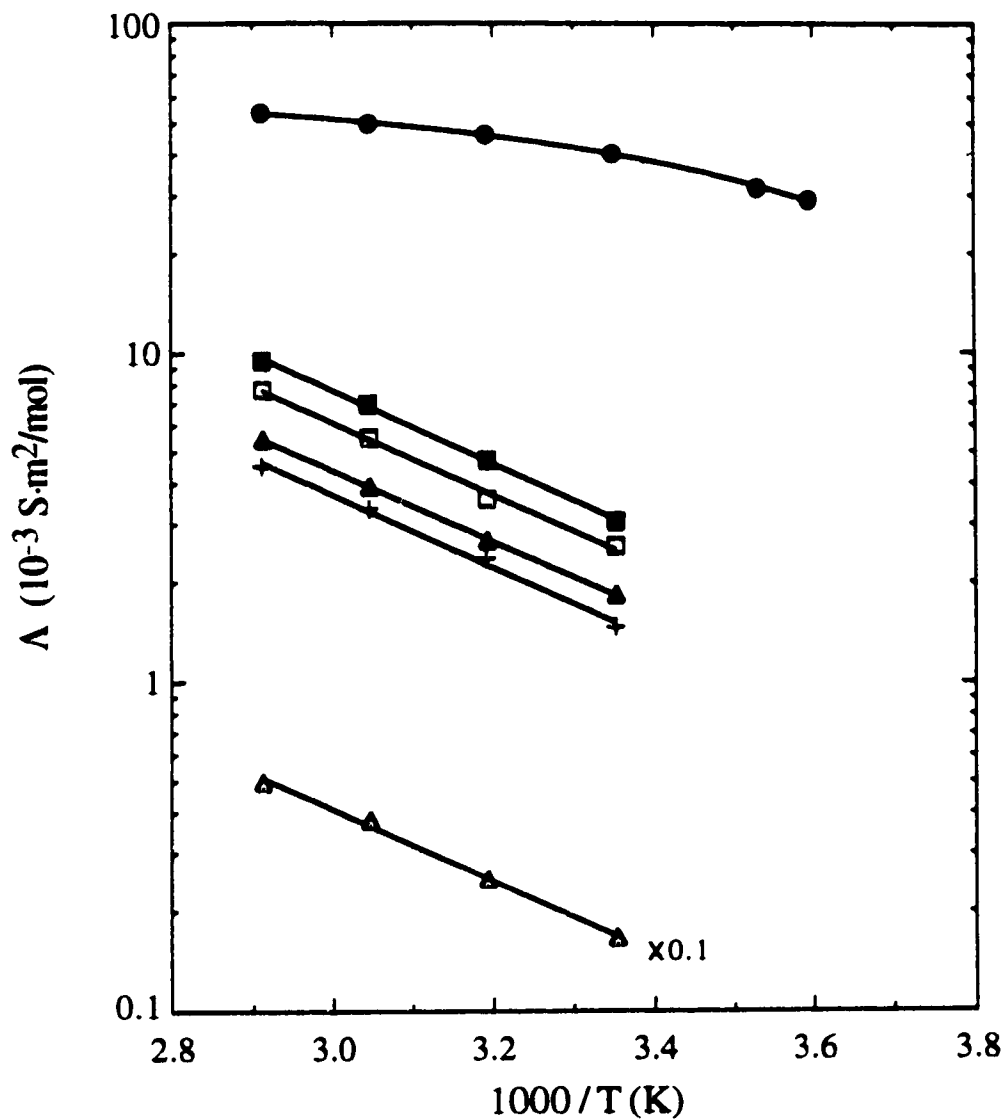


Figure 6-4. Arrhenius plots of Λ of HClO_4 solutions in 1-butanol/water mixed solvents. Symbols representing mol% water are given in Table 3-1. To separate the lines, some values of Λ have been multiplied by the factors indicated.

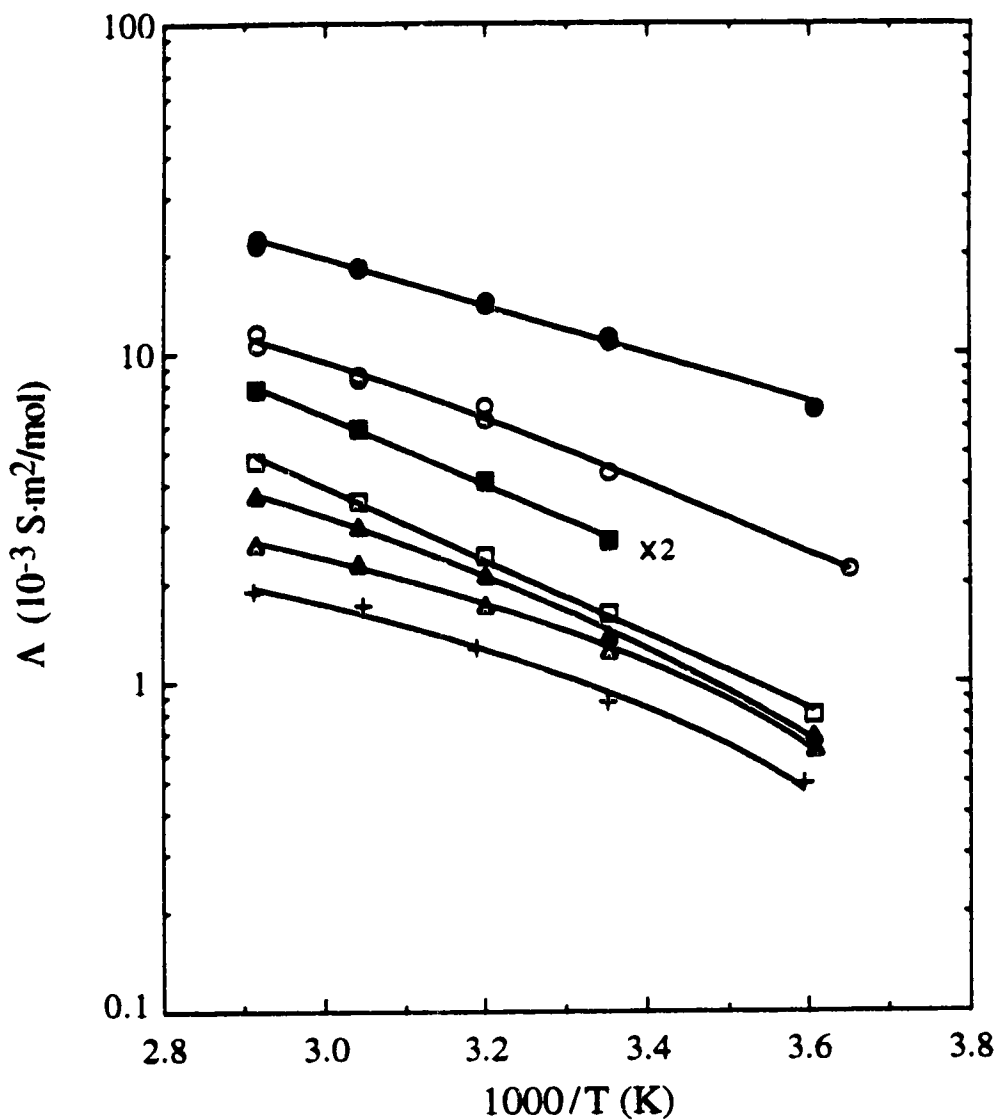


Figure 6-5. Arrhenius plots of Λ of LiNO_3 solutions in *iso*-butanol/water mixed solvents. Symbols representing mol% water are given in Table 4-1. To separate the lines, some values of Λ have been multiplied by the factors indicated.

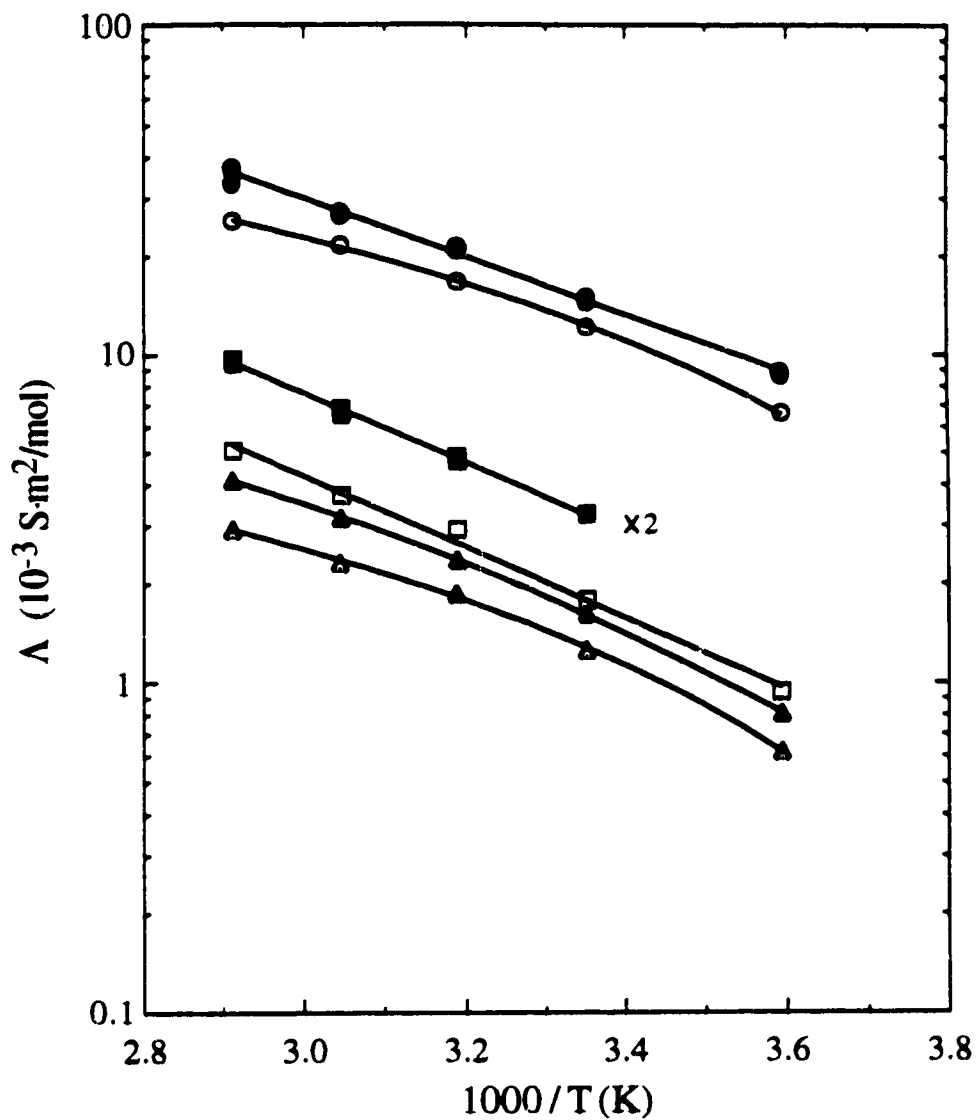


Figure 6-6. Arrhenius plots of Λ of NH_4NO_3 solutions in *iso*-butanol/water mixed solvents. Symbols representing mol% water are given in Table 4-1. To separate the lines, some values of Λ have been multiplied by the factors indicated.

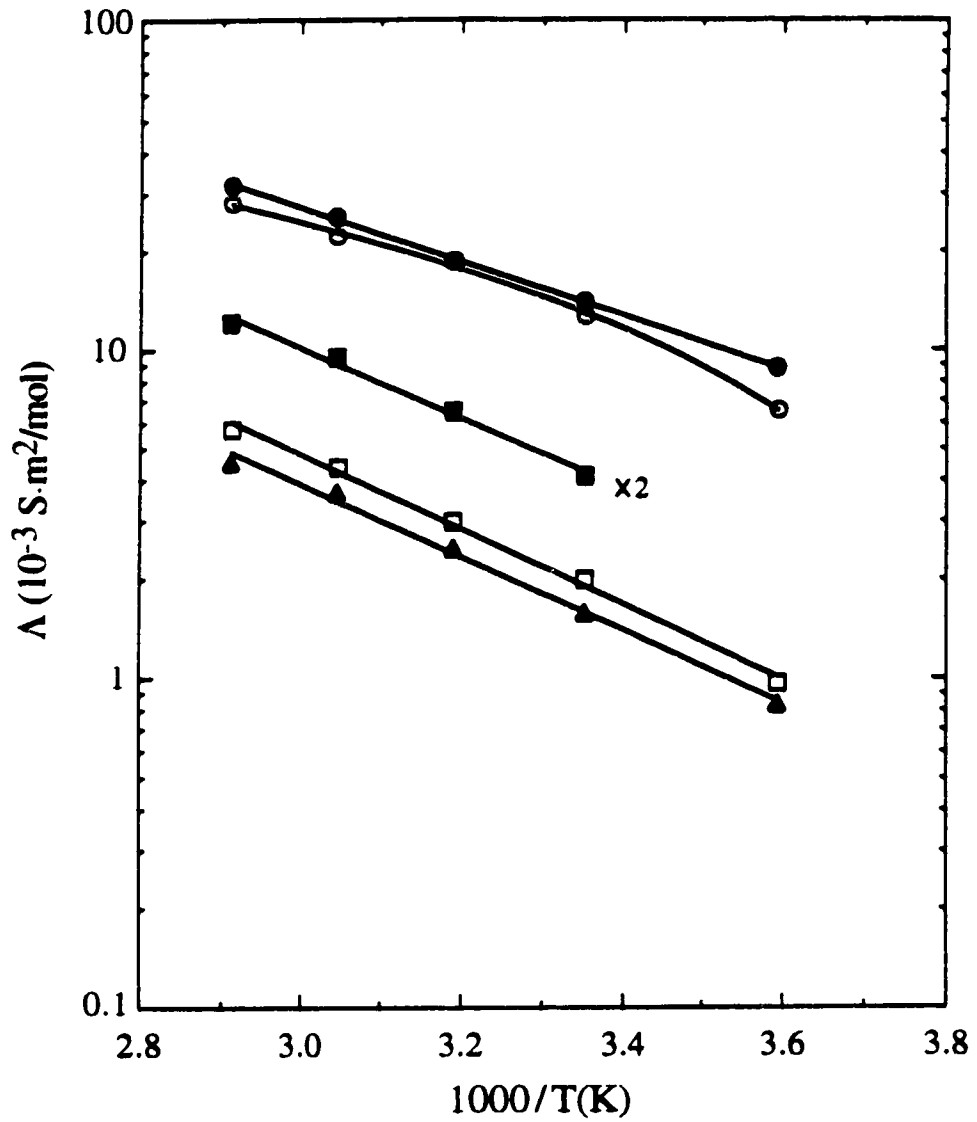


Figure 6-7. Arrhenius plots of Λ of NH_4ClO_4 solutions in *iso*-butanol/water mixed solvents. Symbols representing mol% water are given in Table 4-1. To separate the lines, some values of Λ have been multiplied by the factors indicated.

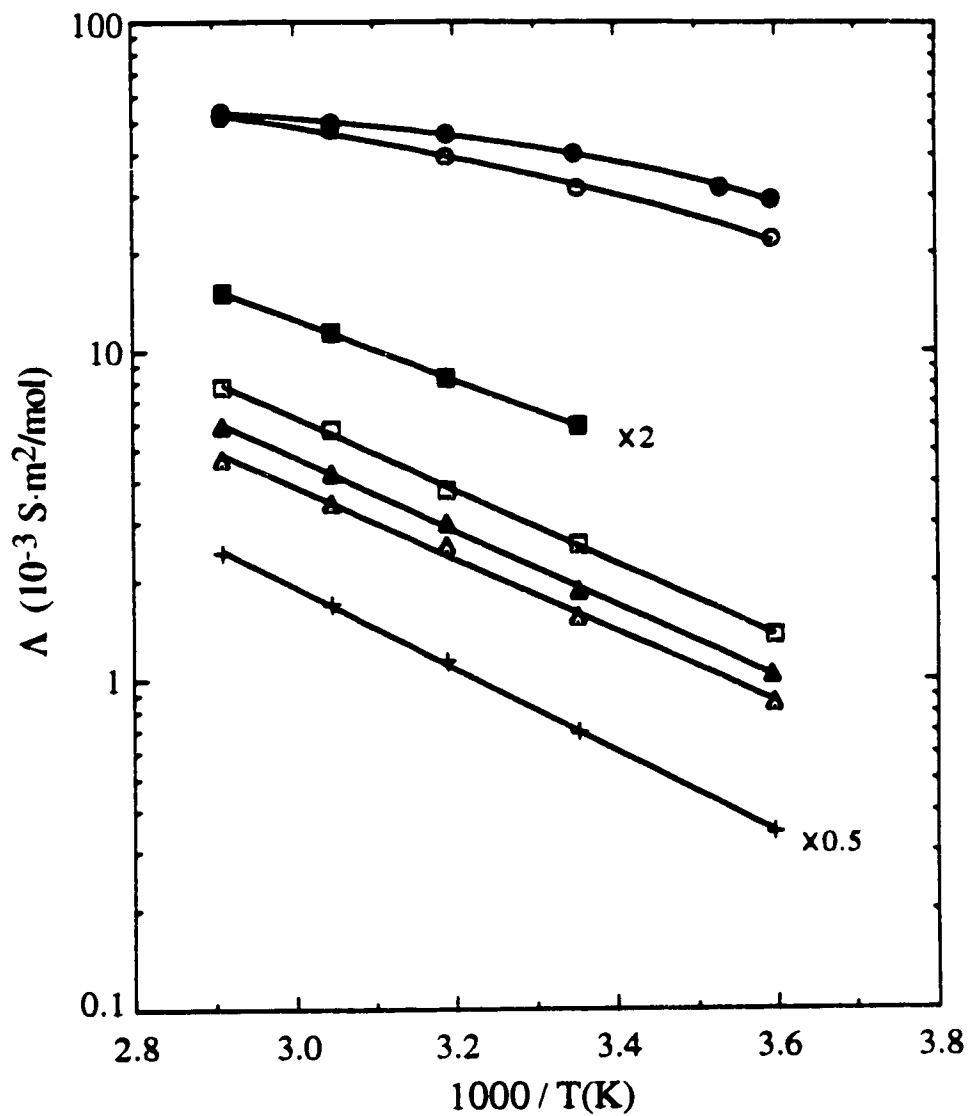


Figure 6-8. Arrhenius plots of Λ of HClO_4 solutions in *iso*-butanol/water mixed solvents. Symbols representing mol% water are given in Table 4-1. To separate the lines, some values of Λ have been multiplied by the factors indicated.

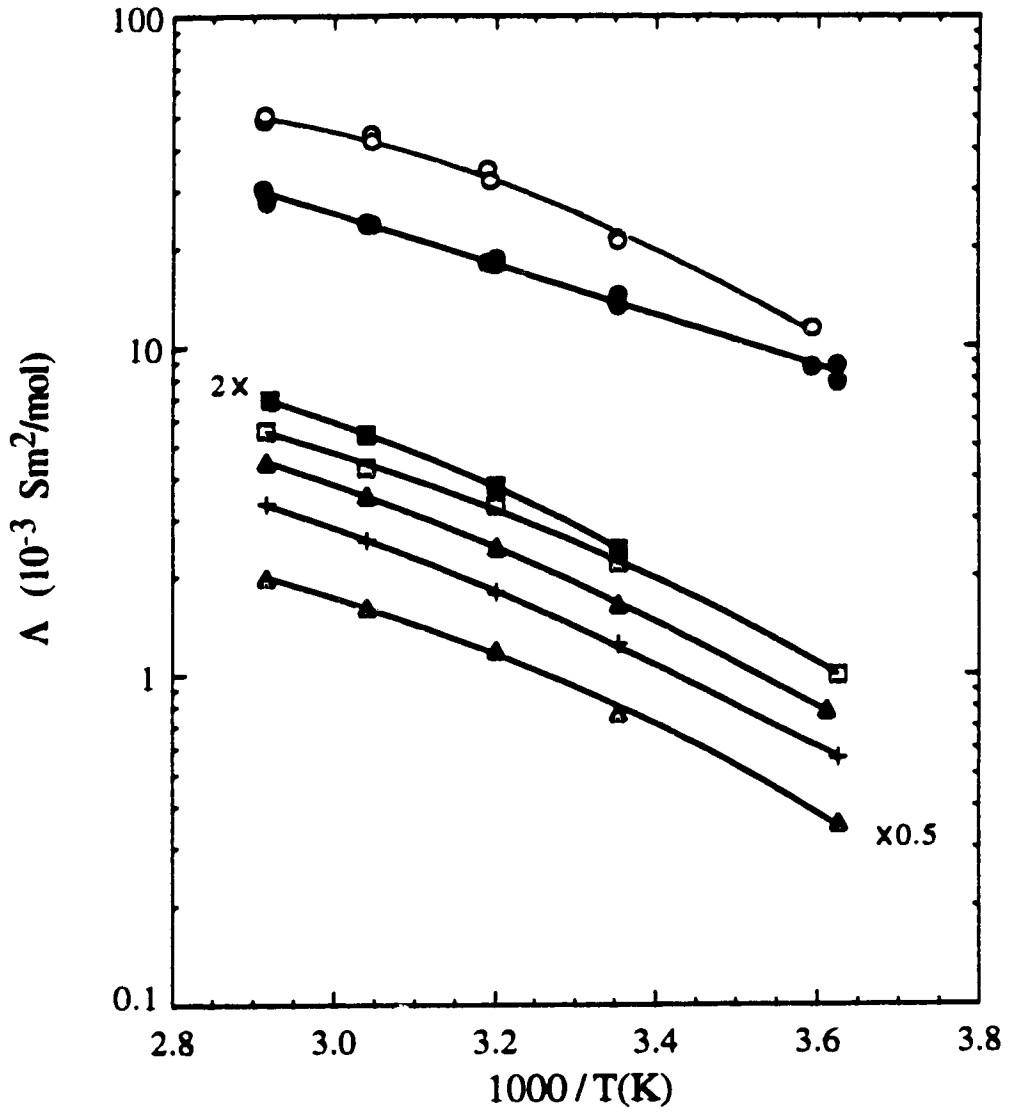


Figure 6-9. Arrhenius plots of Λ of AgClO_4 solutions in *iso*-butanol/water mixed solvents. Symbols representing mol% water are given in Table 4-1. To separate the lines, some values of Λ have been multiplied by the factors indicated.

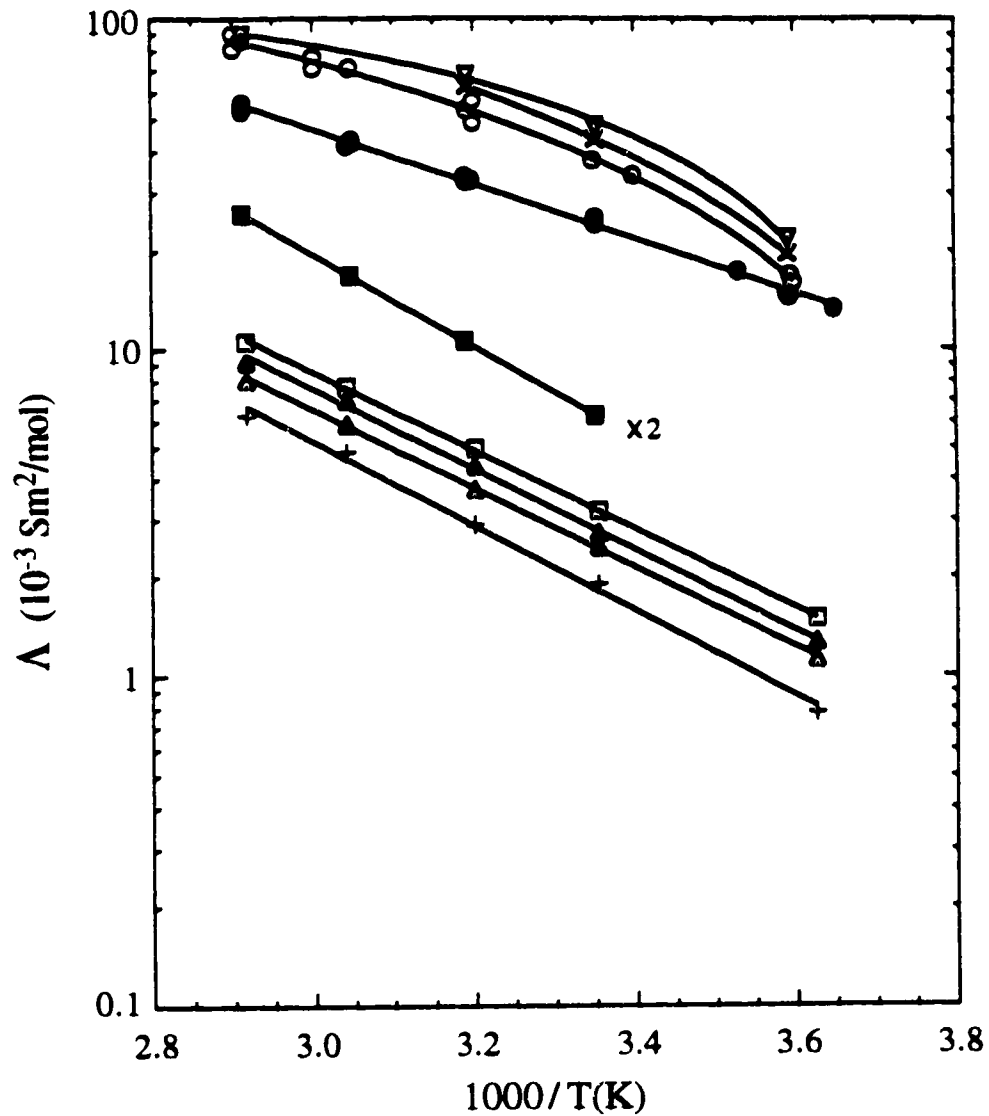


Figure 6-10. Arrhenius plots of Λ of $\text{Cu}(\text{ClO}_4)_2$ solutions in *iso*-butanol/water mixed solvents. Some symbols representing mol% water are given in Table 4-1, with the rest giving here: \times , 99.5; ∇ , 99 mol% water. To separate the lines, some values of Λ have been multiplied by the factors indicated.

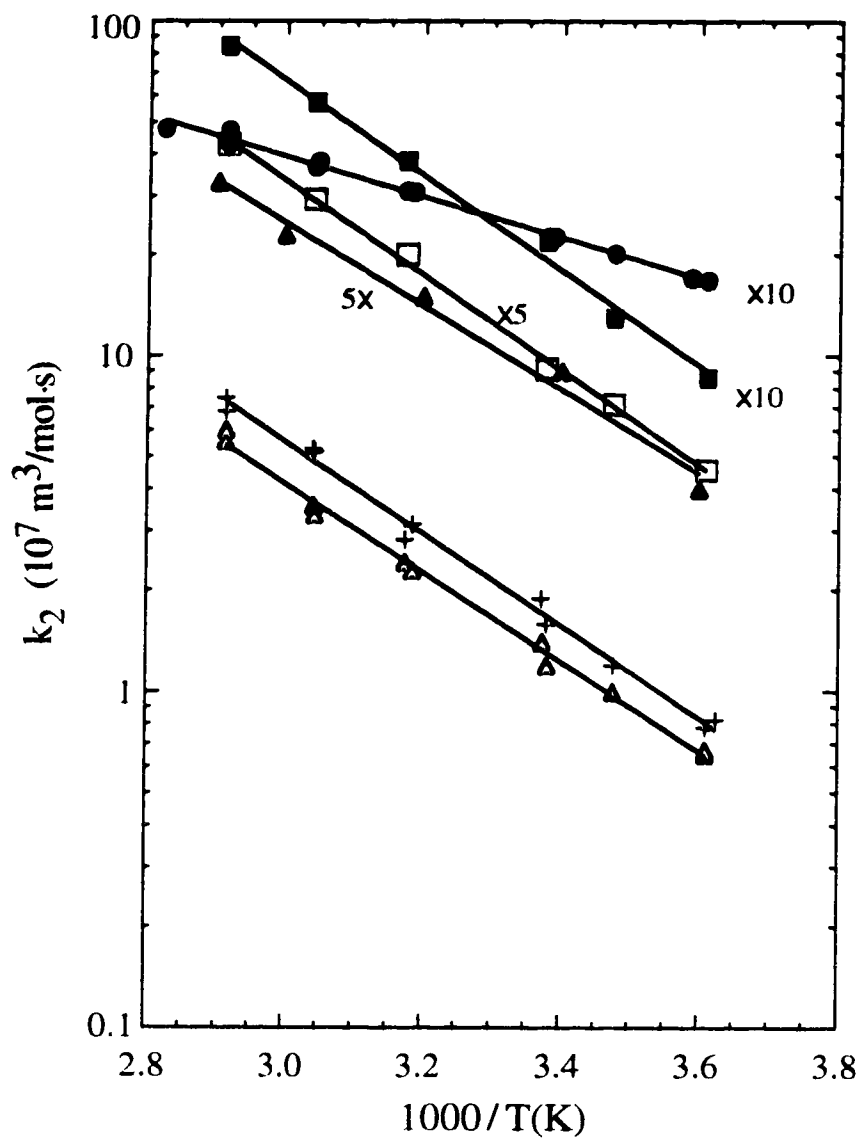


Figure 6-11. Arrhenius plots of k_2 of e_s^- reactions with perchloric acid in 1-butanol/water solvents. Symbols representing mol% water are given in Table 3-1. To separate the lines, some values of k_2 have been multiplied by the factors indicated.

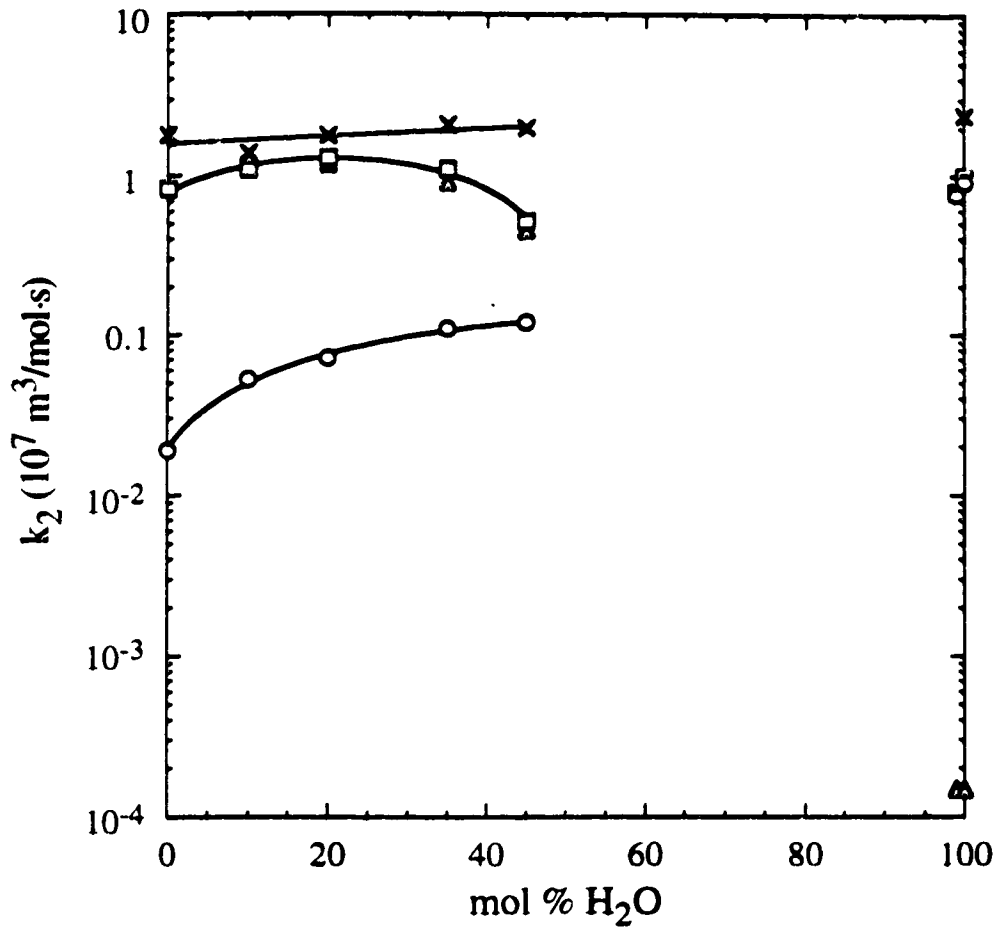


Figure 6-12. Solvent composition dependence of k_2 for $(e_s^- + H_s^+)$ at 298K in 1-butanol/water solvents. O, LiNO₃; □, NH₄NO₃; Δ, NH₄ClO₄; x, HClO₄.

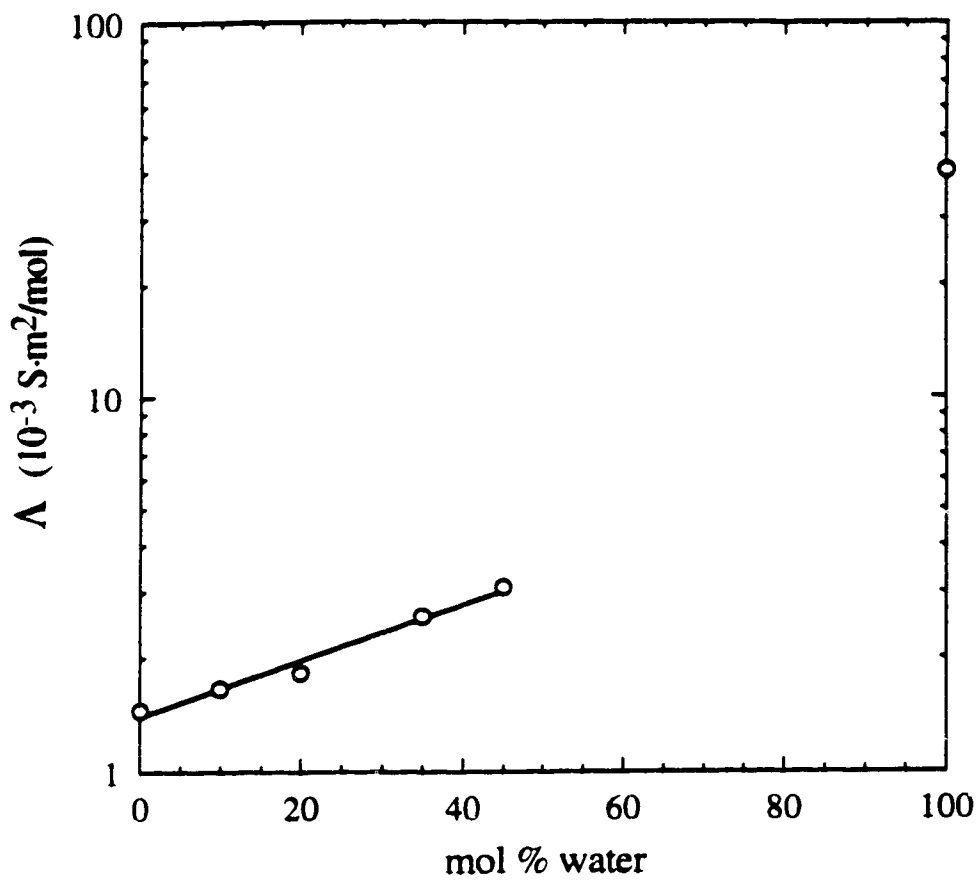


Figure 6-13. Solvent composition dependence of Λ of HClO_4 electrolyte solutions in 1-butanol/water mixed solvents at 298K.

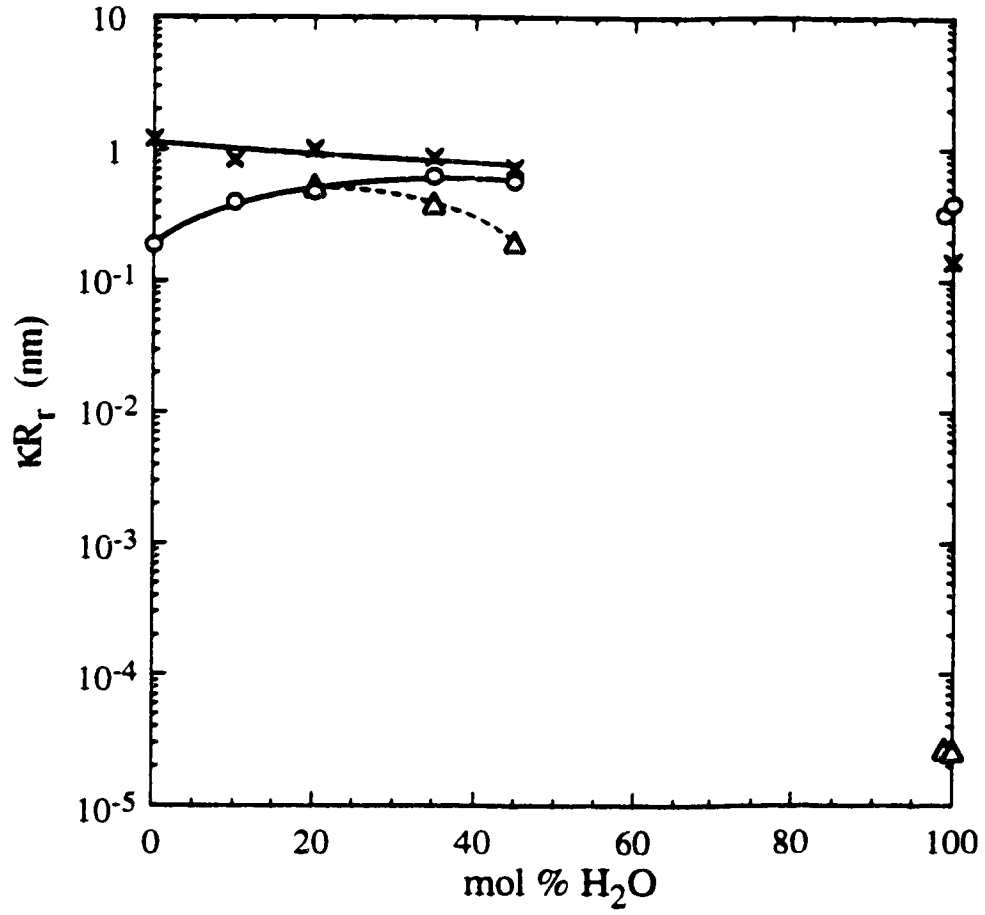


Figure 6-14. Solvent composition dependence of κR_r , equation [6-4], in 1-butanol/water mixed solvents at 298K. Symbols as in Figure 6-12.

References:

1. P. W. Atkins. *Physical Chemistry*. 4th ed. Freeman, New York. 1990. (a) pp. 764-765; (b) pp. 760-761 (note that **B** requires F^2).
2. K. H. Schmidt, P. Han, and D. M. Bartels. *J. Phys. Chem.* **96**, 199 (1992).
3. R. Chen and G. R. Freeman. *Can. J. Chem.* **71**, 1303 (1993).
4. R. Chen, Y. Avotinsh, and G. R. Freeman. *Can. J. Chem.* **72**, 1083 (1994).
5. R. Chen and G. R. Freeman. *J. Phys. Chem.* (*submitted*) 'Solvent Effects on Reactivity of Solvated Electrons with Nitrate Ion in C_1 to C_{10} *n*-Alcohols'. 1994.
6. H. Hayashi, K. Nishikawa, and T. Iijima. *J. Phys. Chem.* **94**, 8334 (1990).
7. H. Hayashi and Y. Udagawa. *Bull. Chem. Soc. Jpn.* **65**, 155 (1992).
8. G. D'Arrigo, J. Teixeira, R. Giordano, and F. Mallamace. *J. Chem. Phys.* **95**, 2732 (1991).
9. G. D'Arrigo and J. Teixeira. *J. Chem. Soc., Faraday Trans.* **86**, 1503 (1990).
10. R. Zana and B. Michels. *J. Phys. Chem.* **93**, 2643 (1989).
11. R. Zana and M. J. Eljebari. *J. Phys. Chem.* **97**, 11134 (1993).
12. B. Marongiu, I. Perino, R. Monaci, V. Solinas, and S. Torrazza. *J. Molecular Liq.* **28**, 229 (1984).
13. P. Debye. *Trans. Electrochem. Soc.* **82**, 265 (1942).
14. M. Anbar. *Adv. Chem. Ser.* **50**, 55 (1965).
15. K. N. Jha and G. R. Freeman. *J. Chem. Phys.* **48**, 5480 (1968).
16. E. J. Hart and M. Anbar. *The Hydrated Electron*. Wiley-Interscience, New York. 1970.
17. J. Jortner, M. Ottolenghi, J. Rabani, and G. Stein. *J. Chem. Phys.* **37**, 2488 (1962).

18. G. Stein. *Isr. J. Chem.* **9**, 413 (1971).
19. P. Han and D. M. Bartels. *J. Phys. Chem.* **96**, 4989 (1992).
20. K. Y. Lam and J. W. Hunt. *J. Radiat. Phys. Chem.* **7**, 317 (1975).
21. C. D. Jonah, J. R. Miller, and M. S. Matheson. *J. Phys. Chem.* **81**, 1618 (1977).
22. R. P. Bell. *The Proton in Chemistry*. Cornell Univ. Press, Ithaca, New York. 1959.
23. References 26-32 in chapter three.
24. W. P. Jencks. *Catalysis in Chemistry and Enzymology*. Dover Publications, New York. 1987. Chapter three and the references therein.

Appendix One

Experimental Methodology

I. Apparatus for Rate Constant Measurement

A. *Sample Cells*

Cells of Spectrosil Quartz from VWR Scientific, and Cells of Suprasil Quartz from Terochem Laboratories were used at atmospheric pressure for temperatures varying from ~275K to ~453K. The inside dimensions of the cell are 10 x 10 x 45 mm, and the optical path length is 10 mm. The cell was topped by a graded seal so that it could be attached to a Pyrex glass tube.

B. *Removal of Oxygen from Samples*

Samples in the cells were bubbled with ultra high pure argon and sealed before the experiment. The bubbling system (Figure A-1) was made by connecting 1 mL syringes to long Pyrex tubes. Pyrex/Teflon stopcocks (No. 72 Canadian Laboratory Supplies Ltd.) at the top of the syringes controlled the gas flow. Bubbling was done through long stainless steel needles (30 cm long, and 0.625 mm inner diameter) attached to the syringes. The rate of bubbling was ~17 cm³/min.

C. Irradiation, Optical, and Control Systems

1. Van de Graaff Accelerator

A Van de Graaff accelerator (type AK-60 2 MeV) manufactured by High Voltage Engineering Corporation was used as the source of high energy electrons. The maximum peak current delivered during a pulsed operation was 150 mA. Pulse widths of 3, 10, 30, and 100 nanoseconds (ns), and 1 microsecond (μ s) were available. Of these only 100ns pulse width was used to obtain an appropriate pulse of 340 fJ (2.1 MeV) electron beam, delivering a dose of \sim 4 Gy (J/kg).

A concrete maze shielded the entrance from the control room to the irradiation room and accelerator. Closing and locking the iron gate at the control room end of the maze sounded a warning buzzer for 15 seconds. It was not possible to operate the accelerator until the cessation of the buzzer. Unlocking the iron gate resulted in immediate shut down of the accelerator.

Steering and focusing of the electron beam was normally done by fixing a piece of phosphorescent paper to the end of the accelerator beam pipe. The paper could be viewed by closed circuit television. Each pulse of electrons caused a visible glow where it struck the phosphor. Accurate steering and focusing were done by adjusting the current in electromagnets. When equipment blocked visual observation of the end of the beam pipe, steering of the beam was done by maximizing the optical absorption of solvated electrons in a water sample.

2. Secondary Emission Monitor (SEM)

A secondary emission monitor indicated the relative dose for each electron pulse. It consisted of three thin metal foils placed inside the accelerator beam pipe perpendicular to the path of high energy electron beam (Figure A-2). These foils were positioned near the exit window and they were made of cobalt-based, high strength alloy (Havar, obtained from the Hamilton Watch Company, Precision Metal Division). This

material (average atomic number 27) was better than gold (atomic number 79) because of less beam attenuation by electron scattering.

The diameter of these foils was 5 cm and they were 0.5 cm apart from each other. The outer two were charged to +50 V relative to the central foil at ground. Passage of an electron pulse generated secondary electrons in the foils. The electrons ejected from the center foil were collected by the outer foils, the net result being a current flow from the center foil. Current flow occurred only during a high energy electron pulse and was measured by a gated integrator, digitized and displayed on a digital readout.

3. *Optical System*

(a) The light source was a high pressure Xenon arc lamp (Optical Radiation Co., model XLN1000) contained in a lamp housing (Photochemical Research Assoc., model PRA ALH220). A rhodium-coated, off axis parabolic mirror (Melles Griot-02 POH 015) placed in the beam path absorbed the UV light with wavelength shorter than 320 nm. Formation of excess ozone was prevented by this. The lamp was run at 1000 W.

A schematic diagram of the path of the analyzing light is shown in Figure A-3. The light shutter was used to protect the sample from unnecessary exposure. It was opened for only 55 ms. The light beam was focused to near the edge of the side of the irradiation cell facing the electron beam by using the above mentioned mirror. The light beam was reflected from front surface aluminized mirrors coated with silicon monoxide, through a 10 cm diameter hole in the 1.2 m thick concrete wall, to the control room. Finally, the light was focused into the monochromator housing by a concave mirror.

(b) Monochromator grating and filters: A Bausch and Lomb monochromator housing, type 33-86-25, was used with the grating type 33-86-03 (700–1000 nm), and a Corning filter type CS-2-64 (700–1000 nm). The light intensity reaching the detector was controlled by adjusting the slits on the monochromator. The wavelength of the

analyzing light was 850 nm with bandwidth 9 nm, to obtain an optimal absorption signal.

(c) Data acquisition and plotting: The light detector (pin silicon photodiode SD 040) was sensitive over the wavelength range 400–1100 nm. The 3 to 97% response time of the detector, amplifier and transient digitizer (Tektronix R7912) was 6 ns. The signal to noise ratio of the differential amplifier (Tektronix 7A13) was increased by using the 5 MHz filter, which gave a system response time of 96 ns. The incident light intensity at the detector, recorded as a voltage on a digital multimeter (Fluke 8810A), was displayed on an oscilloscope (Tektronix R7623). The signals were displayed as plots of voltage against time on a digital plotter (Zeta1200). All information related to the particular signal, such as total light intensity (I_0), dose, temperature, sensitivity, time scale, half-life trace, and cell holder number were also printed on the chart.

4. *Temperature Control System*

(a) Cooling and heating: Temperatures from 277K to 298K were achieved by boiling liquid nitrogen and regulating the temperature of the nitrogen gas by a heater. Liquid nitrogen was boiled at a controlled rate from a 50 L, narrow-necked aluminum Dewar vessel (Lakeshore Cryotonics Inc.). A stainless steel pipe (5 cm diameter) which was fixed to a lid, fitted snugly into the neck of the Dewar. This pipe extended to the bottom of the Dewar. A nichrome heating coil (600W) was attached to the inside of the steel pipe to about 7 cm from the bottom.

A Rubatex foam-rubber pipe (1 meter long) was used to transport the cold nitrogen gas to the sample box. Both ends of the pipe had glass inserts to which a leather seal was connected. Before entering the cell box, the cold gas that came through this pipe flowed through another stainless steel pipe (2.5 cm diameter) that had another nichrome heating wire (0.24 mm diameter, 4 m long) inserted inside it. The temperature of the nitrogen gas was regulated by this heating wire.

A laboratory heat gun (Master Appliance Corporation, Model AH0751) was used to achieve temperatures from 296K to 372K. The nichrome wire heated the air to the required temperature.

(b) Cell holder box: A box insulated with foam glass (Pittsburgh Corning Corporation) contained eight holders which were mounted on a circular (7 cm diameter) aluminum base. The base was connected to a motor so that the cells holder could make clockwise and counterclockwise full cycle rotations when the cells were not being irradiated. Just before irradiation the pre-selected cell stopped in the front of the electron exit window. The gas that flowed through the holes in the aluminum base was stirred by the rotating cell holder before leaving via a hole (2.5 cm diameter) in the lid.

A thermocouple mounted in a cell (Thermocouple cell) filled with solvent monitored the temperature of the system. The temperature controller (Taylor Microscan 1300) utilized a temperature sensor which was fixed to one of the cell holders. A Fluke Digital thermometer (Model 2100A) displayed the temperature of the thermocouple. The temperature of the thermocouple cell and the difference between the temperature setting and the cell holder were plotted on a chart recorder (Clevite Corporation, Model Brush Mark 220). When the chart recorder displayed a steady temperature for a period of 30 minutes the thermal equilibrium in the system was deemed to be established. At this time, the variation of the temperature of the thermocouple cell was only ± 0.1 K.

II. Apparatus for Electrical Conductivity Measurement

A. Impedance Bridge

Conductivity measurements were done with an impedance bridge (type 1608-A, General Radio Co.). It was a self-contained system which included six bridges for the measurements of conductance, capacitance, resistance, and inductance, as well as the internal generator and detectors for AC and DC measurements. To obtain the

conductance reading the variable resistor and capacitor were adjusted until the null balance was achieved. Most of the time the conductance mode (G_p Mode) was used. For the values of conductances less than about 0.6 microSiemen, the bridge was set to one of the capacitance modes (C_p or C_s Modes). Then values of conductance were calculated from the capacitance data. The oscillator frequency was 1 kHz for AC measurement.

B. Conductance Cells

Pyrex conductivity cells (YSI3403) were obtained from Yellow Springs Instrument Co., Inc. The temperature range of the measurements was $\sim 277\text{K}$ to $\sim 353\text{K}$. The cell chamber was 5 cm deep. The overall length was 20 cm and the outer diameter was 1.2 cm.

Graduated cylinders, 25 cm^3 (16 cm long, 1.4 cm inner diameter), were used to contain the electrolyte solutions. In order to have a tight seal between the container and the cell, a rubber adapter made from No. 2 stopper was fixed to the cell. Two layers of Parafilm (American Can Co.) were wrapped around the adapter-container junction to provide a tight seal, especially at high temperatures.

A secondary standard solution (YSI3161, specific conductance of 1000 ± 5 mS/cm) available from Yellow Springs Instrument Co., Inc. was used to calibrate the cells. This solution contained water, 0.002% iodine (an anti-microbial), and potassium chloride (ACS Reagent Grade).

The electrodes of the cells were coated with platinum black which was very important for cell operation. When the electrodes looked gray the cells were replatinized using a replatinizing solution (YSI3140) on a platinizing instrument (YSI3139). The current was kept at about 50 milliamp during the platinization. When a strong clearing of the cells was required they were treated with a solution of equal parts of isopropyl alcohol and 10 M HCl before the replatinization.

C. Constant Temperature Bath

A 10 L glass Dewar filled with water was used to measure conductances at various temperatures (Figure A-4). Inserted in this water were a motor controlled stirrer, a refrigeration unit (Tecumseh Model AE1343 AA), a heating coil, and a knife-heater (Cenco, 53 ohm, 350W). The heating coil was controlled by a variable transformer (Ohmite, Model VT). It was mainly used for the faster change of temperature from one setting to the another. The knife-heater was controlled by a temperature regulating system (Figure A-5). The temperature was measured with a platinum resistance digital thermometer (Fluke, Model 2189A) to ± 0.01 K. A chart recorder (Hewlett Packard, Model 7100B) was used to record the temperature variation in the bath. When the chart recorder displayed a steady temperature for a period of 30 minutes the thermal equilibrium in the system was deemed to be established. At this time, the variation of the temperature in the bath was only ± 0.01 K.

III. Experimental Techniques

A. Sample Preparation

New glassware, including the 10 mm Spectrosil cells, was cleaned according to the following procedure. First they were rinsed with ethanol, and then some concentrated nitric acid was added to them. The acid was rinsed off by washing them many times with distilled water. Then they were washed with potassium hydroxide. Finally they were rinsed many times with distilled water and dried at ~ 383 K in an oven.

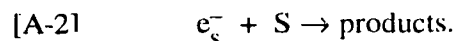
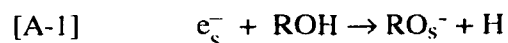
Butanol/water mixed solvents were prepared in a one L volumetric flask, by volume measurements at 298 K. Solid solutes were weighed into 25 mL volumetric flasks on an analytical balance (the precision was 1 mg) and dissolved in the mixed solvent to get the stock solution. Sample solutions were made by diluting aliquots of

stock solution, using micro syringes or volumetric pipettes. Perchloric acid samples were prepared through several steps of dilution from the 70 wt % aqueous solution, and the concentration of the stock solution was checked with the calibrated pH meter. Four to six sample solutions with different concentrations were prepared for each solute. The solutions were poured into quartz optical cells, deaerated by bubbling with ultrahigh purity argon at room temperature at a rate of $\sim 17 \text{ cm}^3/\text{min}$. for 30 minutes, and sealed as illustrated in Figure A-6. Step one took place at room temperature. The syringe needle was then withdrawn to just above the liquid as shown in step two and the argon flow rate was increased. The area around the sealing position was heated by a low flame to flush the volatile substances from the glass wall. The syringe needle was then further withdrawn as illustrated in step three and the seal was made as rapidly as possible. All components of the solution were of low volatility, so their concentration changed negligibly during bubbling.

B. Rate Constant Measurement

1. Half-life and k_{obs} Measurement

The solvated electrons generated in the electrolyte solutions made from the alcohol/water mixed solvents can react with the solvent molecules (ROH) or the solvated ions (S) according to the following equations:



Both reactions are first-order since the concentration of the solvent and of the reactant ions are much larger than that of e_s^- . Therefore, the observed first-order rate constant from the e_s^- optical absorption decay curve is,

$$[\text{A-3}] \quad k_{obs} = k_1 + k_2 [\text{S}] \quad ,$$

where k_1 is the first order rate constant of the reaction [A-1], k_2 is the second order rate constant of reaction [A-2], and [S] is the concentration of the reactant ion.

The optical absorption decay curve of the solvated electrons in each solution was measured at a wavelength which gave the optimal source intensity and e_s^- absorption signal. Figure A-7 shows an example of the decay curve of the solvated electrons in 0.091 mol/m^3 of ammonium nitrate in 1-butanol/water mixed solvent, of 35 mol% water at 315.0K. The optical absorption decay half-life of the solvated electrons was computed as a function of time in each measurement, and recorded along with the optical absorption trace. The half-life was then obtained by measuring the vertical distance between the reference point (the lower + mark in Figure A-7) and the half-life trace. A time-independent half-life horizontal trace corresponds to first-order decay. The decay curve of solvated electrons at the beginning of the decay was sometimes not first order. This initial fast decay could be due to the reaction of e_s^- inside the microzones (geminate reaction). Therefore, the beginning of the trace was ignored for the calculation of half-life in this case. From the half-life of the first-order decay k_{obs} can be calculated,

$$\text{[A-4]} \quad k_{\text{obs}} = \text{Ln } 2 / t_{1/2}$$

where $t_{1/2}$ is the half-life of the first order decay. The k_{obs} value was calculated using an average of two to four half-lives from consecutive measurements for each sample.

2. k_2 and E_2 Measurement

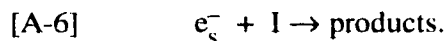
The second order rate constant k_2 obtained from the slope of the plot of the first order decay constants k_{obs} against solute concentration [S] (equation [A-3]). The number of pulses per sample was 2 or 3 at each temperature, and the number of temperatures per sample was 4 or 5. A pure solvent sample was part of each series, so the effect of the $\sim 3 \times 10^{-3} \text{ mol/m}^3$ of aldehyde produced during three pulses would not affect the value of k_2 obtained from the slope of the plot of k_{obs} against added solute concentration. At high concentrations in butanol the plots were curved due to ionic strength effects, in which case initial slopes were used.

The values of k_2 obtained at different temperatures allowed the determination of reaction parameter such as activation energy E_2 . It was derived from the plot of $\ln k_2$ against the reciprocal of the absolute temperature:

$$[\text{A-5}] \quad \ln k_2 = \ln A - E_2 / RT$$

3. Effect of Impurities

(a) Impurity in the Solvent: When the impurity originates in the solvent, the amount of the impurity at each solute concentration is the same.



where I stands for impurity. In this case, We have:

$$[\text{A-7}] \quad k_{\text{obs}} = k_1 + k_i[I] + k_2[S]$$

where [I] is the concentration of the impurity. The effect of the impurity appears in the intercept of the k_{obs} versus [S] plot and has no effect on k_2 which is the slope. If $k_i[I] \gg k_2[S]$ then all half-lives are the same regardless of different solute concentrations. This occurs when the solute is an inefficient electron scavenger and the impurity an efficient electron scavenger. Absence of efficient impurities was conformed by measuring the half-life of the pure solvent.

(b) Impurity in the Solute: When the impurity originates in the solute, the amount of impurity is a fraction p of the solute concentration [S].

$$[\text{A-8}] \quad k_{\text{obs}} = k_1 + (pk_i + k_s) [S] \quad ,$$

since $p \leq 10^{-5}$ for lithium nitrate and ammonium nitrate; ≤ 0.01 for ammonium perchlorate, silver perchlorate, and lithium perchlorate; and ≤ 0.02 for copper(II) perchlorate and aluminum(III) perchlorate, so for a solute of efficient electron scavenger we have,

$$[\text{A-9}] \quad k_2 = pk_i + k_s \approx k_s \quad .$$

If the impurity was an efficient electron scavenger and the solute an inefficient electron scavenger, the value of pk_i could be similar to that of k_s , hence $k_2 = pk_i + k_s$.

C. *Electrical Conductivity Measurement*

Most of the time the conductance mode (G_p) was used. The specific conductance (Λ_{obs} : S/m) was calculated from the following equation,

$$[A-10] \quad \Lambda_{obs} = C L \quad ,$$

where L is the conductance (in S: Siemen) and C is the cell constant (m^{-1}). For conductances in the range: $0.1 < L < 0.6$ mS, the bridge was set to one of the capacitance modes (C_p) and the conductance was calculated from the capacitance data using the following equation,

$$[A-11] \quad L = \omega C_p D \quad ,$$

where ω is the phase angular speed (radian/s) of the AC voltage, C_p is the capacitance (picofarad) and D is the dissipation factor. For conductances $L < 0.1$ mS, the bridge was set to the other of the capacitance modes (C_s) and the conductance was calculated from the capacitance data using the following equation,

$$[A-12] \quad L = \omega C_s D / (1 + D^2) \quad .$$

To test the detection limit of the apparatus, the dry cells were connected to the impedance bridge and the specific conductance was measured. The average dry cell's specific conductance was $1.2 \mu\text{S/m}$, which indicated a lower limit for the electrical conductivity measurement. The specific conductance of pure water used was controlled to be ≤ 0.1 mS/m and those of pure *iso*-butanol or 1-butanol were $\leq 3.0 \mu\text{S/m}$ at 298K. The specific conductance of the mixed solvent varied as a function of composition (an example was shown in Figure A-8). The molar conductance (Λ) was obtained from the plot of specific conductance against solute concentration. The activation energies of the conductivities (E_Λ) were obtained from the plots of the $\ln \Lambda$ against the reciprocal of the absolute temperature.

D. pH Measurement

pH measurements of $\text{Al}(\text{ClO}_4)_3$ aqueous solutions were made with a Fisher Accumet digital pH/ion meter (model 520). The probes are either:

(i) a glass indicating electrode (Fisher No. 13-639-3) and a reference electrode (Fisher No. 13-639-52), or

(ii) a combination microprobe (Fisher 13-620-92 standard Ag/AgCl microprobe combination electrode).

The meter was calibrated with two standard buffer solutions at 298K, SO-B-108 (pH = 7.00 ± 0.01) and SO-B-98B (pH = 4.00 ± 0.01).

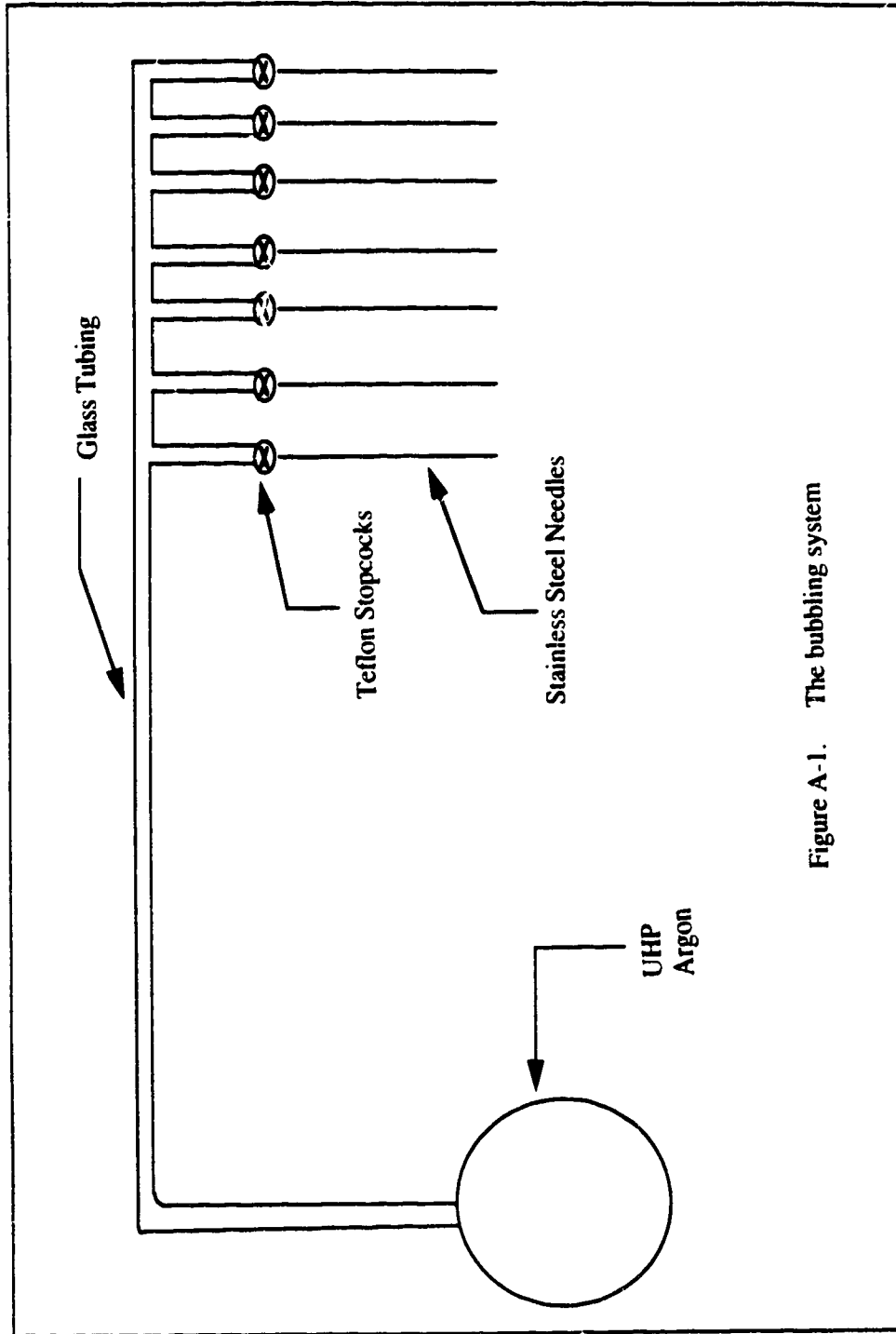


Figure A-1. The bubbling system

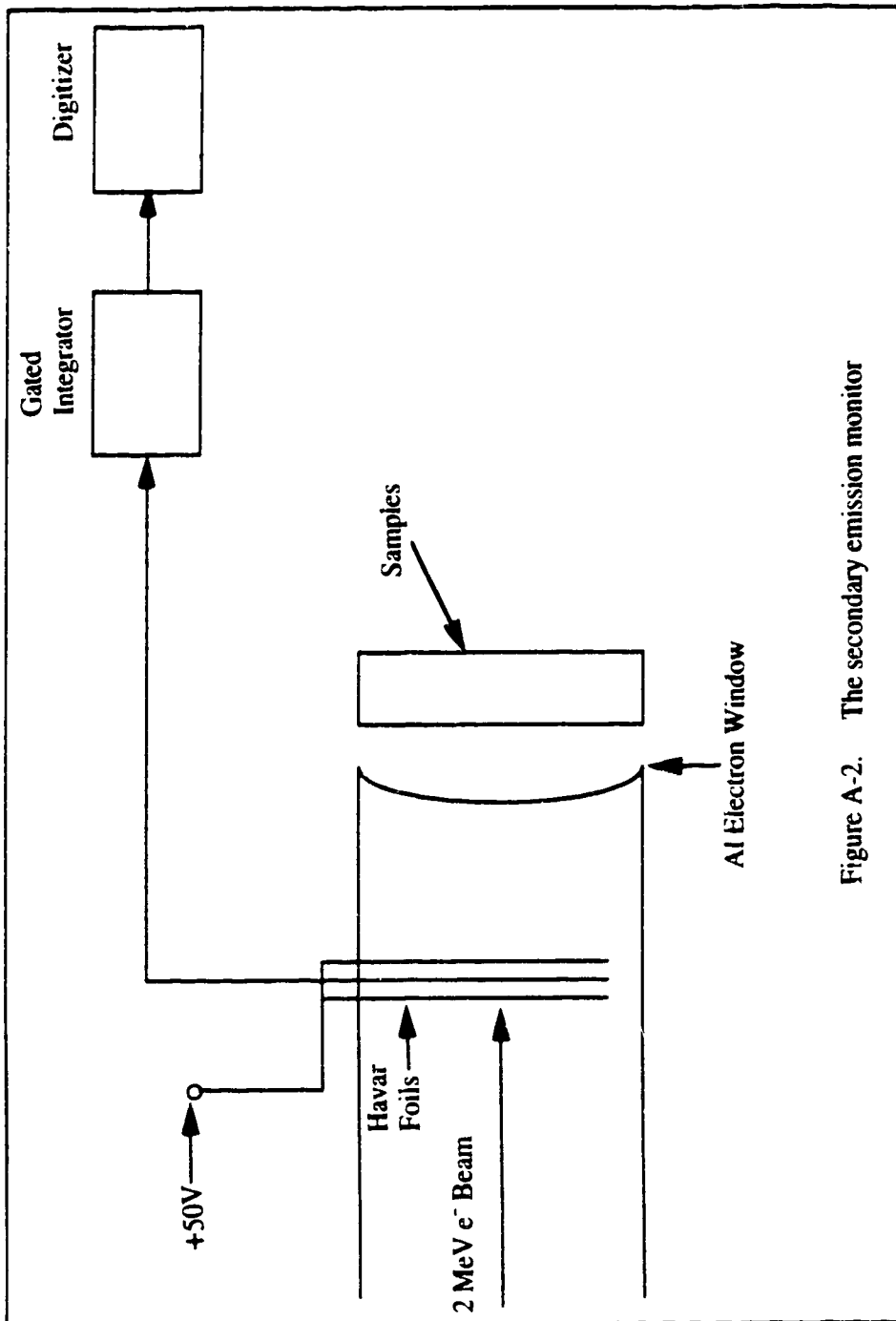


Figure A-2. The secondary emission monitor

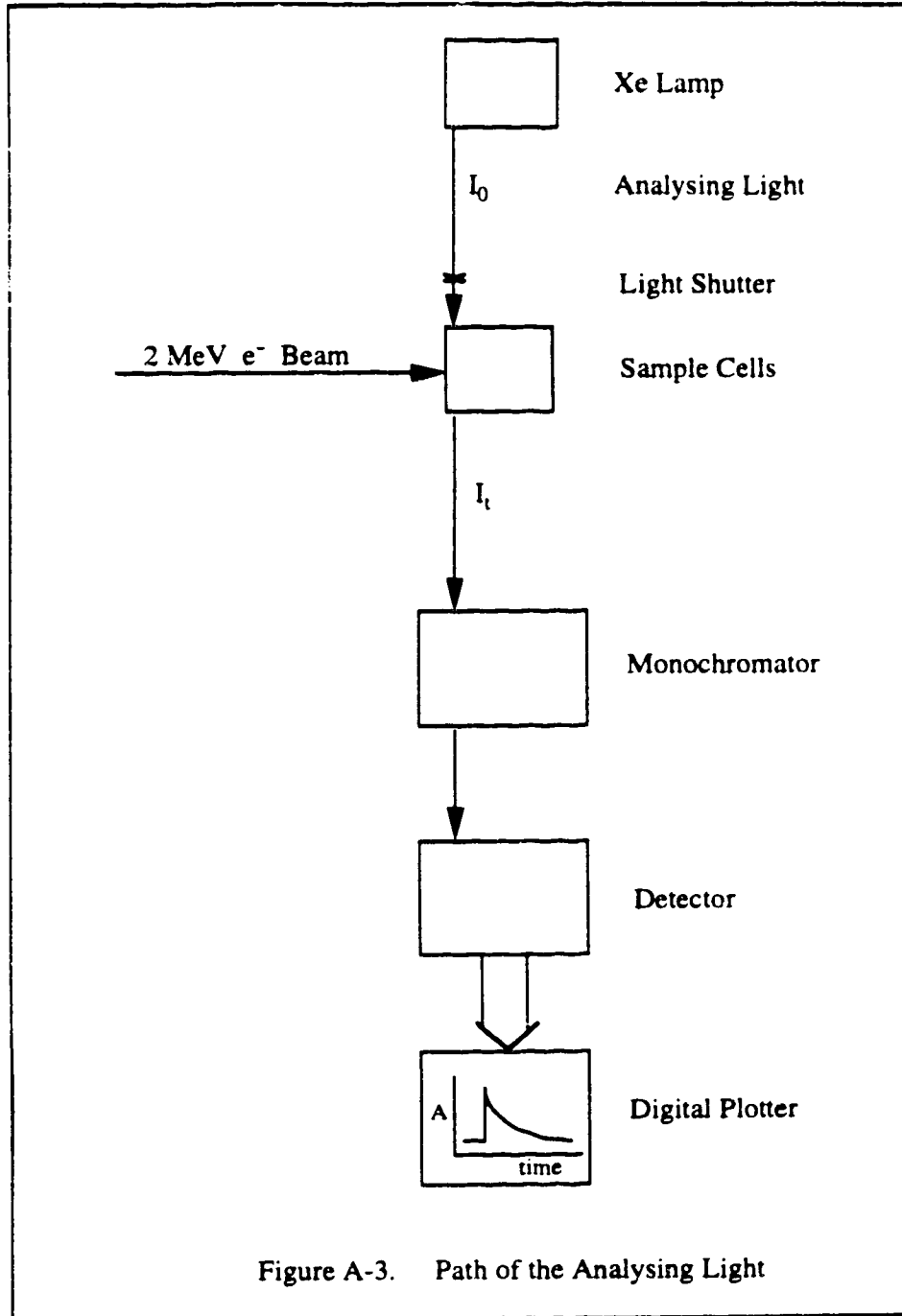


Figure A-3. Path of the Analysing Light

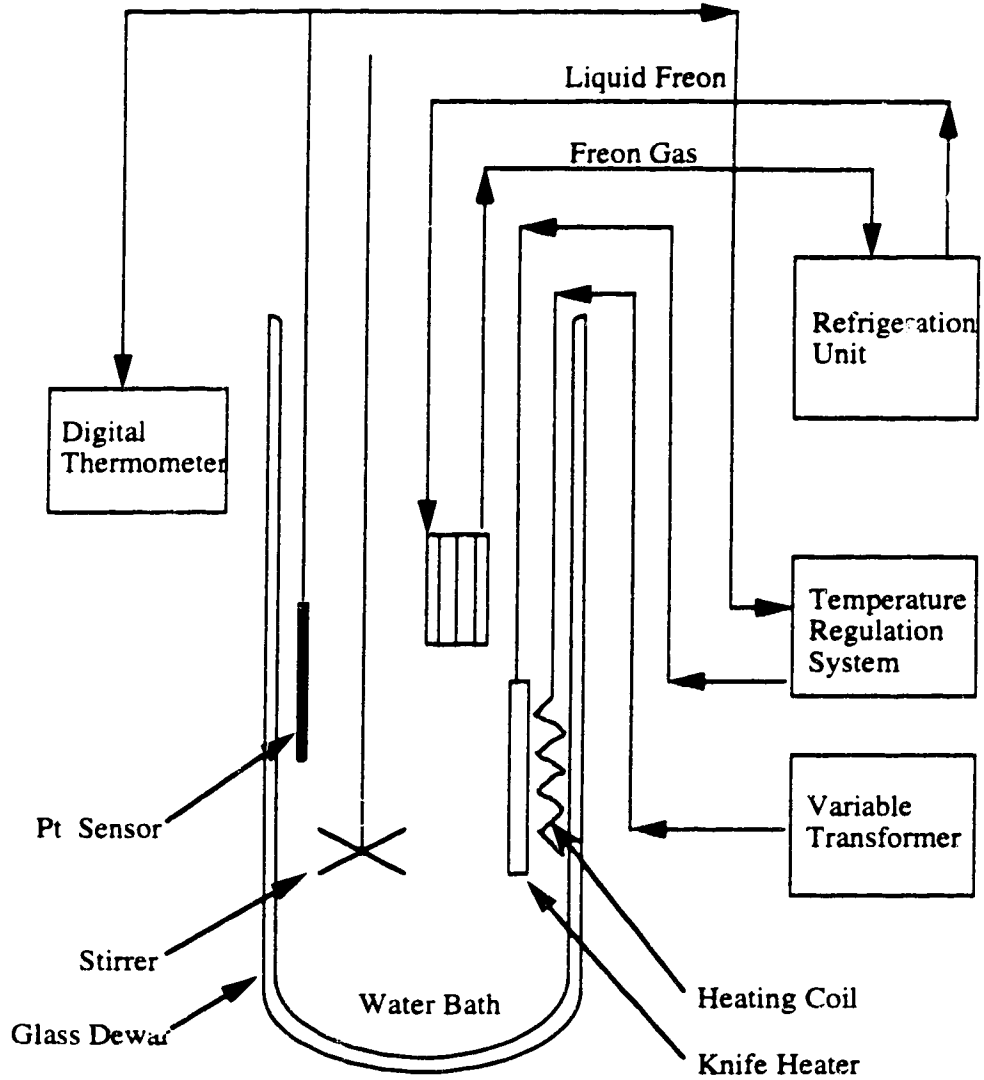


Figure A-4. Temperature Control of the Water Bath

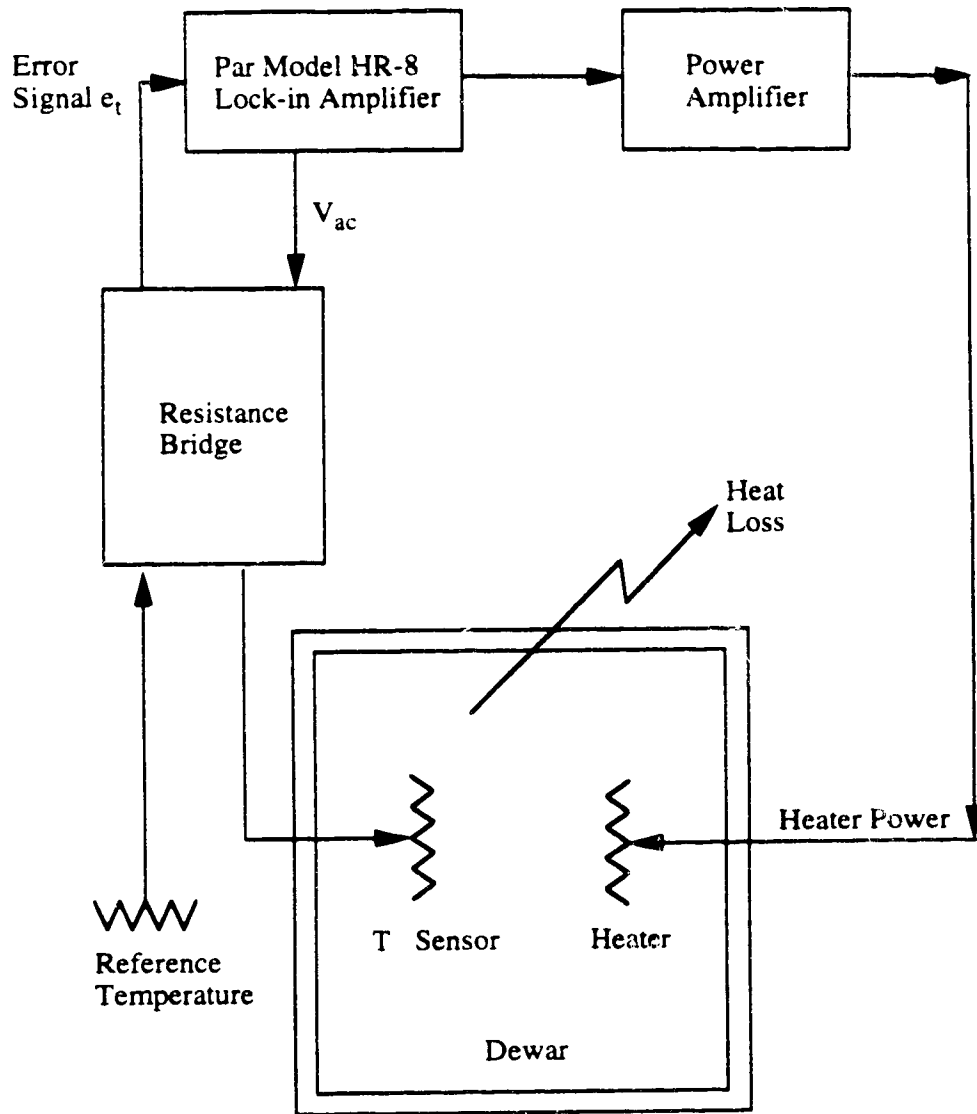


Figure A-5. The Temperature Regulation System

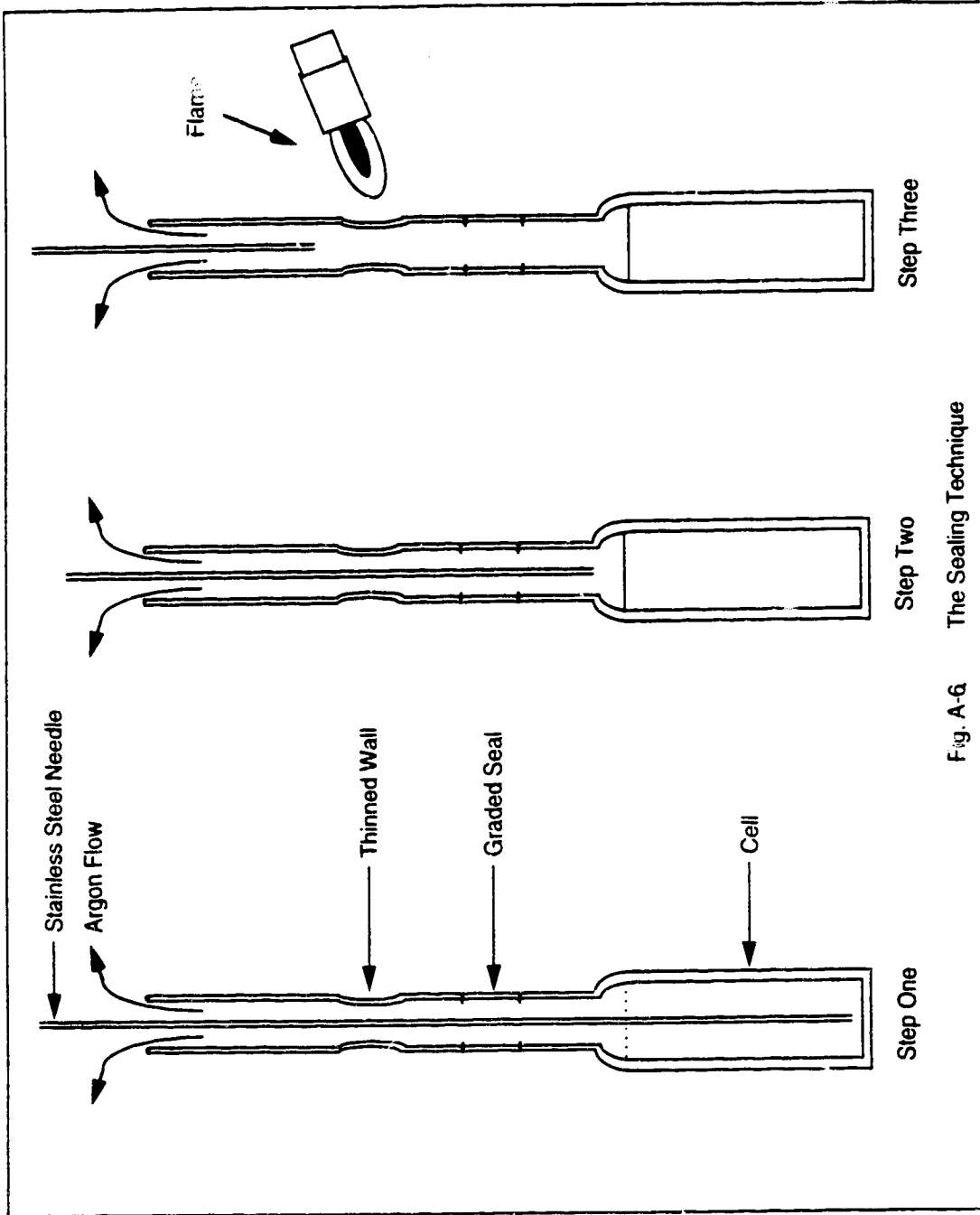


Fig. A-6 The Sealing Technique

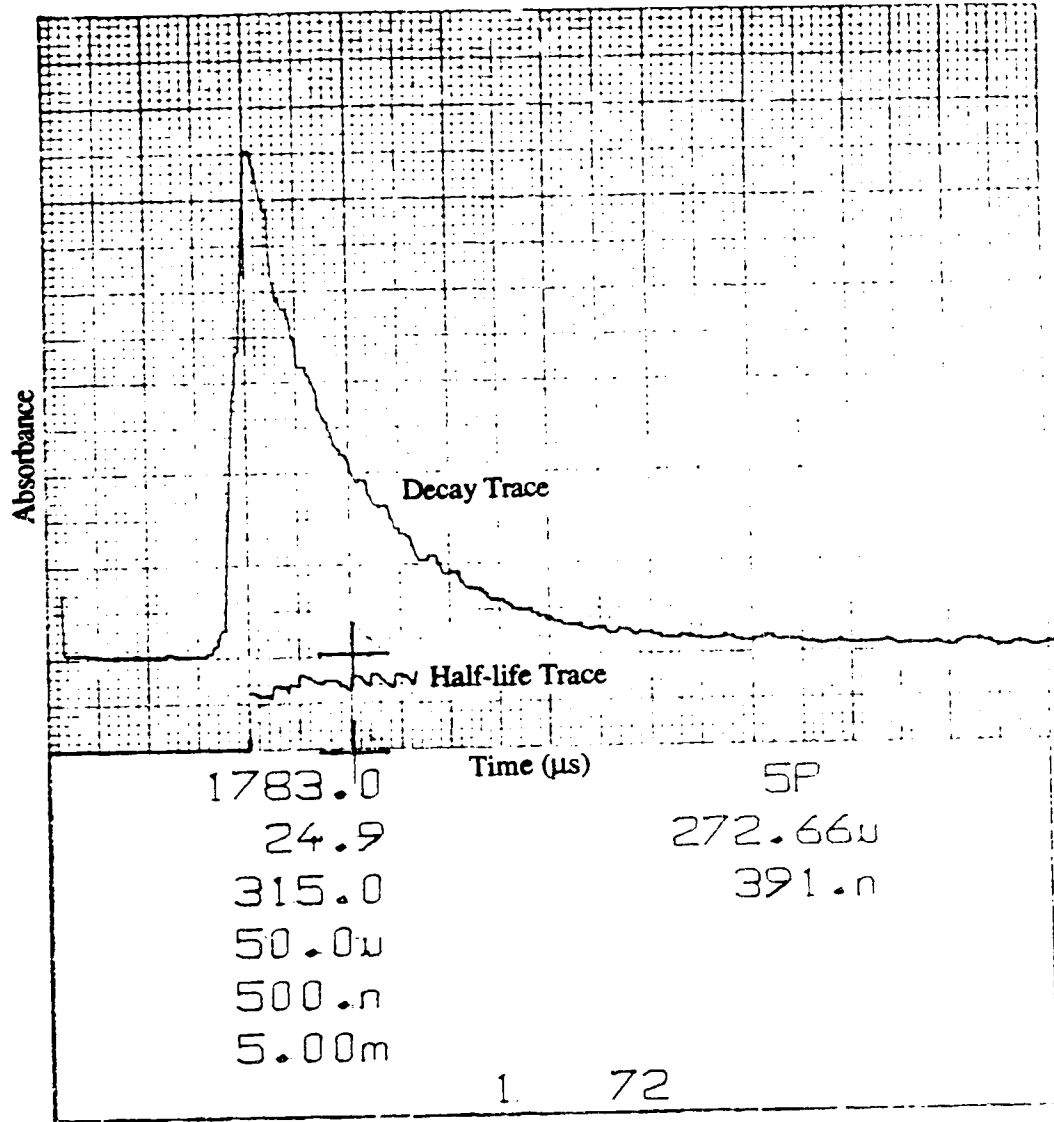


Figure A-7. The typical solvated electron optical absorption trace.

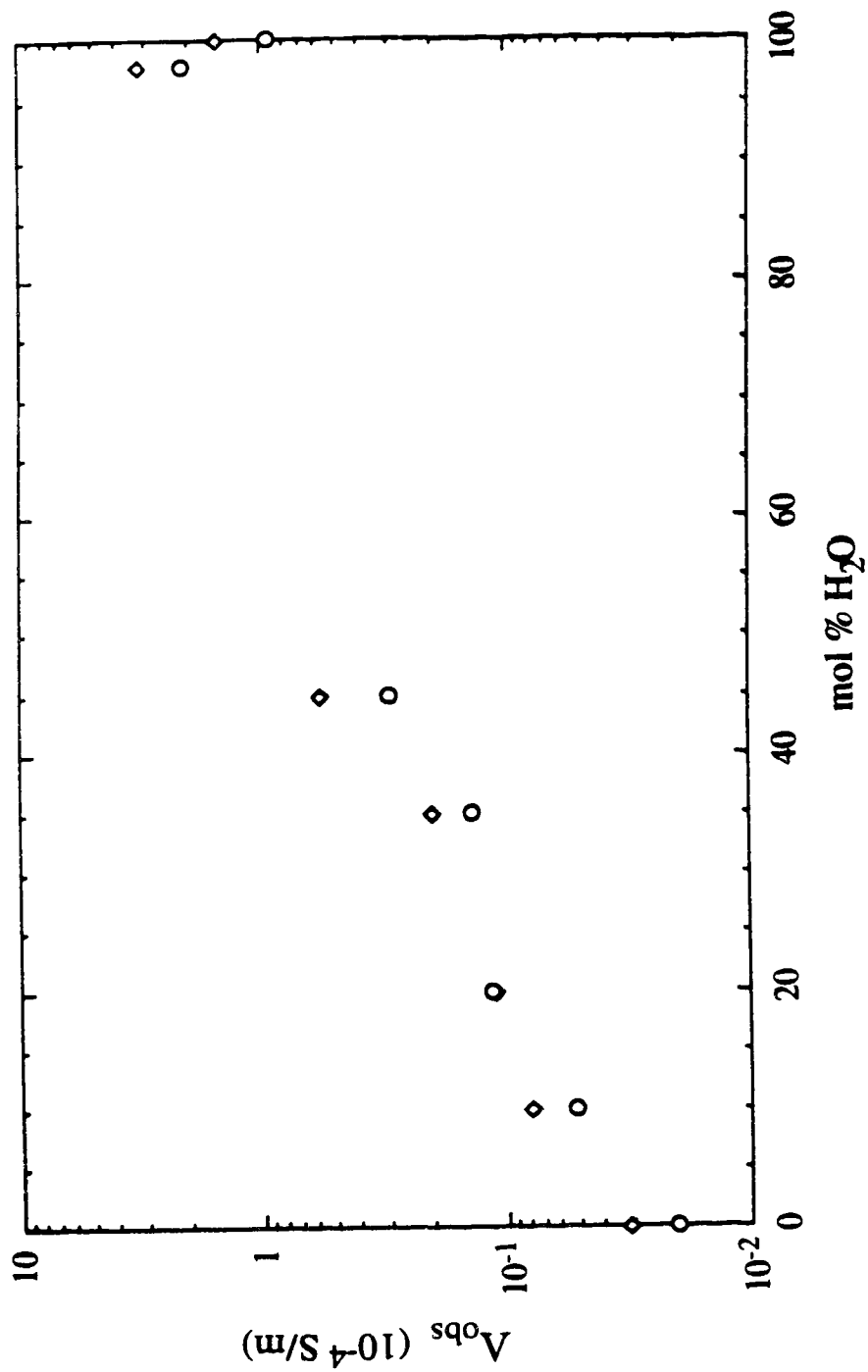


Figure A-8. The specific conductance of pure iso-butanol/water mixed solvents. O: 298K; ◇: 313K.

Appendix Two

Experimental Results

I. Results of Rate Constant Measurement

In this study, the reactions of solvated electrons with lithium nitrate, ammonium nitrate, ammonium perchlorate, and perchloric acid were investigated in 1-butanol/water mixed solvents; and the reactions of solvated electrons with lithium nitrate, ammonium nitrate, ammonium perchlorate, perchloric acid, silver perchlorate, copper(II) perchlorate, and aluminum (III) perchlorate were investigated in *iso*-butanol/water mixed solvents. The reaction of solvated electrons with lithium nitrate was also investigated in 1-hexanol, 1-octanol, and 1-decanol. 1-butanol and *iso*-butanol are not completely miscible with water (see reference 8 in chapter three and reference 7 in chapter four). The measurements were mostly made over the miscible range. For *iso*-butanol/water mixtures, the following mol % water were used: 0, 10.0, 20.0, 35.0, 45.0, 98.0, and 100.0. The 45 mol% is located in the immiscible region for the temperatures less than 293.2K, so the measurement at those temperatures are reported here but not analyzed with the rest of data due to the phase separation. For 1-butanol/water mixture the following mol % water were used: 0, 10.0, 20.0, 35.0, 45.0, 98.0, 99.0, and 100.0. The 98 mol% is located in the immiscible region, so the measurement are reported here but not analyzed with the rest of data due to the phase separation. The rest of mixtures are in the miscible range. The concentration of added salts (C) is in the unit of 10^{-2} mol/m³ unless specified. The percent in the concentration (C) column represents mol % of water in the mixed solvent. The first order rate constant (k_{obs}) is in the unit of 10⁶/s

unless specified. The temperature in the rate constant (k_{obs}) column represents the temperature at which the measurement made.

A. Results of k_{obs} Measurement

Table A-1. The values of k_{obs} of solvated electrons' reaction with lithium nitrate in 1-butanol/water mixed solvents.

C	k_{obs}	k_{obs}	k_{obs}	k_{obs}	k_{obs}	k_{obs}
100%	277.0K	287.7K	296.7K	315.0K	328.1K	343.3K
0.00	0.057	0.074	0.092	0.13	0.18	0.21
1.90	0.16	0.21	0.26	0.38	0.53	0.59
3.81	0.26	0.34	0.46	0.63	0.77	0.96
5.71	0.37	0.49	0.62	0.86	1.03	1.33
7.61	0.49	0.64	0.80	1.14	1.39	1.82
9.52	0.56	0.81	0.96	1.35	1.73	2.11
11.4	0.68	0.88	1.12	1.66	2.05	2.49
C	k_{obs}	k_{obs}	k_{obs}	k_{obs}	k_{obs}	k_{obs}
99%	277.6K	298.3K	314.5K	329.1K	344.2K	
0.00	0.019	0.028	0.042	0.051	0.075	
3.66	0.20	0.35	0.49	0.60	0.79	
7.31		0.60	0.84	1.08	1.39	
9.14	0.47	0.78	1.07	1.39	1.58	
11.0	0.55	0.87	1.26	1.54	2.10	

Table A-1 continued

C	k _{obs}	k _{obs}	k _{obs}	k _{obs}	k _{obs}
98%	296.4K	314.8K	328.6K	343.3K	354.4K
0.00	0.021	0.036	0.047	0.070	0.084
5.05	0.41	0.62	0.82	1.03	1.22
10.1	0.80	1.12	1.54	1.98	2.31
15.1	1.26	1.98	2.39	3.15	4.62
25.2	1.98	3.15	4.08	4.95	5.78
30.3	2.39	3.47	4.62	5.78	6.93

C	k _{obs}	k _{obs}	k _{obs}	k _{obs}	k _{obs}	k _{obs}
45%	277.0K	287.7K	296.4K	315.0K	328.7K	343.3K
0.00	0.028	0.038	0.052	0.088	0.13	0.17
15.6	0.07	0.11	0.14	0.21	0.29	0.38
31.1	0.17	0.25	0.29	0.49	0.63	0.88
46.7	0.26	0.36	0.49	0.71	0.99	1.22
62.2	0.37	0.50	0.65	1.02	1.39	1.98
77.7	0.50	0.63	0.89	1.39	1.88	2.49
93.3	0.59	0.90	1.13	1.73	2.51	3.19

C	k _{obs}	k _{obs}	k _{obs}	k _{obs}	k _{obs}	k _{obs}
35%	277.0K	287.7K	297.0K	315.0K	328.6K	343.2K
0.00	0.03	0.05	0.06	0.10	0.14	0.18
15.8	0.07	0.10	0.14	0.23	0.31	0.46
31.7	0.12	0.18	0.25	0.41	0.58	0.86
47.5	0.22	0.32	0.43	0.83	1.26	1.68
63.3	0.29	0.42	0.61	1.08	1.53	2.37
79.2	0.41	0.61	0.77	1.30	1.95	2.64
95.0	0.47	0.74	0.94	1.62	2.32	3.33

Table A-1 continued

C	k _{obs}	k _{obs}	k _{obs}	k _{obs}	k _{obs}	
20%	297.3K	314.8K	328.6K	343.2K	354.4K	
0.00	0.033	0.051	0.066	0.090	0.12	
26.3	0.15	0.24	0.39	0.61	0.88	
53.7	0.26	0.48	0.83	1.31	1.82	
78.9	0.47	0.82	1.28	2.31	3.15	
105.	0.68	1.24	1.98	3.30	4.62	
132.	0.88	1.61	2.67	4.08	5.33	
158.	1.08	1.92	2.89	5.33	6.93	
C	k _{obs}	k _{obs}	k _{obs}	k _{obs}	k _{obs}	
10%	296.7K	314.9K	328.5K	343.2K	354.4K	
0.00	0.060	0.087	0.12	0.16	0.20	
29.3	0.14	0.28	0.47	0.73	1.14	
58.6	0.28	0.56	0.96	1.69	2.31	
87.9	0.43	0.89	1.48	2.57	3.30	
117.	0.61	1.22	1.98	3.47	4.62	
147.	0.74	1.44	2.48	4.08	5.78	
176.	0.91	1.92	2.89	5.33	6.93	
C	k _{obs}	k _{obs}	k _{obs}	k _{obs}	k _{obs}	k _{obs}
0%	277.0K	287.7K	296.7K	315.0K	328.7K	343.2K
0.00	0.053	0.079	0.091	0.14	0.19	0.23
17.4	0.06	0.09	0.12	0.23	0.36	0.71
34.8	0.07	0.10	0.14	0.29	0.50	0.98
52.2	0.07	0.12	0.17	0.36	0.65	1.27
69.6	0.08	0.13	0.20	0.46	0.77	1.53
87.0	0.10	0.17	0.24	0.58	0.99	1.64
104.	0.11	0.19	0.27	0.62	1.16	1.88

Table A-2. The values of k_{obs} of solvated electrons' reaction with ammonium nitrate in 1-butanol/water mixed solvents.

C 100%	k_{obs} 296.9K	k_{obs} 315.0K	k_{obs} 328.7K	k_{obs} 343.2K	k_{obs} 354.6K	
0.00	0.095	0.10	0.12	0.17	0.21	
2.57	0.29	0.44	0.56	0.71	0.86	
5.14	0.56	0.83	0.99	1.26	1.54	
7.71	0.79	1.14	1.39	1.73	2.04	
10.3	1.08	1.44	1.92	2.31	2.77	
12.8	1.26	1.87	2.39	3.15	3.65	
15.4	1.54	2.31	3.01	3.85	4.33	
C 99%	k_{obs} 278.7K	k_{obs} 296.5K	k_{obs} 314.5K	k_{obs} 329.2K	k_{obs} 344.2K	
0.00	0.022	0.027	0.039	0.055	0.064	
3.32	0.20	0.30	0.44	0.58	0.80	
6.64	0.35	0.57	0.81	1.02	1.20	
9.96	0.51	0.80	1.15	1.54	1.98	
13.3	0.63	0.99	1.48	1.87	2.48	
16.6	0.86	1.33	1.92	2.48	3.01	
19.9	0.99	1.58	2.31	2.89	3.65	
C 98%	k_{obs} 277.0K	k_{obs} 287.7K	k_{obs} 297.0K	k_{obs} 315.0K	k_{obs} 328.6K	k_{obs} 343.2K
0.00	0.021	0.022	0.032	0.046	0.062	0.079
2.27	0.12	0.17	0.20	0.31	0.40	0.55
4.54	0.21	0.28	0.35	0.56	0.66	0.88
6.81	0.31	0.44	0.53	0.78	1.02	1.33
9.08	0.41	0.56	0.70	1.03	1.30	1.70
11.3	0.48	0.65	0.84	1.25	1.59	2.17
13.6	0.61	0.79	1.03	1.62	2.00	2.34

Table A-2 continued

C	k_{obs}	k_{obs}	k_{obs}	k_{obs}	k_{obs}	k_{obs}
45%	277.0K	287.7K	296.4K	315.0K	328.7K	343.3K
0.00	0.022	0.037	0.036	0.079	0.10	0.14
1.32	0.04	0.06	0.09	0.16	0.27	0.43
2.64	0.07	0.11	0.14	0.31	0.52	0.87
3.96	0.10	0.15	0.22	0.49	0.76	1.26
5.28	0.12	0.20	0.28	0.57	1.00	1.65
6.60	0.14	0.24	0.31	0.69	1.22	1.92
7.92	0.17	0.28	0.41	0.81	1.39	2.39
C	k_{obs}	k_{obs}	k_{obs}	k_{obs}	k_{obs}	k_{obs}
35%	277.0K	287.7K	297.0K	315.0K	328.6K	343.2K
0.00	0.021	0.031	0.041	0.065	0.094	0.15
2.27	0.10	0.16	0.23	0.47	0.67	1.15
4.54	0.18	0.34	0.45	0.95	1.48	2.48
6.81	0.30	0.49	0.74	1.39	2.31	3.65
9.08	0.38	0.70	0.91	1.87	2.89	4.95
11.3	0.47	0.91	1.12	2.39	3.47	5.78
13.6	0.62	0.96	1.31	2.89	4.33	6.93
C	k_{obs}	k_{obs}	k_{obs}	k_{obs}	k_{obs}	k_{obs}
20%	277.0K	287.7K	296.4K	315.0K	328.7K	343.2K
0.00	0.03	0.03	0.06	0.07	0.11	0.17
2.69	0.15	0.24	0.31	0.59	0.88	1.39
5.38	0.32	0.46	0.65	1.31	1.82	2.89
8.07	0.50	0.75	0.96	1.87	3.01	4.95
10.8	0.60	0.96	1.39	2.48	3.47	6.30
13.4	0.86	1.39	1.65	3.15	4.95	7.88
16.1	0.94	1.51	1.92	3.65	6.30	7.30

Table A-2 continued

C	k _{obs}	k _{obs}	k _{obs}	k _{obs}	k _{obs}	k _{obs}
10%	277.1K	287.7K	301.4K	315.0K	328.6K	343.3K
2.70	0.14	0.22	0.35	0.54	0.90	1.28
5.40	0.32	0.50	0.81	1.28	1.69	2.48
8.10	0.43	0.71	1.12	1.61	2.57	3.30
10.8	0.57	0.94	1.54	2.24	2.89	4.62
13.5	0.70	1.12	1.73	2.89	3.47	4.95
16.2	0.82	1.28	2.31	3.15	5.33	7.15

C	k _{obs}	k _{obs}	k _{obs}	k _{obs}	k _{obs}	k _{obs}
0%	277.0K	287.7K	296.5K	315.0K	328.7K	343.2K
0.00	0.058	0.080	0.10	0.16	0.22	0.26
2.30	0.13	0.17	0.22	0.36	0.69	0.82
4.60	0.23	0.35	0.45	0.85	1.13	1.69
6.90	0.29	0.43	0.63	1.10	1.68	2.23
9.20	0.41	0.60	0.87	1.41	2.13	2.96
11.5	0.47	0.64	0.95	1.47	2.63	3.65
13.8	0.57	0.86	1.20	1.95	3.47	4.10

Table A-3. The values of k_{obs} of solvated electrons' reaction with ammonium perchlorate in water* .

C	k _{obs}	k _{obs}	k _{obs}	k _{obs}	k _{obs}
water	276.7K	296.5K	313.9K	328.4K	343.1K
0.00	0.54	0.75	1.21	1.86	1.94
8.34	0.57	0.82	1.87	2.56	4.36
16.7	1.00	1.70	3.47	5.17	7.53
33.4	1.12	2.20	3.50	6.13	8.89
41.7	1.10	2.00	4.05	6.74	9.37

* The concentration is in the unit of mol/m³. k_{obs} is in the unit of 10⁵/s.

Table A-3 continued

C	k _{obs}	k _{obs}	k _{obs}	k _{obs}	k _{obs}
water	276.8K	296.7K	314.0K	328.5K	343.2K
0.00	0.37	0.71	1.01	1.28	1.60
36.9	0.70	1.80	3.00	5.73	8.15
49.2	0.89	1.90	3.80	5.98	9.43
61.5	1.10	2.36	4.28	7.15	11.6
73.8	1.40	2.79	5.21	7.92	13.7
86.1	1.40	2.99	5.33	8.01	14.4
98.4	1.40	3.20	5.64	8.72	14.2
C	k _{obs}	k _{obs}	k _{obs}	k _{obs}	k _{obs}
water	276.8K	296.5K	313.9K	328.5K	343.2K
0.00	0.41	0.87	1.06	1.13	1.73
7.22	0.69	1.34	2.20	3.15	4.81
14.4	0.93	1.80	3.05	4.68	7.07
21.7	0.90	1.91	3.22	4.81	7.45
28.9	0.78	1.65	3.05	4.88	8.15
36.1	1.24	2.30	4.33	6.42	10.0
43.3	1.37	2.58	3.87	6.54	10.7
C	k _{obs}	k _{obs}	k _{obs}	k _{obs}	k _{obs}
water	276.9K	297.0K	314.1K	328.5K	343.2K
0.0	0.82	0.86	1.98	2.88	3.47
40.0	1.08	2.19	3.81	6.24	10.0
60.0	1.16	2.52	4.59	7.30	11.6
80.0	1.24	2.77	4.81	8.35	12.4
100.	1.54	3.47	6.03	9.76	15.1
120.	1.56	3.43	6.13	10.0	15.1
140.	1.73	3.79	6.73	11.2	17.3

Table A-3 continued

C	k_{obs}	k_{obs}	k_{obs}	k_{obs}	k_{obs}
water	276.9K	296.7K	313.9K	328.4K	343.2K
0.00	0.49	0.89	1.00	1.34	1.35
10.0	0.75	1.48	2.23	3.77	5.55
24.0	0.63	1.60	2.79	4.68	6.93
38.0	1.08	2.34	3.85	6.36	10.3
66.2	1.25	2.69	4.56	7.22	12.6
80.1	1.44	3.35	5.29	8.45	13.3

Table A-4. The values of k_{obs} of solvated electrons' reaction with ammonium perchlorate in 1-butanol/water mixed solvents.

C	k_{obs}	k_{obs}	k_{obs}	k_{obs}	k_{obs}
99%	278.0K	298.5K	313.9K	328.4K	343.1K
0.00	0.016	0.025	0.034	0.046	0.066
1.37	0.028	0.049	0.084	0.14	0.24
2.73	0.038	0.072	0.12	0.20	0.31
4.10	0.033	0.075	0.12	0.21	0.35
5.46	0.055	0.11	0.17	0.28	0.45
6.83	0.040	0.091	0.16	0.28	0.44
C	k_{obs}	k_{obs}	k_{obs}	k_{obs}	k_{obs}
99%	278.1K	298.4K	313.9K	328.4K	343.1K
6.83	0.032	0.087	0.15	0.27	0.44
13.9	0.036	0.098	0.19	0.33	0.55
20.5	0.059	0.14	0.26	0.44	0.71
27.3	0.071	0.15	0.30	0.46	0.83
34.1	0.11	0.22	0.38	0.59	1.00
41.0	0.072	0.18	0.34	0.56	0.94

Table A-4 continued

C	k_{obs}	k_{obs}	k_{obs}	k_{obs}	k_{obs}
99%	277.6K	296.3K	314.5K	329.1K	344.2K
0.00	0.015	0.027	0.045	0.053	0.069
14.6	0.041	0.10	0.21	0.35	0.60
29.3	0.071	0.18	0.32	0.53	0.82
43.9	0.084	0.18	0.36	0.61	1.02
58.6	0.093	0.22	0.41	0.70	1.20
87.9	0.13	0.29	0.58	0.95	1.51
C	k_{obs}	k_{obs}	k_{obs}	k_{obs}	k_{obs}
45%	282.5K	296.0K	314.7K	329.4K	344.4K
0.00	0.035	0.053	0.071	0.10	0.14
2.11	0.085	0.16	0.31	0.51	0.85
4.22	0.12	0.23	0.51	0.87	1.53
6.33	0.17	0.33	0.66	1.15	1.94
8.44	0.23	0.42	0.86	1.55	2.59
10.6	0.25	0.50	1.05	1.83	3.08
12.7	0.30	0.57	1.33	2.17	4.01
C	k_{obs}	k_{obs}	k_{obs}	k_{obs}	k_{obs}
35%	279.0K	297.7K	314.7K	329.3K	344.4K
0.00	0.024	0.072	0.072	0.10	0.15
2.70	0.14	0.31	0.62	0.99	1.52
5.66	0.27	0.59	1.09	1.88	2.83
8.49	0.41	0.85	1.58	2.64	3.85
11.3	0.50	1.14	2.20	3.56	4.95
14.2	0.62	1.22	2.64	4.18	5.87
16.7	0.72	1.56	2.97	4.85	6.48
C	k_{obs}	k_{obs}	k_{obs}	k_{obs}	k_{obs}
20%	297.3K	314.8K	328.6K	343.2K	354.4K
3.08	0.26	0.44	0.78	1.21	1.66
6.16	0.51	0.80	1.44	2.31	3.61
7.70	0.57	1.00	1.82	2.77	3.87
9.24	0.82	1.44	2.57	4.18	5.64

Table A-5. The values of k_{obs} of solvated electrons' reaction with perchloric acid in 1-butanol/water mixed solvents.

C	k_{obs}	k_{obs}	k_{obs}	k_{obs}	k_{obs}	k_{obs}	k_{obs}
100%	276.9K	287.6K	295.1K	314.9K	328.6K	343.1K	354.3K
0.00	0.069	0.086	0.20	0.16	0.25	0.26	0.32
2.79	0.27	0.34	0.42	0.56	0.69	0.81	0.95
5.59	0.78	0.96	1.08	1.40	1.74	2.02	2.24
8.38	1.22	1.49	1.73	2.33	2.74	3.21	3.65
11.2	1.65	1.93	2.31	2.92	3.52	4.33	4.88
16.8	2.45	3.00	3.65	4.95	5.97	6.86	7.88
C	k_{obs}	k_{obs}	k_{obs}	k_{obs}	k_{obs}	k_{obs}	k_{obs}
98%	277.0K	287.7K	296.6K	314.9K	328.6K	343.2K	
0.00	0.026	0.035	0.050	0.069	0.092	0.12	
2.79	0.32	0.40	0.47	0.63	0.76	0.91	
5.59	0.60	0.78	0.93	1.19	1.52	1.75	
8.38	1.30	1.71	2.04	2.58	3.05	3.43	
14.0	2.20	2.82	3.38	4.62	5.59	6.86	
16.8	2.74	3.38	3.98	5.37	6.66	7.79	
C	k_{obs}	k_{obs}	k_{obs}	k_{obs}	k_{obs}	k_{obs}	k_{obs}
45%	276.9K	287.7K	296.0K	314.9K	328.6K	343.2K	354.4K
0.00	0.022	0.033	0.047	0.071	0.10	0.15	0.18
1.40	0.05	0.07	0.10	0.14	0.19	0.28	0.32
2.79	0.11	0.15	0.22	0.37	0.51	0.75	0.94
4.19	0.27	0.42	0.50	1.00	1.60	2.15	2.89
5.59	0.37	0.53	0.68	1.36	1.90	2.69	3.56
6.98	0.58	0.93	1.22	2.31	3.15	5.21	6.30
8.38	0.62	0.97	1.44	2.60	3.85	5.73	7.70

Table A-5 continued

C	k _{obs}	k _{obs}	k _{obs}	k _{obs}	k _{obs}	k _{obs}
35%	277.0K	287.7K	296.0K	314.9K	328.7K	343.2K
0.00	0.032	0.043	0.055	0.10	0.14	0.25
1.40	0.19	0.31	0.27	0.67	1.07	1.46
2.79	0.35	0.52	0.56	1.33	2.02	3.09
4.19	0.44	0.63	0.77	1.52	2.46	3.73
5.59	0.50	0.70	1.00	2.07	3.01	4.30
6.98	0.66	1.06	1.26	2.84	3.71	5.92
8.38	0.76	1.30	1.68	3.47	5.21	7.62
C	k _{obs}	k _{obs}	k _{obs}	k _{obs}	k _{obs}	k _{obs}
20%	276.9K	287.6K	296.0K	314.9K	328.6K	343.2K
0.00	0.030	0.039	0.048	0.086	0.12	0.15
1.40	0.09	0.13	0.16	0.32	0.51	0.72
2.79	0.12	0.17	0.19	0.42	0.61	0.81
4.19	0.24	0.30	0.32	0.80	1.21	1.90
5.59	0.32	0.43	0.61	1.20	1.74	2.48
6.98	0.38	0.53	0.69	1.36	1.95	
8.38	0.59	0.80	1.17	2.27	3.37	
C	k _{obs}	k _{obs}	k _{obs}	k _{obs}	k _{obs}	k _{obs}
20%	277.0K	296.7K	313.9K	328.4K	343.2K	
0.00	0.030	0.050	0.072	0.092	0.13	
1.86	0.17	0.34	0.62	0.88	1.39	
3.72	0.31	0.63	1.15	1.75	2.59	
5.58	0.48	0.98	1.69	2.48	3.85	
7.44	0.64	1.35	2.45	3.69	5.46	
9.30	0.76	1.73	2.86	4.31	6.13	
10.2	0.84	1.85	3.21	4.75	6.80	

Table A-5 continued

C	k _{obs}	k _{obs}	k _{obs}	k _{obs}	k _{obs}	k _{obs}
10%	277.0K	287.7K	295.8K	314.9K	328.6K	343.2K
0.00	0.037	0.050	0.063	0.10	0.13	0.19
1.40	0.14	0.17	0.23	0.43	0.59	0.88
2.79	0.20	0.30	0.41	0.76	1.13	1.75
5.59	0.41	0.60	0.72	1.43	2.20	3.41
6.98	0.45	0.65	0.89	1.81	2.52	3.85
C	k _{obs}	k _{obs}	k _{obs}	k _{obs}	k _{obs}	
10%	277.0K	296.4K	313.9K	328.4K	343.2K	
0.00		0.06				
1.86	0.16	0.31	0.54	0.81	1.25	
3.72	0.28	0.57	1.03	1.54	2.35	
5.59	0.42	0.85	1.49	2.17	3.29	
7.45	0.49	1.06	1.90	2.90	4.28	
9.31	0.63	1.36	2.29	3.42	5.64	
11.18	0.78	1.63	2.68	3.89	6.86	
C	k _{obs}	k _{obs}	k _{obs}	k _{obs}	k _{obs}	
0%	275.9K	296.6K	313.9K	328.4K	343.2K	
3.00	0.31	0.59	1.10	1.74	2.40	
5.97	0.63	1.22	2.17	3.41	4.89	
8.96	0.88	1.75	2.77	4.68	6.56	
11.9	1.02	2.17	4.18	7.00	8.18	
14.9	1.39	2.85	4.88	7.53	11.3	
17.9	1.53	3.47	5.73	9.63	12.4	
C	k _{obs}	k _{obs}	k _{obs}	k _{obs}	k _{obs}	k _{obs}
0%	277.0K	287.7K	295.9K	314.9K	328.7K	343.2K
0.00	0.054	0.089	0.092	0.13	0.17	0.23
1.86	0.16	0.26	0.36	0.74	0.94	1.64
3.72	0.32	0.50	0.65	1.41	2.15	2.92
5.59	0.46	0.69	0.91	1.65	2.67	4.30
7.45	0.61	0.92	1.30	2.24	3.47	5.64
9.31	0.75	1.16	1.39	2.80	4.25	7.07
11.2	0.82	1.21	1.71	3.59	5.82	8.66

Table A-6. The values of k_{obs} of solvated electrons' reaction with lithium perchlorate in water, 1-butanol, and *iso*-butanol .

C (mol/m ³)	k_{obs}	k_{obs}	C (mol/m ³)	k_{obs}	k_{obs}
water	274.1K	297.3K	<i>iso</i> -butanol	273.6K	297.0K
59	0.041	0.066	0	0.029	0.061
118	0.044	0.078	47	0.055	0.15
236	0.044	0.086	141	0.094	0.14
355	0.054	0.094	235	0.056	0.13
473	0.063	0.11	329	0.056	0.12
591	0.062	0.14	423	0.054	0.13
			470	0.051	0.13
C (mol/m ³)	k_{obs}	k_{obs}			
1-butanol	269.7K	296.8K			
0	0.044	0.093			
88	0.076	0.20			
176	0.068	0.18			
352	0.075	0.19			
440.	0.077	0.20			

Table A-7. The values of k_{obs} of solvated electrons' reaction with lithium nitrate in *iso*-butanol solvent.

C	k_{obs}	k_{obs}	k_{obs}	k_{obs}
<i>iso</i> -butanol	298.5K	314.5K	329.0K	343.5K
0.00	0.14	0.19	0.25	0.37
10.3	0.17	0.27	0.49	0.83
15.5	0.18	0.32	0.58	1.08
25.8	0.20	0.38	0.67	1.20
31.0	0.21	0.39	0.75	1.26

Table A-8. The values of k_{obs} of solvated electrons' reaction with ammonium nitrate in *iso*-butanol/water mixed solvents.

C	k_{obs}	k_{obs}	k_{obs}	k_{obs}	k_{obs}
98%	275.8K	298.6K	313.7K	327.4K	342.0K
0.00	0.042	0.087	0.13	0.15	0.23
1.52	0.086	0.16	0.22	0.28	0.38
3.05	0.14	0.27	0.39	0.45	0.62
4.57	0.20	0.37	0.53	0.67	0.86
6.10	0.26	0.48	0.72	0.88	1.14
7.62	0.35	0.62	0.84	1.15	1.43
9.15	0.39	0.72	1.02	1.26	1.61
C	k_{obs}	k_{obs}	k_{obs}	k_{obs}	k_{obs}
45%	283.2K	296.1K	313.6K	327.2K	341.6K
0.00	0.029	0.056	0.073	0.12	0.17
2.81	0.080	0.16	0.26	0.50	0.85
5.62	0.17	0.27	0.58	1.24	1.73
8.43	0.20	0.41	0.75	1.78	2.48
11.2	0.25	0.50	0.91	1.82	3.01
14.0	0.37	0.64	1.17	2.39	4.08
16.9	0.38	0.72	1.26	2.48	4.62

Table A-8 continued

C	k _{obs}	k _{obs}	k _{obs}	k _{obs}	k _{obs}
35%	275.9K	296.4K	313.7K	327.4K	343.8K
0.00	0.018	0.039	0.061	0.084	0.12
2.06	0.077	0.20	0.38	0.63	1.03
4.13	0.16	0.40	0.78	1.31	2.23
6.19	0.24	0.60	1.24	1.99	3.41
8.26	0.32	0.78	1.65	2.49	4.39
10.3	0.41	1.06	2.19	3.47	4.81
12.4	0.48	1.22	2.27	4.15	5.68
C	k _{obs}	k _{obs}	k _{obs}	k _{obs}	k _{obs}
20%	275.8K	296.1K	313.7K	327.4K	342.0K
0.00	0.016	0.030	0.049	0.059	0.076
1.62	0.10	0.20	0.37	0.60	0.91
3.24	0.16	0.35	0.67	1.05	1.61
4.86	0.22	0.52	0.98	1.59	2.37
6.47	0.28	0.64	1.30	2.01	2.78
8.10	0.35	0.87	1.58	2.41	3.61
9.72	0.49	1.17	2.01	2.95	4.18
C	k _{obs}	k _{obs}	k _{obs}	k _{obs}	k _{obs}
10%	275.8K	296.8K	313.7K	327.4K	342.0K
0.00	0.016	0.032	0.050	0.062	0.087
1.53	0.077	0.18	0.32	0.51	0.76
3.06	0.12	0.29	0.57	0.86	1.37
4.59	0.19	0.43	0.78	1.23	1.72
6.12	0.25	0.57	1.09	1.55	2.24
7.65	0.28	0.69	1.30	2.06	2.67
9.18	0.35	0.77	1.48	2.13	3.22

Table A-8 continued

C	k_{obs}	k_{obs}	k_{obs}	k_{obs}	k_{obs}
0%	276.3K	296.7K	314.0K	327.8K	342.3K
0.00	0.039	0.09	0.10	0.14	0.19
1.40	0.068	0.13	0.27	0.35	0.59
4.20	0.16	0.35	0.58	0.80	1.33
5.60	0.22	0.45	0.67	0.90	1.39
7.00	0.24	0.55	0.99	1.42	2.24
8.40	0.24	0.56	1.10	1.58	2.31

Table A-9. The values of k_{obs} of solvated electrons' reaction with ammonium perchlorate in *iso*-butanol/water mixed solvents.

C	k_{obs}	k_{obs}	k_{obs}	k_{obs}	k_{obs}
98%	277.9K	296.4K	314.8K	329.3K	344.4K
0.00	0.026	0.044	0.061	0.077	0.10
8.45	0.14	0.13			
16.9	0.093	0.18	0.31	0.53	0.87
44.0	0.097	0.21	0.43	0.71	1.23
84.5	0.13	0.31	0.59	0.96	1.59
127.	0.19	0.40	0.80	1.31	2.11
169.	0.21	0.46	0.92	1.45	2.20

C	k_{obs}	k_{obs}	k_{obs}	k_{obs}	k_{obs}
98%	278.2K	298.8K	313.9K	328.4K	343.0K
0.00	0.020	0.033	0.040	0.065	0.076
11.0	0.063	0.13	0.24	0.37	0.62
22.0	0.096	0.21	0.35	0.55	0.92
44.0	0.094	0.23	0.43	0.69	1.15
66.0	0.13	0.31	0.55	0.92	1.48
87.9	0.12	0.31	0.58	0.98	1.65
110.	0.14	0.37	0.67	1.12	1.85

Table A-9 continued

C	k _{obs}	k _{obs}	k _{obs}	k _{obs}	k _{obs}
98%	278.2K	298.9K	313.9K	328.4K	343.1K
0.00	0.016	0.031	0.052	0.060	0.075
2.64	0.033	0.060	0.12	0.19	0.31
5.28	0.029	0.070	0.13	0.22	0.38
7.91	0.043	0.10	0.19	0.31	0.52
10.6	0.053	0.13	0.22	0.39	0.58
13.2	0.073	0.15	0.26	0.43	0.67
15.8	0.067	0.15	0.27	0.43	0.69
C	k _{obs}	k _{obs}	k _{obs}	k _{obs}	k _{obs}
45%	282.1K	299.0K	314.7K	329.3K	344.4K
0.00	0.025	0.073	0.082	0.10	0.15
2.86	0.11	0.24	0.49	0.75	1.18
5.72	0.17	0.36	0.68	1.27	2.13
11.4	0.30	0.63	1.18	2.18	3.69
14.3	0.36	0.69	1.43	2.64	4.59
17.2	0.32	0.71	1.29	2.59	4.81
C	k _{obs}	k _{obs}	k _{obs}	k _{obs}	k _{obs}
45%	282.1K	296.6K	314.7K	329.3K	344.4K
0.00	0.030	0.050	0.073	0.095	0.14
2.40	0.11	0.21	0.41	0.71	1.08
7.19	0.23	0.42	0.91	1.56	2.80
12.0	0.31	0.65	1.27	2.59	3.54
14.4	0.35	0.66	1.61	2.89	4.62
C	k _{obs}	k _{obs}	k _{obs}	k _{obs}	
35%	279.9K	297.3K	314.8K	329.3K	
0.00	0.064	0.043	0.20	0.31	
4.29	0.24	0.44	0.98	1.61	
8.58	0.40	0.87	1.62	2.78	
12.9	0.54	1.16	2.37	4.01	
17.2	0.74	1.49	3.48	5.29	
25.7	0.98	2.15	4.72	7.97	

Table A-9 continued

C	k_{obs}	k_{obs}	k_{obs}	k_{obs}	k_{obs}
20%	275.7K	287.4K	297.5K	314.8K	329.3K
0.00	0.018	0.027	0.037	0.054	0.073
5.01	0.24	0.38	0.60	1.04	1.71
10.0	0.50	0.79	1.16	2.48	3.47
15.2	0.75	1.15	1.80	3.38	4.68
20.0	0.86	1.53	2.21	4.33	6.03
25.0	1.15	1.82	2.72	4.99	7.37
30.0	1.36	2.13	3.18	5.97	9.24

Table A-10. The values of k_{obs} of solvated electrons' reaction with silver perchlorate in *iso*-butanol/water mixed solvents.

C	k_{obs}	k_{obs}	k_{obs}	k_{obs}	k_{obs}	
100%	277.9K	296.4K	313.9K	328.4K	343.6K	
0.00	0.059	0.089	0.13	0.13	0.15	
0.78	0.16	0.29	0.42	0.54	0.63	
1.57	0.39	0.69	1.09	1.36	1.93	
2.35	0.70	1.15	1.95	2.45	3.03	
3.13	0.79	1.39	2.07	2.67	3.61	
3.92	1.06	1.91	2.67	3.81	5.06	
4.70	1.24	2.25	3.38	4.28	5.98	
C	k_{obs}	k_{obs}	k_{obs}	k_{obs}	k_{obs}	k_{obs}
98%	275.8K	286.4K	297.0K	313.9K	327.3K	341.8K
0.00	0.026	0.030	0.037	0.058	0.071	0.094
1.16	0.23	0.33	0.47	0.68	0.92	1.14
2.32	0.48	0.63	0.90	1.35	1.72	2.20
3.47	0.61	0.92	1.18	1.83	2.47	3.33
4.63	0.82	1.14	1.56	2.36	3.30	4.44
5.79	1.05	1.44	2.11	3.15	4.08	6.03
6.95	1.33	1.79	2.43	3.89	5.29	6.19

Table A-10 continued

C	k_{obs}	k_{obs}	k_{obs}	k_{obs}	k_{obs}	k_{obs}
45%	275.8K	286.4K	297.2K	313.7K	327.5K	342.0K
0.00	0.019	0.036	0.035	0.064	0.084	0.11
1.46	0.093	0.15	0.21	0.40	0.72	0.86
2.93	0.15	0.24	0.39	0.69	1.15	1.56
4.39	0.29	0.36	0.61	1.14	2.04	2.41
5.86	0.36	0.51	0.82	1.47	2.85	3.05
7.32	0.47	0.61	1.00	1.78	3.56	3.92
8.78	0.53	0.78	1.21	2.27	4.15	4.62
C	k_{obs}	k_{obs}	k_{obs}	k_{obs}	k_{obs}	
35%	275.9K	295.9K	313.8K	327.5K	342.0K	
0.00	0.032	0.049	0.12	0.18	0.49	
1.02	0.092	0.18	0.41	0.67	0.95	
2.04	0.13	0.29	0.53	0.81	1.21	
3.06	0.21	0.44	0.88	1.41	2.34	
4.08	0.24	0.55	0.99	1.56	2.34	
6.13	0.33	0.81	1.45	2.36	3.45	
C	k_{obs}	k_{obs}	k_{obs}	k_{obs}	k_{obs}	
20%	275.9K	296.4K	313.8K	327.5K	342.5K	
0.00	0.026	0.048	0.07	0.10	0.13	
1.49	0.093	0.21	0.39	0.58	0.87	
2.99	0.17	0.38	0.73	1.07	1.67	
4.48	0.26	0.57	1.14	1.73	2.73	
7.47	0.38	0.88	1.71	2.46	3.41	
C	k_{obs}	k_{obs}	k_{obs}	k_{obs}	k_{obs}	
10%	275.9K	296.1K	313.9K	327.5K	342.1K	
0.00	0.032	0.060	0.082	0.11	0.16	
0.93	0.067	0.13	0.25	0.40	0.60	
1.86	0.10	0.23	0.41	0.63	1.02	
2.79	0.13	0.29	0.58	0.91	1.33	
3.72	0.18	0.38	0.71	1.15	1.72	
5.58	0.26	0.56	1.07	1.70	2.57	

Table A-10 continued

C	k_{obs}	k_{obs}	k_{obs}	k_{obs}	k_{obs}	k_{obs}
0%	275.9K	286.5K	296.8K	313.9K	327.5K	342.0K
0.00	0.037	0.047	0.071	0.099	0.14	0.19
2.79	0.12	0.20	0.27	0.56	0.90	1.33
4.19	0.18	0.28	0.39	0.76	1.28	1.77
5.59	0.19	0.32	0.47	0.94	1.52	2.24
6.98	0.24	0.40	0.51	1.07	1.82	2.68
8.38	0.25	0.43	0.61	1.20	1.99	3.35

Table A-11. The values of k_{obs} of solvated electrons' reaction with lithium nitrate in 1-hexanol, 1-octanol, and 1-decanol solvents.

C	k_{obs}	k_{obs}	k_{obs}	k_{obs}	k_{obs}
1-hexanol	273.9K	296.8K	318.7K	343.2K	353.4K
0.00	0.052	0.095	0.14	0.26	0.32
26.6	0.076	0.26	0.66	1.39	1.73
53.3	0.12	0.36	0.89	1.90	2.48
79.9	0.13	0.41	1.00	2.27	2.89
107.	0.17	0.53	1.16	2.77	3.21
133.	0.20	0.59	1.61	2.89	4.33
C	k_{obs}	k_{obs}	k_{obs}	k_{obs}	k_{obs}
1-hexanol	273.3K	297.0K	319.3K	343.2K	
0.00	0.051	0.075	0.15	0.27	
19.5	0.087	0.25	0.57	1.14	
39.0	0.088	0.29	0.73	1.58	
58.5	0.12	0.41	0.90	2.24	
78.0	0.13	0.45	0.96	2.67	
97.5	0.16	0.51	1.20	2.81	
117.	0.17	0.51	1.35	3.38	

Table A-11 continued

C	k _{obs}	k _{obs}	k _{obs}	k _{obs}
1-octanol	273.6K	296.4K	328.4K	347.8K
0.00	0.12	0.24	0.50	0.82
34.2	0.24	0.53	1.16	1.98
51.3	0.27	0.57	1.41	2.31
68.4	0.30	0.68	1.73	2.89
85.5	0.30	0.70	2.04	3.22
103.	0.34	0.80	1.93	3.33
137.	0.37	0.95	2.24	4.33
C	k _{obs}	k _{obs}		
1-octanol	275.7K	298.6K		
0.0	0.15	0.25		
16.2	0.22	0.45		
32.5	0.23	0.53		
48.7	0.27	0.59		
65.0	0.31	0.67		
81.2		0.72		
97.4	0.35	0.75		
C	k _{obs}	k _{obs}	k _{obs}	
1-decanol	296.2K	313.9K	328.9K	
0.0	0.23	0.41	0.72	
23.2	0.35	0.68	1.14	
46.4	0.44	0.91	1.60	
69.6	0.57	1.10	1.99	
92.8	0.65	1.38	2.38	
116.	0.76	1.48	2.52	
116.	0.77	1.42	2.39	

Table A-11 continued

C	k _{obs}	k _{obs}	k _{obs}
1-decanol	296.4K	314.3K	328.8K
0.0	0.23	0.43	0.73
15.4	0.36	0.64	1.13
38.6	0.48	0.90	1.46
77.2	0.67	1.26	2.02
154.	0.98	1.88	3.09
193.	1.00	1.87	3.19

B. Results of k_2 Measurement

Table A-12. Temperature and composition dependences of k_2 for the reaction of e^-_s with lithium nitrate in 1-butanol/water mixed solvents.

mol % H ₂ O	T (K)	k_2 (10^6 $m^3/mol\cdot s$)	mol % H ₂ O	T (K)	k_2 (10^6 $m^3/mol\cdot s$)
100	277.0	5.5	35	277.0	0.55
	287.7	7.4		287.7	0.87
	296.7	9.2		297.0	1.1
	315.0	13.		315.0	1.7
	328.1	17		328.6	2.5
	343.3	20		343.2	3.6
99	277.6	4.9	20	297.3	0.70
	298.3	7.8		314.8	1.3
	314.5	11.		328.6	2.2
	329.1	14.		343.2	3.6
	344.2	17		354.4	4.6
98	296.4	7.7	10	296.7	0.51
	314.8	12.		314.9	1.0
	328.6	16.		328.5	1.7
	343.3	20.		343.2	3.1
	354.4	23.		354.4	4.0
45	277.0	0.66	0	277.0	0.051
	287.7	0.82		287.7	0.11
	296.4	1.2		296.7	0.16
	315.0	1.9		315.0	0.47
	328.7	2.7		328.7	0.92
	343.3	3.4		343.2	1.6

Table A-13. Temperature and composition dependences of k_2 for the reaction of e^-_s with ammonium nitrate in 1-butanol/water mixed solvents.

mol % H ₂ O	T (K)	k_2 (10^7 $m^3/mol \cdot s$)	mol % H ₂ O	T (K)	k_2 (10^7 $m^3/mol \cdot s$)
100	296.9	0.95	35	277.1	0.40
	315.0	1.4		287.7	0.78
	328.7	1.8		296.3	1.0
	343.2	2.3		315.0	2.1
	354.6	2.6		328.7	3.1
			343.2	5.2	
99	278.7	0.49	20	277.1	0.59
	296.5	0.77		287.7	0.94
	314.5	1.1		296.4	1.2
	329.2	1.4		315.0	2.3
	344.2	1.7		328.7	3.6
			343.2	5.6	
98	277.0	0.43	10	277.1	0.47
	287.7	0.57		287.7	0.74
	297.0	0.72		301.4	1.4
	315.0	1.1		315.0	2.0
	328.6	1.3		328.6	2.8
	343.2	1.7		343.3	3.9
45	277.0	0.20	0	277.0	0.39
	287.7	0.33		287.7	0.57
	296.4	0.46		296.5	0.83
	315.0	0.97		315.0	1.4
	328.6	1.8		328.7	2.1
	343.3	2.9		343.2	3.0

Table A-14. Temperature and composition dependences of k_2 for the reaction of e^-_s with ammonium perchlorate in 1-butanol/water mixed solvents.

mol % H ₂ O	T (K)	k_2 (10^7 $m^3/mol\cdot s$)	mol % H ₂ O	T (K)	k_2 (10^7 $m^3/mol\cdot s$)
100	277.0	0.000082	35	279.0	0.41
	296.7	0.00015		297.7	0.91
	314.0	0.00022		314.7	1.8
	328.5	0.00025		329.3	3.0
				344.4	4.0
99	278.2	0.000085	20	282.0	0.74
	298.5	0.00015		296.3	1.2
	313.9	0.00021		314.6	2.3
	328.4	0.00024		329.4	3.4
	343.1	0.00028		344.4	6.0
45	282.5	0.22			
	296.0	0.41			
	314.7	0.96			
	329.4	1.6			
	344.4	2.7			

Table A-15. Temperature and composition dependences of k_2 for the reaction of e^-_s with perchloric acid in 1-butanol/water mixed solvents.

mol % H ₂ O	T (K)	k_2 (10^7 $m^3/mol\cdot s$)	mol % H ₂ O	T (K)	k_2 (10^7 $m^3/mol\cdot s$)
100	276.9	1.7	45	276.9	0.86
	287.6	2.0		287.7	1.3
	295.1	2.3		296.0	2.2
	314.9	3.1		314.9	3.8
	328.6	3.7		328.6	5.7
	343.1	4.3		343.2	8.4
	354.3	4.8			
100	278.7	1.7	35	277.0	0.91
	295.8	2.3		287.7	1.4
	313.9	3.1		296.0	1.8
	328.1	3.8		314.9	4.0
	343.1	4.7		328.7	5.9
				343.2	8.6
98	277.0	1.7	20	277.0	0.8
	287.7	2.2		296.7	1.8
	296.6	2.6		313.9	3.1
	314.9	3.5		328.4	4.6
	328.6	4.3		343.2	6.6
	343.2	5.1			

Table A-15 continued

mol % H ₂ O	T (K)	k ₂ (10 ⁷ m ³ /mol·s)	mol % H ₂ O	T (K)	k ₂ (10 ⁷ m ³ /mol·s)
20	277.0	0.8	0	275.9	0.82
	296.7	1.8		296.6	1.9
	313.9	3.1		313.9	3.1
	328.4	4.6		328.4	5.2
	343.2	6.6		343.2	6.8
10	277.0	0.6	0	277.0	0.82
	296.4	1.4		287.7	1.2
	313.9	2.3		295.9	1.6
	328.4	3.3		314.9	2.8
	343.2	6.0		328.7	5.3
			343.2	7.5	
10	277.0	0.67			
	287.7	1.0			
	295.8	1.2			
	314.9	2.4			
	328.6	3.6			
	343.2	5.6			

Table A-16. Temperature dependence of k₂ for the reaction of e⁻_s with lithium nitrate in *iso*-butanol solvent.

T (K)	298.2	314.5	329.0	343.5
k ₂ (10 ⁶ m ³ /mol·s)	0.25	0.71	1.3	2.4

Table A-17. Temperature and composition dependences of k_2 for the reaction of e^-_s with ammonium nitrate in *iso*-butanol/water mixed solvents.

mol % H ₂ O	T (K)	k_2 (10^7 m ³ /mol·s)	mol % H ₂ O	T (K)	k_2 (10^7 m ³ /mol·s)
98	275.8	0.42	20	275.8	0.43
	298.6	0.74		296.1	1.1
	313.7	1.0		313.7	2.0
	328.4	1.3		327.4	2.9
	342.0	1.7		342.0	4.2
45	283.2	0.24	10	275.8	0.36
	296.1	0.41		296.8	0.83
	313.6	0.74		313.7	1.6
	327.2	1.5		327.4	2.3
	341.6	2.7		342.0	3.2
35	275.9	0.38			
	296.4	0.98			
	313.7	2.0			
	327.4	3.4			
	343.8	5.2			

Table A-18. Temperature and composition dependences of k_2 for the reaction of e^-_s with ammonium perchlorate in *iso*-butanol/water mixed solvents.

mol % H ₂ O	T (K)	k_2 (10^7 $m^3/mol\cdot s$)	mol % H ₂ O	T (K)	k_2 (10^7 $m^3/mol\cdot s$)
98	277.9	0.00015	35	279.9	0.37
	298.0	0.00026		296.5	0.78
	313.9	0.00046		314.8	1.8
	328.4	0.00058		329.3	2.9
	343.1	0.00079			
45	282.1	0.22	20	275.7	0.44
	299.0	0.40		287.4	0.75
	314.7	0.83		297.5	1.1
	329.3	1.7		314.8	2.1
	344.4	3.0		329.3	2.9

Table A-19. Temperature and composition dependences of k_2 for the reaction of e_s^- with silver perchlorate in *iso*-butanol/water mixed solvents.

mol % H ₂ O	T (K)	k_2 (10^7 $m^3/mol \cdot s$)	mol % H ₂ O	T (K)	k_2 (10^7 $m^3/mol \cdot s$)
98	275.8	1.8	20	275.9	0.47
	286.4	2.5		296.4	1.1
	297.0	3.5		313.8	2.2
	313.9	5.3		327.5	3.2
	327.3	6.9		342.5	5.0
	341.8	9.5			
45	275.8	0.68	10	275.9	0.41
	286.4	0.81		296.1	0.91
	297.2	1.4		313.9	1.6
	313.7	2.4		327.5	2.9
	327.5	4.7		342.1	4.3
	342.0	5.2			
35			0	275.9	0.29
	275.9	0.49		286.5	0.50
	295.9	1.3		296.8	0.70
	313.8	2.2		313.9	1.4
	327.5	3.6		327.5	2.3
	342.0	4.8		342.0	3.5

Table A-20. Temperature dependence of k_2 for the reaction of e^-_s with lithium nitrate in 1-hexanol, 1-octanol, and 1-decanol solvents.

<i>n</i> -alcohol	T (K)	k_2 (10^6 $m^3/mol \cdot s$)	<i>n</i> -alcohol	T (K)	k_2 (10^6 $m^3/mol \cdot s$)
1-hexanol	273.6	0.10	1-octanol	274.7	0.16
	296.9	0.34		297.5	0.40
	319.0	0.83		328.5	1.4
	343.2	2.0		347.9	2.4
1-decanol	296.3	0.52			
	314.1	0.99			
	328.9	1.7			

II. Results of Molar Conductivity Measurement

In this study, the molar conductivities of lithium nitrate, ammonium nitrate, ammonium perchlorate, and perchloric acid electrolyte solutions were measured in 1-butanol/water mixed solvents; and the molar conductivities of lithium nitrate, ammonium nitrate, ammonium perchlorate, perchloric acid, silver perchlorate, copper (II) perchlorate, and aluminum (III) perchlorate electrolyte solutions were measured in *iso*-butanol/water mixed solvents. The molar conductivities of lithium nitrate electrolyte solution was also measured in 1-hexanol, 1-octanol, and 1-decanol. 1-butanol and *iso*-butanol are not completely miscible with water (see reference 8 in chapter three and reference 7 in chapter four). The measurements were mostly made over the miscible range. For *iso*-butanol/water mixtures, the following mol % water were used: 0, 10.0, 20.0, 35.0, 45.0, 98.0, and 100.0. The 45 mol% is located in the immiscible region for the temperatures less than 293.2K, so the measurement at those temperatures are reported here but not analyzed with the rest of data due to the phase separation. For 1-butanol/water mixture the following mol % water were used: 0, 10.0, 20.0, 35.0, 45.0, 98.0, 99.0, and 100.0. The 98 mol% is located in the immiscible region, so the measurement are reported here but not analyzed with the rest of data due to the phase separation. The rest of mixtures are in the miscible range.

Table A-21. Temperature and composition dependences of molar conductivities of lithium nitrate solutions in 1-butanol/water mixed solvents.^a

mol % H ₂ O	T (K)	Λ (10^{-3} S·m ² /mol)	mol % H ₂ O	T (K)	Λ (10^{-3} S·m ² /mol)
100	277.14	6.76	45	278.22	1.12
	298.17	11.2		298.33	2.09
	312.32	14.4		313.50	3.08
	328.91	18.2		328.29	4.27
	343.11	21.5		343.38	5.80
100	298.09	10.9	35	278.20	1.06
	312.42	14.1		298.26	1.94
	328.86	18.4		313.46	2.67
	342.92	22.4		328.21	3.76
				343.30	4.93
100	277.69	6.48	20	278.22	0.98
	298.13	10.3		298.29	1.74
	312.46	13.2		313.51	2.45
	328.89	16.5		328.17	3.38
	342.96	19.9		343.41	4.30
99	278.20	6.30	10	278.27	0.83
	298.22	10.4		298.35	1.50
	313.43	14.8		313.53	2.07
	328.18	18.3		328.19	2.79
	343.39	22.2		343.48	3.31
98	278.32	3.95	0	278.12	0.75
	298.28	7.45		298.35	1.27
	313.52	11.4		313.48	1.79
	328.27	13.0		328.33	2.29
	343.46	16.5		343.47	2.50

^a LiNO₃ concentrations: 0.025-0.25 mol/m³.

Table A-22. Temperature and composition dependences of molar conductivities of ammonium nitrate solutions in 1-butanol/water mixed solvents.^a

mol % H ₂ O	T (K)	Λ (10^{-3} S·m ² /mol)	mol % H ₂ O	T (K)	Λ (10^{-3} S·m ² /mol)
100	278.24	8.70	45	278.22	1.35
	298.25	14.9		298.25	2.35
	313.51	21.2		313.55	3.42
	328.33	26.9		328.25	4.77
	343.50	37.4		343.42	6.41
100	278.36	8.90	35	278.24	1.23
	298.37	15.1		298.33	2.15
	313.53	21.5		313.55	3.07
	328.22	27.1		328.24	4.18
	343.54	33.5		343.41	5.35
100	278.34	8.90	20	278.26	1.16
	298.32	14.6		298.28	1.96
	313.57	21.0		313.51	2.75
100	328.26	27.4		328.22	3.40
	343.45	36.4		343.42	4.25
99	278.23	7.40	10	278.24	0.94
	298.23	13.6		298.28	1.60
	313.43	18.1		313.44	2.18
	328.17	21.7		328.24	2.91
	343.37	26.2		343.46	3.32
98	278.29	7.60	0	278.21	0.77
	298.25	12.1		298.29	1.38
	313.57	15.3		313.52	2.04
	328.28	19.1		328.23	2.60
	343.46	24.4		343.42	2.95

^a NH₄NO₃ concentrations: 0.03-0.2 mol/m³.

Table A-23. Temperature and composition dependences of molar conductivities of ammonium perchlorate solutions in 1-butanol/water mixed solvents.^a

mol % H ₂ O	T (K)	Λ (10^{-3} S·m ² /mol)	mol % H ₂ O	T (K)	Λ (10^{-3} S·m ² /mol)
100	278.34	8.84	45	278.23	1.39
	298.31	14.1		298.24	2.50
	313.26	18.8		313.51	3.69
	328.41	25.6		328.27	5.15
	343.45	32.0		343.44	6.70
99	279.91	8.00	35	278.26	1.40
	298.29	12.7		298.34	2.39
	313.29	16.4		313.58	3.60
	328.29	19.9		328.34	4.90
	343.44	24.2		343.51	6.35
98	278.29	6.60	20	278.24	1.27
	298.24	12.4		298.29	2.22
	313.44	16.2		313.51	3.44
	328.16	20.5		328.33	4.60
	343.45	25.1		343.41	5.42

^a NH₄ClO₄ concentrations: 0.01-0.4 mol/m³ in 99, 45, 35, 20 mol % water mixed solvents. In pure water the low reactivity of NH₄ClO₄ in water required concentrations up to 100 mol/m³ for measurement of k_2 , and the same concentration range (0.08-104 mol/m³) was used for Λ measurement; the Debye-Hückel-Onsager equation (see chapter two) describes the Λ data, so ion pairing is negligible. Λ value reported here in pure water is calculated from the data measured in concentration range 0.08-0.4 mol/m³.

Table A-24. Temperature and composition dependences of molar conductivities of perchloric acid solutions in 1-butanol/water mixed solvents.^a

mol % H ₂ O	T (K)	Λ (10^{-3} S·m ² /mol)	mol % H ₂ O	T (K)	Λ (10^{-3} S·m ² /mol)
100	278.10	29.3	20	298.16	1.83
	283.23	31.9		313.09	2.69
	298.54	40.5		328.19	3.92
	313.35	46.4		343.29	5.47
	328.36	50.0	10	298.12	1.66
	343.61	53.8		313.09	2.51
45	298.15	3.08	0	328.22	3.80
	313.14	4.74		343.14	4.96
	328.36	7.03		298.22	1.46
	343.37	9.52	313.21	2.37	
35	298.19	2.58	0	328.31	3.35
	313.12	3.60		343.48	4.52
	328.27	5.55			
	343.35	7.75			

^a HClO₄ concentrations: 0.03-0.22 mol/m³.

Table A-25. Temperature and composition dependences of molar conductivities of lithium nitrate solutions in *iso*-butanol/water mixed solvents.^a

mol % H ₂ O	T (K)	Λ (10 ⁻³ S·m ² /mol)	mol % H ₂ O	T (K)	Λ (10 ⁻³ S·m ² /mol)
98	273.83	4.40	20	277.27	0.685
	298.12	8.70		298.17	1.38
	312.45	13.8		312.40	2.13
	328.88	17.2		328.87	3.00
	342.95	21.1		343.08	3.73
98	312.44	12.5	10	277.17	0.630
	328.88	16.8		298.15	1.25
	342.97	22.8		312.39	1.72
				328.86	2.31
45	276.92	0.572	0	343.06	2.65
	298.18	1.35		278.18	0.494
	312.42	2.05		298.29	0.870
	328.89	2.97		313.50	1.27
	343.09	3.90		328.21	1.71
35	277.17	0.795		343.44	1.89
	298.14	1.62			
	312.39	2.43			
	328.89	3.57			
	343.06	4.71			

^a LiNO₃ concentrations: 0.04-0.3 mol/m³.

Table A-26. Temperature and composition dependences of molar conductivities of ammonium nitrate solutions in *iso*-butanol/water mixed solvents.^a

mol % H ₂ O	T (K)	Λ (10^{-3} S·m ² /mol)	mol % H ₂ O	T (K)	Λ (10^{-3} S·m ² /mol)
98	278.19	6.65	35	278.24	0.940
	298.35	12.2		298.26	1.79
	313.51	16.8		313.55	2.92
	328.22	21.8		328.17	3.72
	343.42	25.8		343.38	5.10
45	278.32	0.855	20	278.21	0.81
	298.33	1.63		298.33	1.63
	313.52	2.37		313.54	2.37
	328.18	3.44		328.22	3.18
	343.38	4.86		343.44	4.15
45	328.88	3.31	10	278.19	0.62
	343.30	4.75		298.34	1.26
	313.51	2.44		313.60	1.87
				328.31	2.32
				343.41	2.94

^a NH₄NO₃ concentrations: 0.015-0.17 mol/m³.

Table A-27 Temperature and composition dependences of molar conductivities of ammonium perchlorate solutions in *iso*-butanol/water mixed solvents.^a

mol % H ₂ O	T (K)	Λ (10 ⁻³ S·m ² /mol)	mol % H ₂ O	T (K)	Λ (10 ⁻³ S·m ² /mol)
98	278.19	6.57	35	278.27	0.965
	298.28	12.7		298.29	2.00
	313.48	18.8		313.52	3.00
	328.33	22.4		328.17	4.40
	343.43	28.2		343.35	5.74
45	278.19	0.980	20	278.30	0.835
	298.31	2.06		298.34	1.58
	313.52	3.27		313.48	2.49
	328.32	4.77		328.34	3.68
	343.45	6.08		343.49	4.57

^a NH₄ClO₄ concentrations: 0.025-0.17 mol/m³.

Table A-28. Temperature and composition dependences of molar conductivities of perchloric acid solutions in *iso*-butanol/water mixed solvents.^a

mol % H ₂ O	T (K)	Λ (10 ⁻³ S·m ² /mol)	mol % H ₂ O	T (K)	Λ (10 ⁻³ S·m ² /mol)
98	278.01	22.2	20	278.28	1.04
	298.18	31.6		298.19	1.87
	313.40	39.4		313.45	3.00
	328.39	48.0		328.44	4.26
	343.65	52.1		343.69	5.93
45	277.99	1.64	10	278.07	0.85
	298.19	2.96		298.31	1.56
	313.40	4.16		313.44	2.57
	328.42	5.74		328.47	3.46
	343.52	7.60		343.65	4.70
35	277.96	1.37	0	278.03	0.69
	298.18	2.59		298.25	1.39
	313.40	3.78		313.49	2.28
	328.39	5.78		328.47	3.40
	343.60	7.81		343.67	4.87

^a HClO₄ concentrations: 0.015-0.22 mol/m³.

Table A-29. Temperature and composition dependences of molar conductivities of silver perchlorate solutions in *iso*-butanol/water mixed solvents.^a

mol % H ₂ O	T (K)	Λ (10 ⁻³ S·m ² /mol)	mol % H ₂ O	T (K)	Λ (10 ⁻³ S·m ² /mol)
100	275.83	7.84	45	275.83	0.96
	298.10	13.4		298.11	2.43
	312.43	17.9		312.43	3.78
	328.90	23.7		328.87	5.44
	342.97	27.8		342.42	6.95
100	275.80	8.80	35	275.83	1.00
	298.08	14.4		298.11	2.20
	312.42	18.6		312.43	3.31
	328.84	24.0	35	328.87	4.30
	342.91	30.0		342.92	5.60
100	278.28	8.70	20	276.85	0.78
	298.32	13.8		298.09	1.64
	313.48	18.1		312.42	2.46
	328.17	23.7		328.87	3.55
	343.47	30.4		342.91	4.49
98	278.19	11.4	10	275.77	0.71
	298.27	21.4		298.06	1.53
	313.46	34.7		312.39	2.37
	328.26	44.4		328.83	3.22
	343.42	49.0		342.90	3.98
98	298.11	21.1	0	275.79	0.56
	313.19	32.0		298.07	1.24
	328.24	42.4		312.39	1.79
	343.22	50.7		328.83	2.58
					342.89

^a AgClO₄ concentrations: 0.02-0.3 mol/m³.

Table A-30. Temperature and composition dependences of molar conductivities of copper (II) perchlorate solutions in *iso*-butanol/water mixed solvents.^a

mol % H ₂ O	T (K)	Λ (10 ⁻³ S·m ² /mol)	mol % H ₂ O	T (K)	Λ (10 ⁻³ S·m ² /mol)
100	273.96	13.4	98	298.31	38.7
	283.20	17.4		313.56	55.8
	298.23	25.3	98	328.28	71.7
	312.79	32.9			
	328.82	41.9			
	343.53	53.1			
100	278.29	14.8	98 ^b	343.43	79.8
	298.42	24.6		328.19	77.4
	313.54	33.7		313.52	62.8
	328.24	43.3		298.35	50.1
	343.49	54.1		278.29	30.4
100	278.15	14.5	98	277.99	16.9
	298.23	24.1		298.47	37.7
	313.48	32.8		313.38	53.6
	328.13	42.8		328.44	71.2
	343.43	56.1		343.62	86.5
99.5	278.24	19.6	98	298.19	34.3
	298.26	43.8		313.17	56.8
	313.42	63.0		328.22	77.4
				343.39	89.8
99	278.24	21.9	98	278.37	15.5
	298.24	48.1		298.39	33.9
	313.40	67.9			
	343.36	89.8			

^a Cu(ClO₄)₂ concentrations: 0.01-0.16 mol/m³.

^b The order of temperature change is from high to low.

Table A-30 continued

mol % H ₂ O	T (K)	Λ (10^{-3} S·m ² /mol)	mol % H ₂ O	T (K)	Λ (10^{-3} S·m ² /mol)
45	278.28	1.33	10	275.79	1.13
	298.40	3.15		298.07	2.48
	313.56	5.34		312.40	3.73
	328.33	8.44		328.82	5.93
	343.54	13.0		342.88	8.10
35	275.79	1.47	0	275.79	0.78
	298.07	3.04		298.08	1.91
	312.40	4.97		312.40	2.89
	328.82	7.71		328.83	4.84
	342.89	10.6		342.88	6.28
20	275.79	1.27			
	298.07	2.74			
	312.40	4.40			
	328.85	7.03			
	342.89	9.23			

Table A-31. Temperature and composition dependences of the apparent molar conductivities of aluminum (III) perchlorate solutions in *iso*-butanol/water mixed solvents.^a

mol % H ₂ O	T (K)	Λ (10^{-3} S·m ² /mol)	mol % H ₂ O	T (K)	Λ (10^{-3} S·m ² /mol)
100 ^b	298.71	56.8	45	275.79	2.70
	312.40	80.6		298.06	7.64
	328.86	112.		312.38	13.3
	342.93	134.		328.16	21.3
	343.47	150.		343.43	26.5
100 ^c	278.17	26.1	35	275.78	3.45
	298.38	49.1		298.06	6.74
	313.51	75.2		312.40	9.07
	328.36	107.		328.84	14.2
	343.47	150.		342.92	19.8
100 ^d	298.14	40.1	20	275.77	2.92
	313.09	57.7		298.06	5.99
	328.28	75.6		312.40	8.92
	343.36	102.		328.84	13.8
98	278.28	20.1	10	342.89	18.0
	298.36	43.0		275.79	2.10
	313.56	68.2		298.06	5.06
	328.21	110.		312.41	7.49
	343.47	172.		328.84	11.6
98	278.26	25.1	0	342.91	14.8
	298.50	45.0		275.80	1.30
	313.59	67.7		298.08	3.99
	328.27	91.8		312.41	6.77
	343.47	134.		328.85	10.0
				342.93	12.3

^a Al(ClO₄)₃ concentrations: 0.006-0.06 mol/m³ in 98, 45, 35, 20, 10, and 0 mol % water mixed solvents.

^b Al(ClO₄)₃ concentrations: 0.006-0.03 mol/m³.

^c Al(ClO₄)₃ concentrations: 0.013-0.067 mol/m³.

^d Al(ClO₄)₃ concentrations: 0.078-0.31 mol/m³.

Table A-32. Temperature and concentration dependences of the molar conductivities of lithium nitrate solutions in 1-hexanol solvent.

C (mol/m ³)	Λ (10 ⁻⁴ S·m ² /mol)				
	298.15K	313.16K	328.45K	343.43K	353.21K
0.036	4.86	6.75	7.85	8.56	8.41
0.071	4.26	6.22	7.05	7.26	6.61
0.107	4.37	5.68	6.18	6.16	5.48
0.142	4.25	5.37	5.89	5.79	5.15
0.178	4.06	4.88	5.20	4.75	4.17
	298.18K	313.17K	328.39K	343.47K	
0.195	4.14	5.03	5.39	5.13	
0.390	3.50	4.07	4.25	3.92	
0.585	3.01	3.39	3.46	3.03	
0.780	2.71	3.06	3.07	2.76	
1.17	2.56	2.82	2.78	2.44	
	298.22K	313.17K	328.47K	343.48K	
1.50	2.25	2.49	2.36	1.99	
9.01	1.23	1.22	1.15	1.04	
15.0	1.03	1.08	1.03	0.94	
22.5	0.91	0.99	0.96	0.87	
37.5	0.81	0.89	0.91	0.82	
	298.22K	313.26K	328.35K		
2.80	1.75	1.88	1.93		
7.00	1.23	1.28	1.23		
14.0	1.00	1.08	1.09		
21.0	0.92	1.01	1.00		
35.0	0.81	0.92	0.89		

Table A-33. Temperature and concentration dependences of the molar conductivities of lithium nitrate solutions in 1-octanol solvent.

C (mol/m ³)	Λ (10 ⁻⁴ S·m ² /mol)			
	298.22K	313.15K	328.24K	343.45K
0.0274	1.91	1.97	1.94	1.99
0.0547	1.62	1.67	1.71	1.64
0.0821	1.46	1.54	1.55	1.42
0.109	1.27	1.32	1.32	1.17
0.137	1.24	1.29	1.18	1.06
	298.17K	313.14K	328.38K	343.45K
0.162	1.17	1.22	1.18	1.05
0.325	0.91	0.94	0.86	0.74
0.487	0.75	0.74	0.68	0.58
0.650	0.75	0.77	0.69	0.55
0.974	0.61	0.59	0.54	0.45
	298.17K	313.12K	328.39K	343.46K
0.884	0.62	0.64	0.62	0.47
1.47	0.48	0.50	0.44	0.34
2.95	0.38	0.37	0.33	0.27
4.42	0.31	0.31	0.27	0.22
7.37	0.27	0.26	0.24	0.19
	298.22K	313.28K	328.77K	343.47K
2.33	0.46	0.45	0.36	0.33
4.66	0.35	0.34	0.31	0.25
6.98	0.31	0.30	0.25	0.22
9.31	0.30	0.27	0.23	0.20
11.6	0.28	0.25	0.21	0.17

Table A-34. Temperature and concentration dependences of the molar conductivities of lithium nitrate solutions in 1-decanol solvent.

C (mol/m ³)	Λ (10 ⁻⁴ S·m ² /mol)			
	298.24K	313.21K	328.39K	343.47K
0.0581	0.28	0.35	0.36	0.34
0.116	0.28	0.29	0.28	0.20
0.174	0.23	0.28	0.25	0.22
0.232	0.23	0.25	0.22	0.18
0.291	0.21	0.24	0.22	0.18
	298.14K	313.23K	328.36K	343.41K
0.580	0.18	0.18	0.15	0.13
1.16	0.14	0.13	0.11	0.079
	298.21K	313.26K	328.39K	343.50K
0.692	0.15	0.14	0.12	0.092
1.39	0.14	0.11	0.093	0.071
2.08	0.12	0.095	0.079	0.066
2.77	0.11	0.085	0.073	0.059
3.47	0.087	0.071	0.059	0.043
	298.19K	313.22K	328.39K	343.41K
0.251	0.24	0.22	0.20	0.17
0.522	0.18	0.16	0.13	0.11
0.783	0.15	0.14	0.12	0.095
1.04	0.14	0.13	0.11	0.096
1.31	0.13	0.11	0.089	0.071
	298.17K	313.21K		
0.252	0.21	0.21		
0.505	0.16	0.16		
0.757	0.14	0.13		
1.01	0.13	0.12		
1.26	0.12	0.11		

Table A-34 continued

C (mol/m ³)	Λ (10 ⁻⁴ S·m ² /mol)			
	298.18K	313.24K	328.43K	343.44K
0.473	0.19	0.20	0.17	0.155
0.946	0.15	0.14	0.12	0.093
1.42	0.12	0.12	0.10	0.095
1.89	0.12	0.11	0.10	0.085
2.36	0.11	0.10	0.084	0.071